UNIVERSITA' DEGLI STUDI DI MILANO

FACOLTA´ DI SCIENZE MATEMATICHE FISICHE E NATURALI

Dipartimento di Chimica Organica e Industriale

Dottorato di Ricerca in Chimica Industriale

(XXIV ciclo)

TESI DI DOTTORATO DI RICERCA

SYNTHESIS OF PLA HOMO AND COPOLYMERS AND THEIR NANOCOMPOSITES FOR ADVANCED MATERIALS

Tutor: Prof. Giuseppe DI SILVESTRO

Coordinatore: Prof. Dominique ROBERTO

Dott. Luca BASILISSI

Matricola R08298

Anno Accademico 2010-2011

Summary

1. Introduction

1 INTRODUCTION

Even if we are led to think that the plastic is a modern invention, natural polymers like wool, cotton, wood have always existed and they have been used by man since ancient times; it is not easy to identify when the age of macromolecules began, but surely at the beginning of 1900s a strong development of researches for new plastic materials started, greatly contributing to economic and social development, allowing a better quality of life in most of the world population, especially since the '50s; it can stated that we currently live in what may be called "the age of plastic".

The study and development in the field of plastics, since their invention to the present day, have always been designed to improve mechanical and structural properties such as strength, hardness, workability, transparency, in order to obtain materials with better performance and with properties similar to wood, glass, and metal, in order to have polymers that could replace these materials in their applications.

The importance acquired over the years by plastic materials is confirmed by the continuous increase in production volumes, which have grown to reach 275 million tons in 2008. Analyzing the quantity of the main classes of plastics produced in the period 2003-2010, as shown in picture 1, an average increase of 5% per year for all polymers considered can be observed as a further demonstration of a growing market; the only moments of decline can be traced to the oil crises recorded in the mid 70's to early 80's and , less markedly, in 2008-2009, that led to a decrease in production volumes as a result of declining request.

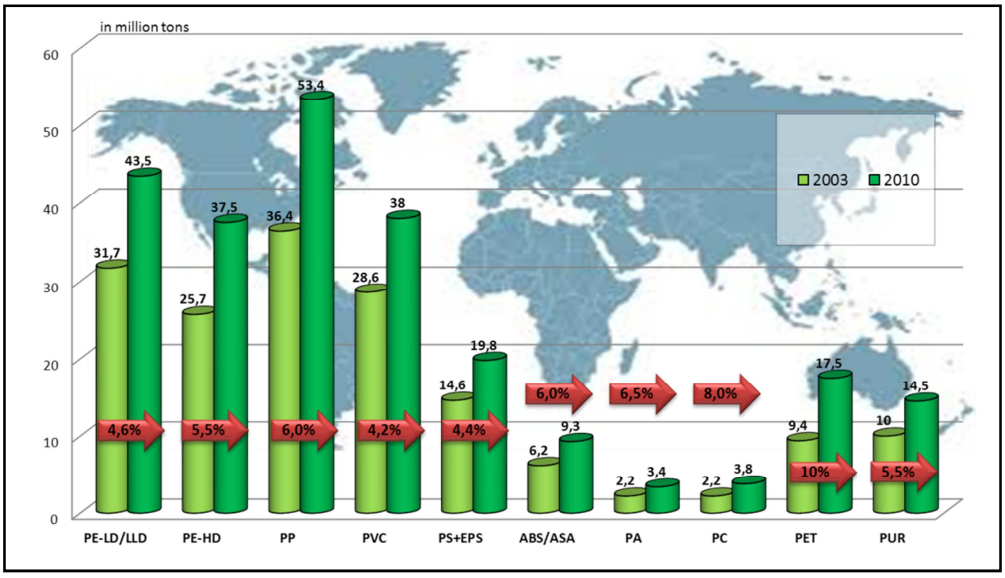

Figure 1: World plastics consumption 2003-2010

It can also be interesting to observe how the world production of plastics shows a almost six-fold increase in the period 1970-2004, growing more than twice than aluminum and even more than six times compared to steel (Figure 2); this trend confirms that polymers could be a more economically and advantageous solution and have improved performance to replace traditional materials.

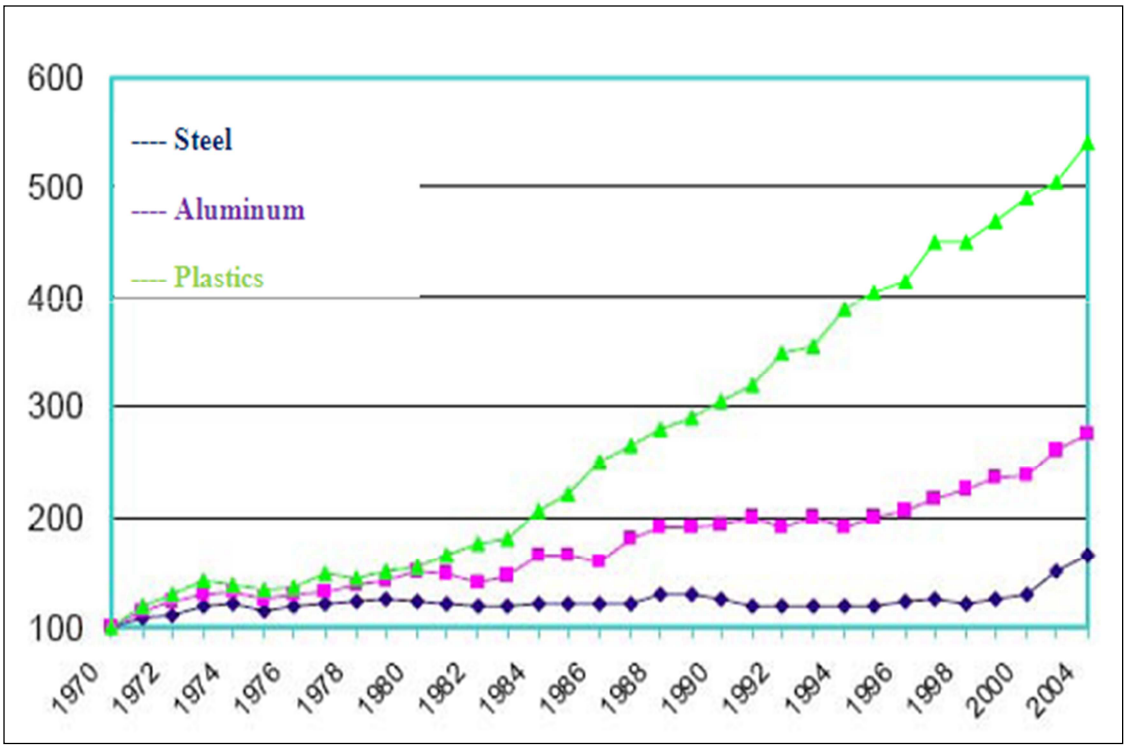

Figure 2: World production: plastics growth Vs other materials

Nowadays the synthetic polymers can be classified in various ways, for example according to their future applications or the mechanism of polymerization, but the more general classification divides polymeric materials into two categories: thermoplastics and thermosets.

In the group of thermoplastic polymers, which accounts more or less 80% of global production, nearly twenty types of polymers are included. PE, PP, PVC, PS and PET alone represent more than 75% of the volume of thermoplastics. In particular, polyolefins (LDPE, LLDPE, HDPE, PP) have the largest market share, which represents 50% of global production.

The main thermoset materials are polyurethane, amino and phenolic resins.

Tables 1 and 2 show the consumption of thermoplastic and thermosetting materials recorded in Europe in 2003, compared to the world consumption; European values account for about 25% market share.

For thermoplastic polymers (Table 1) the value of PE was set as 100 while for the thermosetting polymers (Table 2) the reference is represented by polyurethane resin.

Thermoplastics	Consumption (Mtons)	Relative index (PE=100)
LDPE+LLDPE+HDPE	13482	100
LDPE+LLDPE	8062	59.8
HDPE	5420	40.2
PP	7879	58.4
PVC	5832	43.3
PET	3802	28.2
PS/HPS	3136	23.3
PA	1328	9.9
OTHERS	2678	19.9

Table 1: Consumption of thermoplastics in Europe

Thermosets	Consumption (Mtons)	Relative index (PU=100)
POLYURETHANE	2672	100
AMINO	2630	98.4
PHENOLIC	980	36.7
POLYESTER	490	18.3
EPOXIDIC	398	14.9
ALKYDIC	370	13.8
OTHERS	3100	116

Table 2: Consumption of thermosets in Europe

The application of polymeric materials on the European market is divided into different areas of application and use, with a prevalence of the packaging industry, which alone accounts for 40.1% of total demand in particular for polymers such as polyolefins and PET (Figure 4). This sector is followed by construction (20.4%), automotive (7%) and materials for electrical and electronic equipment (5.6%).

The remaining 26% of plastics is intended for use in a smaller market sectors such as agriculture, furniture, transport and sports equipment (Figure 3).

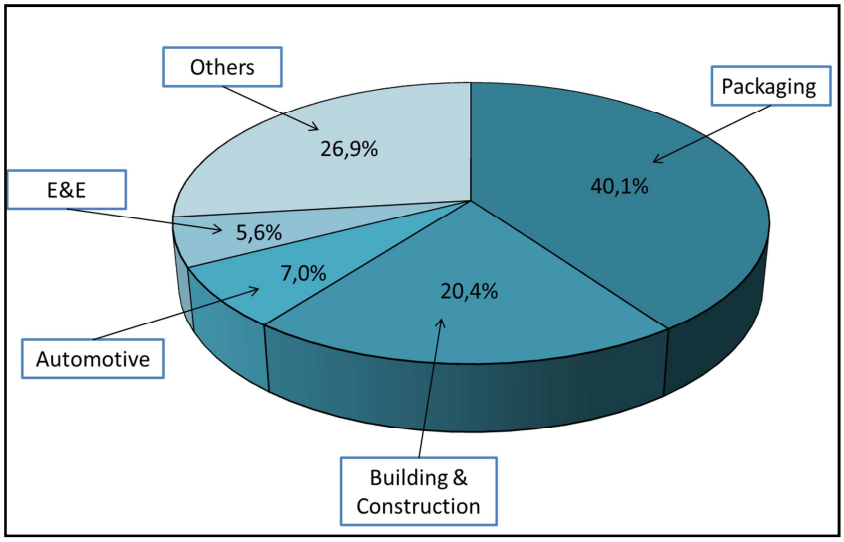

Figure 3: Fields of application of polymeric materials in Europe

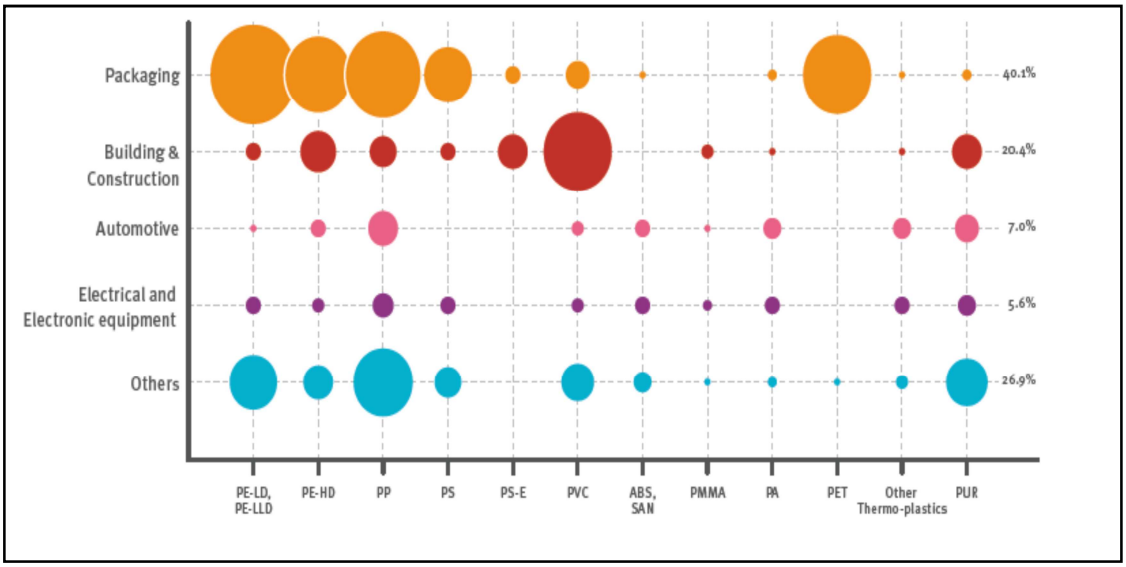

Figure 4: % of plastics used in different fields

1.1 BIOPLASTICS

In the last decade the attention in plastic sector has been facing an issue that was initially non considered, or however underestimated: the environmental impact of plastics derived from petroleum.

The non-degradation of petroleum based polymers is the source of many problems that can greatly influence the future development; the need for a lot of space for collection and disposal, the risk of soil pollution and the development of gas pollutants during the incineration process are factors that must be taken into account, considering the increasing use of plastics. It is true that only 1% each year (22 million tons!) of the total waste produced in Europe is represented by plastic, but the need to find solutions or alternatives reducing the environmental impact is pressing since plastics remain in the environment for a very long time. It is necessary to use the principle of 4R (Reduce, Reuse, Recover, Recycle) to try to transform plastic waste in a resource, but this is not enough to address in a valid way the problem of disposal.

The best solution in the long term is therefore the introduction of biodegradable polymers, whose use must still be synergistic with recovery and recycling to be truly effective; although studied and tested for decades, the use of bioplastics was limited to the medical field as carrier of drugs, support for surgery, tissue engineering, because of their high cost requiring an use in areas that can generate high added values.

In recent years, these biodegradable materials are gaining more and more importance in the market as possible substitutes for conventional plastics due to the possibility to have biodegradables products (degradation either natural or promoted by bacteria) at the end of their life resulting in byproducts that are unharmful or even useful for the environment.

In the next future, bioplastics may also offer economic advantages: the rising price of oil also affects all products connected to it, including derivatives used for the production of traditional plastics so greatly affected by the constant fluctuations in the cost of crude oil recorded because of the many international events in recent years.

The possible applications of bioplastics are many and affect different sectors, both for mass markets (such as packaging or fibers for the textile industry) and niche (such as medical products and engineering applications of special areas where they are already widely used for).

The research, both academic and industrial, is oriented in this direction, but a long and intensive work of research and development is still necessary, considering both the need to verify all structural and environmental conditions that allow the relatively rapid biodegradation of a this plastics and the need to ensure all the physical and mechanical properties essential for the practical use of biodegradable materials in all applications where conventional petroleum based polymers should be replaced.

A material can be defined "bio" if its carbon atoms derive, at least partially, from biological source; the "bio" carbon content is defined as the amount of bio-carbon in bio-plastics, expressed as a fraction or percentage weight by weight of the total amount of carbon present in the plastic material (ASTM D6866).

The concept of biodegradability and organic material are often used incorrectly: it is important to underline that a bioplastic is not necessarily a biodegradable material, as well as a biodegradable polymer is not necessarily a biopolymer. To better understand what is meant by biodegradable material it can be useful to observe the diagram in Figure 5.

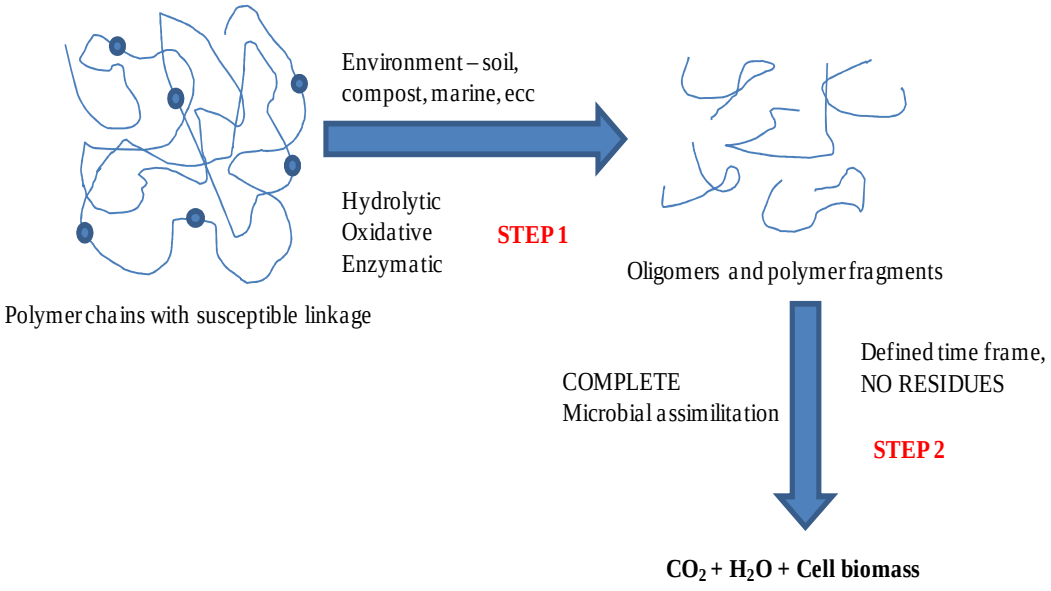

Figure 5: Biodegradation process

The biodegradation process is divided into two phases: the first one is the fragmentation of polymer chains in specific disposal environment, through mechanisms that do not necessarily require the action of enzymes (hydrolytic, oxidative); in the second step the oligomers and low molecular species are converted into water, carbon dioxide and food for microorganisms, without leaving any residue.

It is therefore essential, in order to define a plastic as biodegradable, that the process of biodegradation leads to disappearance of **all** fragments in a **precise time** and in a **specific disposal environment**.
International organizations such as ASTM, ISR, ISO, UNI are actively involved in the definitions and tests to evaluate the biodegradability and compostability of a polymeric material in different environments.
Currently there is still no comprehensive definition, but all existing classifications correlate biodegradability for a specific environment and to a definite test to simulate that environment.
The European standard EN 13432 (ASTM D6400) of 2002, also adopted in Italy under the name of UNI EN 13432, is a rule relating to the characteristics that a material must have to be classified as a biodegradable or compostable:

- Biodegradability; determined by measuring the actual metabolic conversion of the compostable material into carbon dioxide. This property is quantitatively measured using test method EN 14046, the level of acceptance is 90% to be reached in less than 6 months.
- Fragmentation; fragmentation and loss of visibility in the final compost (absence of visual contamination). Measured with a pilot-scale or real composting test (EN 14045). The test material must be degraded, together with organic waste within twelve weeks (3 months). At the end the compost is sieved with a sieve of 2 mm. The residues of test material larger than 2 mm are considered as not having disintegrated. This fraction must be less than 10% of the initial mass.
- No adverse effects on the composting process.
- Low levels of contamination by heavy metals and no adverse effects on the quality of compost.
- Other chemical and physical parameters should not differ from standard compost after the degradation: pH, salinity, volatile solids, N, P, Mg, K.

The biopolymers can be divided into three main groups depending on the production method with which they can be obtained from figure 6:

- polymers from natural sources, used as such or modified (for example, starch or cellulose polymers);
- polymers synthesized from monomers obtained by fermentation (eg PLA, PHA, PHB);
- polymers obtained from fossil monomers that may be demolished by microorganisms.

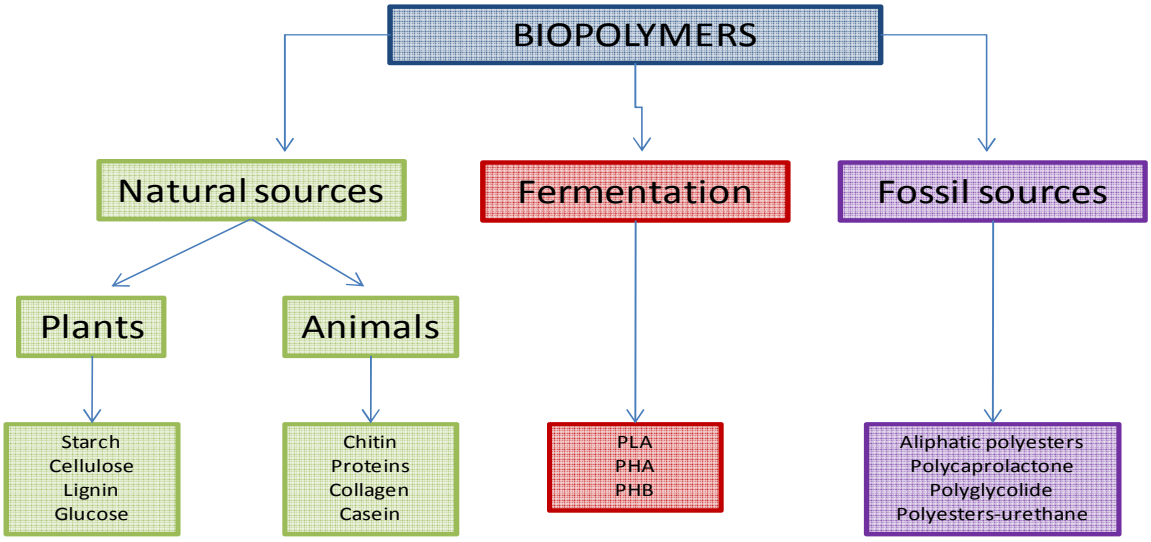

Figure 6: Biopolymers classification

This last category includes biodegradable polymers from non-renewable sources, a series of synthetic materials derived from petroleum such as aliphatic polyesters, aliphatic-aromatic copolyesters, polyester-amides and polyester-urethanes. For most of these materials the primary attack in the mechanism of degradation is a process of hydrolysis, which cleaves the ester bonds, amide or urethane of the polymer without the involvement of enzymes (Figure 5). The aliphatic polyesters are certainly the most widely used class of polymers, easy to synthesize, stable in many environments, but highly biodegradable. Within this class we find a series of condensation polymers derived from the synthesis of diols (ethylene glycol, butane diol, etc..) and acid (adipic acid, succinic acid, etc..).

It is important to note that only some of petroleum based polymers are biodegradable, and that the use of degradable additives does not confer "biodegradability" to non-biodegradable materials because the polymer can’t be consumed by microorganisms.

Similarly not all biopolymers are biodegradable: for example, polyester made from soybean oil is not biodegradable because it is not destroyed by microorganisms even if it comes from a natural source (figure 7).

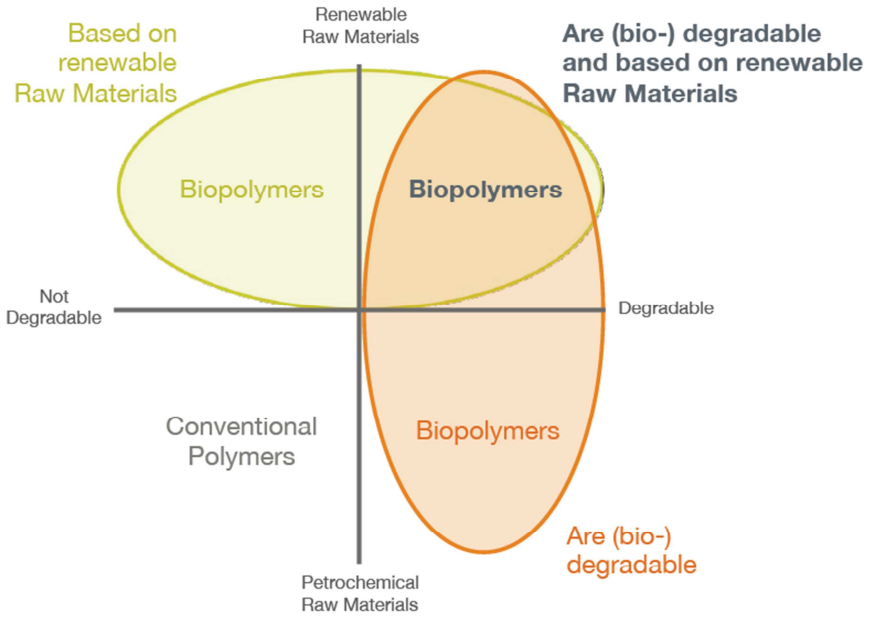

Figure 7: material coordinate system for bioplastics

1.2 POLYLACTIC ACID (PLA)

In this scenario, studies (both academic and industrial) have been focused on one polymer in particular: polylactic acid (PLA), that was discovered for the first time in 1932 by Carothers (DuPont) which obtained low molecular weight species by heating lactic acid under vacuum.
PLA belongs to the family of α-hydroxy acids, is considered biodegradable and compostable and can be obtained from renewable natural sources.
The monomer unit of the PLA is lactic acid (2-hydroxy propionic acid); its carbon atom between the carboxyl group and the hydroxyl function is chiral and therefore allows to obtain different stereoisomeric structures (isotactic polymer chains, syndiotactic or atactic) depending on the configuration of the methyl during the propagation of the polymer chain (figure 8).

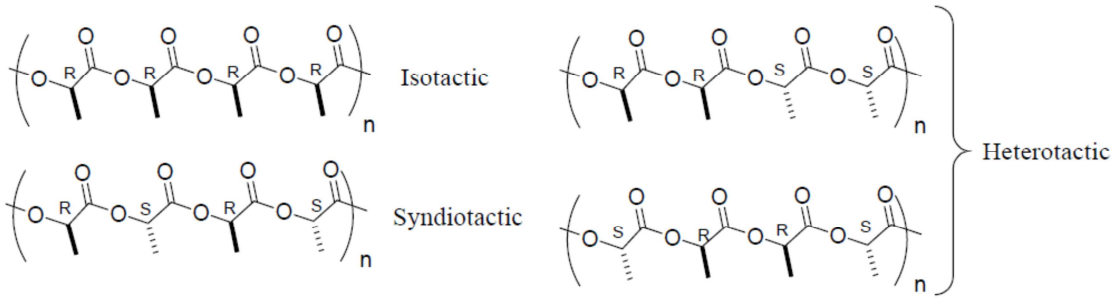

Figure 8: Microstructure of PLA

The microstructure also strongly affects the properties of the material: it is possible to obtain completely amorphous polymer with a Tg between 50 °C and 60 °C, as well as semi-crystalline polymers with melting points between 160 °C and 180 °C.
Initially the use of PLA were confined to the biomedical field (suture[1], drug delivery systems[2], tissue engineering, orthopedics): this was due not only to the high biocompatibility of this polymer with the organism and the ease with which it is absorbed by human organism, but also to the high cost and poor availability on the market, factors that made him a material for applications with high added value.
The cost of PLA is lower than other biopolymers; the increase in interest around the PLA improves the technology of production[3,4], and this fact, with some interesting mechanical properties, makes this polymer attractive as a possible substitute for traditional materials in applications such as food packaging, packaging, bottles, fibers[5-9]. Increasing the production volumes also costs decreases.

PLA is certainly the most promising and interesting biodegradable polymer for large scale applications for which could be assumed a gradual and progressive replacement of traditional materials coming from hydrocarbon. But there are many aspects such as thermal resistance, impact resistance, gas barrier properties that need to be improved because, at present, are lower than those of traditional polymers.

1.3 GOALS OF THE RESEARCH

The objective of this research is the synthesis and the study of the properties of new biocompatible polymeric materials based on PLA, focusing the attention on to two main aspects that may have an effect on the final properties of the polymer:

I. The control of the molecular architecture through the use of appropriate chain regulators able to modify the macromolecular structure.

II. The use of nanoparticles used as such or modified on the surface, added to the polymer matrix.

I.

The importance of changing the molecular architecture of a polymer through the synthesis of complex structures (tree, star, tree-star) is confirmed by the large number of studies in recent years both in academic and industrial field. Complex macromolecular architectures gives to the materials properties (for example low melt viscosity, shear sensitivity) that allows to increase the fields of applications of traditional polymers without changing the transformation processes and without increasing the cost of the final product. Through the modulation of feed, varying the type of regulator chain used or the ratio between two different regulators, it is possible to change the amount and the type of macromolecular species and consequently modulate the properties of the final material.

Star and tree structures of polyamide 6 are an exemplary case, having been the subject of patents and industrial processes used for advanced applications[10].

II.

The use of micrometer-sized mineral fillers added in compounding or, less frequently, in situ polymerization is a very common practice in the polymer industry because it allows to obtain materials with improved properties and lower cost.

The use of traditional micrometric fillers, however, has some disadvantages, such as the lack of dispersion in the polymer having the non homogeneity of the material together with low surface area which requires the use of large amounts of filler in order to have improvements of mechanical properties (i.e. tensile moduls, izod, etc).

In the last years the interest in the field of fillers for polymeric materials has progressively shifted towards the study of systems having very low particle sizes (less than one hundred nanometers) that, given their dimensions, are called nanoparticles.

Among the many features that make this type of mineral fillers interesting as additives for polymeric materials there is certainly their high specific surface area (which can exceed 700 m^2/g), which results in excellent interfacial interaction between polymer and nanoparticles, and consequently, considerable variation in physico-mechanical properties of materials containing them; for this reason even small amounts of nanoparticles dispersed in the polymer matrix can interact giving to the material properties different from the ones of the neat polymer, thus opening the field to new possible industrial applications.

It is therefore clear that the use of nanoparticles as additives in polymer materials is a topic extremely attractive for the features that the systems formed by polymeric matrix and nanofillers could potentially acquire.

The possibility to obtain very interesting variations in the properties of the material even with low percentages of nanofillers allows the preparation of products (such as packaging films or fibers) that cannot be obtained using the traditional micrometer-sized fillers.

For this work have been used a natural nano-sized inorganic clays (montomorillonite) and nanosilica.

A system of surface modification of nanoparticles has been also developed by using the organosilanes as coupling agents in order to modify the interaction between polymer matrix and mineral filler; the use of surface modified mineral fillers can solve, or reduce the problem of the repulsion between the organic phase (polymer) and the mineral phase (nanoparticle) but can also lead to a variation of material properties, depending on the surface modification of the particles is made using silane presenting or not functional reactive groups that are able to react with the polymer matrix or with the monomer during the polymerization reaction.

REFERENCES

[1] Lipinsky, E. S., Sinclair, R. G., *Chem. Eng. Prog.*, 82 (8), 1986, 26.

[2] Dechy-Cabaret, O., Martin-Vaca, B., Bourissou, D., *Chem. Rev.*, 104, 2004, 6147–6176.

[3] Naitove, M., *Plast. Technol.*, 44 (1), 1998, 13.

[4] Enomoto, K., Ajioka, M., Yamaguchi, A., *US Patent 5 310 865*, 1995.

Kashima, T., Kameoka, T., Ajioka, M., Yamaguchi, A., *US Patent 5 428 126*, 1995.

Ichikawa, F., Kobayashi, M., Ohta, M., Yoshida, Y., Obuchi, S., Itoh, H., *US Patent 5 440 008*, 1995.

Ohta, M., Yoshida, Y., Obuchi, S., Yoshida, Y., *US Patent 5 440 143*, 1995.

[5] Steinbuchel A, Doi Y, editors. Polyesters III—applications and commercial products. *Biopolymers*, vol. 4. Weinheim: Wiley-VCH; 2002.

[6] Lunt, J., *Polymer Degradation Stability* 59, 1998, 145.

[7] Edlund, U., Albertsson, A. C., *Adv. Polym. Sci.*, 157, 2002, 67–112.

[8] Drumright, R. E., Gruber, P. R., Henton, D. E., *Adv. Mater.*, 12, 2000, 1841–1846.

[9] Gross, R. A., Kalra, B., *Science*, 297, 2002, 803–807.

[10] Di Silvestro, G. et al., *WO9964496*, 1999.

2. *Raw materials, synthesis and general aspects about PLA*

2 RAW MATERIALS, SYNTHESIS AND GENARAL ASPECTS ABOUT PLA

2.1 LACTIC ACID

The monomer of PLA is lactic acid, isolated for the first time in 1780 by the swedish chemist Scheele from sour milk, and commercially produced in 1881[1]. It is present in many living beings in which it is the end product in the demolition of pyruvic acid under anaerobic conditions playing a basic role related to the energy supply to muscle tissues after an effort. Lactic acid, 2-hydroxy propionic acid ($C_3H_6O_3$), is the simplest of hydroxy acids, soluble in water and highly hygroscopic, it has a chiral center and exists in two enantiomeric forms L (+) and D (-); most of lactic acid is a naturally occurring dextrorotatory, while the D-enantiomer is very rare.

It can be produced industrially on a large scale through two different processes: a petrochemical one or a biotechnological one.

The petrochemical synthesis of lactic acid (2) starts from the acid hydrolysis of lactonitrile (1), a waste product which is obtained by the process of synthesis of acrylonitrile, according to the reactions shown in Scheme 1.

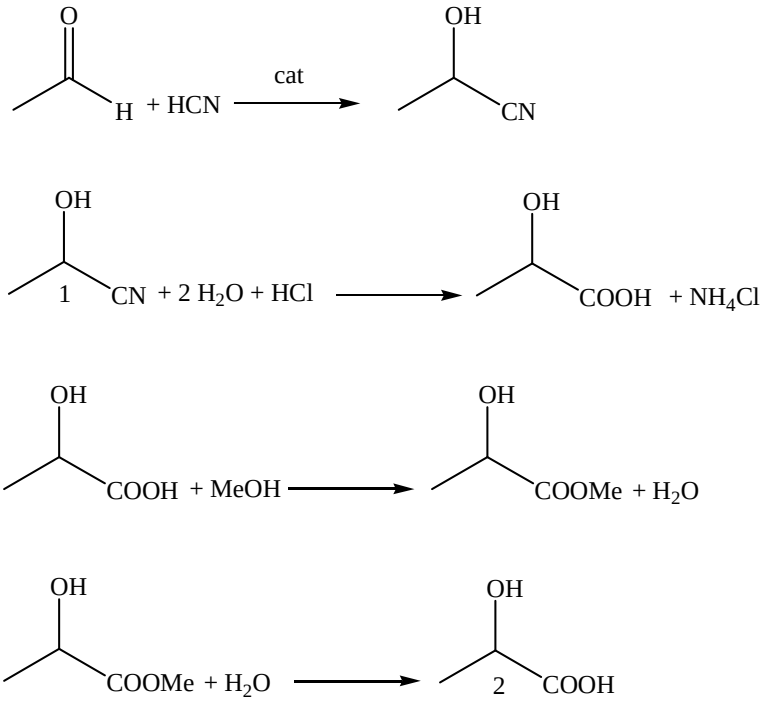

Scheme 1: The synthetic route to lactic acid monomer through lactonitrile

The chemical synthesis of lactic acid leads to a racemic mixture (50% L and 50% D); the two isomers can be separated only by the interaction with a third optically active molecule: this process involves a significant increase in the production cost of enantiomerically pure monomer.

The biotechnological method uses the bacterial fermentation of carbohydrates involving homolactic microorganisms (LAB), such as those belonging to the strain of Lactobacillus, that are able to produce only lactic acid in enantiomerically pure form (L)[1]; the possibility to obtain the monomer in enantiomerically pure form has very important consequences on the properties of the final material. The most widely used microorganisms are Lactobacillus amylophilus, L. bavaricus, L. casei, L. maltaromicus, and L. salivarius.

The raw materials from fermentation (carbohydrate) depend on the kind of microorganisms used in biotechnology process; in general a lot of simple sugars, by-products of agricultural processing, can be used. These sugars include glucose, maltose, dextrose (potato, corn, starch), sucrose (cane sugar, beet sugar), lactose (dairy products)[2].

Currently, 90% of L-lactic acid world production comes from fermentation process, the remaining part is produced synthetically; biotechnological production represents the only valid and competitive method compared to chemical ones, both from an economic point of view and environmental one, relying on a simpler process with lower costs, a wide availability of raw materials and a significant reduction of environmental impact.

Depending on the conditions in which the fermentation is conducted (temperature, pH, type of sugars selected as raw material) LAB can produce either only lactic acid (homofermentative process), or an equimolar mixture of lactic acid, carbon dioxide and ethanol or acetate (heterofermentative process) or a mixture of lactic acid, ethanol, acetate and formate (mixed acid fermentation)[3,4] as reported in figure 1.

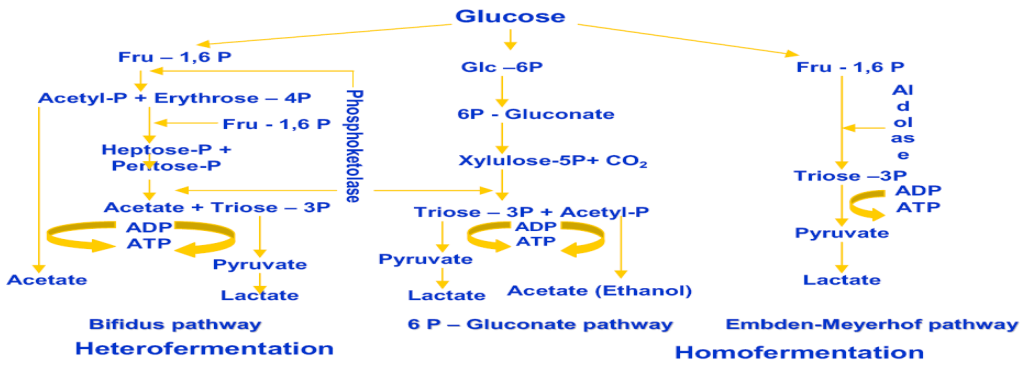

Figure 1: Fermentative process for the production of lactic acid

The homormentative method allows to obtain 1.8 moles of lactic acid per mole of hexose (conversion above 90%) like the heterofermentative method, but with a smaller amount of by-products. The homofermentative method represents therefore the main process adopted industrially, using a pH of 5.4 to 6.4, a temperature of 38-42 °C and low concentrations of oxygen[5].

In order to optimize the fermentation process is important to seek raw materials at low cost and good availability; concerning the source of carbon, the attention has focused on glucose and lactose, sugars readily available.

Among the various sources of nitrogen necessary for the overall process, yeast extract is definitely the best choice for microbial growth and for the production of lactic acid even if not very convenient from the economic point of view contributing over 30% of the total cost of lactic acid, suggesting the need for a cheaper alternative. Some attempts have been made to use other sources of nitrogen from industrial byproducts as growth factors to achieve a partial or complete replacement of yeast, but studies are currently not yet optimized.

However, the main obstacle to the development of the fermentation process is the nature of lactic acid bacteria that require a wide range of growth factors including aminoacids, vitamins, fatty acids, purines and pyrimidines necessary for their proliferation and for biological activity, which significantly raise the overall cost of process[6-9].

Industrially the fermentation is carried out in batch reactors from a 5 to 10% sugar solution which allows to obtain a production rate of about 2 grams of acid per liter of broth culture; to achieve the maximum efficiency of the process various method have been developed to extract lactic acid or neutralize it involving the use of calcium hydroxide or calcium carbonate in order to obtain a solution of calcium lactate which is then acidified to get the lactic acid. The lactic acid thus obtained has an enantiomeric purity of 98% but still contains many impurities such as organic residues, alcohols, acids, esters, making it unsuitable for the polymerization process. Purification process involves vacuum distillation followed by crystallization which allows to obtain lactic acid with a chemical purity higher than 99% and enantiomeric purity of 99.8% [10.11].

2.2 LACTIDE

The lactide, also named 3,6-Dimethyl-1,4-dioxan-2,5-dione ($C_6H_8O_4$), is a cyclic ester obtained by condensation of two molecules of lactic acid followed by dehydration, and exists in three stereoisomeric forms LL, DD and DL depending of the lactic acid isomer used to synthesize it (Figure 2).

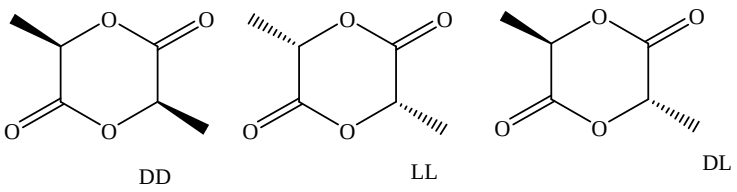

Figure 2: lactic acid isomers

The main method for its synthesis involves the depolymerization of the oligomers of lactic acid at high temperatures in the presence of catalysts (Figure 3).

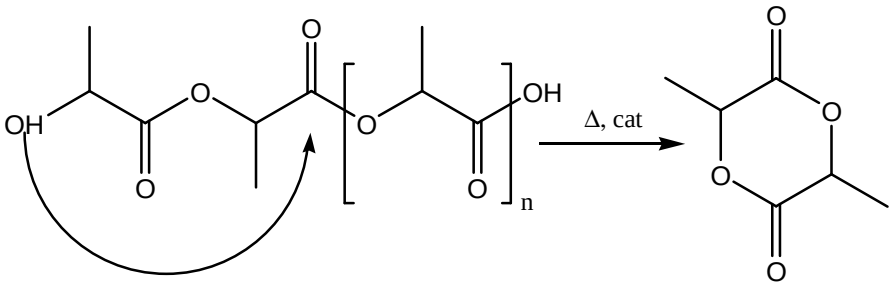

Figure 3: Production of lactide from lactic acid oligomer

Lactic acid is heated at a temperature below 180 °C under vacuum in order to promote the formation of a low molecular weight prepolymer. The oligomers thus obtained and the catalyst (tin octanoate) are heated to a temperature between 190 °C and 260 °C and allowed to react under vacuum. The lactide vapor formed is removed by distillation in order to shift the reaction equilibrium towards the formation of cyclic dimer. The lactide obtained, cooled and collected at a temperature between 60 and 90 °C, however contains a number of impurities which do not allow the immediate use in polymerization and that are removed through crystallization, extraction or distillation.

Several aspects of the synthesis of lactide, such as operating temperature, kind of catalyst, purification techniques were evaluated to identify the best operating conditions in order to optimize the production process by improving the separation between the cyclic dimer and the oligomers and the chemical and enantiomeric purity of the lactide[12-15].

2.3 SYNTHESIS OF PLA

There are two main methods for synthesizing PLA, depending if lactic acid is used as a starting monomer (direct polycondensation 1), or if lactide (ring-opening polymerization 2) is used, as shown in figure 4.

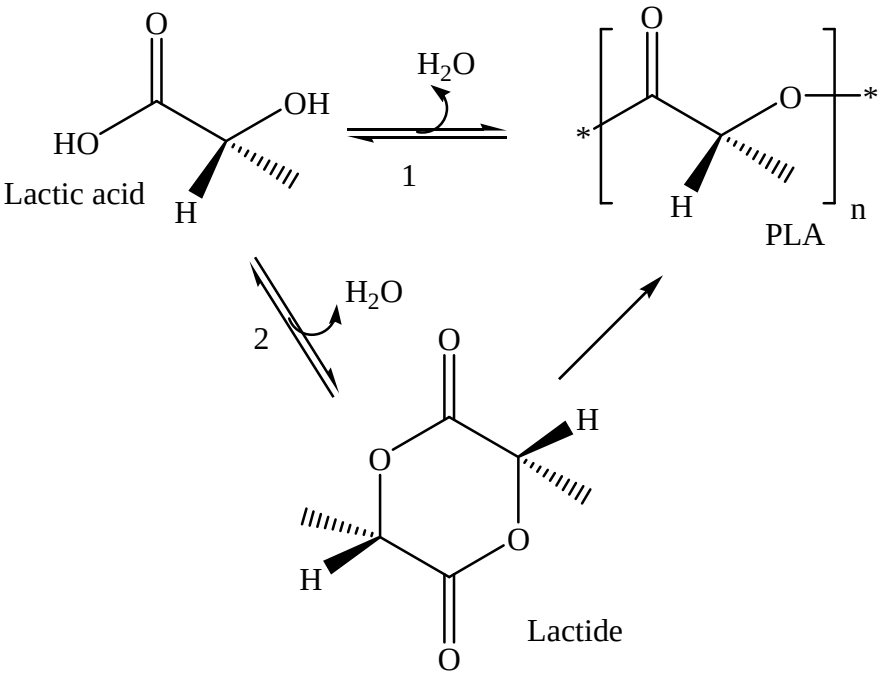

Figure 4: Polymerization routes to polylactic acid

Basing on the synthesis of the intermediate cyclic of lactic acid, lactide, NatureWorks LLC, the first worldwide company to produce PLA, has developed and patented a process for low-cost continuous production of polilactic acid[61]; the methodology combines the advantages, both economic and environmental, of synthesizing both lactide and PLA into a single bulk process rather than in solution, obtaining for the first time a commercial compostable product made from renewable resources.

The process begins with the condensation reaction of a lactic acid solution to produce a pre-polymer with low molecular weight. These oligomers are then converted into a mixture of stereoisomers of lactide using tin-based catalysts to increase the speed and selectivity of the reaction; the mixture thus obtained is purified by vacuum distillation. The process of production and purification of lactide is the phase that most contributes in raising the cost of synthesis due to the high degree of purity required to obtain high molecular weight PLA having good mechanical properties. The monomer thus obtained is polymerized by a ring-opening polymerization in bulk, totally eliminating the use of solvents. After the end of reaction, the residual monomer is removed under vacuum and recycled to be reused again (Figure 5).

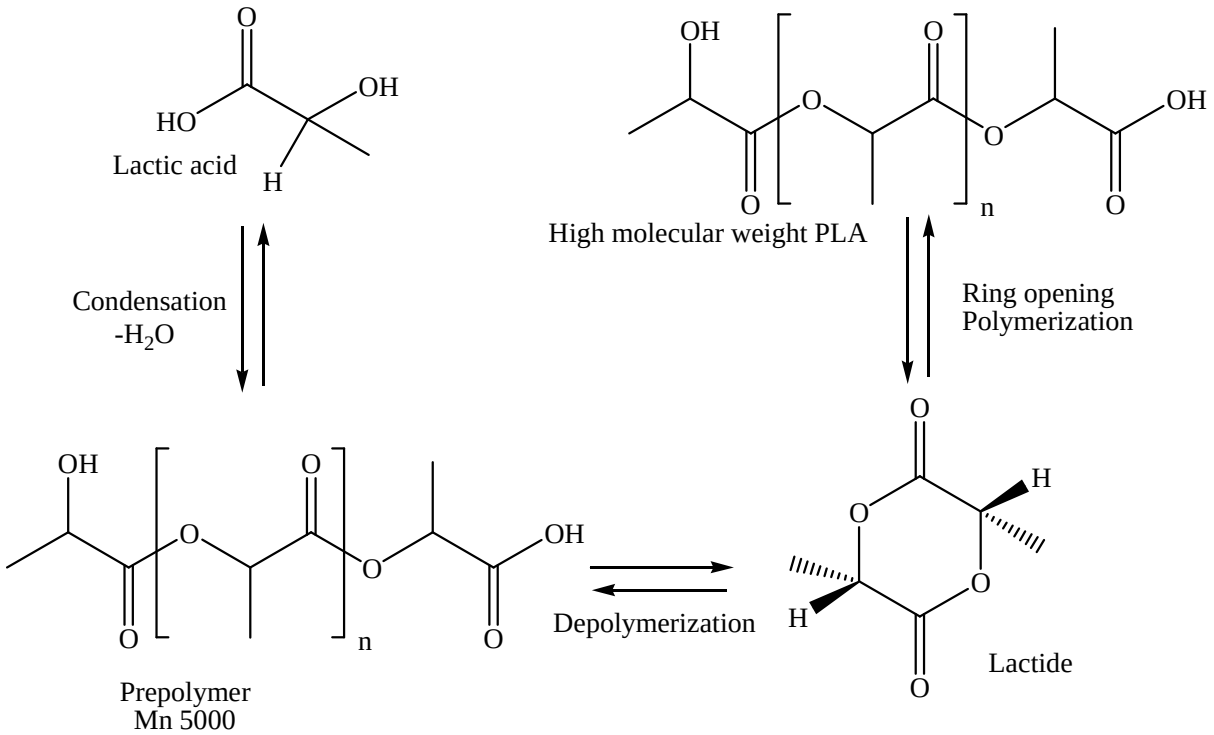

Figure 5: PLA production via prepolymer and lactide polymerization

This process is currently used for the production of PLA on a large scale in a plant located in Nebraska (USA) capable of producing 300 million tons/year; referring to data provided by different companies in 2009 there are currently several companies involved in the production of PLA through various synthetic methodologies: the main companies are listed in Table 1:

Company name/ location	Trade name	Production capacity (metric tons/year)	M_w (Da)	M_n (Da)	Process used
Nature Works (Cargill/Teijin)/ NB, USA	NatureWorks PLA (Eco PLA)	140,000	NA	$1.22x10^4$ (94% L-LA content)	Solvent free Melt PC/ROP
Toyota (Shimadzu Co.)/ Kyoto, Japan	LACTY™ 5000 LACTY™ 2012 Eco-plastic	>100	$2.89x10^5$ $1.6x10^5$	$1.7x10^5$ $1.883x10^5$ (100%L-LA content)	ROP
Dupont / USA	Medisorb	NA	$1.0x10^5$	NA	ROP
Purac plc. / Netherlands	Purasorb® PL	NA	$3.5x10^5$	$1.5x10^5$	ROP/ solution PC
Mitsui Chemicals Co./ Japan	LACEA	500	NA	NA	Solution PC
Birmingham Polymers/ AL. USA	LACTEL	NA	NA	NA	NA
Toyobo/ Japan	Vyloecol	NA	$43x10^3$	NA	NA
Hisun Biomaterials Co. Ltd. / China	REVODE	5,000	NA	$70x10^3$	NA

Table 3: PLA producers

In addition to these companies, which satisfy most of the world demand for PLA, there are other producers, such as Kanebo Limited Gohsen/Australia (Lactron), Kaneka Corporation/Japan/USA (Kanepearl PLA foam), Toyota Motor Corporation/USA (Toyota Ecoplastics U'z series), and others that however produce smaller quantities of polylactic acid.
As can be seen from the table, most of the processes are based on ROP of lactide, sometimes used in combination with the polycondensation of lactic acid.

2.3.1 Polycondensation of lactic acid

The direct polymerization starting from lactic acid proceeds through the elimination of water by condensation. This is an intermolecular esterification reaction between hydroxyl and carboxyl groups of lactic acid catalyzed by acid species, in particular Lewis acids and protic acids.

In the literature there are several studies to identify the most efficient catalytic system to synthesize an high molecular weight polymer[22-24] limiting the racemization of the system; tin-based catalysts are the most used catalytic system because they allow to obtain high molecular weights in short reaction times.

However, it has been shown that a catalytic system consisting of a binary metallic compounds activated by an acidic species is much more efficient than the system composed by a single metal[21].

Moon and coworkers[21] have suggested a mechanism (Scheme 2) to explain the combined action of the metal catalyst and protic acid, which in the example is indicated by the acronym TSA. The end groups of PLA form a coordinated bond with the catalytic metal center (Sn II) of the species (2) obtained by elimination of HCl from tin chloride dihydrate.

The hydroxyl and carboxyl groups present in PLA promote dehydration and the formation of Sn-OH species (3). The amount of hydroxyl and carboxyl terminal decreases increasing the molecular weight and when it is enough high, the center of coordination of the catalyst is not occupied by end groups (3); the hole that is created promotes side reactions, especially the formation of lactide, causing racemization and coloration of the polymer.

These two undesirable phenomena are related to reaction temperature, curing time, type of catalyst and change not only the surface of the polymer (the material could be yellow, brown, black) but also the material properties that are related to the microstructure; the presence of protic acid considerably lowers the change of color and increases the rate of growth of the polymer chain by acting as a ligand for the catalytic site (4) and (5): it is not involved in the process of esterification, and therefore it can occupy the free coordination site preventing side reactions.

Moreover, the presence of a strong acid promotes the dehydration process of compound 3 to give compound 5 via intermediate 4 as shown in scheme 2.

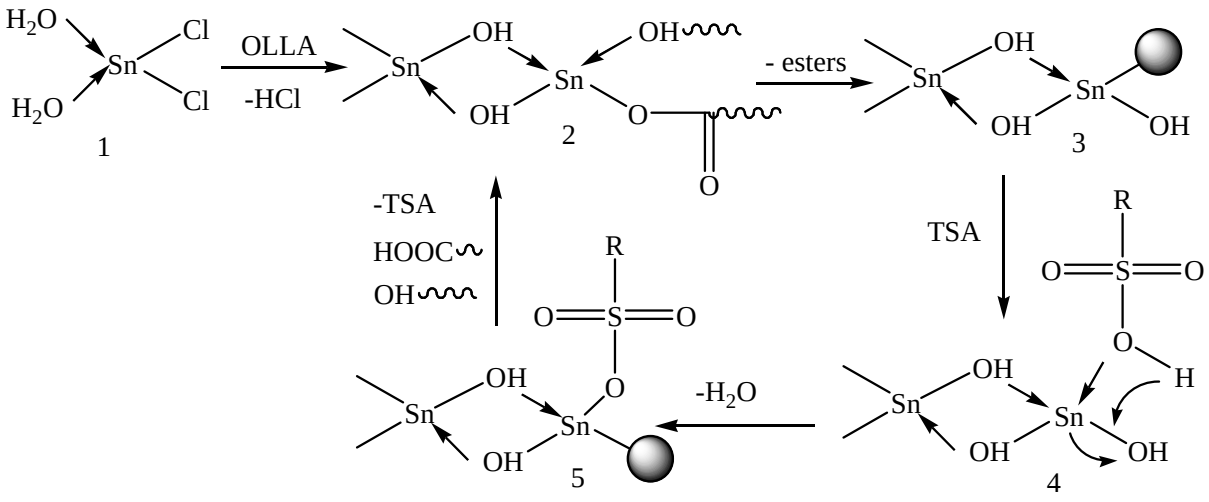

Scheme 2: Hypothetical condensation mechanism by the action of the Sn(II) and Sn(II)–TSA systems

The amount of protic acid should be equimolar respect to the catalyst to avoid deactivation of the catalytic system that would occur in case of an excessive use of TSA; the deactivation is probably due to the decrease in the number of vacant sites available for coordination of the polymer chains because these sites are occupied by the acid.

Polycondensation of lactic acid is an esterification reaction and therefore proceeds, as occurs in all these kind of reactions, with the formation of an equilibrium (Figure 6) in which water produced must be removed from the reaction system in order to shift the equilibrium of the polycondensation towards the formation of the polymer.

For this purpose it is necessary to operate in vacuum between 120 °C and 175 °C. Under these conditions, water produced by the process can be distilled increasing the speed and the conversion of the reaction. However, the establishment of an equilibrium between free lactic acid, water and the polymer formed, together with the intrinsic polarity of the system, makes it difficult to completely remove water, thus limiting the growth of the polymer chain; with this methodology polymers with a low molecular weight are obtained, brittle, that can not be used in any application requiring good mechanical properties. In addition, polymerization reaction is in competition with the formation of lactide and it is important to minimize the latter because it is not possible to eliminate it.

Lactide, as well as lactic acid and low molecular weight species, is volatile in the reaction conditions under vacuum and this factor causes the loss of too much material.

To overcome this problem is necessary to provide the reactor with a reflux system in order to bring the lactide and low molecular weight species that evaporate in the boiler, shifting the equilibrium towards the formation of the polymer. Reflux can be accomplished in two ways: with a special heated distillation column, or using some solvent in the reaction mixture. The heated distillation column must be maintained at a temperature allowing condensation of lactide and low molecular weight species that should fall back into the boiler of reaction without crystallizing.

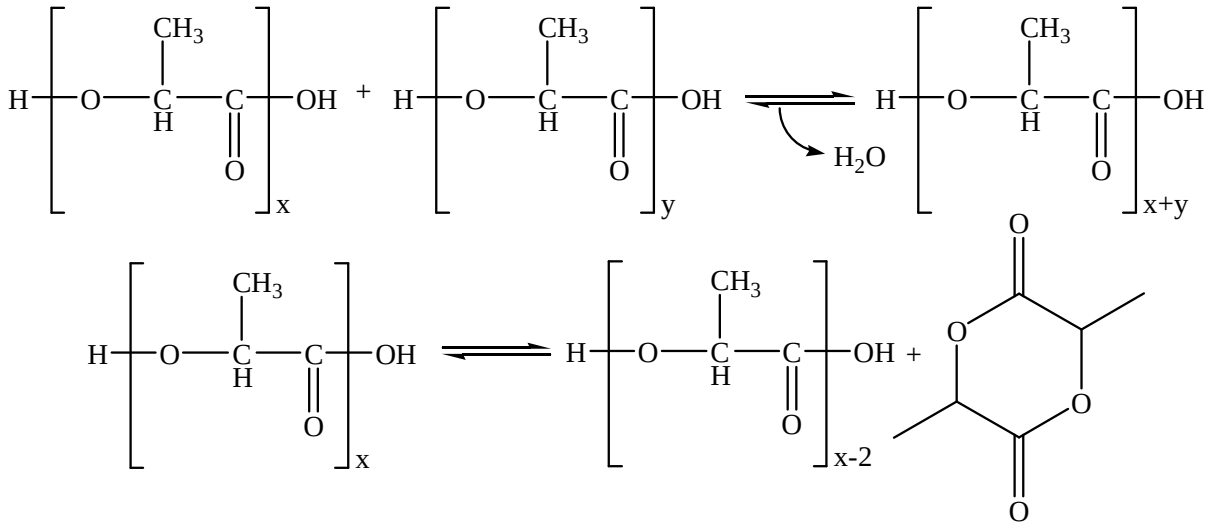

Figure 6: Two reaction equilibria involved in polycondensation

The equilibrium between water and lactic acid may be modified by working in the presence of an organic solvent[16,17] that can dissolve the low molecular weight species and lactide having boiling temperature in vacuum similar to the one of lactide (146 °C at 10 mmHg).

To obtain a polymer with a high molecular weight and better mechanical properties it is possible to use a multifunctional agent in order to obtain hydroxy-terminated species, linear or star shaped - depending on the number of functional groups of the agent used - that are able to react with diisocyanates in a chain extension process giving a polymer with high molecular weight values[18,19].

With all these precautions the process of obtaining PLA from lactic acid can greatly improve, but there are still several drawbacks that limit the use of this synthetic route: the polymers obtained are brittle, polymers have too low molecular weight values to be processed and used in various applications of interest. Furthermore, the time required for the polymerization is still very long for a possible application on an industrial scale.

There are also several issues related to the need to evaporate and recover any solvent used for the polymerization, to the coloration of the polymer and an to an increase tendency to racemization, as observed by Carothers in 1932[20]; for all these problems several studies are required before producing PLA on a large scale with the condensation process.

2.3.2 Ring Opening Polymerization (ROP)

The ring-opening polymerization (ROP) of lactones and lactide is the most widely used synthetic route for the synthesis of aliphatic polyesters with an high control of the macromolecular structure and of the values of molecular masses and distribution.

The growing interest about this kind of material, mainly due to their biodegradability, has stimulated a lot of studies about this polymerization process with a particular interest on reaction mechanism, characteristics of monomers, type of initiators and catalysts[25-29].

The control of polymerization reactions is possible only working in a very strict reaction conditions, taking into account not only the thermodynamic aspects associated with the mechanisms of ring opening, but also the choice of solvent, reaction temperature, onset of equilibrium, amount and the type of catalysts that act on the kinetics of reaction, the initiators that are responsible for controlling the molecular weight and finally time of polymerization.

The key factor that determines whether a cyclic ester can be converted into the corresponding linear polymer or not is the thermodynamic stability of the cyclic structure compared to the one of the polymer. Table 2 shows the values of enthalpy, entropy and free energy for the conversion of cycloalkanes to the corresponding linear polymers; as shown, polymerization is thermodynamically favored for all cycles except for 6 atoms ones.

The order of reactivity for the other cycles is 3, 4> 8> 5, 7 and it is related to the tension deriving from bond angles of cyclic structures and to their spatial conformation.

$(CH_2)_n$ n	ΔH_{lc} (kJ/mol)	ΔS_{lc} (J/mol-°C)	ΔG_{lc} (kJ/mol)
3	-113.0	-69.1	-92.5
4	-105.1	-55.3	-90.0
5	-21.2	-42.7	-9.2
6	+2.9	-10.5	+5.9
7	-21.8	-15.9	-16.3
8	-34.8	-3.3	-34.3

Table 2: Thermodynamics of polymerization of cycloalkanes at 25°C

ΔH is the key factor affecting ΔG for rings with three and four atoms, while ΔS is more relevant for systems having 5 and 6 atoms; for larger rings the contribution of ΔH and ΔS is comparable. If both values are negative, an increase in temperature leads to an increase in the values of ΔG: above a certain value of temperature the free energy is positive and therefore the polymerization reaction is less favored.

For all kind of structures the presence of substituents on the ring leads to a decrease in reactivity. The concept can therefore be also applied to the polymerization of lactones: the larger the ring, the lower the reactivity for the polymerization process[30].

Polymerization of cyclic esters is usually carried out in solution (THF, toluene, dioxane) or in bulk, but it is also possible to operate in suspension and emulsion: the choice of solvent is very important and is not only related to the solubility of reagents and products, but also to the polarity and solvation power, aspects that can affect the rate of polymerization[31]. Temperature is another key parameter, since it should be closely monitored to avoid intra and intermolecular side reactions (trans-esterification, backbiting); usually bulk polymerizations are conducted at temperatures between 100 °C and 150 °C, while for solution reactions temperatures are lower and linked to the type of solvent chosen.

Dubois and coworkers[32] observed that polymerization of lactide in toluene at 75 °C under strict control proceeds without any side reactions, while increasing the temperature of 10 °C there is an increase of the polydispersity of the system due to backbiting reactions.

As mentioned previously, only few cyclic compounds are able to polymerize spontaneously, most of them requires an initiator or a catalyst promoting the ring opening reaction.

Organometallic compounds based on tin[33], aluminum[34], zinc[35] (oxides, carboxylates, alkoxides) and rare earth[36] elements are among the most widely used catalysts for the ROP of lactones; the type of initiator used will affect also the mechanism of ring opening, which can be carbocationic, anionic or via “insertion and coordination”: the last two are the ones that allow to obtain polyesters with high molecular weight and lower values of racemization.

Organometallic catalysts can generate a problem for the use of these polymers in areas such as biomedical or pharmaceutical because these are fields that require high purity of the materials and the absence of toxic pollutants: for this reason the removal of the catalytic species is necessary when the catalyst used is not compatible with biological systems.

Over the past ten years several number of researches has been done to develop new catalytic systems that are able to promote the enzymatic ROP of cyclic esters[37,38] and overcome the toxicity of metal systems; the interest for these catalytic systems is considerable also because it is possible to work in milder conditions and with greater control of stereochemistry (and often the catalyst could be recycled) but so far the polymers obtained with these catalysts don't have molecular weight values comparable with those of polyesters synthesized with the classical catalytic systems.

The initiators for the anionic ring opening polymerization of cyclic esters are alkali metals, alkali metal oxides, metal complexes with crown ethers; depending on the reaction conditions, the type of monomer and the initiator used, the polymerization can proceed with a living mechanism or with controlled mechanism[42]. The reaction is promoted by the attack of negative charge of the nucleophilic initiator on the carbonyl carbon or on the alkyl carbon bonded to the oxygen, depending on the type of initiator used, and leads to the formation of a linear polyester; the polymerization then proceeds through a new attack on one of the two terminal carbons forming alkoxylated terminal groups or carboxylates terminal groups (Scheme 3).

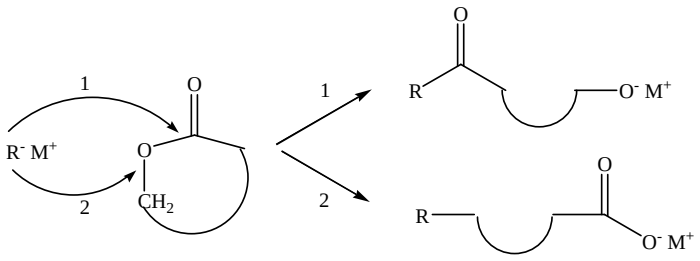

Scheme 3: Initiation of Ring-opening Polymerization of Lactones

Polymerization initiated by weak bases proceeds through mechanism 2, and then carboxylate ions are the propagating species; on the contrary, using a strong base the most common mechanism is the number 1, in which alcoholate is the species that promotes the reaction, although both mechanisms may occur. Carboxylates and alkoxides of some metals with free "d" orbitals, such as aluminum and tin, are very efficient initiators able to promote the ROP through a mechanism of coordination and insertion (Scheme 4).

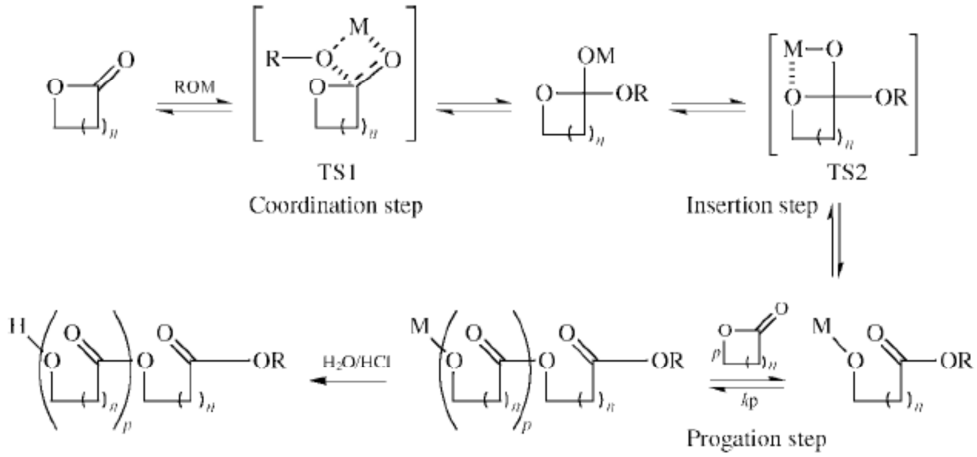

Scheme 4: The coordination–insertion mechanism for ROP of lactones and lactides

The first step of the reaction is the coordination of the catalytic species (ROM species in scheme 4) to the carbonyl of the monomer; the attack breaks the acyl carbon-oxygen bond with the simultaneous insertion of the metal species[39,40]. The energy of each transition state (TS1 and TS2), together with the steric and electronic properties of the monomer, determine which is the kinetic determinant state between the coordination and the insertion[41] mechanism.

The reactivity of the initiator also depends on the combination of steric and electronic properties; in general carboxylates are weaker nucleophiles than alkoxides and therefore tend to act more as catalysts rather than real initiators of the reaction. For this reason they are often used in the presence of species with a free proton, typically an alcohol, which acts as an initiator.

The use of these organometallic catalysts in the ROP conducted at high temperatures or for long reaction times leads to intra-and intermolecular reactions of trans esterification causing an increase in the polydispersity of the polyesters.

2.3.3 Ring Opening Polymerizatio of Lactide

The reaction of ring-opening polymerization is the synthesis that is commonly used, even industrially, for the production of high molecular weight PLA.

Among intiators and catalysts used in the ROP, compounds based on tin (II and IV) oxides and carboxylated, and especially tin 2-ethylhexanoate [tin octanoate Sn $(Oct)_2$] are those that are more frequently used in the polymerization of lactones, thanks to their versatility, ease of use and excellent solubility in lactones and lactide; moreover the Food and Drug Administration approved tin octanoate as an additive that can be used in substances that are food contact. It is one of those catalysts that, as mentioned above, must be activated *in situ* with substances having a mobile hydrogen; in particular a large variety of compounds with hydroxyl functionality were investigated in literature[32,43,44]. If these substances are not added, impurities can act as initiators (for example humidity).

Molecular weight of the polymer can be easily controlled by varying the amount of species with OH groups included in the feed. The mechanism of polymerization with this catalyst system is quite complex and there are several works in the literature in which it is represented[44-47]. The activated monomer mechanism involves the coordination of the monomer with the catalyst to activate it, then the polymerization proceeds through the nucleophilic attack of the hydroxyl group of the initiator with the insertion of the monomer in the metal-oxygen bond, promoted by electronic rearrangement. The hydroxyl group of the added monomer, coordinated with tin atom will keep the catalyst active for the propagation of the chain. The reaction ends after hydrolysis with formation of a terminal hydroxyl group.

An alternative mechanism involves the formation of a complex between alcohol and $Sn(Oct)_2$ before the polymerization; the complex obtained promotes the opening of lactide (Scheme 5).

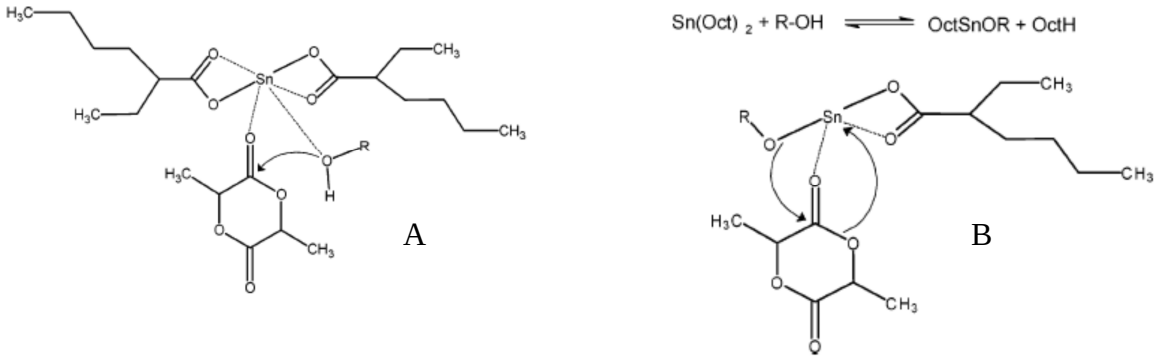

Scheme 7: Activated Monomer Mechanism for ROP of Lactide (A) and Tin Alkoxide Complex Initiated Polymerization of Lactide (B)

The use of tin octanoate allows to obtain high molecular weight polymers with conversions above 90% and with levels of racemization lower than 1% as reported in literature by Kricheldorf and Serra[48].

The polymerization is first order respect to the lactide and the catalyst; the nucleophilic attack of the complex between tin and alcohol to the carbonyl carbon of the monomer is kinetically determining in the ROP of lactide.

At the polymerization temperature, the formation of octanoic acid coming from the dissociation of the ligand during the propagation phase may disrupt the coordination of the monomer and inhibit or slow down the process of birth and propagation of the reactive species.

The kinetics of reaction can be accelerated increasing the amount of alcoholic initiator or using a larger amount of catalyst: in the first case, however, the increase of initiator further adjusts the length of the macromolecular chains, lowering the molecular weight that is closely related to [monomer]/[OH groups] ratio, whereas in the latter case, increasing the percentage of catalyst accelerates side reactions in addition to promoting the coloration of the polymer.

The study of the ROP of lactide, especially in academia, is not only limited to the use of tin octanoate as a catalyst, but several other compounds have been tested evaluating the ability to promote the opening of the lactide. Examples of polymerization of meso lactide in the presence of aluminum alkoxides or zinc-based complexes are presented in literature[49-51]; complex structure (M(AcAc)n, M = Nd, Y, Zn, Zn, Fe, Co, Ni) promote the polymerization of meso lactide with a conversion close to 99% for all tested metals[52]. Dubois and colleagues have conducted a lot of studies on the polymerization of lactide in the presence of aluminum isopropoxide confirming the insertion and coordination mechanism similar to what occurs in the presence of $Sn(Oct)_2$ and with a strong control on the molecular masses and on the values of polydispersity[32,53].

Compounds such as lanthanum and yittrio have been studied by McLain[54], Feijan[55]: they show that these metals work with a mechanism of coordination and insertion very similar, promoting the polymerization of lactide with a reaction rate that is much higher than the one observed in the presence of catalysts based on Al and Sn.

Recent developments in the field of catalysis for the polymerization of lactide are focused on the use of systems such as metal-free organic catalysts or enzymes catalysts. Hedrick and colleagues were the first to report the use of -(dimetilammino) pyridine (DMAP) in the polymerization of lactide[56]; the use of organic catalysts or enzymes represents an attractive and cheaper alternative for the ROP of lactide especially for applications that do not allow the use of metals.

2.4 SOLID STATE POLYMERIZATION (SSP)

A relatively small amount of literature, including patents, is available about the post-polycondensation of PLA[57-59], but considering also the information on other classes of polymers such as polyamides or polyesters like PET, this technique appears to be effective not only for the synthesis of PLA starting from oligomers, but also for the increase of molecular weight and the removal of residual monomer or low molecular weight species.

This is a very simple process, easy to do, that involves both physical and chemical aspects being controlled by three different parameters: mobility of the chains in the amorphous phase, reaction kinetics and removal of volatile products to shift the equilibrium of the process.

The polymer is heated to a temperature above the glass transition temperatures but below the melting temperature, in order to increase the mobility of the chains and promote the reaction between the end groups in the presence of a catalyst that can be the same used during polymerization. The removal of by-products using vacuum or strong flow of inert gas is necessary to promote the process. The SSP involves the amorphous region of the polymer where the reactive groups are present; since it operates at temperatures lower than the ones of bulk polymerization, and also considering the reduced mobility of terminal reactive groups, the time required to obtain high molecular weight species can be very long[60].

Although the reaction time is high, molecular masses obtained with the SSP are not obtainable through the process in bulk or in solution, due to the high viscosity of the system and the arising of hydrolytic and oxidative degradation phenomena.

The technique is mainly used to increase the molecular weights of PLA obtained by polycondensation of lactic acid, while in the case of ROP the SSP can be used to eliminate the residual monomer.

2.5 PLA PROPERTIES

Thermal and mechanical properties, and biodegradability of PLA are closely related to the molecular weight and the ratio of L and D isomers of lactic acid and their distribution within the polymer chain[62], as well as glass transition temperature and melting temperature.

The PLA can be either amorphous or semi-crystalline, depending on the stereochemistry of the units present in the chain and on its thermal history.

The ability to control the stereochemistry of the polymer allows to have a very accurate control of speed and degree of crystallinity, the basic parameters for the control of material properties, as well as the processability of the polymer. An high content of L-isomer produces a PLA with high crystalline content, while levels of D-isomer higher than 15% lead to the formation of an amorphous polymer; it is preferable to have high crystalline content of PLA to obtain materials with good properties.

The use of meso-lactide, or a mixture of D and L lactide forms the atactic PDLLA, fully amorphous, with properties different from those of PLLA and PDLA, which are semicrystalline.

For the amorphous PLA, glass transition temperature (Tg) determines the upper limit of use of the material, while for the semi-crystalline PLA both the Tg temperature that the melting temperature (Tm) are important parameters to determine the application range.

Both these temperatures are strongly influenced by the composition of the isomers in the chain. Commercial PLA is a semi-crystalline polymer obtained from the LL form of lactide having a melting temperature between 160 °C and 180 °C and a glass transition temperature between 55 °C and 60 °C. Its crystal structure consists of spherulites composed of lamellae separated by amorphous regions.

The values reported in table 3 show the effect of a stereoregular structure on the mechanical properties of PLA.

Property	L-PLA	DL-PLA
Glass transition temperature (T_g)	60-65 °C	50-60 °C
Melting point (T_m)	184 °C	Amorphous
Specific gravity	1.24	1.25
Tensile Strenght (MPa)	55.2-82.7	27.6-41.4
Elongation (%)	5-10	3-10
Modulus (MPa)	2758-4137	1379-2758
Inherent viscosity (dl/g)	0.90-1.2	0.55-0.75

Table 3: Physical properties of PLA

The stereochemical composition of the PLA has a large influence on the kinetics of crystallization, the shape and size of spherulites, the degree of crystallinity; both the size of spherulites and the percentage of crystallinity are important for the melting point of the polymer.

A pure PLLA melts at 180 °C, but this value can be lowered even at 130 °C increasing the presence of stereo defects in the chain until a totally amorphous polymer is obtained from meso-lactide, in which is not possible to observe a melting point.

Crystallinity is also necessary for applications in which the material must have mechanical strength, thermal and chemical stability, low permeability, while a lower crystalline content can lead to benefits in terms of processability of the material - that can be worked at lower temperatures - reducing the risk of oxidative and hydrolytic degradation and also formation of lactide.

Crystallinity in the polymer can be induced in two different ways: through the use of nucleating agents, or subjecting the material to a rapid mechanical stress that can promote the formation of crystals. Both crystallinity and molecular weight influence the properties of polylactic acid. The solubility of PLA is strongly linked to the degree of crystallinity, the molecular mass and the presence of other co-monomer units in the chain; the amorphous polymer is soluble in many organic solvents such as ketones, tetrahydrofuran, benzene, dioxane, chlorinated solvents, while the semi-crystalline PLA is dissolved only in chlorinated or fluorinated organic solvents. Water and hydrocarbons are non-solvent for the polylactic acid.

Mechanical properties of PLLA are much more interesting than the one of PDLLA and his behavior changes significantly increasing crystallinity: elasticity values, strength, impact, and thermal stability are better in crystalline PLA in comparison to the values increasing the percentage of amorphous fraction in the macromolecular chain.

As noted by Moon and coworkers[63], PLA thermal and mechanical properties become constant for values of molecular weights higher than about 70000 Daltons. Its properties can be modulated also through the copolymerization of lactide (or lactic acid) with monomers such as glycolide, caprolactone or other lactides and lactones, or by the addition of chain extenders and plasticizers.

2.6 THERMAL STABILITY

In order to use PLA as a biodegradable replacement for traditional plastics, rapid and complete depolymerization at the end of the life cycle of the material is definitely considered as a good thing, but for the applications in which PLA is used a high thermal stability is required; a process of thermal degradation can indeed adversely modify the viscosity of the material and thus worsen the mechanical properties generating in addition, for example, the development of fumes and volatile substances.

Thermal degradation of PLA is a first order reaction, which includes several mechanisms that promote radical and non radical depolymerization reactions, hydrolysis, racemization, oxidative degradation, transesterification and backbiting, and leads to the formation of low molecular weight species including lactide and other cyclic oligomers, carbon dioxide and carbon monoxide, acrylic acid, methane, ethylene and other products obtained by the fragmentation of the polymeric chain[64].

The thermal degradation of polylactic acid is influenced by the amount of catalyst used for the polymerization and by the presence of low molecular weight species such as lactide or oligomers that lower the starting degradation temperature increasing the speed of degradation; compounds based on tin and magnesium are among the metals that mainly promote the formation of lactide from PLA. Reducing the presence of reactive end groups increasing the molecular weight or blocking them by end-capping reaction are two strategies to increase the thermal stability of the PLA.

Polylactic acid stereo complexes have a thermal stability that is higher than the one of PLA homopolymer because of the strong interactions between the two enantiomers, PLLA and PDLA; for example, the stereo complex prepared from a 1/1 mixture of L and D homopolymers has higher thermal stability than the one of the two homopolymers at 260 °C, but degradation rate is still comparable[65]: intermolecular interactions between the two enantiomeric species thus increase the thermal resistance by increasing starting degradation temperature, but once activated, the process of degradation proceeds with the same kinetics observed for PLA homopolymer.

2.7 HYDROLYTIC STABILITY

Hydrolytic degradation is one of the features that make PLA interesting for many application areas: in technical applications (such as packaging) this type of process must be avoided during the synthesis, processing and use, but it should occur once the product reaches the end of life. In biomedical applications hydrolytic degradation is used for controlled release devices, sutures, implants.

Polylactic acid is stable under normal conditions of use for several years, but it degrades rapidly in a few weeks when subjected to conditions of temperature and humidity typical of the environments in which composting is running. Hydrolytic degradation rate depends on the molecular mass of the polymer and the percentage of crystallinity and can be accelerated by the presence of catalysts. Demolition takes place in two distinct phases: the first one is a non-enzymatic degradation of the chains giving oligomers and lower molecular weight species; then a rapid degradation is promoted by enzymes.

Polylactic acid can be hydrolyzed both in the solid state and in melted at high temperatures; rate of hydrolysis is higher for temperatures above the glass transition because of the greater mobility of the system.

The mechanism of hydrolytic degradation of PLA could be a random mechanism or can proceed through terminal ester bond breaking; since the number of ester bonds present in the chain is much higher than the number of terminal ones, it is statistically more likely that the mechanism by which degradation occurs is the random mechanism[66].

As already observed regarding thermal stability, also resistance to hydrolytic degradation of PLA can be improved by minimizing the amount of residual monomer present and operating in the absence of moisture; the amount of water present at the equilibrium in the acid can be adjusted by controlling morphology (crystallinity and orientation of the crystals) of the polymer. Amorphous PLA is more susceptible to hydrolytic degradation because it has higher permeability and greater water absorption.

Hydrolysis can be controlled by changing the morphology of the polymer through stereochemical control, minimizing the presence of end groups that promote hydrolytic degradation or, as already observed for the thermal degradation, using PLLA/PDLA stereo complexes, which show higher hydrolysis resistance compared to that observed for pure homopolymers.

REFERENCES

[1] Hartmann, M. H., in D. L. Kaplan (Ed.), *Biopolymers from Renewable Resources*, Springer-Verlag, Berlin, 1998, pp. 367–411.

[2] Karin, H., Hahn-Hagerdal, B., *Enzyme and Microb. Technol.*, 26, 2000, 87.

[3] Thomas, T. D., Ellwood, D. C., Longyear, M. C., *J. Bacteriol.*, 138, 1979, 109.

[4] Smith, J. S., Hillier, A. J., Lees, G. J. J., *Dairy Res.* 42, 1975, 123.

[5] Kharas, G. B., Sanchez-Riera, F., Severson, D. K., in D. P. Mobley (Ed.), *Plastics From Microbes*, Hanser-Gardner, Munich, 1994, pp. 93–137.

[6] Cheng, P., Mueller, R. E., Jaeger, S., Bajpai, R., Eannoti, E. L., *J. Ind. Microbiol.*, 7, 1971, 27.

[7] Moat, A. G., "Biology of lactic, acetic and propionic acid bacteria" in Demain, A. L. and Solomon, N. A. eds. *Biology of Industrial Microorganisms*, Boston: Butterworths, 1985, pp. 174 – 80.

[8] Payot, T., Chemaly, Z., Fick, M., *Enzyme Microl, Technol.*, 24, 1999, 191.

[9] Tejayadi, S., Cheryan, M., *Appl. Microbiol. Biotechnol.*, 43, 1995, 242.

[10] Breugel, J. V., Krieken, J. V., Baro, B. C., Lancis, J. M. V., Vila, M. C., *WO056693*, 2000.

[11] Datta, R., Tsai, S., Bonsignore, P., Moon, S., Frank, J., *FEMS Microbiology Reviews* 16, 1995, 221–231.

[12] Mueller, M., *EP261572A1*, 1988.

[13] Bhatia, K. K., Lin, K., Nash, R. S., Stambaugh, T. W., *WO9302075*, 1993.

[14] Gruber, P. R., Hall, E. S., Kolstad, J. J., Iwen, M. L., Benson, R. D., Borchardt, R. L., *WO9509879*, 1995.

[15] Yamaguchi, Y., et al., *US5502215*, 1996.

[16] Miyoshi, R., et al., *US5574129*, 1996.

[17] Proikakis, C. S., Tarantili, P. A., Andreopoulos, A. G., *J. Elastom. Plast.*, 34, 2002, 49–63.

[18] Hiltunen, K., Seppala, J. V., Harkonen, M., *J. Appl. Polym. Sci.*, 63, 1997, 1091–1100.

[19] Spaans, C., Biomedical polyurethanes based on 1,4-butanediisocyanate: an exploratory study. *PhD thesis. The Netherlands: University of Groningen*, 2000.

[20] Carothers W., et al., *J. Am. Chem. Soc.*, 54, 1932, 761.

[21] Moon, S. I., Lee, C. W., Miyamoto, M., Kimura, Y., *J. Polym. Sci. Part A: Polym. Chem.* 38, 2000, 1673–1679.

[22] Ajioka, M., Enomoto, K., Suzuki, K., Yamaguchi, A., *Bull. Chem. Soc. Jpn.,* 68, 1995, 2125.

[23] Hiltunen, K., Seppala, J. V., Haerkoenen, M., *Macromolecules*, 30, 1997, 373.

[24] Ki Woong, K., Seong, I., *Macromol. Chem. Phys.,* 203, 2002, 2245-2250.

[25] Lofgren, A., Albertsson, A. C., Dubois, P., Jerome, R., *Macromol. Sci. ReV. Macromol. Chem. Phys.* 35, 1995, 379.

[26] Albertsson, A.C., Varma, I. K., *Advances in Polymers Science,* 157, 2002, 1-40.

[27] Stridsberg, K. M., Ryner, M., Albertsson, A. C., *Advances in Polymers Science*, 157, 2002, 41-65.

[28] Mecerreyes, D., Jerome, R., Dubois, P., *Ad. Polym. Sci.,* 147, 1999, 1.

[29] Kricheldorf, H. R., Kreiser-Saunders, I., *Macromol. Symp.,* 103, 1996, 85.

[30] Dubois, P., Coulembier, O., Raquez, J. M., *Handbook of ring opening polymerization*, Ed.; Wiley- VCH, Weinheim 2009.

[31] Saegusa, T., Fujii, H., Kobayashi, S., Ando, H., Kawase, R., *Macromolecules* 6, 1973, I.

[32] Dubois, P., Jacobs, C., Jerome, R., Teyssie´, P., *Macromolecules*, 24, 1991, 2266–2270.

[33] Kricheldorf, H. R., Lee, S.-R., Bush, S., *Macromolecules* 29, 1996, 1375–1381.

[34] Wang, Y., Hillmyer, M. A., *Macromolecules*, 33, 2000, 7395–7403.

[35] Chamberlain, B. M., Cheng, M., Moore, D. R., Ovitt, T. M., Lobkovsky, E. B., Coates, G. W., *J. Am. Chem. Soc.*, 123, 2001, 3229–3238.

[36] Portinha, D., Belleney, J., Bouteiller, L., Pensec, S., Spassky, N., Chassenieux, C., *Macromolecules,* 35, 2002, 1484–1486.

[37] Kobayashi, S., Uyama, H., Kimura, S., *Chem. Rev.,* 101, 2001, 3793.

[38] Gross, A., Kumar, A., Kalra, B., *Chem. Rev.,* 101, 2001, 2097.

[39] Kowalski, A., Duda, A., Penczek, S., *Macromol. Rapid Commun.,* 19, 1998, 567.

[40] Kricheldorf, H. R., Kreiser-Saunders, I., Boettcher, C., *Polymer*, 36, 1995, 1253.

[41] Von Schenck, H., Ryner, M. Albertsson, C. A., Svensson, M., *Macromolecules*, 35, 2002, 1556–1562.

[42] Penczek, S., Duda, A., et al., *Prog. Polym. Sci.,* 32, 2007, 247–282.

[43] Jalabert, M., Fraschini, C., Prud'Homme, R.E., *J. Polym. Sci. Part A.,* 45, 2007, 1944-1955.

[44] Kowalski, A., Duda, A., Penczek, S., *Macromolecules,* 33, 2000, 689–695.

[45] Du, Y. J., Lemstra, P. J., Nijenhuis, A. J., Vanaert, H. A. M., Bastiaansen, C., *Macromolecules*, 28, 1995, 2124.

[46] Duda, A., Penczek, S., Kowalski, A., Libiszowski, J., *Macromol. Symp.*, 153, 2000, 41.

[47] Kowalski, A., Duda, A., Penczek, S., *Macromolecules*, 33, 2000, 7359.

[48] Kricheldorf, H. R., Serra, A., *Polym. Bull.*, 14, 1985, 497–502.

[49] Ovitt, T. M., Coates, G. W., *Polym. Prepr.*, 41, 2000, 385.

[50] Cheng, M., Attygalle, A. B., Lobkovsky, E. B., Coates, G. W., *J. Am. Chem. Soc.*, 121, 1999, 11583.

[51] Ovitt, T. M., Coates, G. W., *J. Am. Chem. Soc.*, 121, 1999, 4072.

[52] Sun, J., Cui, L., Wu, L., *Gongneng Gaofenzi Xuebao*, 9, 1996, 252.

[53] Dubois, P., Jerome, R., Teyssie, P., *Makromol. Chem., Macromol. Symp.*, 42/ 43, 1991, 103.

[54] McLain, S. J., Ford, T. M., Drysdale, N. E., *Polym. Prepr.*, 33, 1992, 463.

[55] Stebels, W. M., Ankone, M. J. K., Dijkstra, P. J., Feijan, J., *Macromolecules*, 29, 1996, 3332.

[56] Conner, E. F., Nyce, G. W., Myers, M., Mock, A., Hedrick J. L., *J. Am. Chem. Soc.*, 124, 2002, 914.

[57] Shinno, K., Miyamoto, M., Kimura, Y., Hirai, Y., Yoshitome, H., 1997; 30:6438–44.

[58] Ren, J,. Zhang, N., Wang, Q., *CN1718607A*, 2006.

[59] Zhou, Z., Xu, W., *CN 1594393A*, 2005.

[60] Chen, F. C., Griskey, R. G., Beyer, G. H., *AIChE J*, 15, 1969, 680–685.

[61] Gruber, P. R., Hall, E. S., Kolstad, J. J., Iwen, M. L., Benson, R. D., Borchardt, R. L., *US 5142023*, 1992.

[62] Garlotta, D., *J. Polym. Environ.*, 9, 2001, 63–84.

[63] Moon S., Kimura Y., *Polym. Int.*, 52, 2003, 299–303.

[64] McNeill, I. C., Leiper, H. A., *Polym. Degrad. Stab.*, 11, 1985, 267-285.

[65] Tsuji, H., Fukui, I., *Polymer*, 44, 2003, 2891-2896.

[66] Henton, D. E., Gruber, P., Lunt, J., Randall, J., Polylactic acid technology, in A. K. Mohanty, M. Misra and L. T. Drzal. (Ed.), *Natural Fibers, Biopolymers, and Biocomposites*, CRC Press, USA, 2005, pp. 527-577.

3. SEC Calibration

3 SEC CALIBRATION

3.1 GENERAL PRINCIPLES ABOUT CALIBRATION

Spectra coming from Sixe exclusion chromatography (SEC) analyses can provide important information on the sample analyzed, like data relating to the average molecular weight and molecular weight distribution.

SEC columns are able to separate molecular species having different hydrodynamic volume or, in other words, having different molecular mass; therefore species with different dimensions will come out of separation columns with different retention time in relation to their molecular size that.

A SEC chromatogram is reported on a two-dimensional diagram with retention times on the abscissa and the intensity of the electrical signal on the ordinate, which leads to a relative amount by weight. To refer the results to molecular masses it is necessary to make a conversion of the x-axis, correlating retention time or retention volume to the molecular weight; therefore a relationship between molecular mass and retention time is necessary: the mathematical equation that shows the dependence between them is precisely the function of the calibration curve.

A general equation that shows the nature of the dependence of the two quantities involved in the process of converting the scale of the x-axis is shown below:

$$\log(M_{ni}) = f(V_{ri}) \qquad 3.1)$$

in the equation 3.1) M_{ni} represents the molecular weight of species i, with a retention volume V_{ri}.

Calibration curve, which is obtained experimentally for a chromatographic system, is valid only for the couple polymer-eluent/chromatography system for which was obtained; in fact, the hydrodynamic volume of a polymer is inevitably influenced by the medium in which is dissolved and with which it interacts. Considering this, it is easy to understand that parameters obtained in specific experimental conditions cannot be used to interpret SEC analyses conducted in different conditions.

Standards for calibration can be either monodisperse, or with a value of polydispersity greater than 1.1. In the first case, with monodisperse samples, it can be assumed that $M_p \approx M_w \approx M_v \approx M_n$, and this approximation is much better as the polydispersity index is close to one.

In this case, the knowledge of any of the values of the average mass polymer is required; viscosimetric analysis, titration of end groups or light scattering analysis allows to obtain one of the values. Alternatively it's easier to buy commercial monodisperse standards having a known value of average molecular weight. Standard samples must be injected into the chromatographic system to be calibrated and for each sample the retention time, corresponding to the maximum of the peak of the SEC chromatogram, will be associated with the value of the average molecular weight determined for the same standard; in this way couples of values (M_n, t_r) will be obtained. These couples of point are then used in a two-dimensional diagram, plotting log (Mn) Vs t_r. Points are interpolated with a polynomial curve of an appropriate order.

The simpler polynomial curve is, of course, a straight line, but for columns filled with polystyrene gels, such as those currently in use in research laboratories, a linear calibration does not represent correctly the relation between the variation of the logarithm of the molecular masses and the corresponding change in retention time. A good approximation can be obtained using a polynomial interpolation of third order, while higher orders allowing a better interpolation of the points are even too accurate to be trusted. In order to have a good calibration, it is very important to have a good number of standards that can cover all the range of retention times interesting from an analytical point of view considering the polymers that must be analyzed.

Unfortunately, it is not always possible to have monodisperse standards because of high costs or of the difficult to synthesize proper samples.

To overcome this problem SEC system can be calibrated with polidisperse standards for which the approximate equality of the average molecular weights is no longer valid. In this case at least two different values of average molecular masses for each standard must be known to calibrate the system with polidisperse samples through the calibration procedure commonly called *broad calibration*.

3.2 UNIVERSAL CALIBRATION

The accuracy of the calibrations performed using monodisperse standards is certainly higher than the procedure with polydisperse samples, and for this reason many attempts were made to find a correlation between calibrations, obtained with monodisperse standards, for a particular system polimer1-eluent, and the calibration needed for a polimer2-eluent systems, where polimer2 represents a polydisperse polymer.

Based on this goal a method of universal calibration[1] has been proposed as a result of numerous studies about homopolymers and copolymers with different chemical and geometric structures. The philosophy of the methodology was based on the assumption that steric exclusion chromatography is controlled only by the hydrodynamic volume of the eluted species or by a parameter related to it: viscosimetric studies of dilute solutions of synthetic polymers indicate that macromolecules in solution can be represented as an equivalent hydrodynamic sphere[2]: it follows that the intrinsic viscosity $|\eta|$ can be defined by the following Einstein relation:

$$|\eta| M = 0{,}025 N_A V_h \qquad 3.2)$$

in equation 3.2) V_h is the hydrodynamic volume of the equivalent sphere, N_A is the Avogadro's number and M the molecular mass of polymer species with volume V_h. A curve plotting $|\eta| M$ against V_r must hold for all polymers and the concept of invariance of the product $|\eta| M$ is the heart of the theory of universal calibration.

Another equation which relates the intrinsic viscosity with the molecular mass of a polymeric species is expressed by the following Mark-Houwink equation:

$$|\eta| = K M^{a} \qquad 3.3)$$

K and α are constants for a specific polymer-solvent-temperature system.

Having the ability to construct a calibration curve with monodisperse samples, using standard of polystyrene (readily available) and knowing the values of K and α for standard polymer and for the polymer that will be analyzed with the calibrated system, it is possible to use Mark-Houwink equation and the concept of universal invariance of the $|\eta| M$ product to obtain the calibration curve for the polymer to be analyzed.

The simple mathematical basis of the conversion are listed below considering two polymers 1 and 2:

$$|\eta|_1 M_1 = |\eta|_2 M_2 \qquad 3.4)$$

replacing in 3.4) the values of $|\eta|$ described by the equation of Mark-Houwink:

$$K_1 M_1^{a_1+1} = K_2 M_2^{a_2+1} \qquad 3.5)$$

converting 3.5) to the logarithmic form:

$$\log K_1 + (a_1+1)\log M_1 = \log K_2 + (a_2+1)\log M_2 \qquad 3.6)$$

reordering 3.6) to underline $\log M_2$:

$$\log M_2 = \frac{a_1+1}{a_2+1}\log M_1 + \frac{1}{a_2+1}\log\frac{K_1}{K_2} \qquad 3.7)$$

considering a third order calibration curve:

$$\log M = A + BV_r + CV_r^2 + DV_r^3 \qquad 3.8)$$

replacing expression 3.8) in equation 3.7):

$$A_2 + B_2V_r + C_2V_r^2 + D_2V_r^3 = \\ = \frac{a_1+1}{a_2+1}(A_1 + B_1V_r + C_1V_r^2 + D_1V_r^3) + \frac{1}{a_2+1}\log\frac{K_1}{K_2} \qquad 3.9)$$

The equality in equation 3.9) is verified for the following relations between the coefficients of polynomial interpolation of a calibration curve and the respective coefficients of the second and third order curve:

$$A_2 = \frac{a_1 + 1}{a_2 + 1} A_1 + \frac{1}{a_2 + 1} \log \frac{K_1}{K_2} \qquad B_2 = \frac{a_1 + 1}{a_2 + 1} B_1$$

$$C_2 = \frac{a_1 + 1}{a_2 + 1} C_1 \qquad D_2 = \frac{a_1 + 1}{a_2 + 1} D_1 \qquad 3.10)$$

Given this, the conversion from a calibration curve to another one is immediate; having the interpolation coefficients obtained by a calibration with monodisperse standards, it is possible to obtain the four coefficients to construct the calibration curve regarding the polymer for which the monodisperse samples are not available. Of course, it is essential to know the parameters K_1, α_1, K_2, α_2, which can be found in the literature or determined experimentally by viscosity measurements and analysis that can provide the average molecular weight.
In our case monodispersed polystyrene have been used as standard samples, and conversion is carried out to obtain a calibration for PLA using the following values for K and α parameters of Mark-Houwink equation for polystyrene in methylene chloride:

$$K_{ps} = 1{,}43 * 10^{-2} \qquad a_{ps} = 0{,}691 \qquad 3.11)$$

For PLA the following values[3] have been used:

$$K_{PLA} = 1.31 * 10^{-2} \qquad a_{PLA} = 0{,}777 \qquad 3.12)$$

By the correction is possible to express the results obtained by the integration of a polylactic acid SEC curve (average molecular weight and polydispersity index) in terms of PLA. Figure 1 shows the calibration curves for polystyrene and PLA.

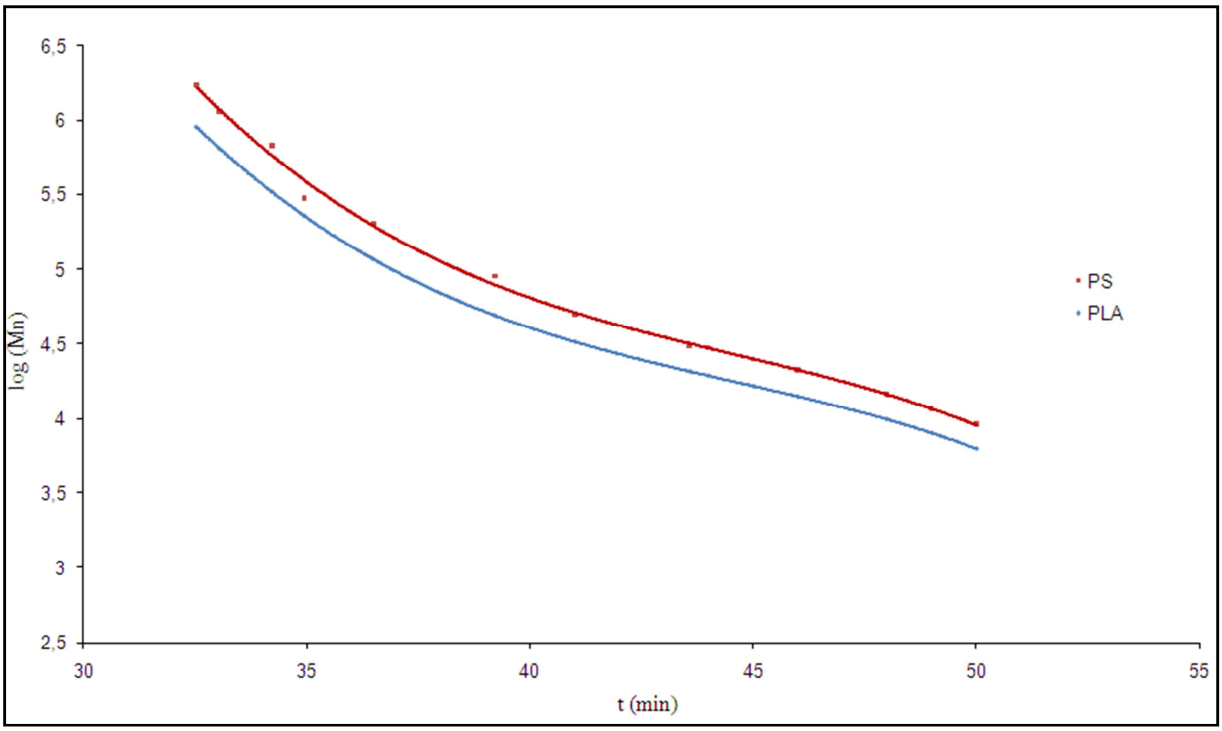

Figure 1: Comparison between calibration curves expressed in PS and PLA

3.3 CALIBRATION WITH PLA SAMPLES

Generally Mn, Mw and D values of polymers are expressed in terms of polystyrene equivalent. The molecular weight of polylactic acid is significantly lower than the one determined with a calibration based on polystyrene standards, due to the different behavior of PLA and PS in the same solvent[4-6]. A system of absolute calibration to express data relative to the polymers synthesized in terms of equivalent linear PLA has been developed.

In chapter two the possibility to have a high control of molecular masses and their distribution working under very controlled reaction conditions in the presence of solvents or in bulk but at temperatures not exceeding 130 °C were discussed. In this way it is possible to obtain polymers with a Mw/Mn ratio close to 1, as for the standard polystyrene commonly used for calibration of SEC systems.

PLA synthesized in this work have not a Mw/Mn ratio close to 1, but there is a gradual re-distribution of species, due to backbiting and transesterification reactions, which leads to a widening of the molecular masses distribution curve, as happens for all polycondensation polymers, as will be discussed in chapter 4 (figure 2).

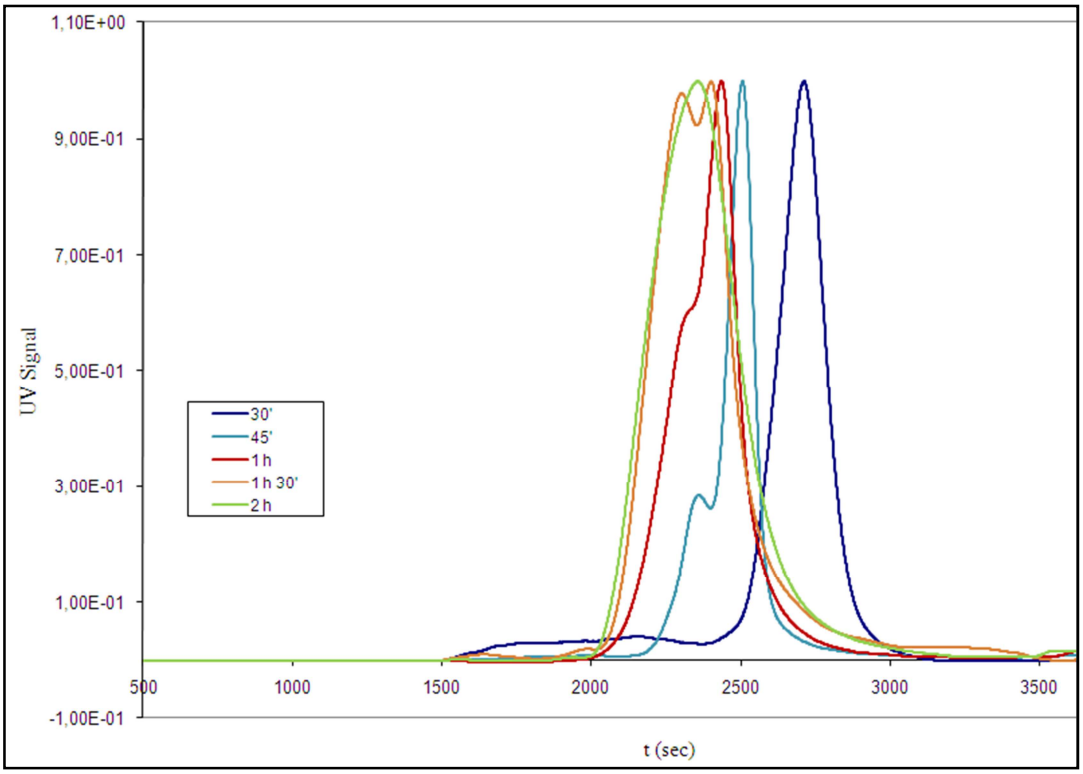

Figure 2: Increase in molecular weight distribution as a function of polymerization time

As SEC curves in Figure 2 show, molecular masses distribution curves change by increasing polymerization time. For very short polymerization times (blue curve 30') molecular weight distribution is very narrow, typical of a ROP polymerization. Increasing the reaction time an increase in molecular weight is observed, but it is also clear how the curves tend to widen, with the progressive appearance of a shoulder in the area corresponding to higher molecular weight species. The uneven distribution (curve 45', 1h, 1h30') is due to the backbiting and transesterification reactions that, at temperatures and conditions in which the polymerization is carried out (typical of an industrial process of synthesis of the PLA) cause a rearrangement of the macromolecular chains.

For long reaction time (curve 2h) curve has a wider and more uniform distribution.
In this situation the value of molecular weight distribution tends to an equilibrium value close to 2, typical of polymers obtained by polycondensation. Figure 3 shows a comparison of the SEC curves of two PLA obtained via ROP, with different reaction times, and a polymer synthesized from lactic acid by a polycondensation process.

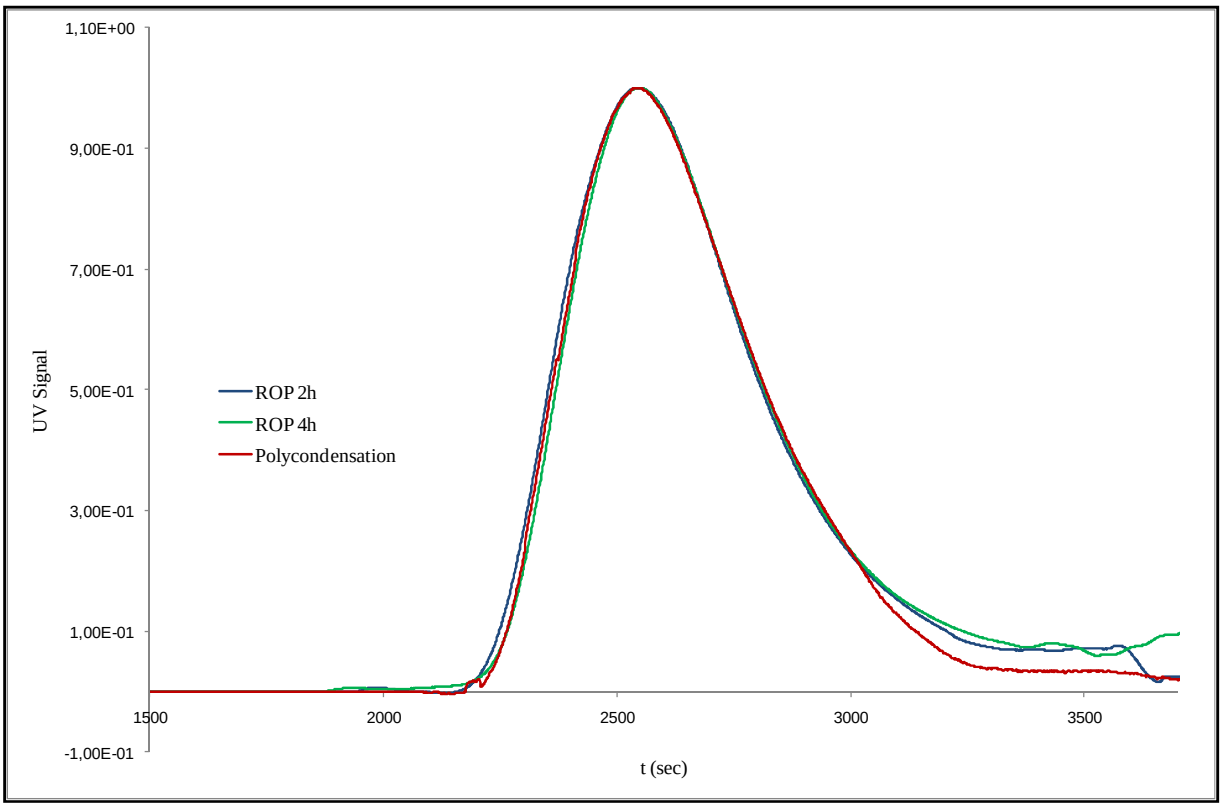

Figure 3: Comparison between distribution of PLA synthesized via ROP and polycondensation

It is interesting to note that, under the operating conditions used for the synthesis via ROP, the molecular weight distribution reaches an equilibrium after 2 hours and increasing the reaction times no changes were observed in D but only in the molecular weight values.
The polymer represented by the red curve was obtained by polycondensation of lactic acid with a conversion of 97% , therefore the reaction can be considered complete.
It can be seen that the molecular masses distribution of the two polymers deriving from lactide is virtually identical to that of PLA synthesized starting from lactic acid, confirming that an equilibrium between species for long times ROP polymerization at high temperatures was really established.
Based on these observations it was decided to develop a calibration system by addressing the problem with a different philosophy than the procedure based on the concept of universal

calibration; it was decided to exploit Flory[7] equations, which describe the distribution curve of molecular masses for polymers obtained by polycondensation reactions: these polymers have a statistical reaction distribution of D = 2. The decision to use this methodology has been taken because of the behavior observed for PLA obtained via ROP in our synthetic conditions, that reach an equilibrium for long polymerization times. For this reason we decided not to use monodisperse PLA samples prepared in solution, whose synthesis will be described in chapter 4.

Eight samples of PLA were synthesized starting from lactide and using two different monofunctional regulators with low volatility under reaction conditions, 1-heptanol (E) and 1-tetradecanol (T), in order to obtain polymers with different molecular weight. The synthesis time was held constant (two hours) for all the syntheses, to operate under the same reaction conditions and allow the establishment of equilibrium, even if increasing the amount of chain regulator - and therefore the number of hydroxyl function - reaction kinetic is increased. The samples thus synthesized are considered standard PLA with different average molecular numeral weight and therefore it is assumed that the polydispersity index, which describes the distribution of molecular masses is 2.

This procedure has been used under one of the two hypothesis of this work; the second one involves the assumption of the validity, within the limits of experimental errors, of the results obtained from the determination of the end groups of PLA by ^{1}HNMR analysis; hydroxyl terminal groups were measured by ^{1}HNMR[8] and not through titration because the polymer is easily hydrolyzable.

With all these consideration it is possible to compare the real GPC curve obtained from SEC analysis with the theoretical curve expressed by Flory theory[7] built using as input data only the quantity of terminal hydroxyl groups.

Considering a distribution of 2 for the standards PLA, we can say that the maximum of the real SEC curve corresponds to a molecular weight value equal to the value of the average molecular weight (Mw).

Knowing the values of end groups, the theoretical curve can be constructed from Flory equation reported below:

$$P_n = np^{(n-1)}(1-p)^2 \qquad 3.13)$$

Pn is the amount, in moles, of the species with degree of polymerization *n* and *p* is the conversion of the reaction:

$$p = 1 - \frac{\text{total terminal groups}}{2 * \text{mol of monomer}} \qquad 3.14)$$

For PLA:

$$p = \frac{\text{mol of polymer}}{\text{mol of monomer}} \qquad 3.15)$$

Moreover, since each polymer chain (both regulated and non regulated) has a hydroxy terminal group, the 3.15) becomes:

$$p = 1 - \frac{\text{OH groups}}{\text{mol of monomer}} \qquad 3.16)$$

It should be remembered that the resulting GPC curve gives a distribution of the eluted amount according to the molecular weight: so every time it returns a value that represents the total weight of all the molecules that have that elution time and therefore have the same molecular mass.

Equation 3.13) represents a distribution of quantities in moles as a function of the degree of polymerization; it is therefore necessary to pass from the theoretical equation expressing resulting data as a function of moles to the real GPC curve; therefore it is necessary multiply the expression for the molecular mass of a single molecule in order to obtain, for each value of *n*, the total weight amount for the considered species having on the ordinate the same variable for the real curve and for the theoretical one.

This is essential to make a comparison.

The new equation is here reported:

$$M_m nP_n = M_m n^2 p^{(n-1)}(1-p)^2 \qquad 3.17)$$

Mm is the molecular mass of monomer unit in the chain (72 g/mol for PLA).

For each value of *n*, the relative weight amounts is calculated: the distribution curve can be transposed in a two dimensional graphic. Figure 4 shows a theoretical Flory curve for a terminal hydroxyl value of 187.06 meq/kg corresponding to the value found for standard 2, synthesized with 1-heptanol.

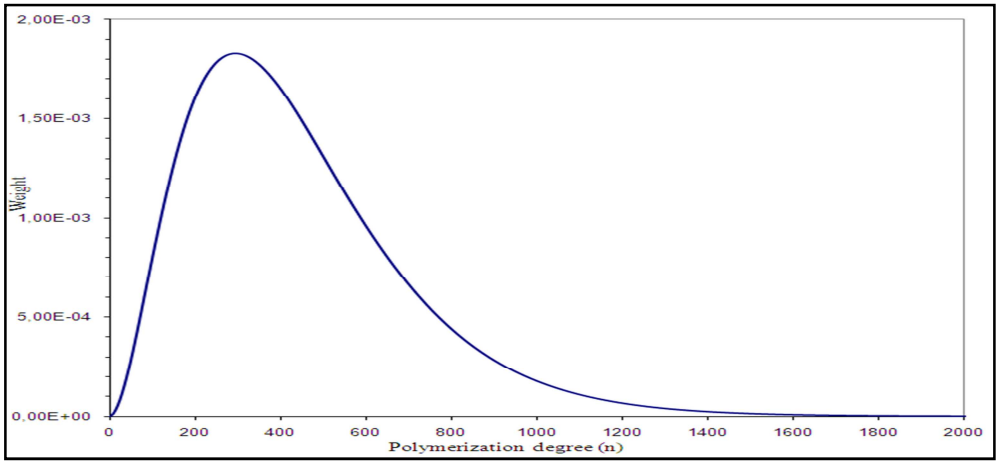

Figure 4: Flory theoretical curve calculated for a OH terminal groups value of 187.06 meq/kg

The next step involves a comparison between theoretical curve and real curve; the real curve is shown in Figure 5.

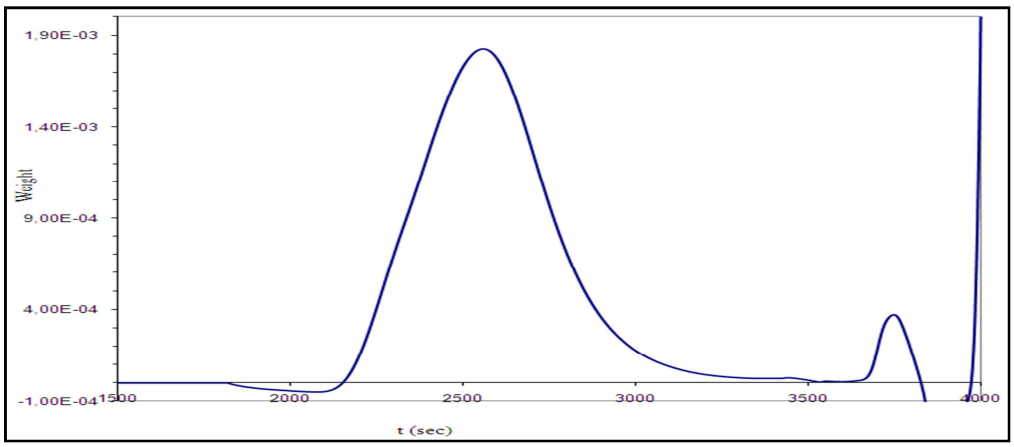

Figure 5: SEC curve reported at the same intensity of the curve in Figure 4

Calibration is necessary to go from the scale of the theoretical curve, which has the molecular weight on the x-axis (Figure 4), to the experimental one which has time on the abscissa (frigure 5); the equation for a third order calibration curve expressed in t (time) is the following:

$$\log M = A + Bt_r + Ct_r^{\,2} + Dt_r^{\,3} \qquad 3.18)$$

A, B, C, D are the parameters of polynomial interpolation.

Defined these steps the points for calibration curve can be defined. A value on ordinate for the theoretical curve is chosen; the corresponding *n* value is obtained plotting the intercept with the abscissa axis. The same ordinate value for the real curve is taken and the intercept to x-axis is determined: since on the abscissa of real curve, time is plotted, with this procedure the first pair of points (n, t) is obtained. Repeating the procedure for different ordinate values and for all the standard samples, many points allowing to get through the third order polynomial interpolation, an accurate calibration curve can be obtained. Calibration curve will also be extended for a sufficiently wide range of elution times to allow a correct integration of real GPC curves of several samples with high, medium and low molecular weight. In the construction of the calibration curve it was noted that the polymers synthesized covered very well the area of medium and low molecular weights but not that of high molecular weights, so another linear polymer (NR) was synthesized, without using a chain regulator to obtain a PLA sample whose molecular weight was going to fall in the left area uncovered by the 8 samples previously synthesized. Table 1 shows the values of end groups of the samples synthesized for calibration.

Sample	OH (meq/Kg)
Std 1 E	133.61
Std 2 E	187,06
Std 3 E	405,56
Std 4 E	653,59
Std 1 T	93,06
Std 2 T	166.83
Std 3 T	276,40
Std 4 T	572.74
Std 5 NR	16,71

Table 1: terminal groups for standard PLA

The two different chain regulator were used to evaluate if there might be some influence due to the greater length of the chain in 1-tetradecanol compared to 1-heptanol.

The percentages comonomers used are 0.5%, 1%, 2% and 4% in order to cover a large area of molecular weights. The amount of end groups of each polymer was determined by ^{1}HNMR analysis; DPn and Mn values upon which it is based the development of calibration were calculated from OH groups.

Figure 6 shows the GPC curves of some standards used for calibration.

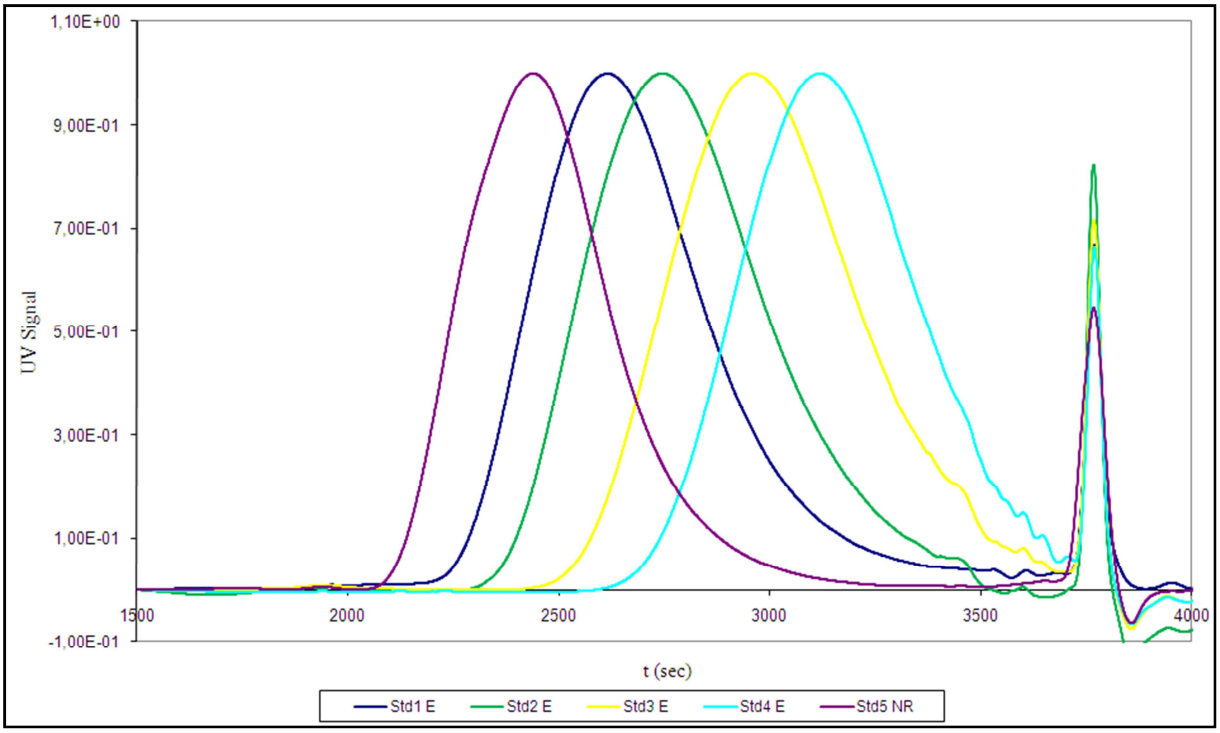

Figure 6: GPC curves of standards for calibration

Figure 6 shows that standard 5 NR covers the area of the high molecular weights left uncovered by the samples synthesized with monofunctional monomers.

From SEC curves of each sample the points necessary for the construction of calibration curves were obtained; figure 7 shows the comparison between calibration curves obtained using 1-heptanol and 1-tetradecanol as monofunctional chain regulators. To assess the real influence of the two alcohols, points deriving from standard NR 5 have not been considered.

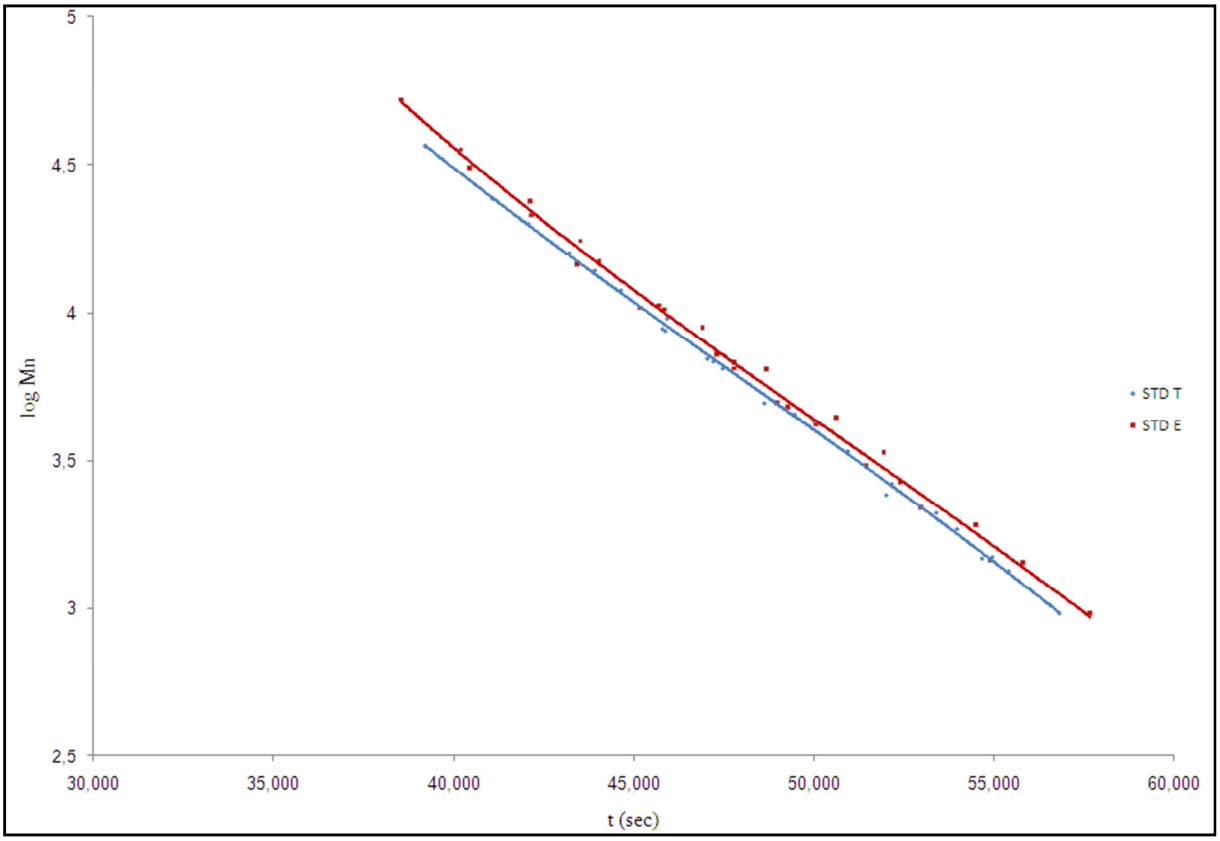

Figure 7: calibration curve obtained with 1-heptanol and 1-tetradecanol

Figure 7 shows how the alcohol used as chain regulator influences the shape of the curve especially in the area of low and high molecular weights. This is explained by the fact that polymer with the same molecular weight (determined via ^{1}HNMR), synthesized using 1-heptanol as chain regulator, has lower retention time because its hydrodynamic volume is lower than that synthesized with 1-tetradecanol. Once observed the effect of monofunctional comonomer on the behavior of the curve, the effect of the seven carbon atoms of difference existing between 1-heptanol and 1-tetradecanol on the curves was determined. This procedure was performed to have a curve independent from the nature of the chain regulator.

The difference between the intercept values (log Mn) of the two curves represents the influence that the seven carbon atoms present in 1-tetradecanol and not in 1-heptanol have on the molecular weight of the polymer. This difference was used to correct the curve of 1-heptanol.

The new points thus obtained are the log Mn values of the hypothetical curve obtained without the use of chain regulators.

These values were added to the points obtained from the curve of the standard NR 5, synthesized without any comonomer.

Figure 8 shows the comparison between the three calibration curves experimentally determined and theoretically derived in terms of linear non regulated polymers.

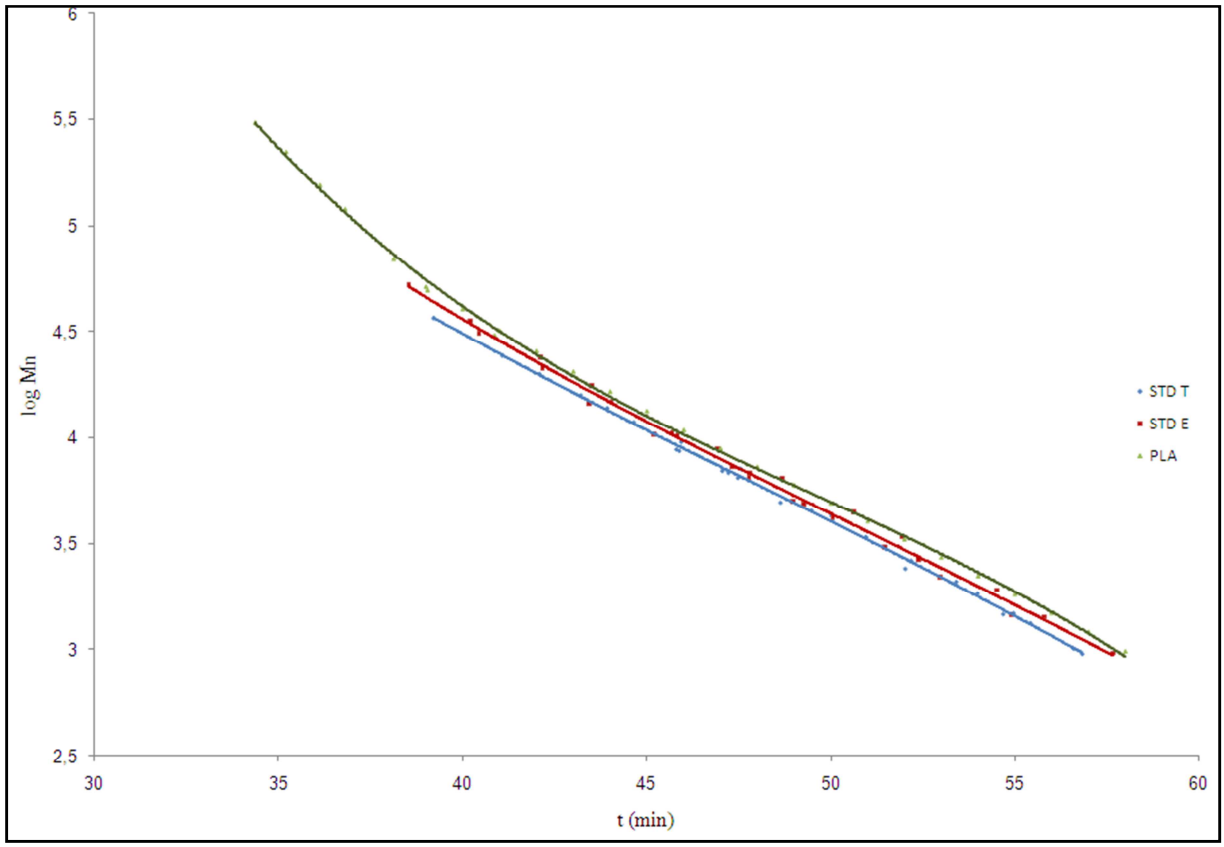

Figure 8: comparison between theoretical calibration curve without regulation and experimental calibration curves

The third-order calibration curve obtained by this way covers a range of molecular weights wider than that of the two curves obtained using monofunctional alcohols, allowing a better study of molecular properties of polymers synthesized in this research project, allowing a better correlation between molecular masses, structures and properties of polymers.

Figure 9 shows the calibration curve obtained in this work.

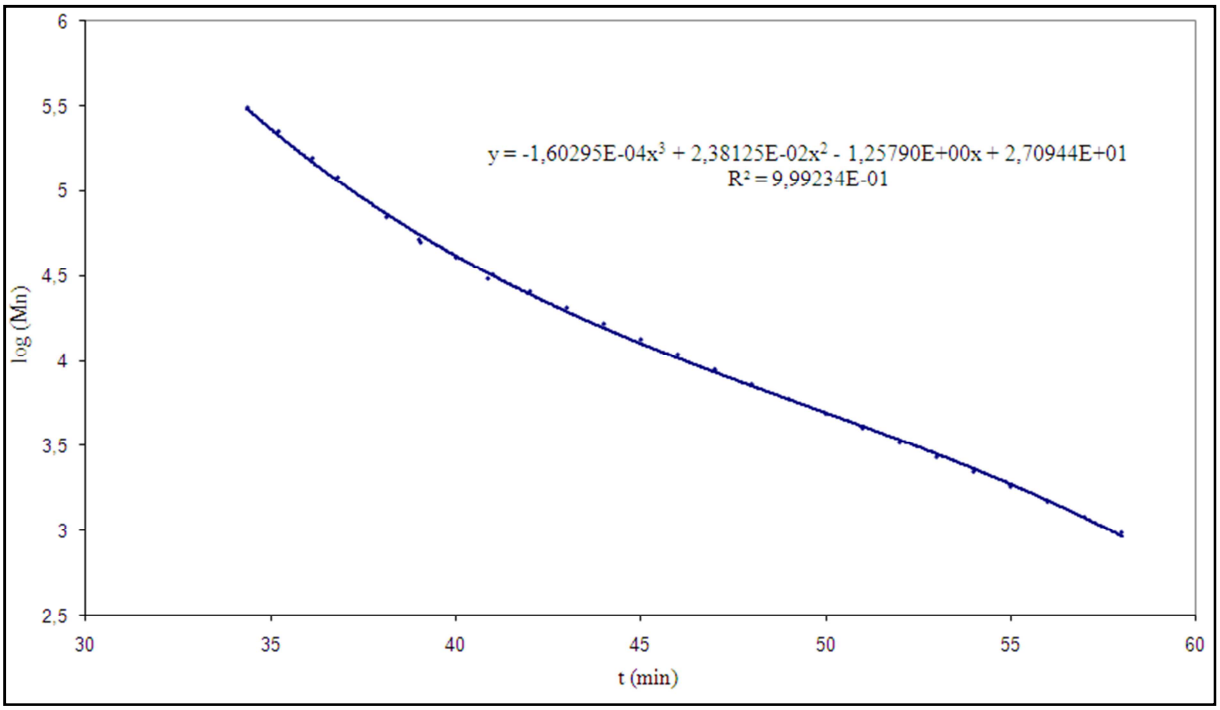

Figure 9: linear PLA calibration curve

The range of retention times of this curve is between 34.4 minutes and 58.0 minutes, which corresponds to a range of molecular weights between 480354 and 1509 Dalton, thus allowing an accurate analysis of both systems with a high molecular weight and oligomers.

Figure 10 shows the comparison between the calibration curve obtained with polystyrene standard and the calibration curve obtained in this work expressed in terms of PLA.

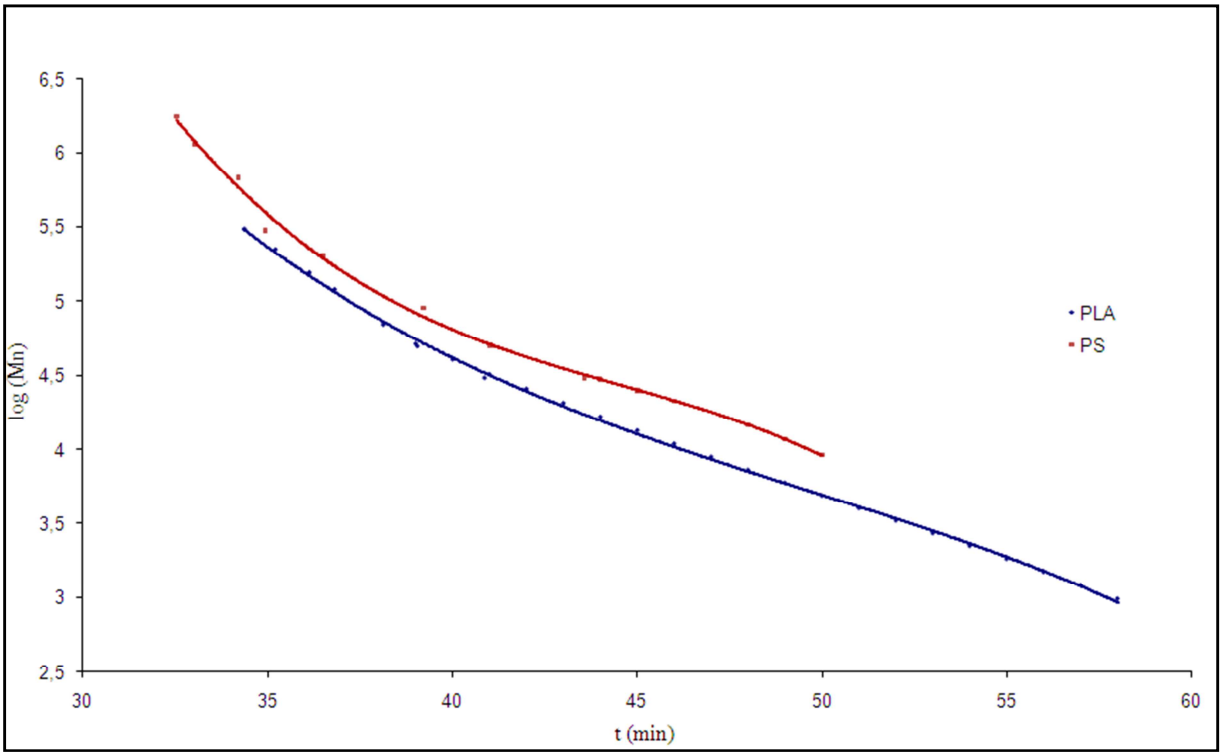

Figure 10: comparison between PS and PLA calibration curves

From Figure 10 it is clear the difference between the two calibration curves that does not involve a simple geometrical shift of the PS curve, since the two third-order polynomial curves cannot be considered similar.

This shows how the behavior of the PLA in the presence of the solvent used for SEC analyses is totally different from that of polystyrene.

Figure 10 shows that, for any values of time considered on x-axis, the corresponding molecular weight obtained on y-axis is always lower for PLA.

Considering two species with the same elution time, and therefore the same hydrodynamic volume, it is evident that expressing the value of weight in terms of polystyrene equivalent leads to an overestimation.

REFERENCES

[1] Grant, D.M., Cheney, B.V., *J. Am. Chem. Soc.*, 89, 1967, 5315-5319.

[2] "Steric Exclusion Liquid Cromatography of Polymers", *Cromatographic Science Series*, Vol. 25, Ed. J. Janca, 1984.

[3] Vargas, L. F., Welt, B. A., Seliga, J., Brennan, A. B., Teixeira, A. A., Balaban, M. O., Beatty, C. L., *Journal of Applied Packaging Research*, 1(3), 2007, 181-190.

[4] Biela, T., et al., *Macromol. Symp.*, 183, 2002, 1.

[5] Save, M., et al., *Macromol. Chem. Phys.*, 203, 2002, 889.

[6] Tillier, D., et al., *Macromol. Chem. Phys.*, 205, 2004, 581.

[7] Flory, P. J., *"Principles of Polymer Chemistry"*, Cornell University Press, 1971.

[8] Jalabert, M., Fraschini, C., Prud'Homme, R.E., *J. Polym. Sci. Part A*, 45, 2007, 1944-1955.

4. Solution polymerization of lactide

4 SOLUTION POLYMERIZATION OF LACTIDE

Solution polymerization of lactide is a technique used to synthesize PLA with an high control of molecular masses and polydispersity, due to very controlled reaction condition necessary for this kind of syntheses. The use of solvents, the long reaction times, high costs associated with the need to operate with extremely pure reagents make this method unsuitable for industrial production of PLA, but very useful for synthesizing polymers as standards, or as model molecules to study some mechanistic aspects of reaction.

In the first part of the thesis it was decided to synthesize a series of controlled molecular weight polymers, using chain regulators with a different number of reactive functionalities; comonomers having hydroxyl functional groups were chosen as benzyl alcohol (T1), 1,6 hexanediol (T2), trimethylolpropane (T3) and pentaerythritol (T4) (Figure 1).

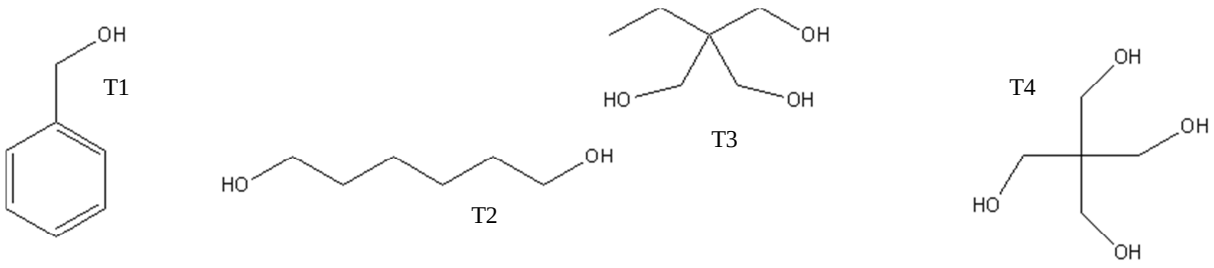

Figure 1: comonomers used in PLA solution polymerization

Since the molecular weight of PLA is controlled by the amount of OH groups in the feed, it is possible to design polymers with different values of Mn by changing the [monomer]/[comonomer], ([M]/[CM]), ratio obtaining systems having different arm lengths depending: the length of each arm depends on the [monomer]/[comonomer] ratio. Moreover changing the different number of hydroxyl groups of the reactive comonomers gives the possibility to synthesize linear or stars polymers with different number of arms, depending on the functionality of the comonomer itself.

To increase the control on the final structure of the polymer, as well as the values of molecular mass and polydispersity, reactions were carried out in solution, in order to reduce the number of collisions between the species for a better control of the system.

The solvent was dehydrated before polymerization, and lactide and comonomers were purified by crystallization or distillation to eliminate the impurities that could affect the chain growth.

Bulk polymerization do not allow to obtain high molecular weight polymers with a narrow distribution of molecular masses because the temperature required to avoid backbiting and transesterification reactions (that increase the polydispersity of the system) is below the melting temperature of high molecular weight PLA. Therefore when DPn get high the polymer is not melt but solidifies and the growth of the macromolecular chain is interrupted: this leads an increase in D value.

As reported by De Jong[1] and coworkers, using the synthesis in bulk at 130 °C is not possible to obtain a degree of polymerization greater than 30 and also polydispersity values are higher than those obtained by solution polymerization[2].

Figure 2 shows the GPC curves of two polymers synthesized in bulk at a 130 °C (red curve) and in solution at 60 °C, using THF as solvent (green curve); for both samples the [monomer]/[comonomer] ratio was the same in order to obtain two polymers with a DPn of 200 lactic units, corresponding to a Mn value of 14400 Dalton.

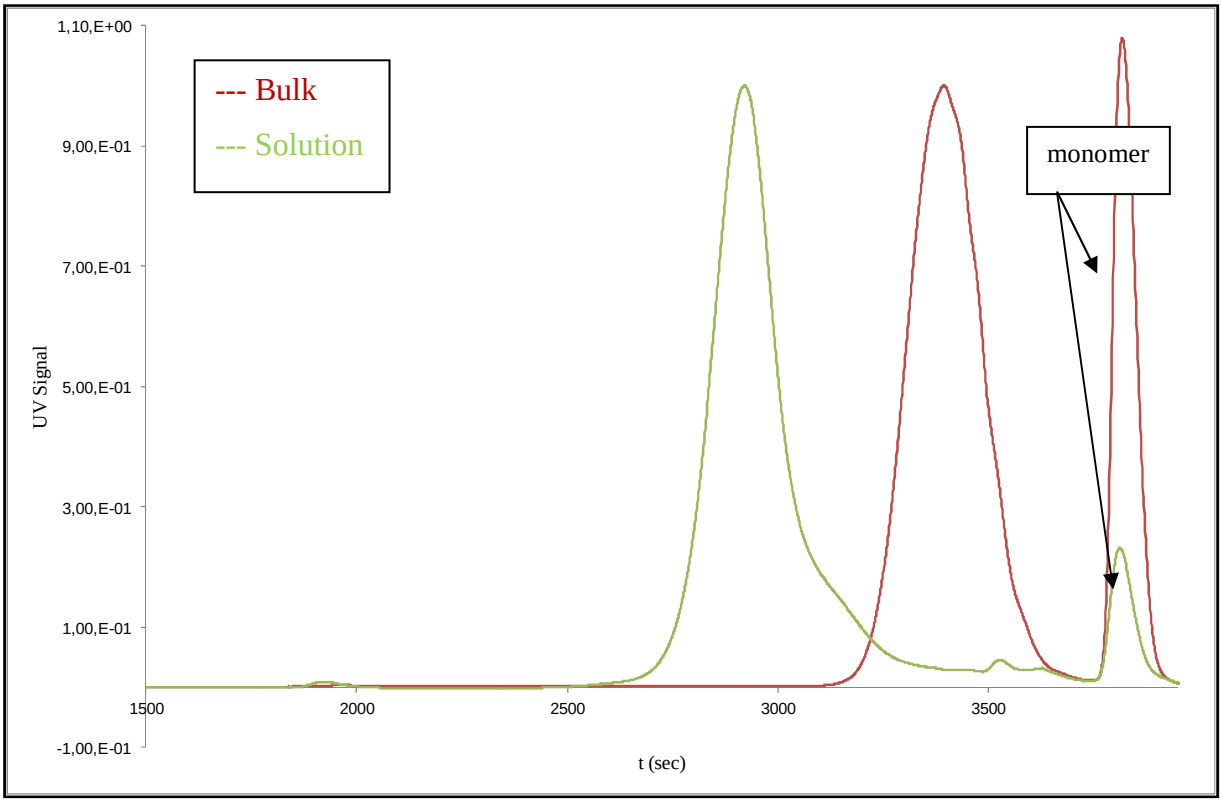

Figure 2: SEC curves of PLA obtained by bulk and solution polymerization

Figure 2 shows that both polymerization process allows good control of polydispersity values, which is close to 1 Differences are relative to the chain growth; in solution polymerization the monomer is almost completely consumed and the molecular weight calculated by ^{1}HNMR analysis is 12960 Dalton, in accordance with the programmed one, while in bulk process macromolecular chains have grown until the melting temperature of the polymer has become higher than the one of the reaction (130 °C). In this condition the polymer is then solidified and therefore the polymerization process stops without reaching a complete monomer conversion, as evidenced by the peak of the unreacted lactide which is significantly higher.

Bulk polymerization, conducted at low temperatures to have good control over molecular weights and polydispersities, can not therefore be used for the synthesis of high molecular weight PLA.

The synthesis of high molecular weight polylactic acid with narrow polydispersity needs to be performed in solution, using a solvent that is able to solubilize polymers with high DPn: by this way is possible to control the molecular parameters of the polymer.

4.1 SOLVENT EFFECT

The choice of solvent used for polymerization process is a critical and delicate aspect that can greatly affect the reaction. The solvent should be selected according to several factors, such as polarity, ability to solubilize the monomer and the polymer and, the solubility of the comonomers used as chain regulators; it is essential that all components are dissolved to have an homogeneous system. As reported in literature[3,4] the polymerization kinetic of lactide and the conversion is strongly influenced by the type of solvent used.

In literature standard solvents for the polymerization of lactide are toluene, THF and dichloromethane. The first two were used, since they allow to operate at higher temperature, thus reducing the time required for the synthesis. As mentioned earlier the choice of solvent is essential for the synthesis, as GPC curves show in Figure 3.

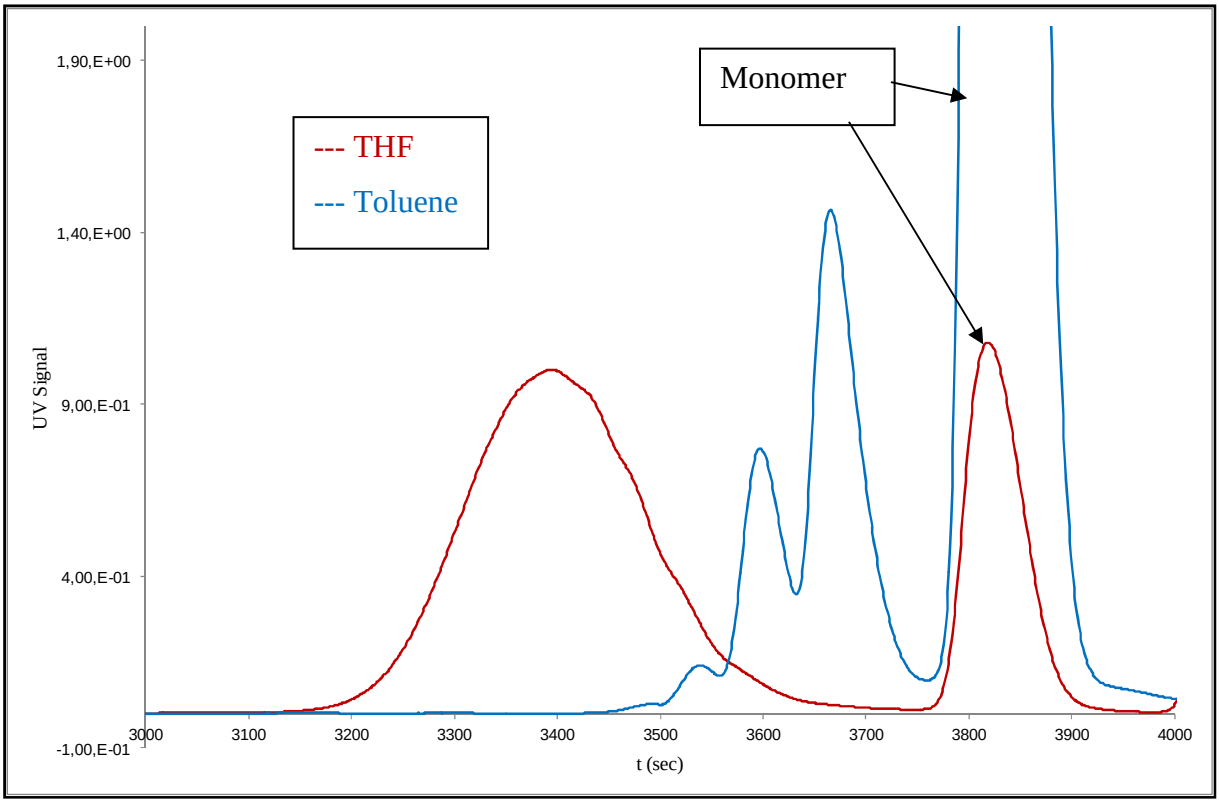

Figure 3: lactide polymerization in toluene and THF

Figure 3 shows that chain growth rate is much higher using THF rather than toluene. After 4 hours, while in THF the presence of high molecular weight species and a decrease in the amount of residual monomer is observed, in toluene reaction is much slower and there are only low molecular weight oligomeric species, as well as a large amount of unreacted monomer. This is due to the lower polarity of toluene compared to THF in addition to the lower solubility of lactide. Looking at the conversion values for two oligomers, having [lactide]/[T1] ratio of 15, shown in the graph of figure 4 the big difference between the reaction rates in the two solvents are clearly visible.

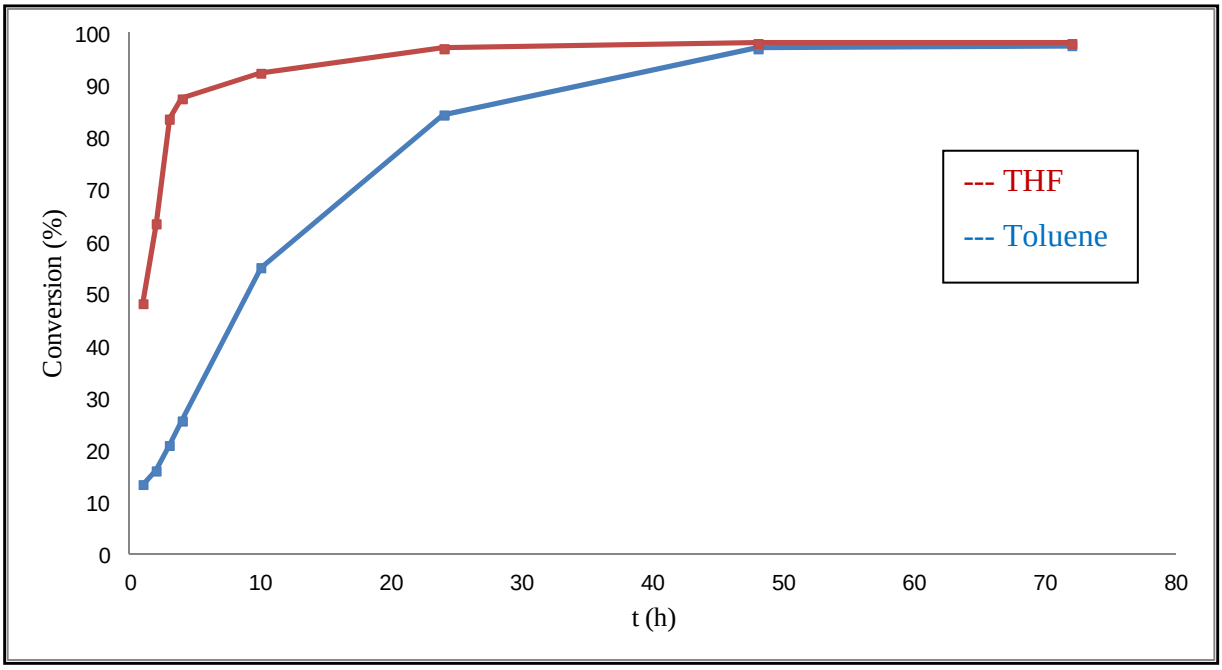

Figure 4: % of conversion Vs time

Analyzing the conversion, determined by ^{1}HNMR analysis, as function of time can be seen as the beginning of polymerization in tetrahydrofuran is extremely fast, so since after one hour of reaction the conversion is about 50%; chain growth proceeds with a high speed until it reaches a conversion of 90%, at then a decrease in speed due to the decrease in the concentration of monomer in solution can be observed: a plateau is reached after 24 hours from the beginning of the polymerization reaction. Comparing the data obtained for the polymerization in THF with those of the reaction in toluene is evident that the reaction rate in toluene is significantly lower, especially at the beginning of the reaction and undergoes further reduction when conversion is just over 50%, probably due to the lower solubility of the polymer in this solvent; the time required to have a total consumption of the monomer introduced in feed is more than 50 hours, more than twice in comparison to THF, although reaction was 70 °C, ten degrees higher than the one used for tetrahydrofuran.

The choice of solvent is therefore also crucial to avoid excessively long polymerization times, which could promote the competition between chain growth and side reactions favoring the latter and therefore leading to a more difficult control of molecular masses and polydispersity.

4.2 CONTROLLED MACROMOLECULAR ARCHITECTURE PLA OBTAINED BY SOLUTION POLYMERIZATION

4.2.1 Synthesis of low molecular weight species

After checking the different rates of polymerization in the two solvents, a series of oligomers was synthesized, using the comonomers described in Figure 1. Although the reaction kinetic is very slow using toluene, for low values of the [monomer]/[comonomer] ratio both solvents were used to assess whether, at least for the lower molecular weights, it is also possible to use toluene as solvent for the reaction, obtaining values close to the programmed ones .
Table 1 shows the feed and the molecular properties of the samples synthesized in toluene and THF.

[M]/[CM]	Comonomer	Solvent	Mn SEC PS	Mn SEC PLA	Mn ^{1}HNMR (DPn)	D
15	T1	THF	1372	1292	1160 (16)	1.19
15	T2	THF	1312	1228	1008 (14)	1.20
15	T3	THF	1248	1226	1126 (15)	1.14
15	T4	THF	1305	1217	1008 (14)	1.11
15	T1	Toluene	1395	1100	1152 (16)	1.15
15	T2	Toluene	1310	1144	1080 (15)	1.10
15	T3	Toluene	1246	1218	1008 (14)	1.13
15	T4	Toluene	1248	1225	1008 (14)	1.09

Table 1: feed and molecular properties of PLA with [M]/[CM]=15

As already discussed in chapter 3, molecular weight values expressed as PLA equivalent are closer to the one measured by ^{1}HNMR than values expressed as PS equivalent.
Data in table 1 show that both THF and toluene are good solvents for the polymerization of lactide: molecular weight can be controlled, values are in agreement with the feed, and polydispersity for all samples is always close to 1.

Mn values determined by SEC analysis are not affected by the hydrodynamic volume contraction caused by the presence of star like macromolecules, linked to the different nature of the comonomers used, probably because of the low [M]/[CM] ratio does not allow the star species to take a more compact conformation in solution than the linear species.

Molecular weight values obtained by chromatographic analysis with polystyrene calibration are higher than those measured by ^{1}HNMR due to the higher hydrodynamic volume of polystyrene in solution compared to PLA, as discussed previously in chapter 3.

After testing the functionality of both systems with very low DPn values the degree of polymerization was increased in order to verify if both solvents could be used to obtain high molecular weight polymers.

Eight new samples, described in table 2, were synthesized with planned DPn = 100; polymerization conditions were maintained identical to those used for the synthesis of polymers with DPn of 15, and the only variable parameter was the time required to complete the reaction.

Observing the progress of the reaction it was immediately clear that the use of toluene is not suitable for the synthesis of PLA with higher molecular weight ([monomer]/[monomer] = 100) due to poor solubility of polylactic acid in hydrocarbon solvents; increasing the value of Mn as the conversion increases, a partial precipitation of the polymer is observed, resulting in non-homogeneity of the system, with all kind of comonomers.

Because of this a quantitative conversion cannot be achieved, and Mn values obtained are lower than ones planned.

SEC analysis confirms what is observed: beyond a certain value of molecular weight, when precipitation occurs, there is no further increase in the Mn values, but only a broadening of the distribution curve with appearance of a shoulder in the area of low molecular weight caused by the non-uniformity of the macromolecules growth process (Figure 5).

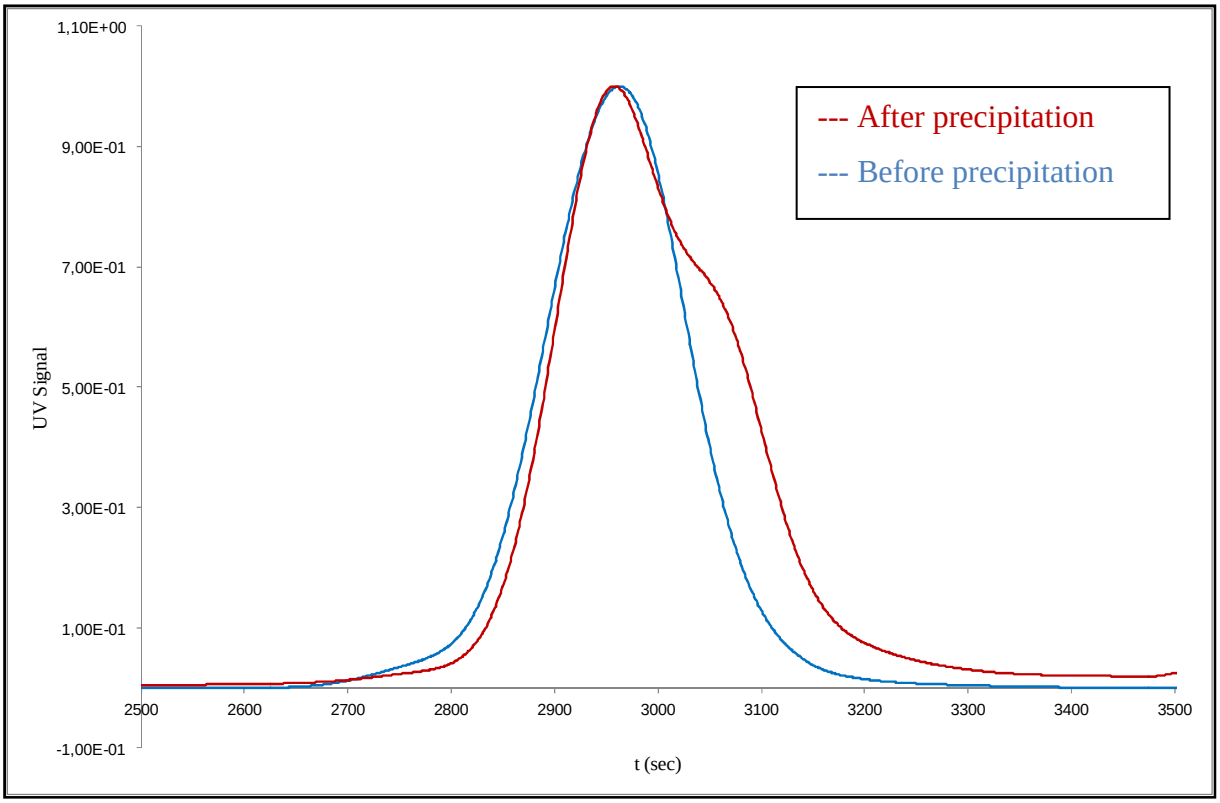

Figure 5: increasing in polydispersity after PLA precipitation

Keeping constant the programmed value of DPn using THF as solvent, polymers with molecular weight values close to those planned and with a good control of the polydispersity are obtained, as can be seen from the data in table 2.

[M]/[CM]	Comonomer	Solvent	Mn SEC PS	Mn SEC PLA	Mn ^{1}HNMR (DPn)	D
100	T1	THF	6912	6552 (91)	6480 (90)	1.18
100	T2	THF	5915	6271 (87)	6408 (89)	1.19
100	T3	THF	6840	6217 (86)	6408 (89)	1.19
100	T4	THF	6744	6485 (90)	6552 (91)	1.18
100	T1	Toluene	4870	4525 (62)	4176 (58)	1.26
100	T2	Toluene	4936	4639 (64)	4680 (65)	1.36
100	T3	Toluene	5000	4700 (65)	4464 (62)	1.27
100	T4	Toluene	4380	4070(56)	3960 (55)	1.30

Table 2: feed and molecular properties of PLA with [M]/[CM]=100

Polydispersity of the samples synthesized in toluene are higher than those of polymers obtained in tetrahydrofuran because when molecular weight value gets higher, the solubility of PLA in toluene is too low.

4.2.2 Synthesis of high molecular weight species

The synthses previously reported show that in THF it is possible to synthesize polymers with high DPn values with an excellent control of molecular masses and distribution; therefore other samples with higher molecular weight were synthesized. A [M]/[CM] ratio of 100 has set for T1 containing polymer and is held constant the number of repeat units for each arm changing the comonomers, to obtain PLA with different total DPn of 200, 300, 400, as reported in table 3.

Comonomer	[M]/[CM]	DPn for each arm	Total DPn	Programmed Mn
T1	100	100	100	7200
T2	200	100	200	14400
T3	300	100	300	21600
T4	400	100	400	28800

Table 3: molecular characteristics of star PLA with constant arm length

Table 4 shows the values of molecular weight and polydispersity of PLA synthesized. It is interesting to note that there is always an high discrepancy between the value obtained from the analysis of end groups by ^{1}HNMR, corresponding to the real Mn value, and the molecular weight values obtained by SEC analyses; this because of the different performance of the calibration curves in the PLA and PS, which becomes more pronounced in the area of medium and high molecular weights.

[M]/[CM]	Comonomer	Solvent	Mn SEC PS	Mn SEC PLA	Mn ^{1}HNMR (DPn)	D
100	T1	THF	7026	6412 (89)	6446 (90)	1.12
200	T2	THF	17116	11835 (164)	12960 (180)	1.16
300	T3	THF	31924	17642 (245)	19584 (272)	1.11
400	T4	THF	43578	25794 (358)	27648 (384)	1.11

Table 4: feed and molecular properties of PLA with a arm length of 100

SEC curves of polymers described in table 3 are reported in picture 6.

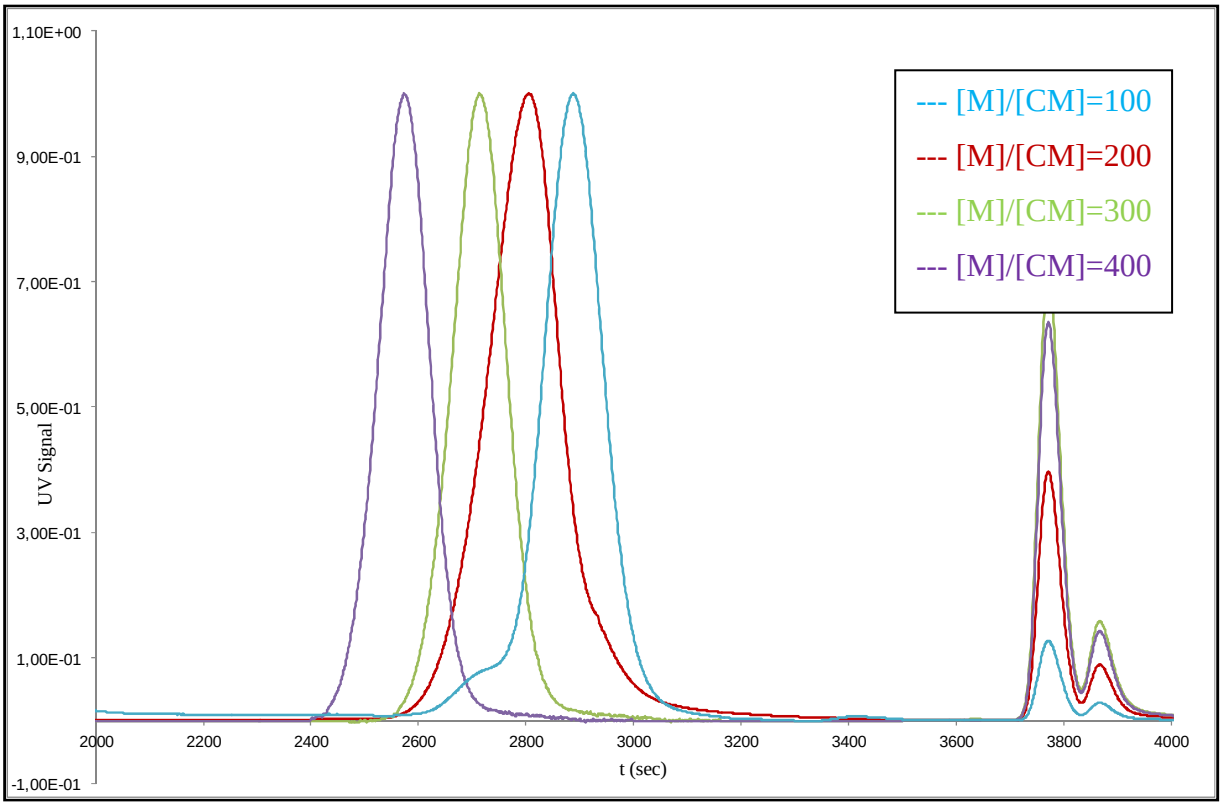

Figure 6: SEC curves of PLA with the same arm length

SEC curves in figure 6 show again how solution polymerization in THF allows to control the molecular parameters of polymers synthesized: curves do not exhibit non-homogeneities related to interference with the process of chain growth, even for samples with higher molecular weight.

The values of molecular weight and degree of polymerization are in agreement with the [M]/[CM] ratio, confirming that in the absence of factors that can disturb the polymerization it is possible to achieve complete consumption of the monomer. Polydispersity is close to 1 for all polymers, regardless of the type of comonomer used.

^{1}HNMR shows that comonomers is linked to the polymer chains and there are no free hydroxyl functionalities which have not reacted. These data further confirm the regularity of the structures obtained, as already confirmed by molecular weight values and especially by polydispersity values, obtained from the SEC analyses. Figure 7 shows the ^{1}HNMR spectrum of PLA synthesized using T3 species as comonomer: in the area between 4.5 ppm and 3 ppm only the signals related to terminal CH and to CH_2 of the comonomer directly bound to the polymer chain are present, while the signals related to unreacted CH_2OH of T3 do not appear.

Thes data correlated with SEC curve show that the polymer is formed by chain starting from the OH groups of the comonomers, confirming the homogeneity of the macromolecular structure.

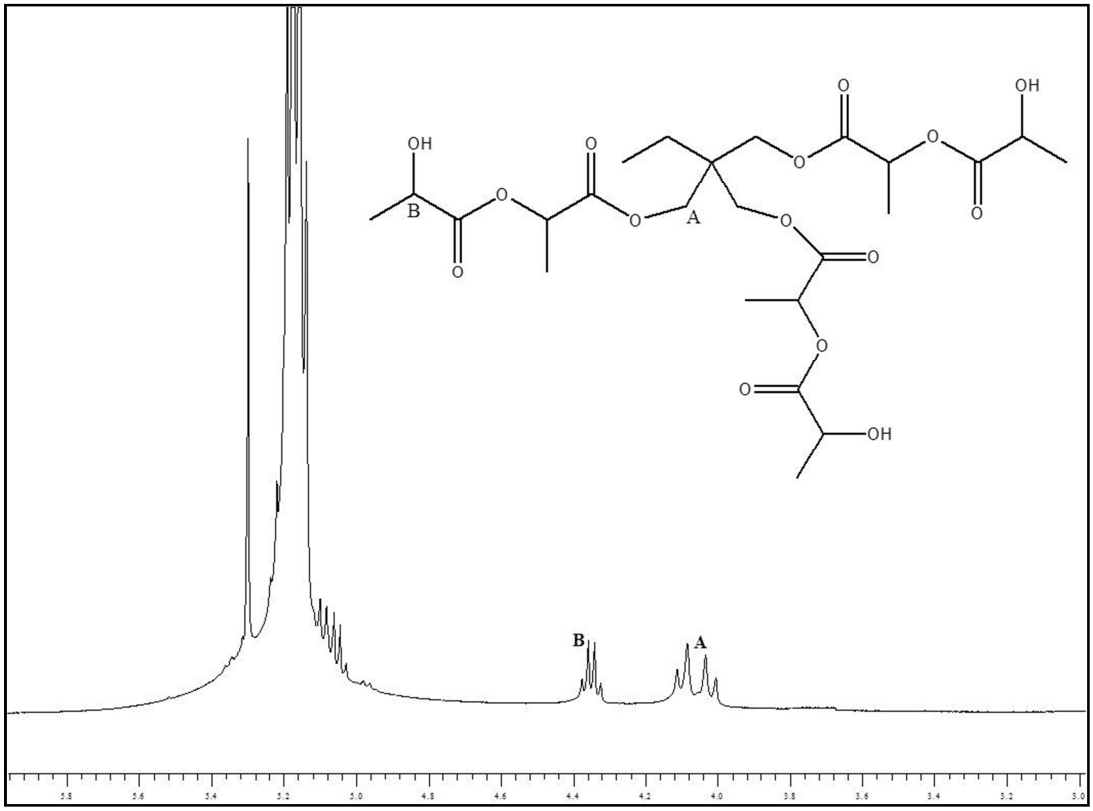

Figure 7: NMR spectra of PLA with T3

NMR can evidence the presence of unreacted comonomers, but if comonomer has only partially reacted and if chains don't simultaneous start from OH groups of comonomer probably NMR spectra is similar to one reported in picture 7; in this case GPC curves would be very different. The increasing of the polydispersity indicates the presence of a variety of macromolecular species characterized by different molecular masses, indicating a lack of homogeneity of the system.

In conclusion solution polymerization is thus certainly useful for understanding the mechanisms that regulate the polymerization of lactide, as well as to synthesize model molecules with an high control of molecular weight values and polydispersity, but requires, as we have seen, to operate under controlled conditions to avoid side reactions that can compete with the propagation of the chain.

4.3 RELATION BETWEEN POLYMERIZATION TIME AND POLYMER STRUCTURE

Among the many factors that must be monitored to control the polymer structure, purity of reagents and polymerization time are the most important ones.

In this regard, while it is noted that there is not a significant difference between the polymerization carried out using highly purified reagents and the reaction with commercial monomers and comonomers, it is interesting to observe the effect of polymerization time on the shape of the molecular weights curve. Figure 8 shows the GPC curves of two samples with the same feed [M]/[CM] ratio of 300, but different reaction time. Increasing polymerization time there is a moderate increase in the molecular masses, and the predominant phenomenon is a broadening of the distribution curve, especially from the area of low molecular weight, reaching a Mw/Mn equilibrium ratio typical of polycondensates. D value is significantly higher than the the one of the PLAs previously synthesized by controlling the kinetics of the reaction, and it is quite similar to a typical distribution of polymers synthesized through a polycondensation process.

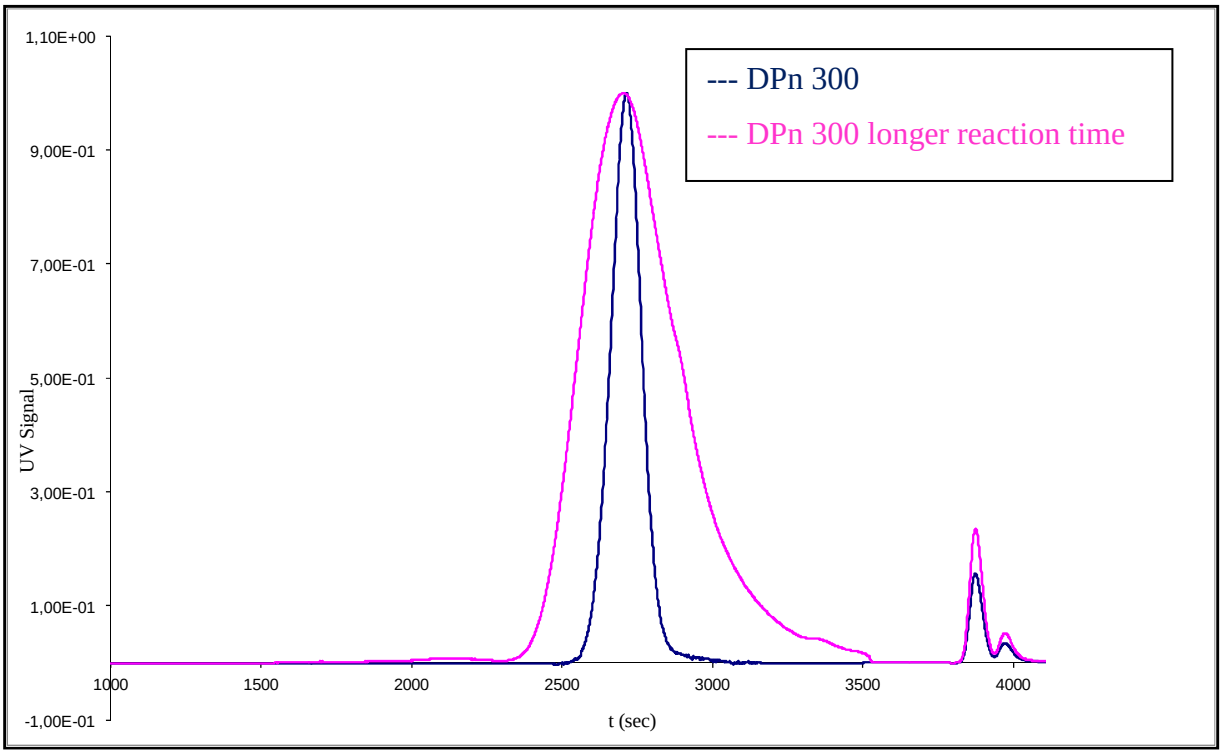

Figure 8: effect of polymerization time on D and Mn values

D value for polymer synthesized with longer reaction time reaches a value of 1.40, which is a typical value of the systems obtained by polycondensation in the presence of a trifunctional comonomer,[5]. In literature, the increase in molecular weight distribution has been studied by several research groups[6,7], who attributed the phenomenon to several factors, such as side reactions that interfere with the macromolecular chain growth mechanism, caused by high temperatures and long reaction times; the presence of impurities can also promote polymerization process competing with the function of comonomer.

As already mentioned before, the use of non purified did not bring any change in the molecular masses distribution curve; in literature is reported a ^{13}CNMR spectra of PLA that shows, in the presence of side reactions such as epimerization, a multiplicity of signals in the methine region[8] (Figure 9).

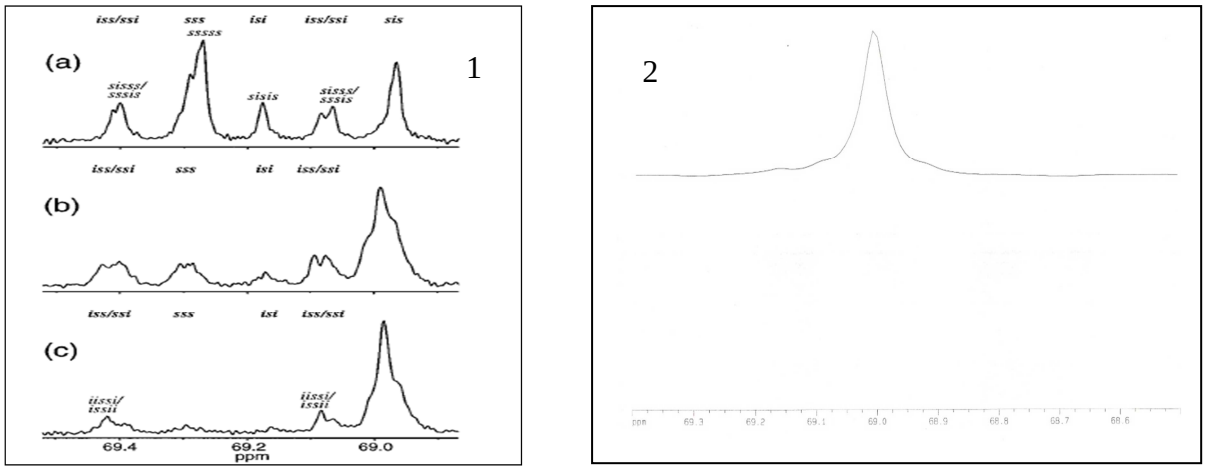

Figure 9: ^{13}CNMR of PLA in presence of epimerization(1) and without epimerization (2)

Comparing the two spectra in figure 9, PLA synthesized for this work (2) have only signals relating to the methine of L-lactic units: there are no undesired species coming from epimerisation reactions. On the contrary in the spectrum shown in literature[8] there are many different signals. The increase of the distribution is not therefore linked to a variation of the stereochemistry of the polymer, but probably caused by backbiting or transesterification reactions.

To verify this hypothesis several PLA with [M /[CM] ratio of 15 have been synthesized in the same reaction conditions used for the samples described in table 1, simply increasing the polymerization time beyond those necessary to achieve the total conversion.

MALDI-TOF technique was used to characterize these samples (Figure 10). The spectra show the presence of two different distributions of molecular masses, one for sequences with an even number of monomer units and the other, unexpected given the nature of the starting monomer (lactide) that should lead only to an even number of repeating units, due to the uneven sequences.

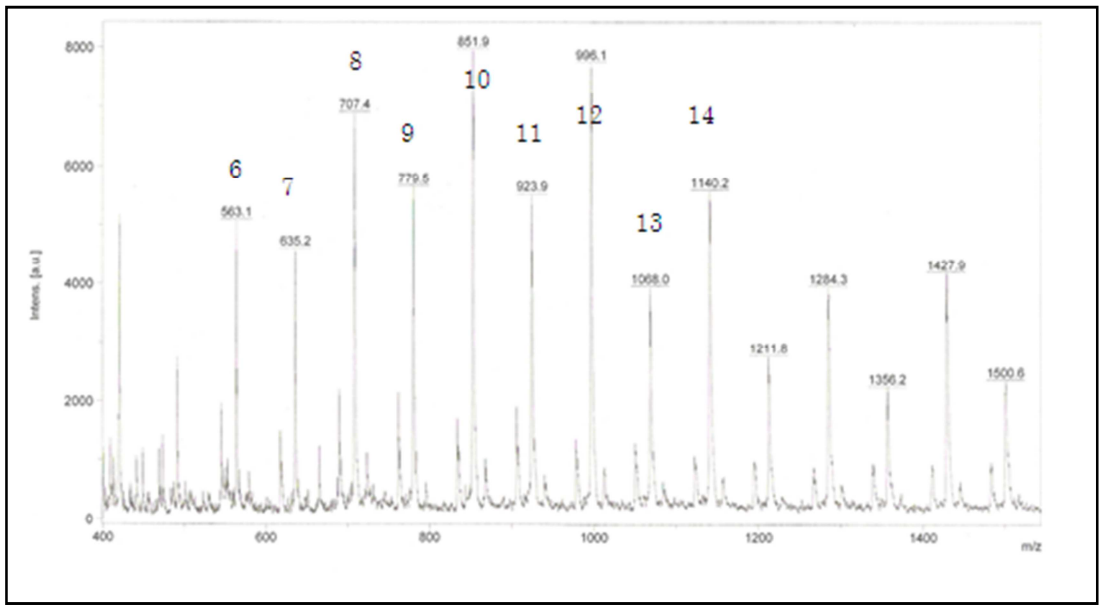

Figure 10: MALDI-TOF spectra of PLA with Dpn of 15

MALDI-TOF spectra in figure 10 shows the presence of species with an uneven number of lactic units in the chain, a phenomenon related to transesterification or backbiting reactions that may occur extending the reaction time caused by the attack of last repetitive units on internal lactic unit of polymer chain, resulting in the formation of a chain that can have an uneven number of lactic species. Working with these reaction conditions, D value tends to grow reaching typical values obtained in the polycondensation reactions that depend on the conversion achieved and on the [M]/[CM] ratio in the feed.

4.4 CONCLUSIONS

Solution polymerization is very efficient for the synthesis of PLA, even at high molecular weight, for polymers that require a strict control of the macromolecular parameters.

It is possible to synthesize polymers with programmed molecular weight in order to design the final characteristics of the PLA. The polarity of the monomer requires a careful choice of reaction solvent to avoid precipitation phenomena which may affect the progress of polymerization and then change the molecular weight and polydispersity of the polymer: for this reason THF is suitable for this type of synthesis.

The use of comonomers having different reactive hydroxyl functionality allows to synthesize PLA with controlled molecular weight: the data obtained by ^{1}HNMR analysis show that there is agreement between the values actually achieved and those planned in the absence of factors that may disturb the process of growth.

Polymers are obtained with a very narrow molecular weight distribution, close to 1, further proof of the high control system that can be achieved with this technique. Controlling some parameters, in particular increasing the polymerization time a plateau of the conversion curve is reached: an increase in the values of polydispersity of the polymers compared to those recorded under optimal conditions is observed; molecular weight distribution tends to a equilibrium value typical of polycondensates because of backbiting reactions and/or transesterification reactions promoted by excessive polymerization time.

The synthesis of PLA in solution is certainly a good technique to prepare ideal model systems for which the equality of species is required. This synthesis is obviously not applicable on industrial scale to produce commodities, due to the high costs and necessary precautions for the use and disposal of solvents, as well as the high reaction times required.

On the other hand monodisperse PLA obtained with controlled conditions could be used in high added value biomedica applications (drug delivery system, etc.) were monodisperse samples are often required.

In later chapters will be described how the structure of a polymer is related to its molecular and rheological properties.

REFERENCES

[1] De Jong, S. J., Van Dijk-Wolthuis, W. N. E., Kettenes-van den Bosch, J. J., Schuyl, P. J. W., Hennink, W. E., *Macromolecules*, 31, 1998, 6397–640.

[2] Jalabert, M., Fraschini, C., Prud'Homme, R.E., *J. Polym. Sci. Part A*, 45, 2007, 1944-1955.

[3] Sun, J., Wu, L., Chinese Journal of Polymer Science, 14(4), 1996, 324-329.

[4] Köhn, R. D., Pana, Z., Sunb, J., Liang, C., Catalysis Communications, 4(1), 2003, 33- 37.

[5] Yuan, C.M., Di Silvestro, G., Speroni, F., Guaita, C., Zhang, H., Macromol. Chem. Phys., 202, 2001, 2086-2092.

[6] Dubois, P., Jacobs, C., Jerome, R., Teyssie, P., Macromolecules, 24, 1991, 2266-2270.

[7] Kowalski, A., Libiszowski, J., Duda, A., Penczek, S., Macromolecules, 33, 2000, 1964-1971.

[8] Takur, K. A. M., Kean, R. T., Hall, E. S., Macromolecules, 30, 1997, 2422-2428.

5. Study of star shaped PLA

5 STDUY OF STAR SHAPED PLA

5.1 THEORY OF POLYMERS WITH STAR ARCHITECTURE

The synthesis of polymers with controlled macromolecular architecture has always been one of the objectives of academic and industrial research to obtain polymers with rheological and mechanical behavior different from that of standard materials.

This approach is widely used, for example, in the field of polyamides, that are the subject of several papers in the literature describing the use of different kind of multifunctional comonomers, used to modify macromolecular architecture.

Regarding PLA, the state of art is quite different: polymers with complex architecture are described in the literature, typically star or dendrimer systems, but most academic papers aim at understanding the mechanism of polymerization in the presence of polyfunctional molecules and obtaining a structure as homogeneous as possible, while there are no studies concerning a possible use of macromolecular architecture control to improve the properties of the polymer, topic that will be discussed in this work.

Two different methods can be used to synthesized a systems with this particular type of molecular architecture: convergent synthesis and divergent synthesis.

Both synthetic routes require the availability in the reaction mixture , although at different times, of a star agent that must have at least three identical reactive functional groups, complementary in terms of reactivity, to the functional groups provided by the monomer molecules.

Defining RA_f the molecule of star agent having *f* functional groups of type A and if in the reaction there is an AB type monomer, the formation of macromolecules with star-shaped structure can occur for the growth of polymer chains of type -BA-BA-BA- at least on three functional units of the comonomer. RA_f agent is like a starting ramification point from which several arms, formed by AB monomer units, can growth.

Figure 1 shows a representation of a star shaped macromolecule.

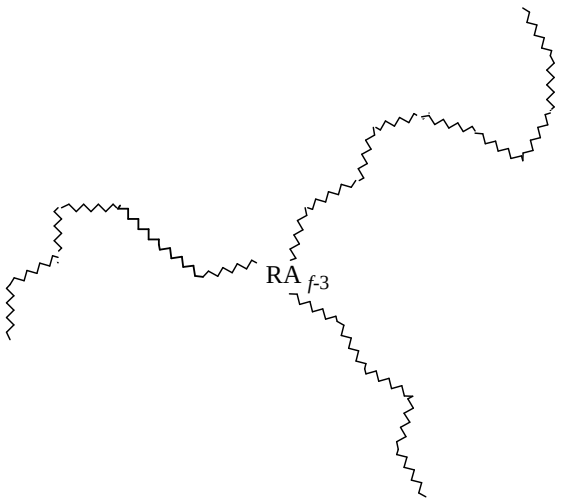

Figure 1: three arms star shaped macromolecule

In figure 1 the represented macromolecule is a star species with three arms and the comonomer has still available a number of A reactive groups equal to f-3; moreover the length of the arms should not necessarily be the same for all the branches that originate from the central comonomers, but generally these sizes vary from arm to arm on a statistical basis of growth.

Theoretically the multifunctional agent can be copolymerized with an AA and BB monomers or with an AB monomers.

The copolymerization of star agent with AA and BB monomers, however, shows a serious problem, related to the possibility of formation of stars with arms terminated both with functional groups of type A and type B; in this case the condensation of two star-shaped macromolecules with the formation of a multiple star could occur. This iper-star structure may further react with other macromolecules with the formation of a multifunctional cross-linked structure. Crosslinked materials, in these cases, are generally undesirable because they are not processable, usually brittle and not extrudable from plants running continuously.

The growth of the chains from comonomer during lactide polymerization is based on the ring-opening reaction promoted by the functional group A of the comonomer therefore group A will always be the terminal group of the chain; therefore it is not possible to have a reaction between two or more star macromolecules and the reaction mixture is composed of linear and star species of finite size.

The multifunctional comonomer in this case acts as a multifunctional chain regulator. The greater the amount of reactive groups in the feed with the comonomer the lower the molecular weight of the final polymer.
The star agents used in polymerization must have some intrinsic characteristics to give the polymer chemical and technological desired properties.
Comonomer must have:

- *Thermal stability*, necessary because the polymerization temperature is high and a possible degradation of the monomer leads to a yellowing of the polymer, and to a lower molecular weight.
- *High purity*, required to achieve very high molecular weight and therefore high performance materials. The purification of the product is facilitated if it can be obtained by crystallization.
- *Colorless*, to avoid problem with materials that must not be colored during processing.
- *Easy to synthesize and cheap*, because the synthesis and the use of comonomers in polymerization reaction must not affect significantly the total production cost of the polymer.

The comonomers used in this work are mainly four: an hexa-functional polyol (T6), a tetra-functional polyol (T4), a tri-functional polyol (T3), a bi-functional alcohol (T2) and a mono-functional alcohol (T1); the last two molecules do not act as star agents, because they can allow the growth of one or two polymer arms, creating linear macromolecular species. Alsothe behaviorof multifunctional agents with carboxyl reactive groups has been tested but, as already mentioned in chapter 2, acid functions interfere with the polymerization process and not allow to obtain the desired structure.

Structures of the comonomers used for the synthesis of star systems are here reported:

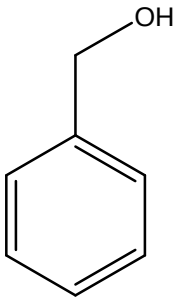

T1

Benzyl alcohol

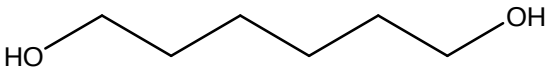

T2

1,6 Hexanediol

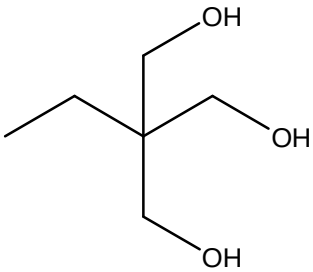

T3

Trimethylolpropane

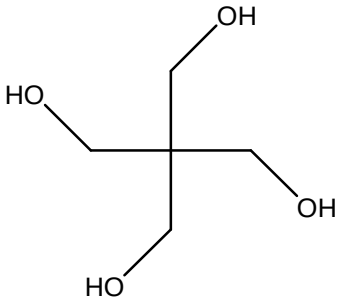

T4

Pentaerythritol

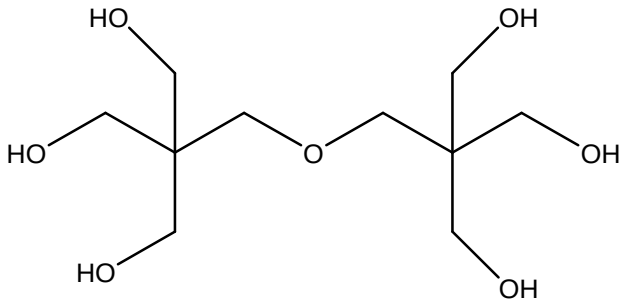

T6

Dipentaerythritol

The most important feature ofof polymers with star architecture is the decrease in hydrodynamic volume in comparison to linear polymers of the same nature which have the same molecular weight (Mn). This feature results in a lower viscosity of the polymer melt during its processing, for example during a process of injection molding. It follows that the material at a temperature T1, has a viscosity similar to a linear polymer with the same molecular weight at the temperature T2>T1. In other terms, at the same processing temperature, a star polymer is able to fill in better a mold than a linear polymer: for these reasons materials with a star architecture are suitable for the molding of complex objects with special shape or low thickness. Moreover there is an energy saving (the injection machine uses less power to process the material) and a simple processing step.

5.2 DISTRIBUTION AND CALCULATION OF MOLECULAR WEIGHT OF STAR POLYMERS

5.2.1 Flory theory

Academic studies regarding modified architecture polymers date back to Flory, who was the first to study polymerization reactions in the presence of multifunctional agents having two or more reactive groups of the same nature. His studies were conducted on the process of polycondensation of caprolactam. During these studies he assumed that all functional groups of star agent were reacted and that in the reaction mixture were present molecules with a number of arms equal to the number of functional groups of multifunctional agent (full star chains). The experimental evidence of the presence of terminal amino groups, even if he used a multifunctional agent with acid groups, led him to consider that in the reaction mixture were not only the full star molecules, but also the linear molecules that do not react with the multifunctional agent.

Basing on these considerations, Flory, developed a statistical theoretical model[1] calculating average molecular weight, numeral molecular weight and the fraction of linear species for polycondensation products of AB monomers in the presence of multifunctional agents RA_f.

This model was intuitively valid for reactions with total conversion and in presence of very small concentrations of star agent, because only in these conditions the statistical hypothesis of complete reaction of functional groups of the star agent could occur. In fact in his works Flory aimed to achieve a complete star polymer therefore he pushed her reactions to high degrees of conversion. Equation 5.1 provides the distribution of molecular masses for the full star species basing on the model developed by Flory.

$$\left(\frac{\overline{x_w}}{\overline{\overline{x_n}}}\right)_b = 1 + \frac{b(1-L)(1+Q)}{[b(1-L)+(Q+L)]^2} \qquad 5.1)$$

Subsequently, after several years from the original work of Flory in 1948, Farina[2] resumed the same concepts proposed by Flory and developed the equations for the calculation of the polydispersity of star polycondensed polymers. Only recently, in 2001, Yuan[3] reconsidered the scheme at the base of the kinetic model of Flory to develop a more complete statistical model.

5.2.2 Farina theory

Farina, in a research aimed at preparing polyamides with modified molecular weight distribution to study their chemical-physical and technological properties, approached the study of the general equations for the distribution of molecular masses of polymers obtained by polycondensation in the presence of the monomer and of a multifunctional chain regulator with a general structure R_{af}.

The polymer thus obtained were considered, approximately, as homogeneous mixtures of non-regulated chains (linear species) and chains regulated by the co-monomer with a number of arms equal to the number of groups of the multifunctional reagent; as already reported in Flory hypothesis, it was not considered the possibility that star macromolecules could be constituted by a number of arms lower than the number of reactive groups present in the monomer. Following this philosophy, Farina[2], considering the theory of Flory and the properties of polymer blends, developed the following mathematical expression for calculating the distribution of molecular masses:

$$D = 2 - \frac{(f-1)^2}{f} x_{w2}^2 + \frac{(f-1)(f-2)}{f} x_{w2} \qquad 5.2)$$

X_{w2} indicates the fraction weight of polymer with the comonomer unit, in other words the fraction weight of regulated macromolecules. The equation proposed by Farina is easier to understand than the rigorous treatment proposed by Flory and allows to calculate the index of dispersion with an error lower than 1%, much smaller than the experimental errors usually made with the analytical techniques that allow to determine the value of polydispersity index, like for example size exclusion chromatography (SEC).

Recently Yuan[3] developed a statistical model that is more complete and complex than that proposed by Farina.

5.2.3 Yuan model

In Yuan model[3], analytical expressions of the average numeral degree of polymerization (DPn), the average weight degree of polymerization (DPw) and the dispersion index, D, of different polymeric species are obtained as a function of monomer conversion of functional groups of the RA_f.

$$P_{r-i} + P_i \xrightarrow{k_C} P_r \qquad r > i = 1,2,..., \; P_1 = AB$$

$$RA_f + P_r \xrightarrow{f\,k_C'} P_r^1 RA_{f-1}$$

$$P_r^1 RA_{f-1} + P_i \xrightarrow{k_C} P_{n+i}^1 RA_{f-1}$$

……

$$P_r^l RA_{f-l} + P_i \xrightarrow{(f-l)k_C'} P_{r+i}^{l+1} RA_{f-l-1}$$

$$P_r^l RA_{f-l} + P_i \xrightarrow{k_C} P_{r+i}^l RA_{f-l} \qquad l = 1,2,..., f$$

Figure 2: reaction scheme proposed by Yuan

In figure 2, Pr is the pure linear chain, which has not undergone any act of reaction with the RA_f comonomer and it is formed only by repeating units of r monomer. Pr_lRA_{f-l} represents the species branched with r monomer units and for which only *l* functional groups of the comonomer is reacted: this species can be defined as star with *l* arms, which, for *l* = 1 and *l* = 2 are really linear macromolecules, even if containing multifunctional monomer unit; there are also unreacted (f-l) groups of the comonomer.

Unlike Flory[1] therefore, there are three different types of linear species: one coming from the polycondensation of the AB monomer (linear primary) and those coming from the reaction of one or two functional groups of comonomer (linear star).

It is possible to define a star macromolecule only if at least three functional groups of the comonomer are reacted.

A very complex kinetic reaction scheme as as the one proposed by Yuan, needs some approximations to be solved considering all species in it. The hypothesis include:

1) the assumption of equal reactivity of functional groups of the polymer chain, regardless of the length of the chain;
2) the equal reactivity of the functional groups of the comonomer, regardless of the time they react, which is equivalent to assume that the steric impediment of arms is irrelevant;
3) the absence of side reactions not considered in the kinetic model.

Basing on these fundamental hypothesis, the kinetic constants in the reaction scheme proposed in figure 1 have the same value. Yuan proposed the following expression for the calculation of the distribution of molecular masses:

$$D(\lim) = \left(a + 1 + \frac{1}{f} \right) \left(1 - \left(\frac{fa}{1 + fa} \right)^{f} \right) \qquad 5.3)$$

a is the C_0/N_0 ratio in the feed. Then is possible to conclude that:

- The molecular weight of the polymer essentially depends on the initial C_0/N_0 ratio: the lower is this value, the higher the molecular weight that can be obtained with a total reaction conversion.
- The distribution of the molecular weight decreases increasing RA_f comonomer functionality.
- The index of dispersion, D, depends not only from the functionality f, as described in the model of Farina, but also by the molar ratio between monomer and comonomer in the feed.

Yuan model shows that polymers with a star architecture have an higher complexity than the one suggested by Flory and Farina in their models. For this reason, to take advantage of polymeric materials with a star architecture, it is necessary to optimize the production process in order to optimize the ratio between the different species, linear or with star architecture, constituting the final material. The fraction of the star is responsible for the decrease in melt viscosity during processing, while the linear part gives the material good mechanical properties.

5.3 STUDY OF PLA STAR POLYMERS

PLA has a structure different from a polyamide, both from the point of view of the length of monomer unit both in terms of the chemical bonds along the chain, therefore it is necessary to determine if the structures obtained in the presence of comonomers have a distribution of molecular masses similar to that expected from the model of Yuan, and if it is possible to use this type of architecture for the synthesis of macromolecular materials useful in some applications.

In this chapter the study of polymerization of lactide in the presence of RA_f multifunctional agents will be discussed, to define the complexity of these reaction systems and evaluate what are the effects of the presence of comonomers on molecular and rheological properties of PLA.

In the literature there are many works in which the PLA is synthesized in the presence of multifunctional agents having reactive hydroxyl groups to obtain star structures[4,5], but in these case the attention is focused on low molecular weight systems that are synthesized for mechanistic studies , while there are no studies about the correlation between macromolecular architecture and the properties of engineering materials, topic for the industry.

In chapter 4 the synthesis of star shaped PLA was already considered; in that case solution polymerization with four different multifunctional species, defined as T1, T2, T3 and T4 (respectively, with one, two, three and four hydroxyl groups that can react with the monomer forming the ester bonds) was used. Polymerization under controlled conditions allows to obtain model structures but these cannot be applied in the industry, both for the complexity of the synthetic method and for the final properties of the polymers. For these reasons in this chapter the synthesis of star systems prepared through bulk polymerization will be discussed in order to obtain some information about the methodology but also about a possible industrial application of this synthesis.

T1 and T2 comonomers do not give species with star architecture but only linear macromolecules; however, they have been used as chain regulators because they allow to obtain simpler structures to verify the results obtained with different analytical techniques.

It is important to remember the importance of thermal stability of multifunctional agents at high temperatures and during the polymerization reactions, fundamental to obtain PLA with high molecular weight and a decrease of the polydispersity index of the molecular masses of the species forming the polymer.

5.3.1 Evaluation of comonomers reactivity in bulk polymerization

A fast and practical way to evaluate how a comonomer behaves during the polymerization process is to synthesize oligomeric materials regulated using a high amount of multifunctional agent. By this way the effect of comonomers on the polymerization process will be greatly increased.

At first reactions were conducted in the presence 10% m/m of multifunctional agent respect to the lactic acid units in the feed.

The reaction was carried on by ROP of lactide promoted by the hydroxyl groups of the multifunctional regulator catalyzed by a tin species; the polymerization was conducted at 190 °C for 90 minutes and at the end the polymer had about 3% of unreacted monomer, measured by ^{1}HNMR analysis. Table 1 shows the feeds and the molecular properties of these oligomeric species.

Sample	Comonomer	% Tx	Mn SEC	D
1	T1	10	903	2.048
2	T2	10	923	1.448
3	T3	10	921	1.356
4	T4	10	867	1.302
5	T6	10	1023	1.174

Table 1: feed and molecular properties of PLA oligomers

These oligomers were analyzed by SEC to determine their molecular weight and their distribution. It is also important to verify if, as expected, this technique is valid for the study of star architecture PLA obtained by bulk polymerization.

Figure 3 shows the SEC curves of the oligomers described in table 1.

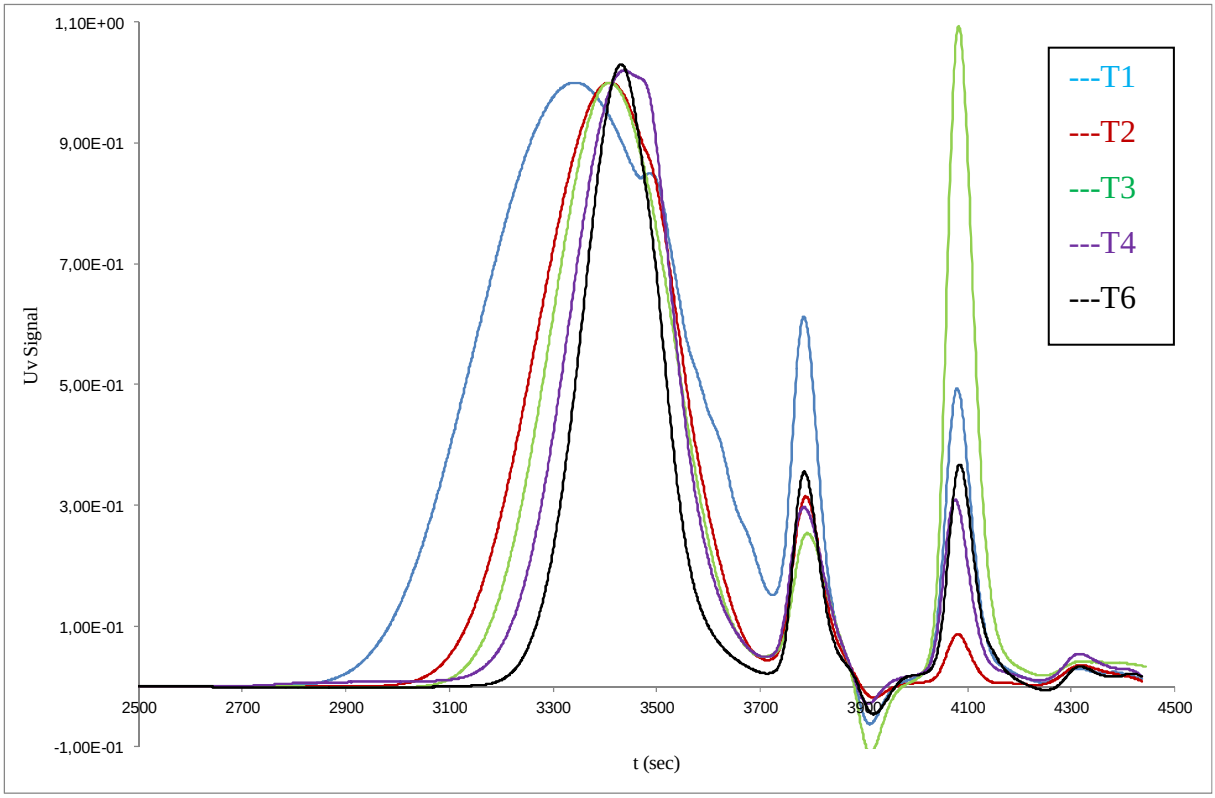

Figure 3: SEC curves of PLA oligomers

SEC curves reported in figure 3 show clearly the effect of multifunctional comonomers on the molecular properties of PLA, especially on the polydispersity index of the system; by increasing the number of reactive groups in the T_x comonomers, a marked narrowing of the curve of the polymer was observed, compared to a similar material synthesized in the presence of T1. Also T2 comonomer (red curve), which gives only linear species, shows a decrease of D values in comparison to the oligomer synthesized with T1 comonomer (blue curve).

The effect becomes even more pronounced in presence of comonomers with functionality greater than two, which give polymers with star architecture. The black curve, referring to the polymer with T6 comonomer, has a very narrow molecular weight distribution, close to 1.

Figure 4 shows the SEC curves of oligomer synthesized with 10% of T3 comonomer.

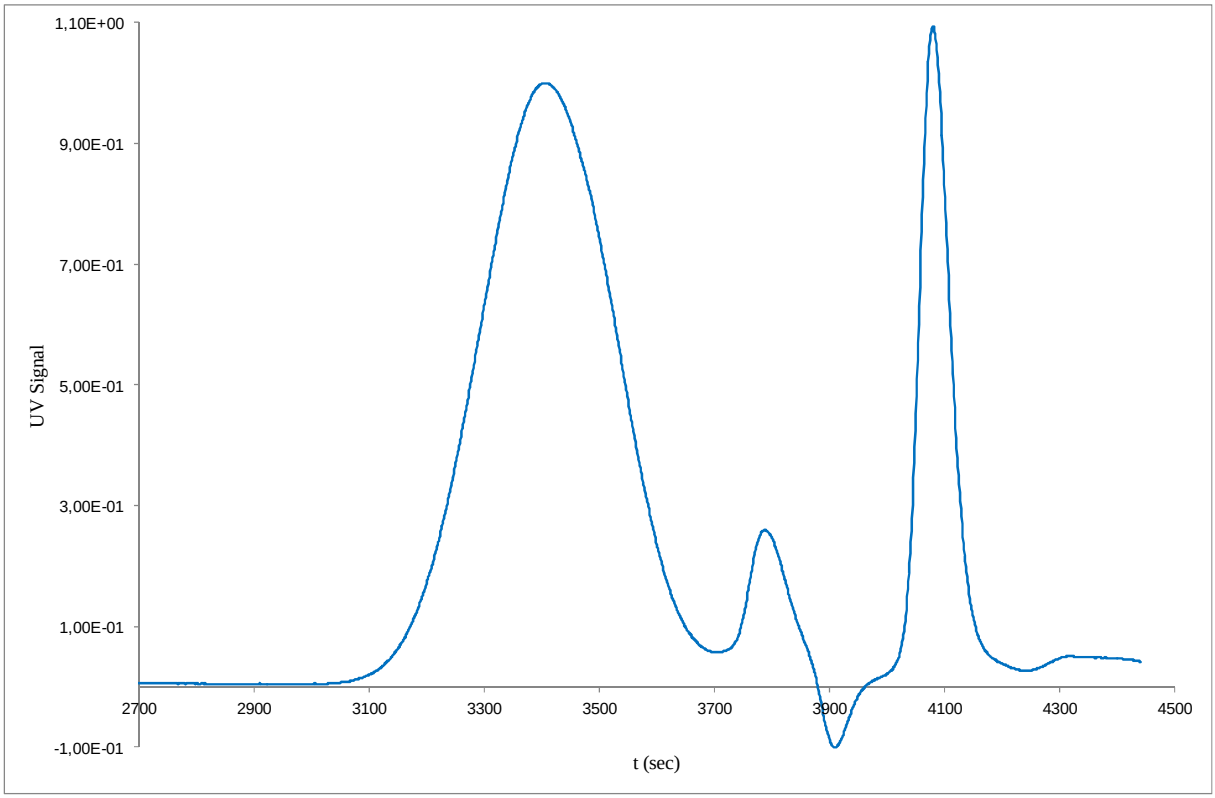

Figure 4: SEC curves of PLA with 10% of T3

Figure 4 shows that the T3 comonomer has effectively worked as a star agent modifying the macromolecular architecture of the polymer. Molecular masses distribution is narrower compared to that of oligomers without any comonomer. Data obtained by the integration of the curve, expressed as linear PLA basing on the SEC calibration system described in chapter 3, and reported in table 1 further confirm the effect of comonomers on the molecular properties of PLA. Both the Mn value and the distribution of molecular masses are affected by the presence of T3 comonomer.

Further experimental evidence may also be observed for a higher average molecular weight oligomers obtained with 5% m/m of T3 multifunctional agent (half of the quantity used for the sample reported in figure 4).

Figure 5 shows the SEC curve of PLA oligomer with 5% of T3 multifunctional agent.

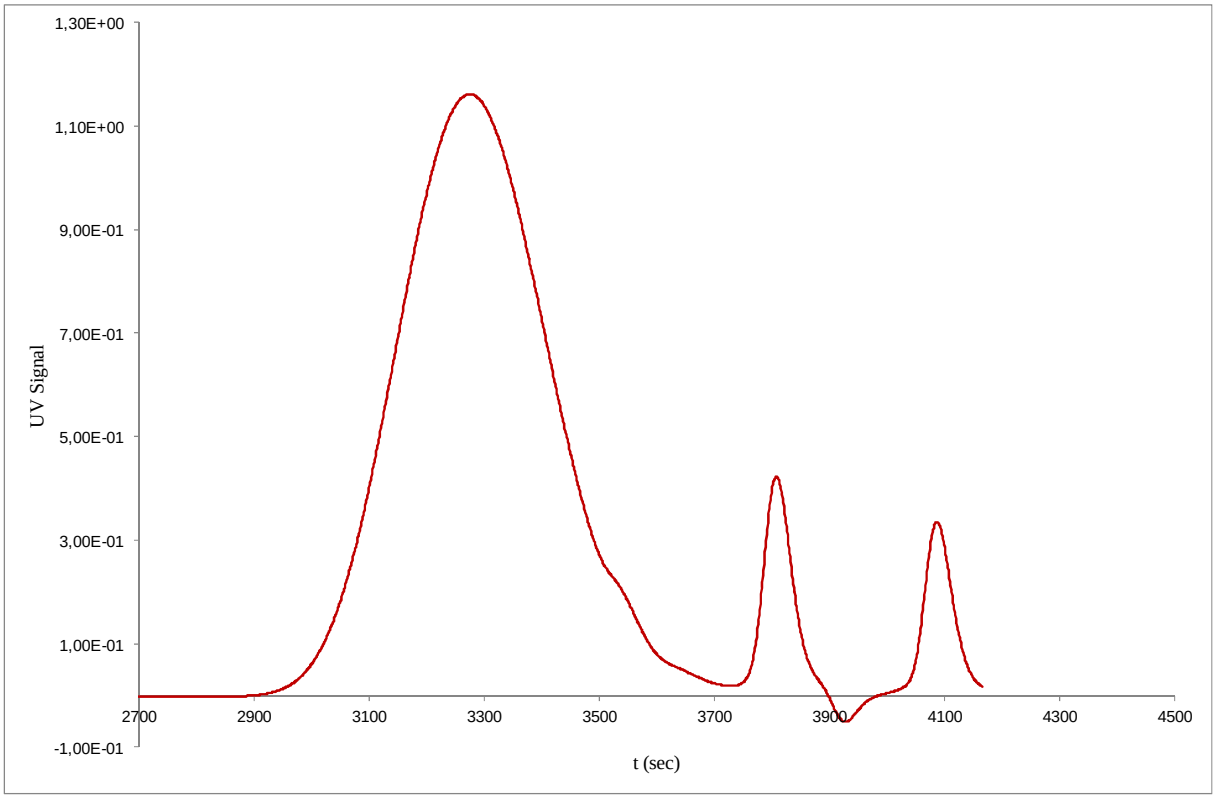

Figure 5: SEC curves of PLA with 5% of T3

Integrating the SEC curve for the sample shown in figure 5 the following values of average molecular weight and molecular weight distribution are obtained:

Mn: 1676 D: 1.386

The comparison between the values obtained for the polymer synthesized with 5% of T3 and those of the oligomer with 10% of the same comonomer shows that the method used for the synthesis of these materials allows to obtain a restriction on the distributions of molecular masses, and also allows to obtain an increase of Mn by increasing the [lactide]/[comonomer] ratio in the feed; the polymers always have a narrow distribution of molecular masses.

In chapter 4 the effect of factors such as polymerization time and reaction temperature was discussed concerning the solution polymerization of lactide because these parameters can lead to a broadening of D values up to values typical of a polycondensation process. Analyzing the data reported in table 1, and also observing the SEC curves in figure 3, oligomers synthesized in bulk, without strictly controlled reaction conditions, have a distribution of molecular masses that is different from that of polymers obtained by solution polymerization; D values are similar to the ones of materials obtained by polycondensation process.

The spectra of the oligomers were analyzed by ^{1}HNMR to get a further confirmation of the behavior of multifunctional comonomers during the polymerization. Oligomers were analyzed in order to see if there were different species, as predicted by Yuan model, statistically formed in the presence of star comonomer. Using pentaerythritol (T4), the species that may be present in the final oligomer are;

- Pentaerythritol

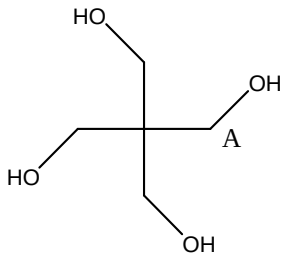

5.4)

- Mono-reacted pentaerythritol

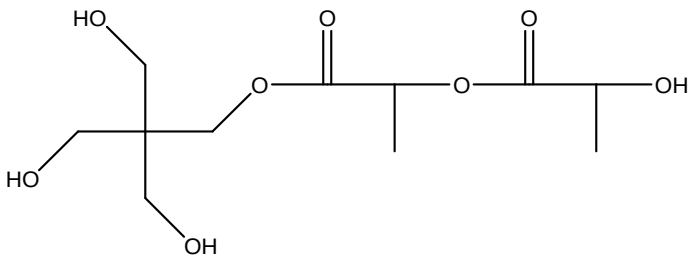

5.5)

- Bi-reacted pentaerythritol

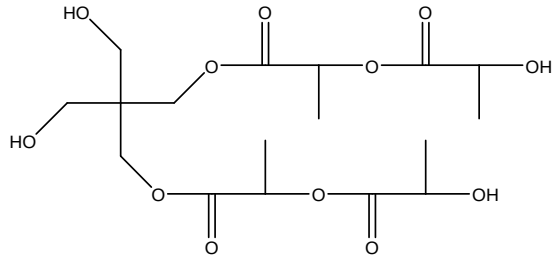

5.6)

- Tri-reacted pentaerythritol

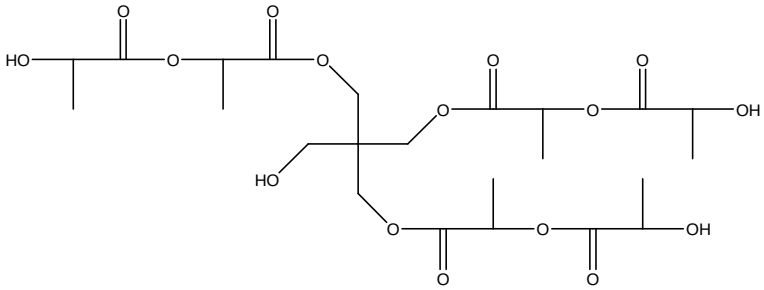

5.7)

- Totally reacted pentaerythritol

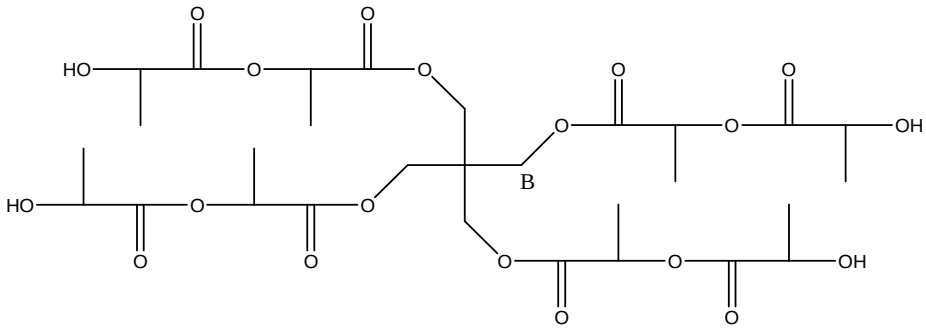

5.8)

Looking at the structure from 5.4) to 5.8) ^{1}HNMR signals of the two protons of the CH_2 group (A) bound to oxygen were used to determine the type and number of species present in the reaction mixture. Indeed, the presence of a different number of substitutions on the pentaerythritol should originate a variety of signals and a chemical shift towards lower fields if the hydroxyl group of the regulator reacts with the monomer promoting the formation of the chain (B), compared to the case in which it remains unreacted (A).

Figure 6 shows the ^{1}HNMR spectra of the oligomer containing 25% of T4.

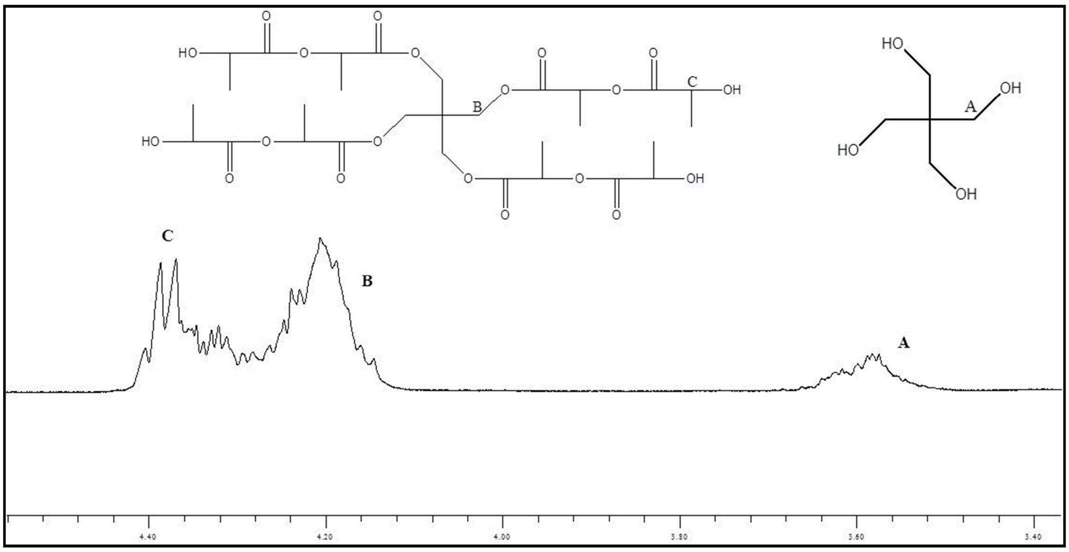

Figure 6: ^{1}HNMR spectrum of oligomer with 25% of T4

^{1}HNMR spectrum in figure 6 shows that there is no multiplicity in the signal on CH_2 of T4 (B), but only one signal is present, due to a structure in which all the functionalities of the comonomer are reacted with lactide. To further verify this observation a ^{13}CNMR spectrum was collected, shown in Figure 7.

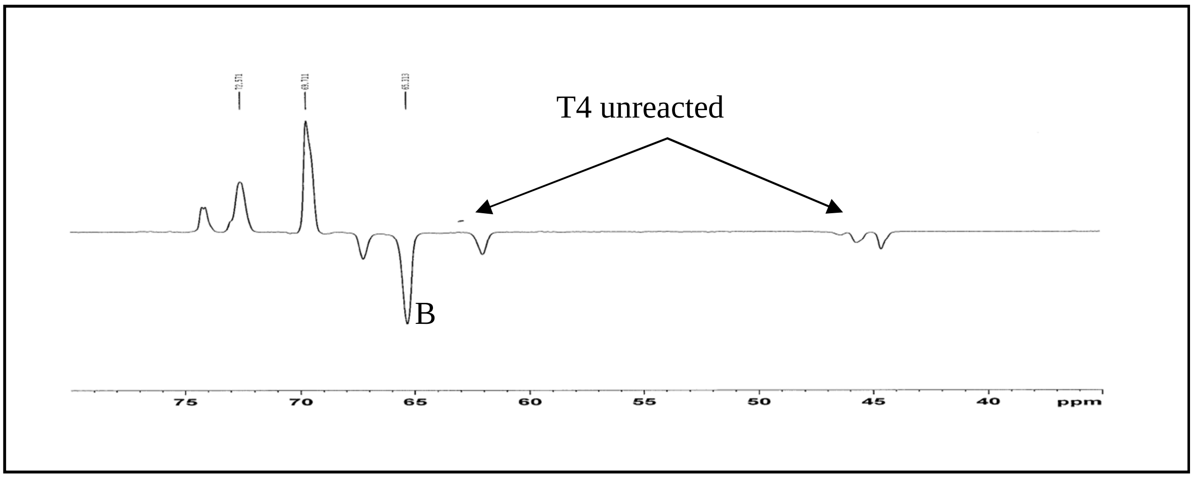

Figure 7: ^{13}CNMR spectrum of oligomer with 25% of T4

Also ^{13}CNMR spectra of figure 7 confirms what ^{1}HNMR has already shown: there is no multiplicity of signals that can confirm the presence of different species represented in figures from 5.4) to 5.8), but only species 5.8), totally reacted and a lower residue of unreacted T4 comonomer (5.4).

To better understand the expected results it can been useful to observe the spectrum of figure 8 in which an oligomeric system based on trimesic acid and caprolactam is reported. The image was taken from the doctoral thesis of Ph.D. Hermes Farina[6]. In this case all the possible different protons are found in the NMR spectrum, suggesting that all species provided by Yuan model are actually present in the reaction mixture. There are not only the fully star macromolecule, as suggested by Flory model, but also all species in which the multifunctional comonomer is not completely reacted.

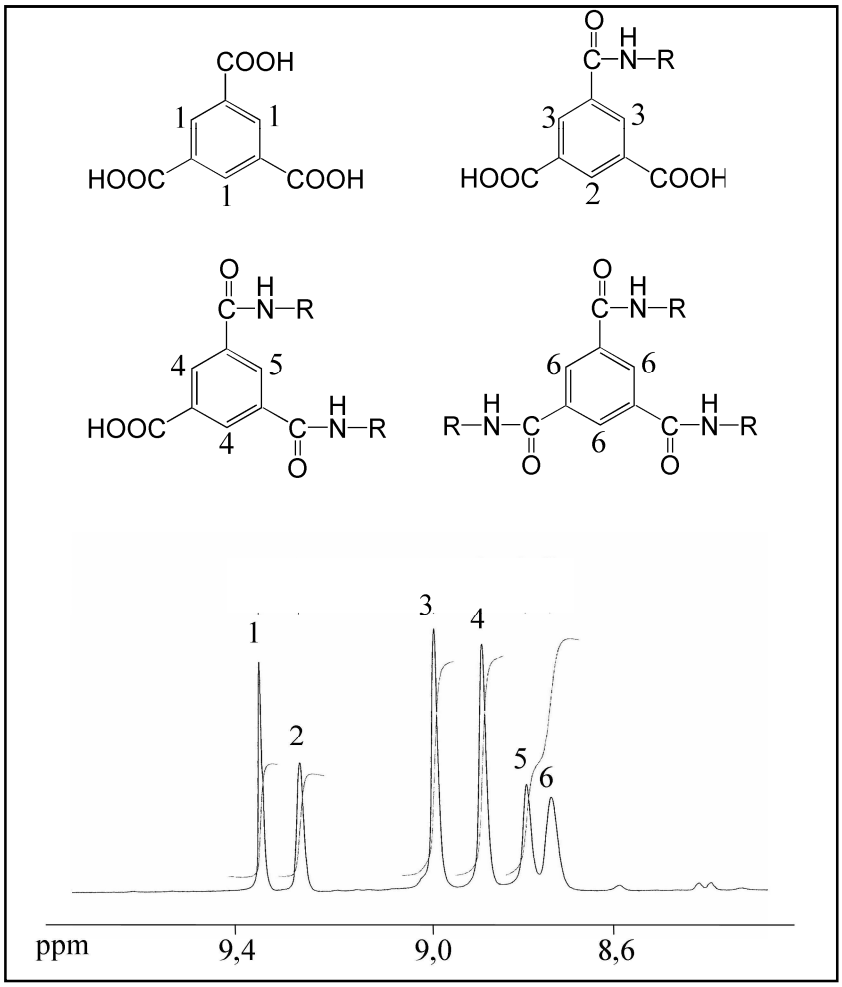

Figure 8: ^{1}HNMR spectrum of samples with a caprolactam/trimesic acid ratio of 3

[1]HMNR spectrum of PLA synthesized using the T3 comonomer as a chain regulator was considered in comparison to the spectrum of Figure 8; figure 9 shows that in this case there is not any multiplicity of signals that may suggest the presence of a mixture of different species, but similar to what observed for T4 comonomer, there are only signals of the CH_2 of T3 completely reacted (B), the signals of lactic units terminal chain (C) and also a signal of a small amount of completely unreacted comonomer (A), exactly as observed in the spectrum of figure 6.

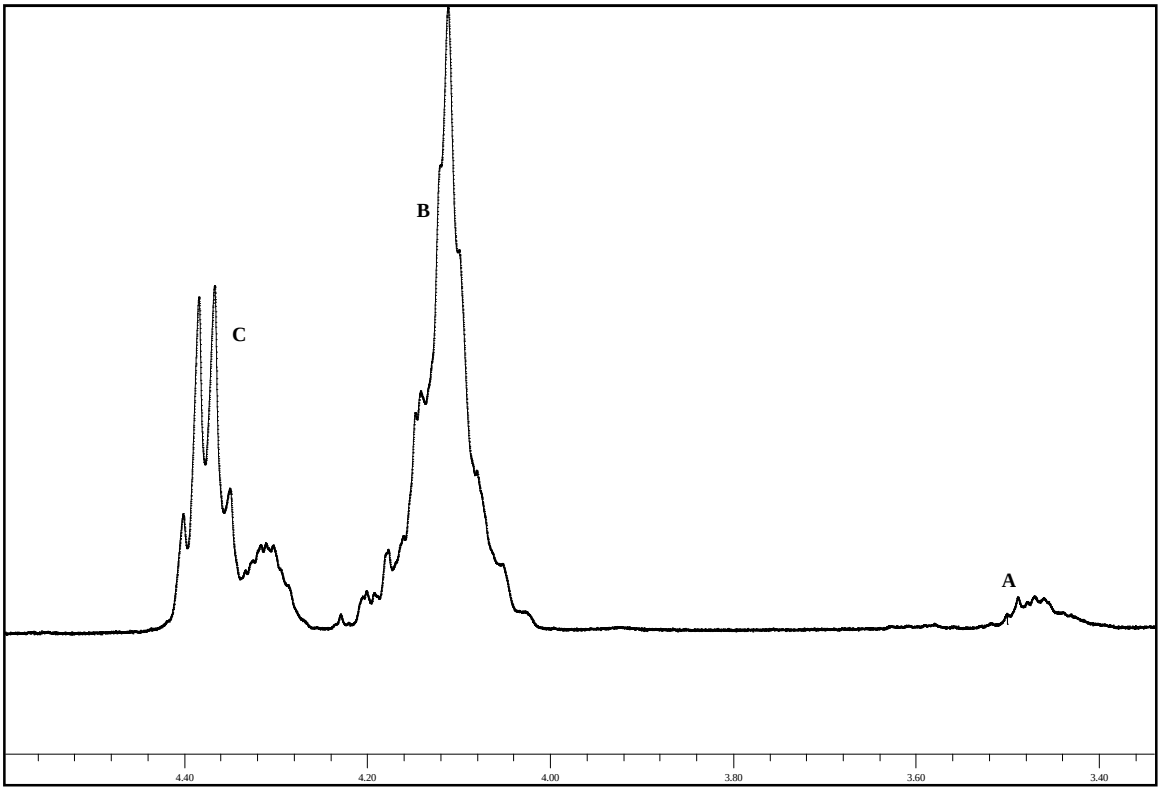

Figure 9: [1]HNMR spectrum of oligomer with 10% of T3

To further confirm these data, an oligomer was synthesized, using T3 as but with only 30' and not 120' as reaction time, to verify if for shorter reaction times the different species considered in the theoretical model were present. The proton spectrum relative to the latter sample is shown in Figure 10.

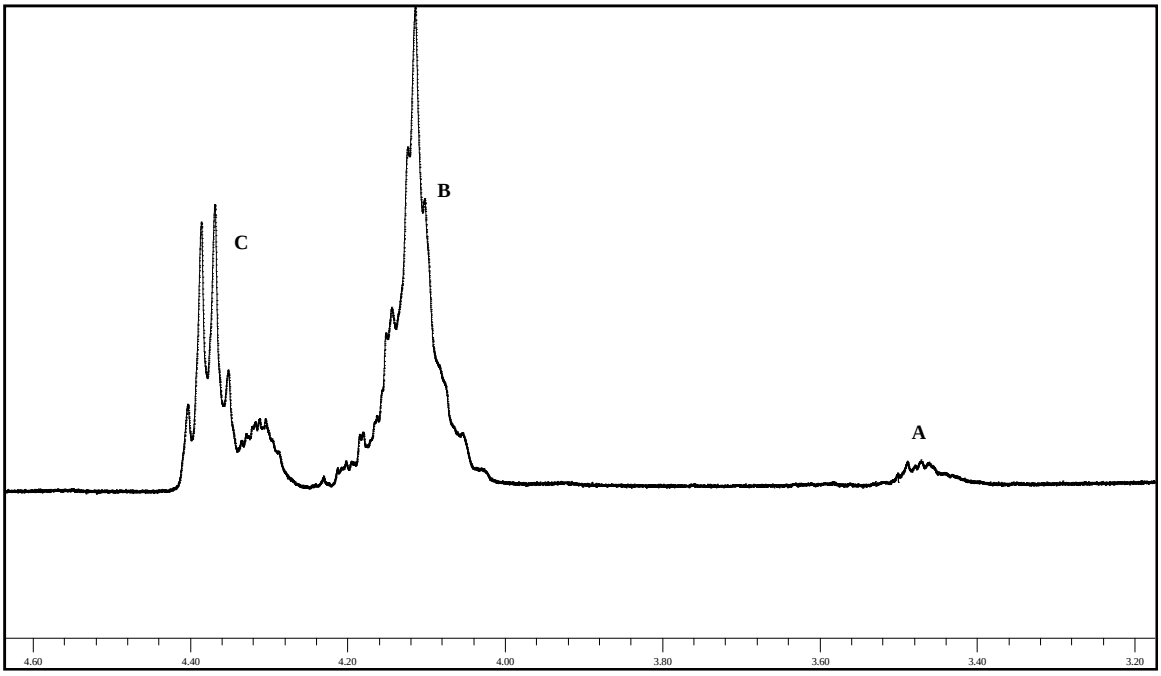

Figure 10: ^{1}HNMR spectrum of oligomer with 10% of T3 synthesized in half an hour

The spectra in figure 9 and 10 are perfectly identical in the area of methylene of comonomers, therefore time does not influence the number of reacted or unreacted arms of the multifunctional comonomer.

By analyzing all the data collected it can be stated that the polymerization of lactide, even in the presence of high amounts of comonomer, is promoted by the nucleophilic attack of the hydroxyl groups of the comonomer T_x to the lactide ring. All the reactive groups of T_x are involved in the initiation of chain growth, with high reaction rate and without any distinction; it is not possible to identify the different species only partially reacted because from each arm a macromolecular chain starts.

This type of mechanism is similar to the one observed for an anionic polymerization and is confirmed by the fact that for short reaction times the molecular weight distribution is very narrow, a behavior typical of polymerization that proceeds by an anionic mechanism, as reported in chapter 4.

During the polymerization, transesterification reactions occur and involve the rearrangement of the chains that lead to a final value of polydispersity typical of the polymers obtained by polycondensation and predicted by the theoretical model. However, these reactions take place on internal chain ester groups and do not involve the core, probably due to the increased stability of its bonds and/or increased steric hindrance. This explains why in the NMR spectra there is no multiplicity of signals.

5.4 POLYMERIZATION WITH T1, T3, T4, T6 COMONOMERS

5.4.1 Effect of comonomer % on PLA molecular weight

The chemical nature of PLA chain is characterized by a short monomer unit in which there are only three carbon atoms. The macromolecule of PLA is also weak due to the presence of an oxygen atom in the chain near to an electron attractor group such as carboxyl group. These two reasons require for PLA to have very high molecular weights, 90000 g/mol (polystyrene equivalent) or 50000 g/mol (PLA equivalent) to obtain materials with good mechanical properties, which can have a industrial application; lower molecular weight PLAs have poor mechanical properties and cannot find applications.

Therefore it is important the choice of reaction conditions to obtain high-performance materials.

Using the same synthetic method used for the synthesis of the oligomers four samples of PLA were synthesized, using different quantities of T4 comonomer, in order to verify the effect on polymerization process on the final material. In particular what was the best concentration range to be used for the synthesis of polymers with good properties was searched.

The feed and the values of molecular masses and polydispersity of these samples are shown in table 2.

Sample	Comonomer	% Tx	Mn SEC	D
1	T4	0.125	31424	1.538
2	T4	0.25	24290	1.504
3	T4	0.5	10082	1.420
4	T4	1	5523	1.311

Table 2: feed and molecular properties of PLA with different %m/m of T4

The data reported in table 2 show that the T4 has really worked as chain regulator because Mn values determined by SEC analysis decrease with increasing the amounts of T4 in the feed, and the distribution of molecular masses is narrow compared to that obtained for the synthesis of not regulated linear polymers.

Molecular weight values show that using theoretical model to study the behavior of star agents is possible to obtain polymers with a restriction on the distribution of molecular masses, but also with numeral average molecular weight increased by increasing the [lactide]/[comonomer] ratio; in other words, decreasing the amount of multifunctional agent Mn increases while the polydispersity of the material is low. It is also interesting to note that increasing the concentration of tetra functional agent there is a great decrease in the distribution value of molecular masses. Figure 11 shows the SEC curves of the four samples synthesized with the tetra functional comonomer: both Mn values and molecular mass distributions reflect the values reported in table 2.

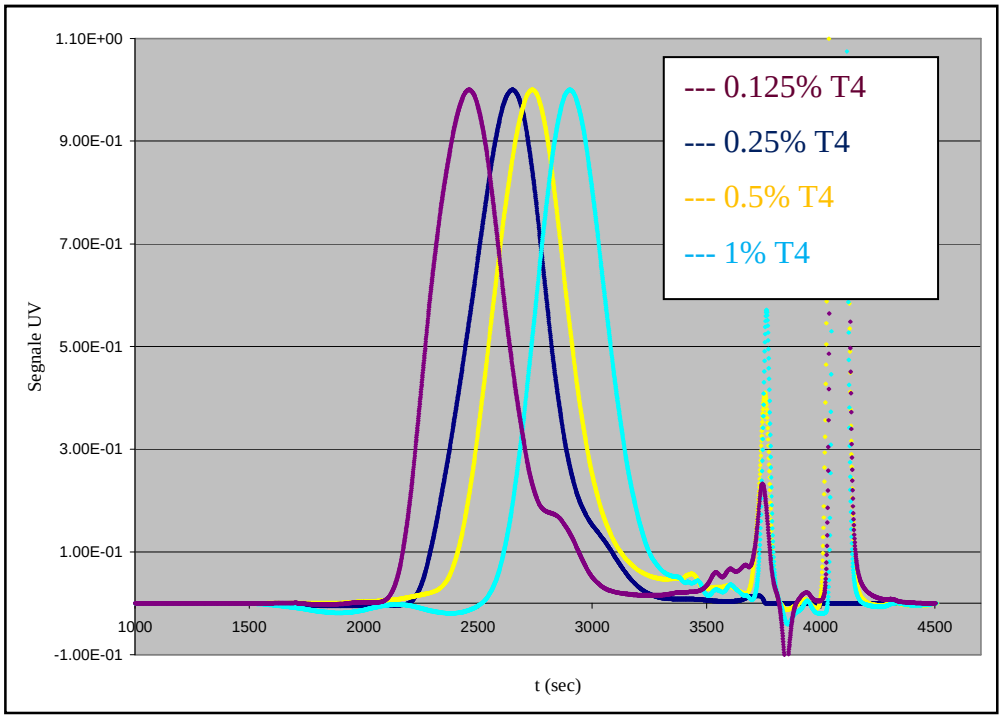

Figure 11: SEC curves of PLA with different % of T4

As mentioned before, however, PLA must have a molecular weight of about 50000 g/mol in order to obtain materials with good mechanical properties that make them suitable in fields different from the biomedical one; polymers reported in table 2 have Mn values too low to have an interesting mechanical and rheological behavior, especially if the polymers with T4 up to 0.25% are considered. For this reason the study on the behavior of the PLA in the presence of multifunctional agents was continued using an amount of comonomer between 0.05% and 0.125% m/m.

5.4.2 Star shaped PLA with low amount of multifunctional comonomers

In section 5.4.1 it was said that high molecular weight is necessary to obtain polymers with good mechanical and rheological properties: for this reason the amount of multifunctional agent used to modify the macromolecular architecture must be very low. Then several star architecture PLA with feeds and molecular properties that are summarized in table 3 were synthesized.

Sample	Comonomer	% Tx	Mn SEC	D
0	-	-	56909	1.982
1	T1	0.05	55186	1.888
2	T1	0.0625	49951	1.883
3	T1	0.125	27802	1.895
4	T3	0.05	69910	1.652
5	T3	0.0625	67588	1.644
6	T3	0.125	30600	1.605
7	T4	0.05	121834	1.668
8	T4	0.0625	103321	1.658
9	T4	0.125	31424	1.611
10	T6	0.05	66270	1.512
11	T6	0.0625	63520	1.509
12	T6	0.125	32691	1.482

Table 3: feed and molecular properties of star shaped PLA

Table 3 shows that the change of the number of multifunctional agent reactive groups affects the Mn values of polymers, determined by SEC analysis, and also the polydispersity; it is possible to modulate the molecular weight and the polydispersity modifying the type of comonomer in feed.

For small concentrations (0.05% and 0.0625%) of T3, T4 and T6 Mn values are similar or higher than the ones of linear polymers; the multifunctional agents work as chain extenders, and this effect is particularly noticeable when T4 is present. Increasing the concentration of the multifunctional agent (0.125%) a dramatic decrease of the average molecular weight is observed. The polymers synthesized in the presence of T1, which does not act as a chain extender but only as a chain regulator, have always average molecular weight values lower than the non regulated linear PLA and Mn gets lower as the amount of T1 increases.

The trend of Mn values is also confirmed by the SEC curves of the same samples.

In figures 12, 13, 14 and 15 are shown the SEC curves of PLA synthesized with T1, T3, T4 and T6 compared with the unregulated linear PLA.

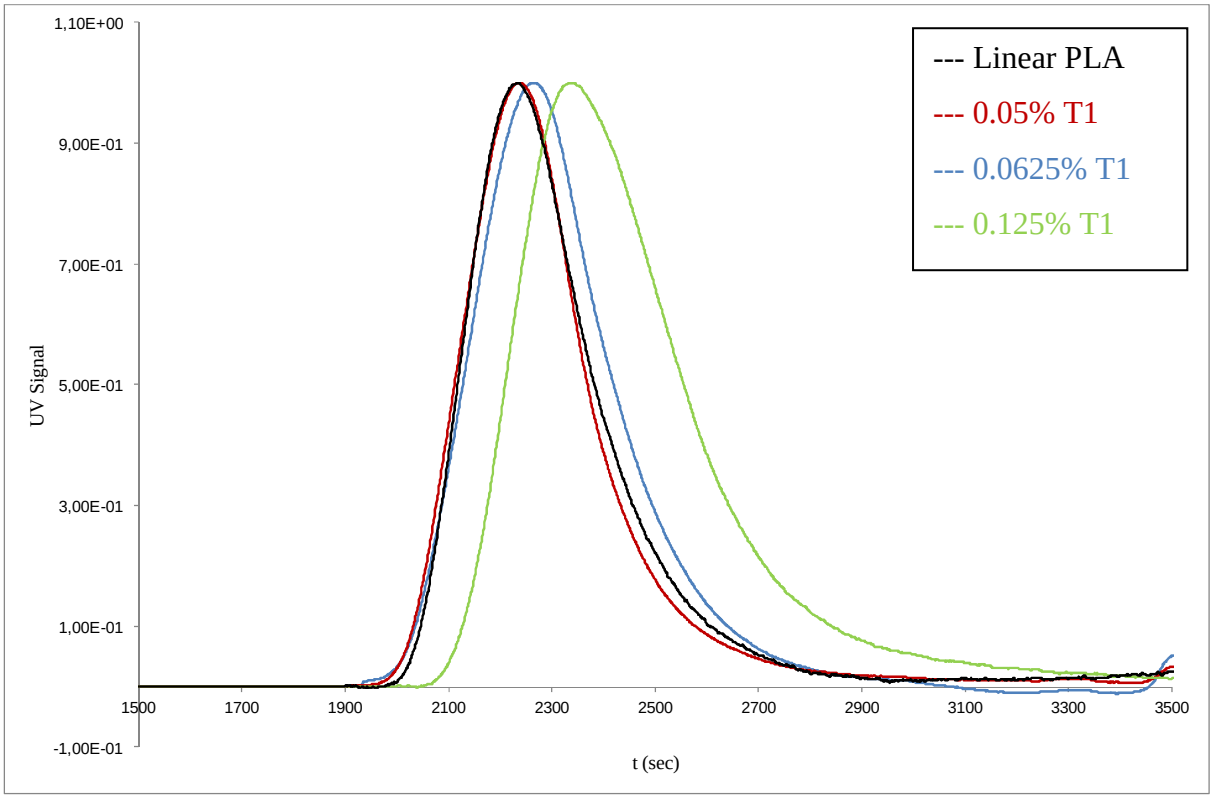

Figure 12: SEC curves of PLA with different % of T1

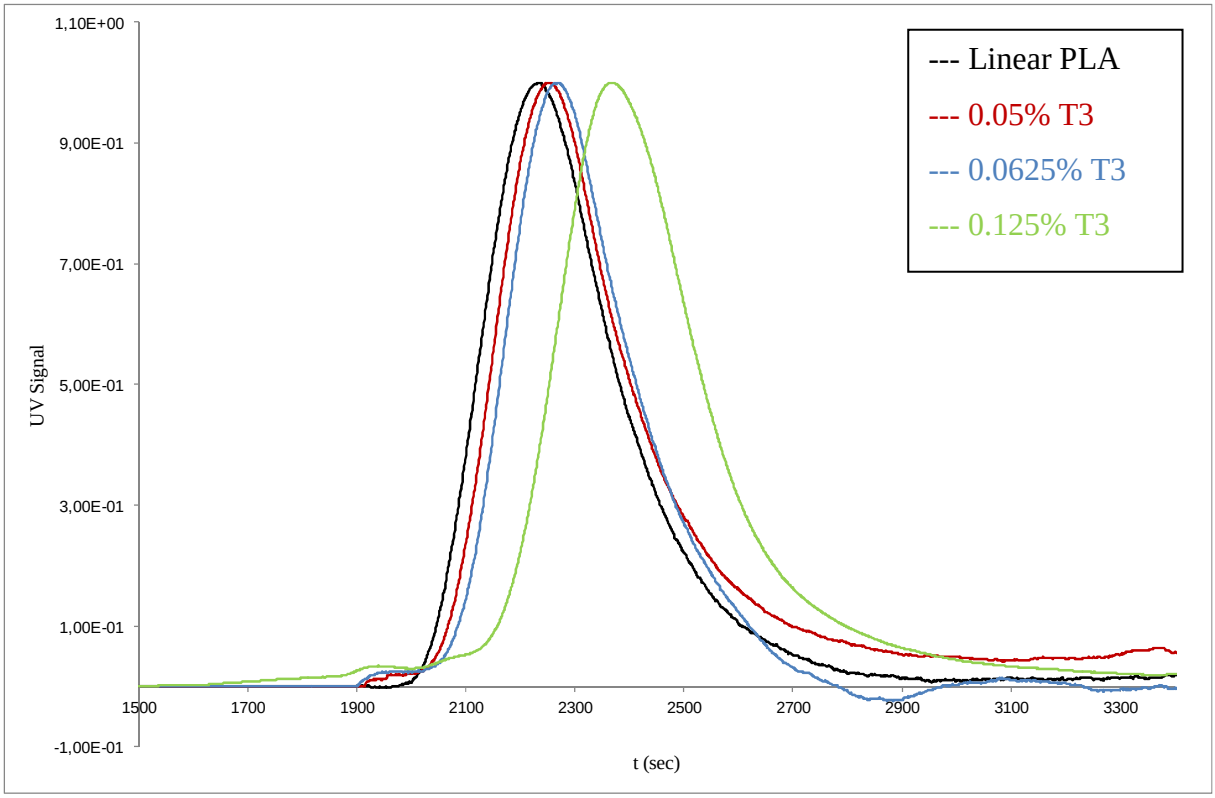

Figure 13: SEC curves of PLA with different % of T3

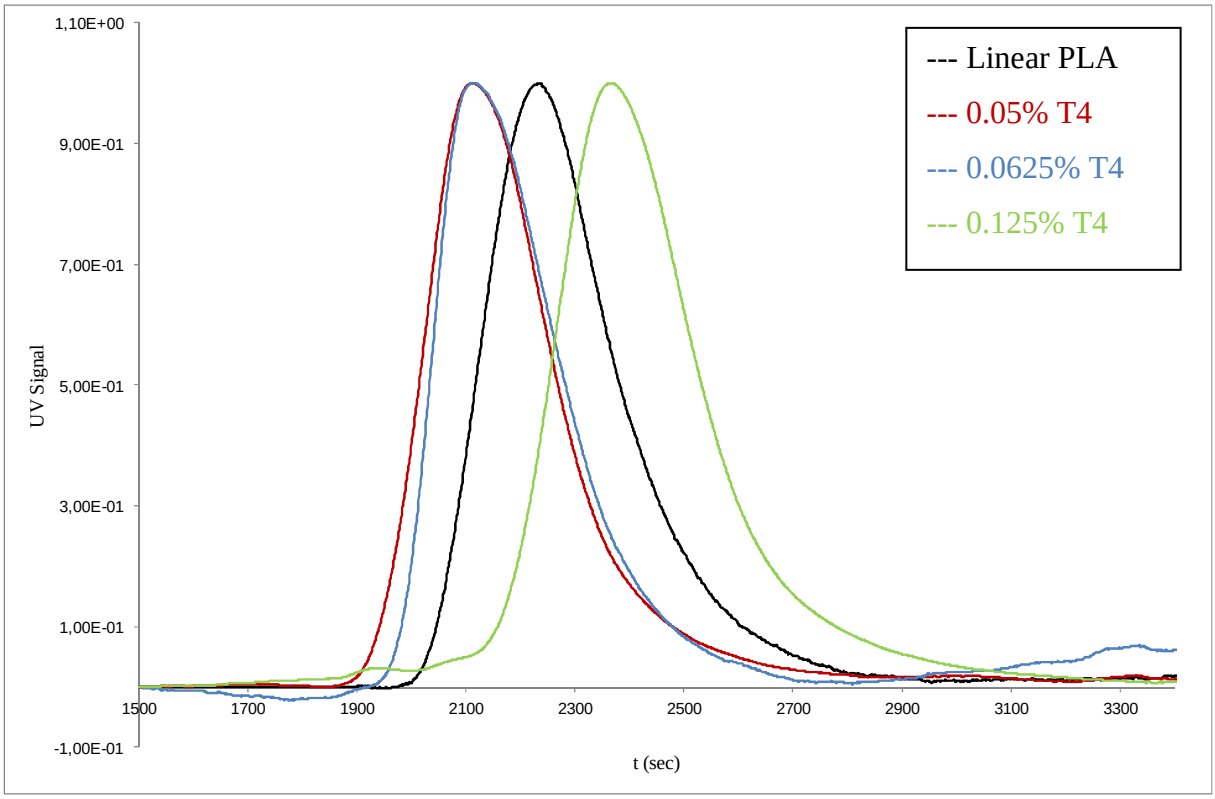

Figure 14: SEC curves of PLA with different % of T4

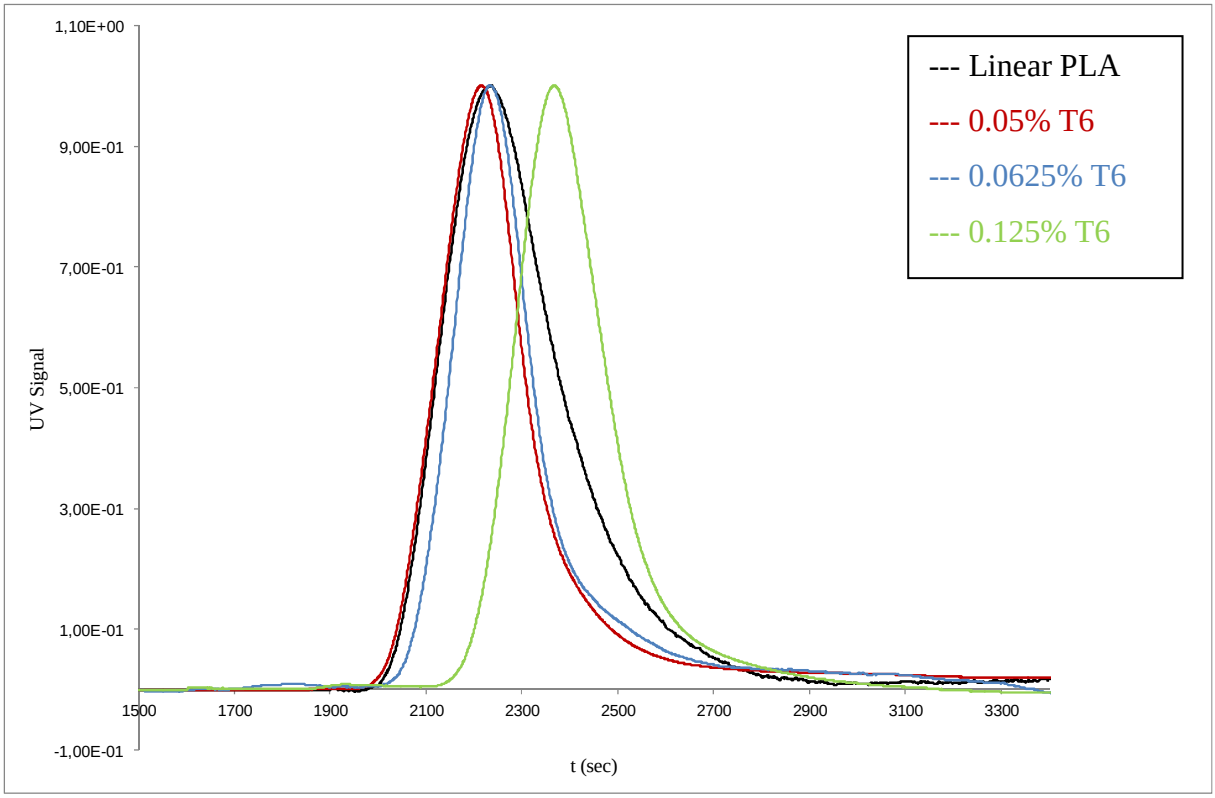

Figure 15: SEC curves of PLA with different % of T6

Looking at the pictures above it can be seen the high regulation of molecular masses and distribution in PLA with the 0.125% of comonomer; it is also clearly visible the action of chain extenders of comonomers T3, T4 and T6 when they are used in smaller concentrations. The percentages of comonomer used for the synthesis of polymers, in particular 0.05% and 0.0625%, necessary to obtain materials with good molecular weight values, is to be very low and thus the effect of the comonomers on Mn values and on polydispersity is not so strong as in polymers synthesized with higher amounts of multifunctional agents.

Figure 16 shows that SEC curves of PLAs synthesized with the 0,125% of T3, T4 and T6 have the maximum of the peak shifted to smaller hydrodynamic volumes compared to the linear polymer regulated with T1, despite the higher molecular masses of these materials having star architecture, as shown in table 3.

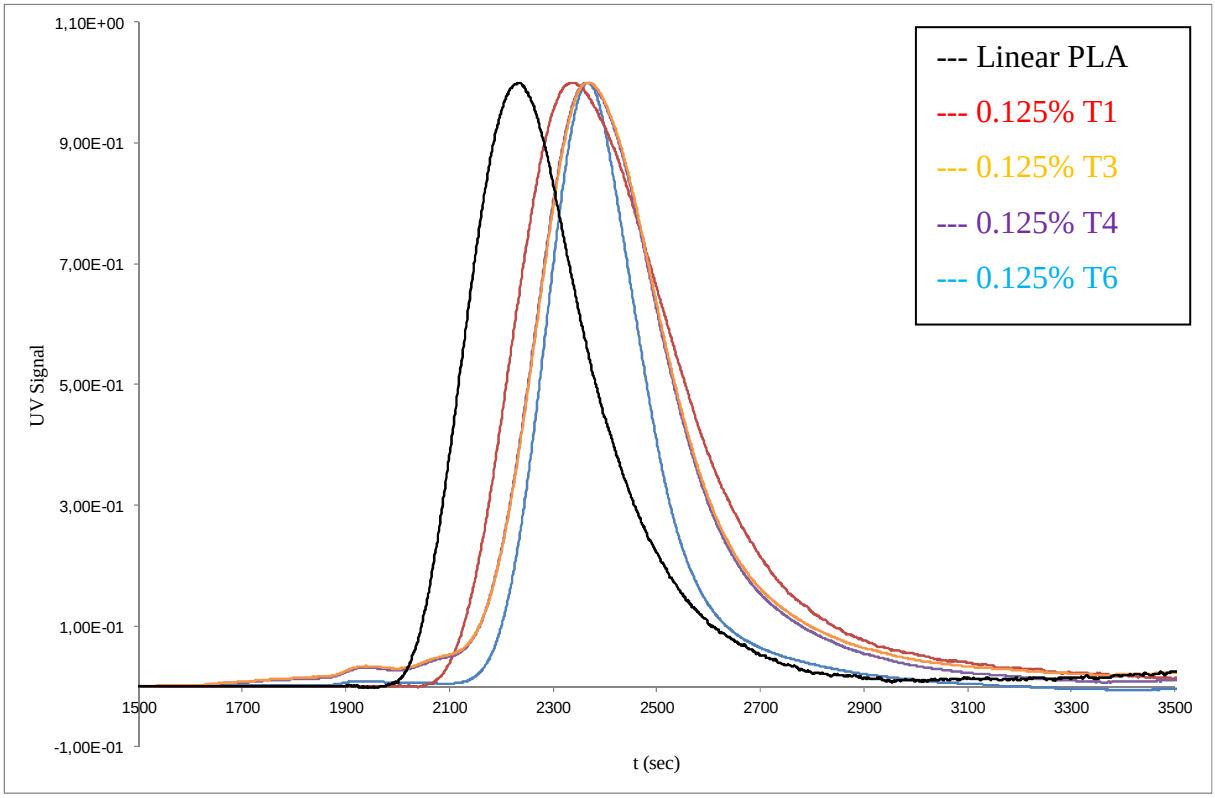

Figure 16: SEC curves of star shake PLA

A feature of star polymers, also described by the theoretical model, is the restriction of molecular masses compared to linear polymers, that has a polydispersity index of about 2. The SEC analysis is an excellent analytical technique to estimate D values and is commonly used for this purpose.

The SEC curves of figure 16 show the wider molecular masses distribution for PLA synthesized with T1 in comparison to the one of PLA with T3; the difference is greater for the polymers with the same molar percentage of T4 and T6, for whom the effect is higher because of the high number of reactive functional groups.

Looking at the SEC curves of figure 16 the effect of multifunctional agents on the polydispersity of the polymers is visible even with very small percentages of comonomers, lower than those used for example in the synthesis of oligomers, described in this chapter at paragraph 5.3.1.

5.5 RHEOLOGY OF PLA WITH MACROMOLECULAR STAR ARCHITECTURE

In a star shaped PLA, as already reported in the introduction to this chapter, a desired feature is the higher fluidity of the melt. This behavior makes it easier the process the polymers and makes the material fill molds quicker and better than a polymer with a similar molecular weight but a linear architecture. This property, and consequently the resulting technological advantage, is widely used in the field of polyamides, particularly for the polyamide 6, but in the literature the use of star shaped PLA used to improve the processing has not been reported, probably because, as already mentioned, PLA has a structure requiring very high molecular weight values to have good properties.

In this work the viscosity of star-PLAs was evaluated in order to study the rheological behavior of these materials compared to a linear PLA.

Samples described in section 5.3 and summarized in table 3 were considered.

Analyses were performed using a rotational rheometer: it is an instrument which works in the fields of shear rates lower than those of a capillary rheometer. While capillary rheometer is dedicated to measures that reproduce the conditions of industrial processing, the rotational rheometer better underlines the different behavior of various materials in molten state in relation to the macromolecular architecture. Physica MCR 300 rotational rheometer was used in this work, with a parallel plate geometry (Φ = 25 mm), useful for the analysis of polymeric materials. PLA has a melting temperature of about 170-180 °C and rheological tests were conducted at 190 °C, approximately 10-15 °C above the melting temperature. The rheological curves were obtained in experiments of frequency sweep from 100 Hz to 0.01 Hz with a constant deformation (strain) equal to 5%. In practice, applying a controlled shear rate, the resulting stress is determined.

Considering also the nature of the polymer studied, that are easily degradated at high temperatures, and using the experience gained by the research group with another class of polymers very sensitive such as polyamides, an analytical methodology has been developed optimizing the time of analysis, minimizing any time related to the inclusion of the sample in the furnace and reducing the time required to restore the temperature within a range of ± 0.1 °C above the temperature of analysis.

In order to have a good repeatability in the analysis on the same sample and a better comparison between the analysis of different samples it is important to always run experiments having approximately the same duration.

The samples were treated with a solid state polycondensation (SSP) overnight under mechanical vacuum at 150 °C, for two reasons: the first one is because PLA is a polymer very sensitive to humidity and therefore requires a thorough process of drying to avoid that traces of moisture during the analysis at high temperatures lead to random hydrolysis of the ester bonds in the polymer chains and to a degradation of the polymer molecular weight.

Secondly SSP process eliminates the residual monomer, whose presence could lower the viscosity of the polymer.

Figure 17 shows the curves of complex viscosity as a function of shear rate for PLA obtained in the presence of the same molar percentage of T1, T3, T4 and T6. By comparison also the curve of the linear PLA is present and used as a reference.

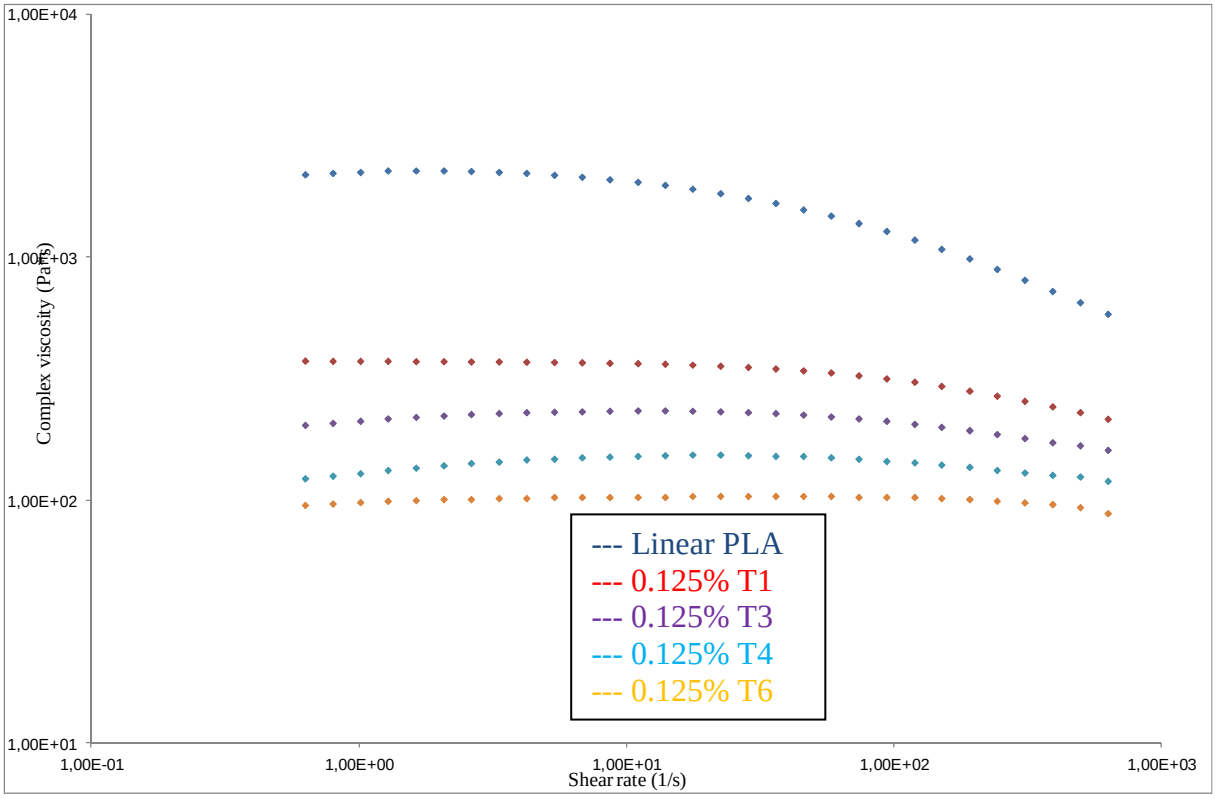

Figure 17: rheological curves of PLA regulated with T1, T3, T4 e T6 comonomers

The rheological curves in figure 17 show that with the same percentage of multifunctional comonomer introduced in the polymer, to obtain materials with the same programmed Mn, there is a decreasing of the complex viscosity of the PLA increasing the number of hydroxyl functional groups in the comonomer. There is therefore the typical effect on the behavior of polymer having star architecture in the molten state.

It should be noted, however, that the viscosity of these star systems is significantly lower than that of unregulated linear PLA; probably this difference between the rheological curves shows that these materials could not be used in applications requiring good mechanical properties.

Figure 18 shows the rheological curves of PLA synthesized in the presence of different amounts of T3 comonomer.

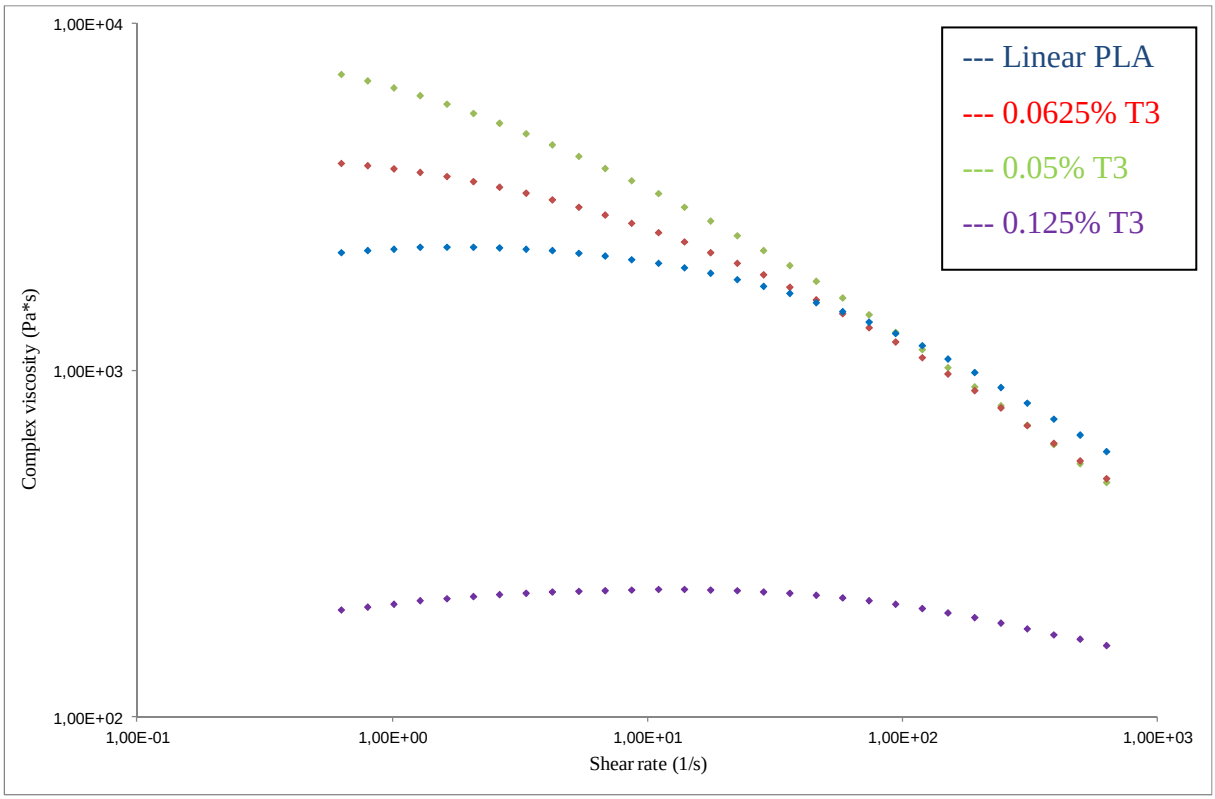

Figure 18: rheological curves of PLA regulated with T3 comonomer

Figure 18 shows that the higher the percentage of the comonomer, the lower the viscosity of the melt, as would be expected by analyzing the molecular weight values of polymers measured by SEC analysis and reported in table 3.

It is also interesting to note that with the lowest percentages of comonomer (0.0625% and 0.05%), the chain extender behavior of the multifunctional chain regulator leads to an increase in viscosity at low shear rate values compared to the linear PLA, while for high values of stress, the viscosity is lower than that of the polymer not regulated.

This phenomenon is related to the behavior of chain extender exercised by the multifunctional comonomer, while with 0.125% of regulator the rheological curve of star PLA has significantly lower viscosity values, as discussed above.

Table 4 shows the complex viscosity values measured at the lowest angular speed, where the differences between samples are greater.

Sample	Comonomer	% Tx	Complex viscosity (Pa*s)
0	-	-	$2.19*10^3$
1	T1	0.05	$1.60*10^3$
2	T1	0.0625	$1.17*10^3$
4	T3	0.05	$7.15*10^3$
5	T3	0.0625	$3.96*10^3$
7	T4	0.05	$1.58*10^4$
8	T4	0.0625	$9.80*10^3$
10	T6	0.05	$3.70*10^3$
11	T6	0.0625	$2.71*10^3$

Table 4: complex viscosity values of star shake PLA at $6.28*10^{-1}$ s^{-1}

Data reported in table 4 show that polymers with T4 and T6 comonomers have a behavior similar to that shown in figure 18 for the PLA synthesized with the T3 comonomer: an increase of viscosity in the presence of small amount of multifunctional regulator is observed, in comparison to unregulated polylactic acid. In accordance with the molecular weight values reported in table 3 the polymers synthesized with T4 comonomer have significantly higher viscosities, and also the viscosity of polymers synthesized with T6 comonomer is higher than the one of linear unregulated PLA, even if the effect is lower than the one observed for similar polymers prepared with T3 and T4..

PLAs synthesized with T1 show an increase in viscosity when decreasing the percentage of comonomers, in accordance with the Mn values reported in table 3, but the rheological curves are lower than the unregulated linear polymer since there is no effect of chain extension.

The experimental results show that it is possible to obtain PLA with high fluidity by adjusting the structure of the polymer with multifunctional comonomers, able to give a star architecture, that act on the molecular weight values and on distribution of the masses, especially when used in the amount up to 0.125%.

The characteristics of PLA, however, force to have a very high molecular weights to be sure that the material has good mechanical properties. For this reason is not possible to use large amounts of comonomers, therefore very low (for example 0.05% and 0.0625%) amount of multifunctional comonomers must be used; acting as chain extenders, they lead to an increase in viscosity in comparison to the unregulated linear polymer. With these low amount of star agents the effect of narrowing of the molecular masses is still visible but less marked than the one that could be achieved with higher percentages of comonomers.

REFERENCES

[1] Schaefgen, R., Flory, P. J., *J. Am. Chem. Soc.*, 70, 1948, 2709.

[2] Farina, M., *"Variazione della distribuzione delle masse molecolari in policondensati a stella"*.

[3] Yuan, C. M., Di Silvestro, G., Speroni, F., Guaita, C., Zhang, H., *Macromol. Chem. Phys.*, 202(10), 2001, 2086.

[4] Atthoff, B., Trollsas, M., Claesson, H., Hedrick, J. L., *Macromol. Chem. Phys.*, 200, 1999, 1333-1339.

[5] Korhonen, H., Helminem, A., Seppala, J. V., *Polymer*, 42, 2001, 7541-7549.

[6] Farina, H., *Sintesi di polimeri con architettura controllata ad albero e/o stella mediante policondensazione,* PhD Thesis AA 2005-2006.

6. Study of PLA with tree macromolecular architecture

6 STUDY OF PLA WITH TREE MACROMOLECULAR ARCHITECTURE

6.1 THEORY OF SYSTEMS HAVING TREE ARCHITECTURE

In literature there are several examples about highly branched polymer obtained by condensation of AB_n monomers. Flory, was both a pioneered in the study of star architecture polycondensates and also a pioneer in the study of hyper branched polycondensation polymers[1]. He studied the polycondensation of AB_n monomers and developed a statistical model in which functional groups A and B have opposite reactivity and able to react with any other complementary group; n is the number of groups of type B present in the monomer. The theory developed by Flory predicts that the polycondensation of AB_n monomers leads to the synthesis of high molecular weight polymers, randomly branched.

The macromolecules of these polymers contain a functional group A and a number of unreacted B groups depending on the degree of polymerization of the polymer:

$$(n-1)x+1 \qquad 6.1)$$

x is the number of monomeric units in the chain. According to Flory theory these polymers, if appropriately synthesized, do not reach the gel point, are soluble and can be melted; he also developed several equations for calculating the distribution of molecular masses and their moments. From Flory theory it results that the polydispersity index of polymers increases with the degree of polymerization.

Thirty years later, Kricheldof[2] studied the co-polymerization of AB monomers with BA_2 monomers. In particular he studied the polycondensation of 3-(trimethylsiloxy) benzoyl chloride in the presence of 3,5-(bis-trimethylsiloxy) benzoyl chloride to synthesize a poly (3-hydroxybenzoate) with branched structure. In this work, non-crosslinked polymers were synthesized regardless of the degree of conversion.

In 1988 Webster and co-workers[3] synthesized hyper-branched polyarylene using BA_2 type monomers and in 1997 Yan and co-workers[4] calculated the molecular weight distribution and other molecular parameters for polymers derived from the polycondensation of BA_2 monomers.

Also these authors, as already noted by Flory, found that the index of polydispersity of these polymers is very large; this feature can be explained by that larger molecules have a greater number of functional B groups, compared to smaller ones, and therefore can better react with a A group of another molecule. The result is a bigger molecule with an higher probably to react. This statistical factor means that small molecules have lower probably to grow, while larger one have a better chance to grow further; this implies that a wide distribution of molecular masses is obtained.

Subsequently, starting from the restriction of polydispersity index in star polymers, as already known, Hult[5] and coworkers synthesized hyper-branched polymers in the presence of star comonomers to obtain a reduction in the polydispersity of these polymers.

Subsequently Yan and coworkers[6] developed a kinetic model of growth for polycondensates obtained from BA_2 monomers in the presence of RB*f* multifunctional agents as a star point; the synthesis of these type of hyper-branched polymers did not lead to materials with good mechanical and structural properties.

In two recent reviews Long[7] and Voit[8] accurately describe the fundamental mechanisms of the synthesis of hyper-branched polyesters confirming that the ability to modulate the degree of branching and the length of the arms of the polymers, avoiding the gel point, are key factors to control the rheological behavior, the processability and the thermal characteristics of the materials; these parameters are very important in polymer processing.

As for the synthesis of aliphatic polyesters with branched structure starting from cyclic monomers(also including lactide) several hyper-branched systems are described in literature: these polymers are obtained through the insertion of elements connected to the main chain or they are dendrimers[9,10].

The use of ABn monomers as branch points to obtain hyper branched structures to increase the molecular masses of polymers is described by Frey and coworkers[11]: they use dimethylolpropionic acid to obtain structures having an high branching degree in caprolactone polymers. Frey[12] again studied the use of the same acid in lactide polymerization catalyzed by tin octanoate: in this work he shows for the first time the involvement of hydroxyl and carboxylic groups of multifunctional agent in the growth process of PLA polymer chains.

After the work of Frey[12], Storey[13] used the same type of multifunctional agent in the polymerization of lactide: in contrast to what observed by Frey, Storey states that only the hydroxyl groups of the comonomer are directly involved in the growth of the chain, giving rise only to linear species, while the carboxyl functionality reacts in a second step with a diisocyanate molecule able to connect two different polymer chains obtained from dimethylolpropionic acid.

In this case the multifunctional agent does not completely react directly with the monomer, probably due to the non-reactivity of the carboxylic groups in the lactide/tin octanoate system and to the adverse reaction kinetics of the ester bond formation. The conclusions of Storey and coworkers[13] coincide with what our research group observed about the non-reactivity of the carboxyl group in lactide polymerization. For this reason, as later shown in this chapter, it was decided to use solid state polycondensation (SSP) to obtain the non-crosslinked branched structures.

The small number of papers present in literature regarding the possibility of increasing the molecular weight and properties of the PLA through the use of multifunctional agents is also reflected in the industrial field, where this type of macromolecular architecture is not used for the production of materials.

6.2 PLA WITH TREE MACROMOLECULAR ARCHITECTURE

In chapter 5 the synthesis of star shaped PLAs with high fluidity of the melt has been described. Star macromolecular architecture is obtained adding a multifunctional RA_f agent to the reaction mixture; on the other hand, using comonomers with A_nB_m general formula in the feed, with n and/or m greater than 1, branching points are introduced, that create chains that can end with a functional group A or with a complementary group B. These molecules, unlike the star-shaped ones, can react either with other similar macromolecules or with the monomer or with the A_nB_m comonomer, giving new branches. The result in this case is not a regulation of the macromolecular chain; branched macromolecules with different degree of branching are obtained; branching tends to increase increasing conversion and A_nB_m comonomer concentration, reaching very high values of molecular masses. Given the nature of the PLA (having short repeating unit and ester bonds, that don't create hydrogen bonds between the chains as happens in polyamides), a branched system might be more functional for the increase of the properties of the polymer in comparison with a star polymers.

A hyper-branched structure of a tree statistics polymer obtained by the reaction of an AB type monomer with a AB_2 comonomer is shown in figure 1.

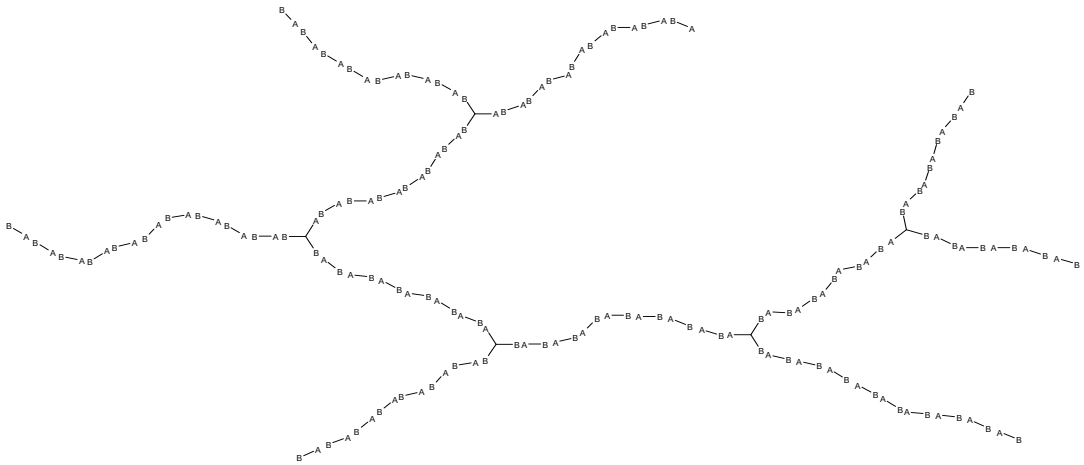

Figure 1: macromolecule with statistical tree structure obtained from a polymerization of AB monomer with AB_2 comonomer

The polymerization of AB_2 comomonomer leads to an hyper-branched structure, very compact , like a dendrimer; these structures have generally very low solubility even at low DPn values due to the high symmetry of the oligomers. A particular dendrimeric structure is shown in figure 2.

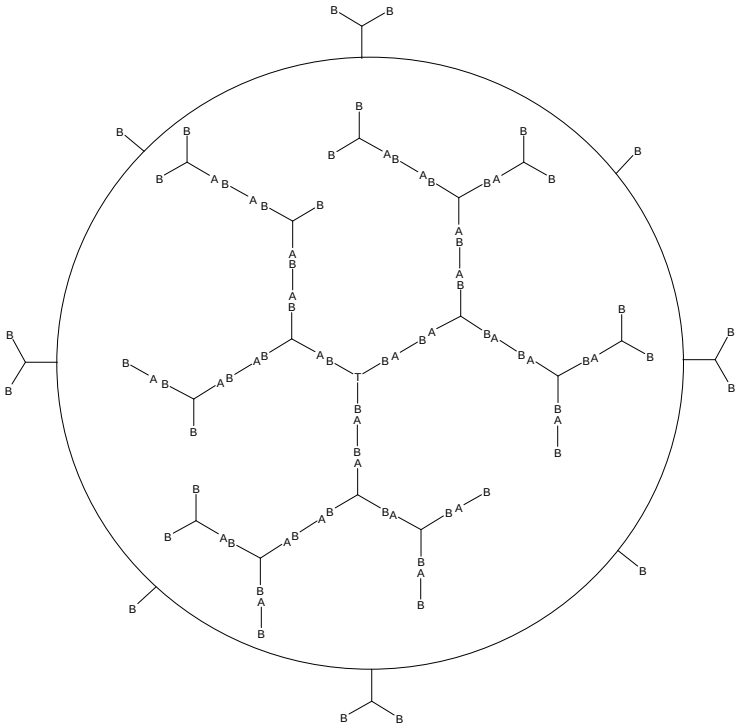

Figure 2: example of a dendrimer obtained from AB_2 comonomer polymerization

Dendrimers, as reported in section 6.1, are studied in the polymerization of lactide, but the topics of the works reported in literature are academic, focusing for example on the study of polymerization mechanisms or on the study of structures obtained using this type of comonomer. A few practical applications are present in literature, ant they are however to biomedical field(i.e. drug carrier molecules).

Comonomers chosen to synthesize polymers with tree macromolecular architecture, as described in chapter 5, must have features that allow not to affect the final properties of the material: they must be thermally stable at the temperature of polymerization, they must have high purity, they must not give color to the final polymer and they should have prices allowing their industrial use.

In this work we used two types of BA_2 comonomers: 5-aminoisoftalic acid (AIA) and dimetilolpropionic acid (DMP), whose structures are shown below.

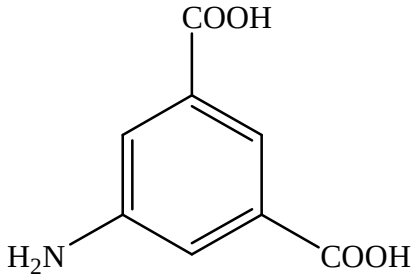

5 - aminoisoftalic acid

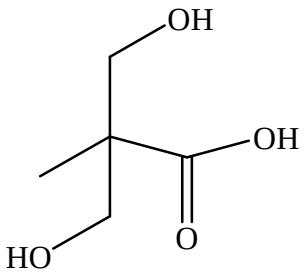

Dimetilolpropionic acid

The main property of PLAs with statistical tree macromolecular architecture is a significant increase in melt viscosity in comparison to linear PLA. The high melt viscosity of these polymers could allow to use them, for example, in blow-molding process.

The carboxyl functional groups present in the comonomers, as mentioned above, do not react during the process of polyaddition and do not contribute to the growth of the chain and the formation of the complex architecture; the two molecules act as mono-functional regulators (5 – aminoisoftalic acid) and as bi-functional comonomer (dimetilolpropionic acid).

For this reason it is necessary to treat the polymer with a post-polycondensation process that promotes the reaction between the carboxyl groups of the comonomers and the free end groups of the polymer in order to obtain a branched structure.

The study of tree statistical PLA required the synthesis of polymers with different concentrations of AIA and DMP. Synthesis conditions are similar to those developed for the production of linear and star architecture PLAs. First a series of samples containing an increasing amount of comonomer have been synthesized in order to verify the reactivity of branching agent. The first syntheses were performed using DMP because it is more compatible with PLA, and to verify if there was a reactivity of the carboxyl group of DMP, as shown in the work of Frey[12], or if it acted only as a bi-functional regulator, as reported by Storey[13]. For this reason all the polymers were analyzed before the post-polycondensation process.

Table 1 shows the feed and the molecular properties of the samples synthesized with dimetilolpropionic acid.

Sample	Comonomer	% Tx	Mn SEC	D
1	DMP	0.125	33836	1.677
2	DMP	0.25	28392	1.651
3	DMP	0.5	11187	1.647
4	DMP	1	7664	1.639

Table 1: feed and molecular properties of PLA with DMP

The values of molecular weight and polydispersity show that DMP acts as a bi-functional agent, thus confirming the non-reactivity of the carboxyl group in the polymerization of lactide.

Figure 3 shows the SEC curves of samples described in table 1.

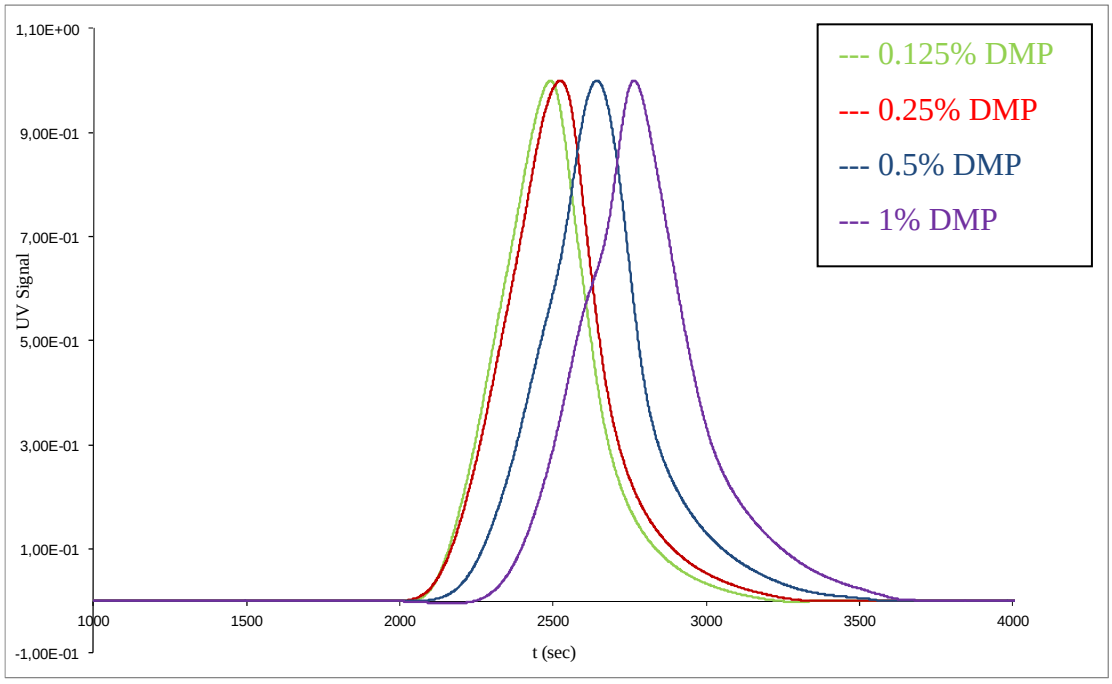

Figure 3: SEC curves of PLA with DMP

SEC curves in figure 3 show that DMP acts as bi-functional comonomer.

Similarly to what was done for DMP syntheses using 5 – aminoisoftalic acid were performed, to evaluate the behavior of the comonomer.

Table 2 shows the feed and the molecular properties of the samples synthesized with 5 – aminoisoftalic acid.

Sample	Comonomer	% Tx	Mn SEC	D
1	AIA	0.125	29420	1.862
2	AIA	0.25	25425	1.866
3	AIA	0.5	12798	1.890
4	AIA	1	9559	1.901

Table 2: feed and molecular properties of PLA with AIA

AIA comonomer acts as a mono-functional regulator and not as chain branching agent, confirming the non reactivity of carboxy groups observed also with DMP.

Figure 4 shows the SEC curves of samples described in table 2.

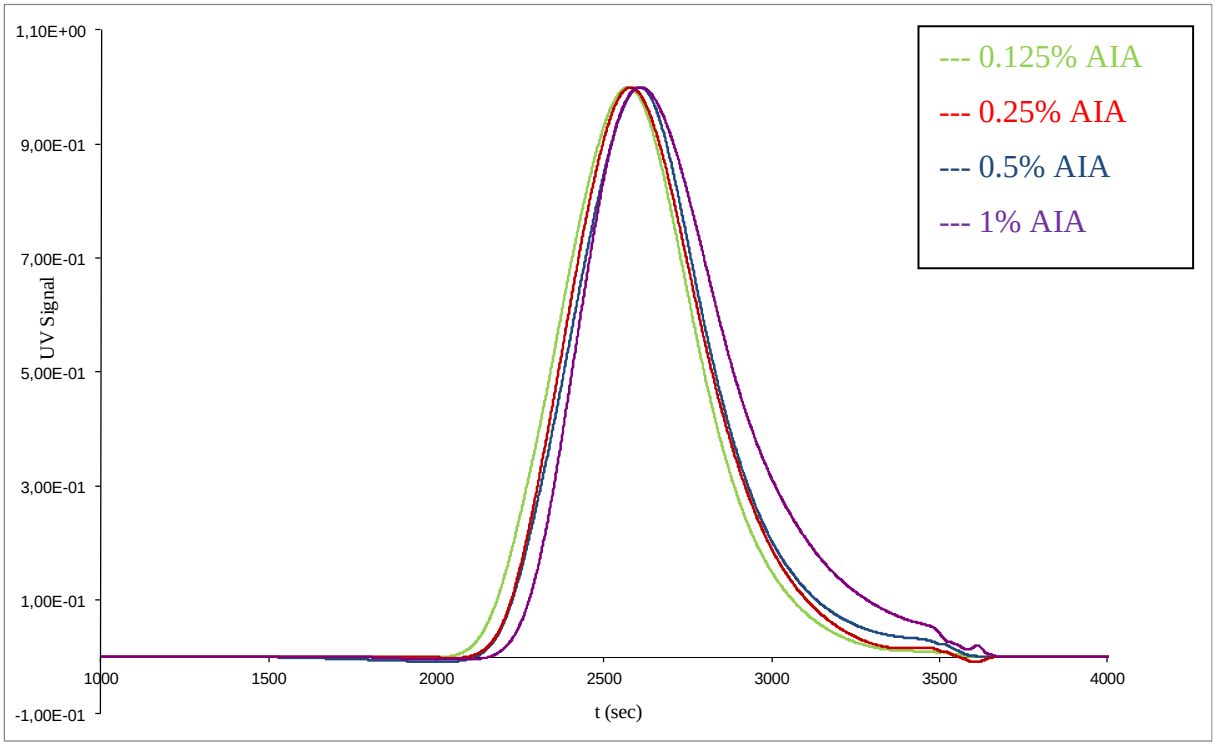

Figure 4: SEC curves of PLA with AIA

These tests show that the carboxyl group is not reactive in the polymerization conditions, making it impossible the formation of tree structures during the synthesis.

The comonomers behave as mono-functional agent (AIA) or bi-functional agent (DMP) and therefore they regulate the molecular weight that decreases increasing the percentage of comonomer added in the feed.

To obtain branched structures is therefore necessary to use SSP technique, in order to promote the reaction of the free carboxyl groups of comonomers with terminal hydroxyl groups of the polymer chains, thus forming the branches.

The SSP conditions require to operate at a temperature between the Tg and Tm, so that the chains acquire mobility to react, with the advantage that by working in the solid phase there is no risk of degrading the polymer.

The post-polycondensation was conducted at 150 °C under mechanical vacuum ($8*10^{-2}$ mbar) for 12 hours.

SEC curves reported in figure 5 show the effect of SSP process on polymer synthesized in the presence of 0.25% of DMP.

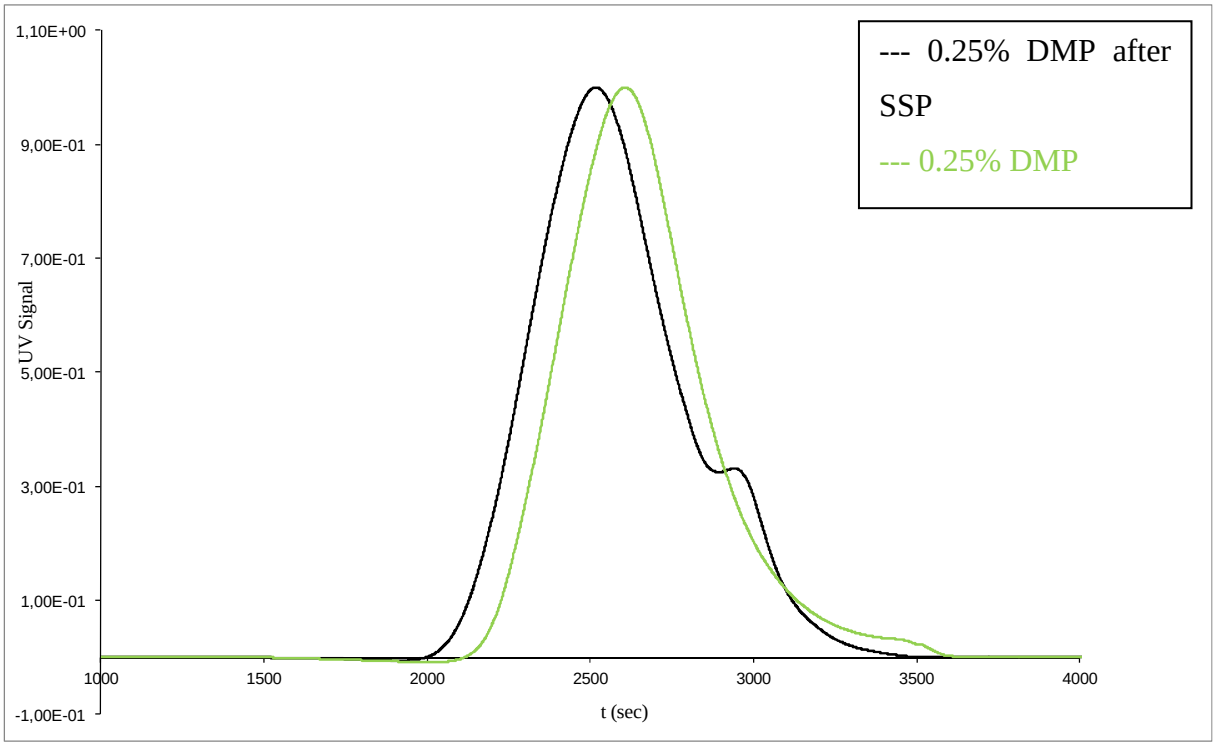

Figure 5: SEC curves of PLA with DMP before and after SSP process

The SEC curves in figure 5 show that SSP process has an effect on the molecular weight, which is incremented, but also on the polydispersity of the system. An evident broadening of the molecular masses distribution is present and a shoulder in the left area of the curve appears, probably due to the growth of existing chains or the formation of new species from lactide still present in the system reacting under SSP conditions.

Table 3 shows the values of molecular weight of the samples with AIA and DMP after SSP process.

Sample	Comonomer	% Tx	Mn SEC	D
0	-	-	56909	1.982
1	AIA	0.05	53818	2.010
2	AIA	0.0625	51100	2.000
3	AIA	0.125	39832	2.114
4	AIA	0.25	25649	2.147
5	AIA	0.5	13025	2.190
6	AIA	1	8882	2.330
7	DMP	0.05	54719	1.986
8	DMP	0.0625	49714	1.970
9	DMP	0.125	40171	2.001
10	DMP	0.25	27082	2.105
11	DMP	0.5	22728	2.113
12	DMP	1	13578	2.258

Table 3: feed and molecular properties of PLA with AIA and DMP

The values in table 3 confirm the formation of branched structures after the SSP process: post-polycondensation reaction not only increased Mn values, but also increased significantly the polydispersity index of these materials that are higher than those shown in tables 1 and tables 2.

As already noted in chapter 5, in relation to the star-architecture systems, even for polymers having tree architecture it should be underlined that the molecular weight values reported in table 3 for polymers with comonomer higher than 0,125% m/m are quite low to give polymers with good mechanical properties.

According to a first hypothesis, SSP process creates branching thanks to the reactions of carboxylic groups of the comonomers but these reactions are probably not enough to increase

significantly the length of PLA macromolecules. In other words, the equilibrium of the polycondensation reactions limits the branching of the chains.

On the other hand assuming a high conversion of carboxyl groups in SSP process and then an increase of branching increasing the concentration of multifunctional monomer, we can assume that highly branched chains are not long and therefore more compact ,resulting in a decrease in hydrodynamic volume and consequently in Mn values measured by SEC analysis.

Contrary to what happens to star systems in which, when multifunctional comonomer is 0.05% and 0.0625% m/m, an increase in molecular mass compared to the linear and not regulated polymer is observed, table 3 shows that this is not true for tree system, which have lower molecular weight values than linear PLA also using low amount of comonomers. This behavior has been observed in chapter 5 for polymers regulated with T1 (and similarly with a bi-functional comonomer). This observation supports the first of the two hypotheses reported above.

It will nevertheless be interesting to study if, despite the lower hydrodynamic volumes , there is an effect of tree architecture on the complex viscosity of these materials.

Figures 6 and 7 show the SEC curves of PLA samples synthesized with DMP and AIA after the SSP process.

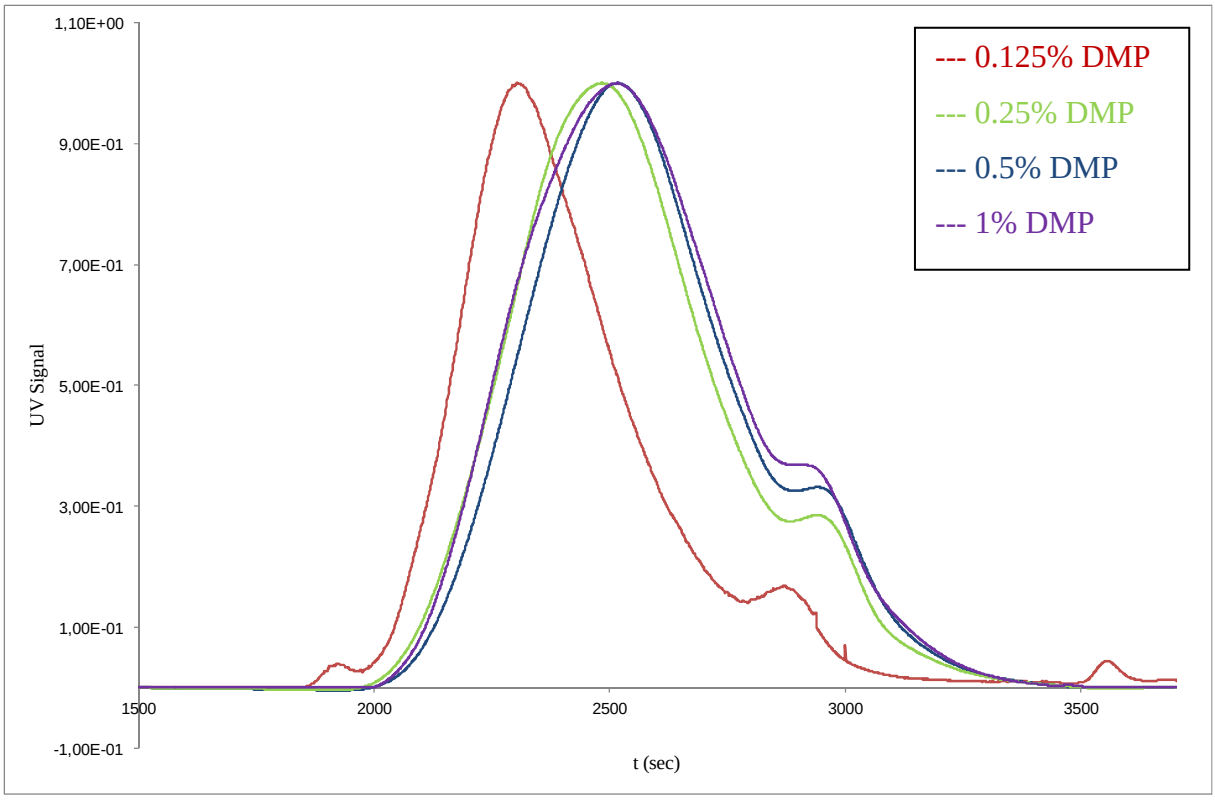

Figure 6: SEC curves of PLA with DMP after SSP

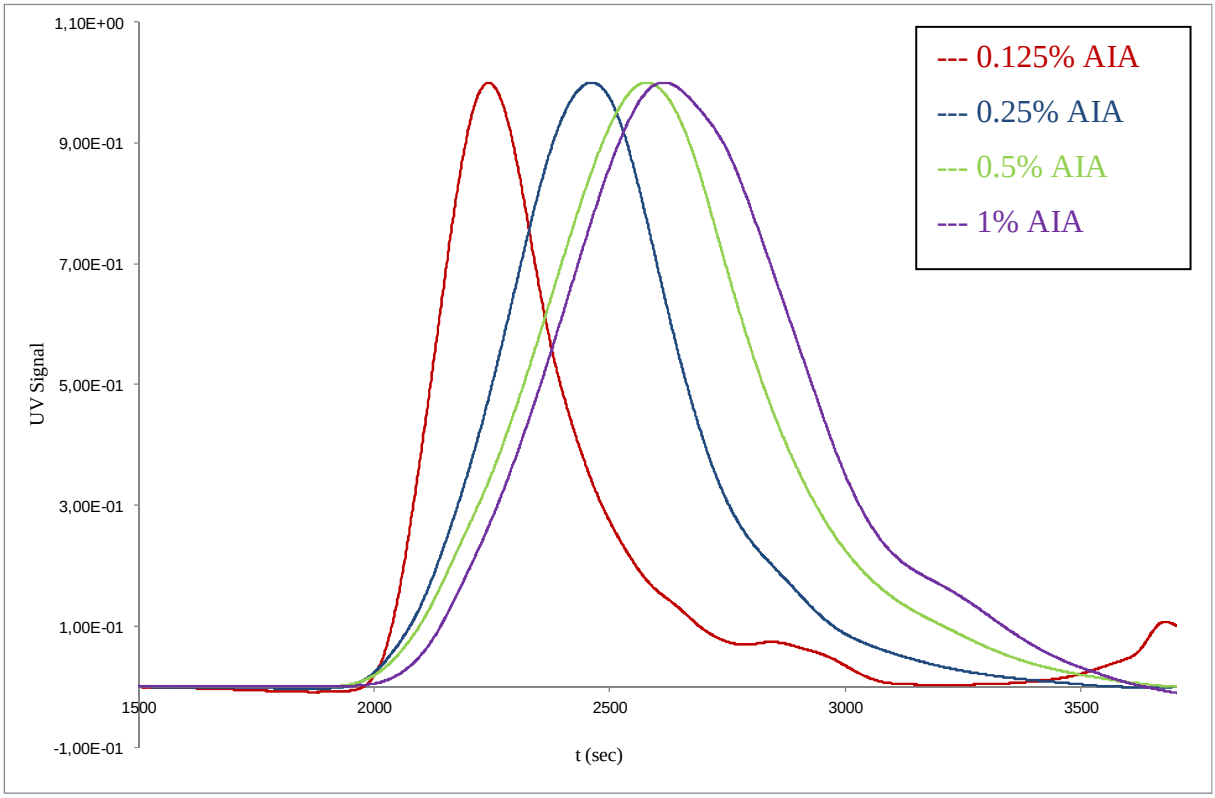

Figure 7: SEC curves of PLA with AIA after SSP

Figures 6 and 7 show that increasing the amount of 5 – aminoisoftalic acid and the amount of dimetilolpropionic acid the distribution of molecular masses increases and in particular the increase is clearly visible with concentrations higher than 0,125%.

SEC curves of PLA with DMP the presence of a double distribution can be observed, becoming more pronounced and more evident when comonomer quantities increase; the same behavior can be observed in PLAs synthesized with AIA, but the shoulder at low hydrodynamic volumes is less pronounced.

This phenomenon is not observed in linear PLA after a SSP process, and can therefore be attributed to the presence of the branching comonomer that, in SSP conditions, promotes the formation of species with different degrees of branching.

Similarly to what has been done for polymers with star-shaped architecture, also for tree system the effect of the addition of small amounts of comonomer was evaluated, using quantities lower than 0,125%, especially 0.05% 0.0625% m/m.

Decreasing the amount of multifunctional agent in the chain an increase of the Mn values is observed, as expected: the molecular weight is controlled by the amount of hydroxyl or amino groups in the feed, as previously observed. Also in these polymers there is an increase of molecular masses distribution after SSP process and polydispersity values are slightly lower than those observed for PLA synthesized with higher amounts of branching comonomer.

Figure 8 and 9 show the SEC curves of polymers synthesized with lower amount of DMP and AIA.

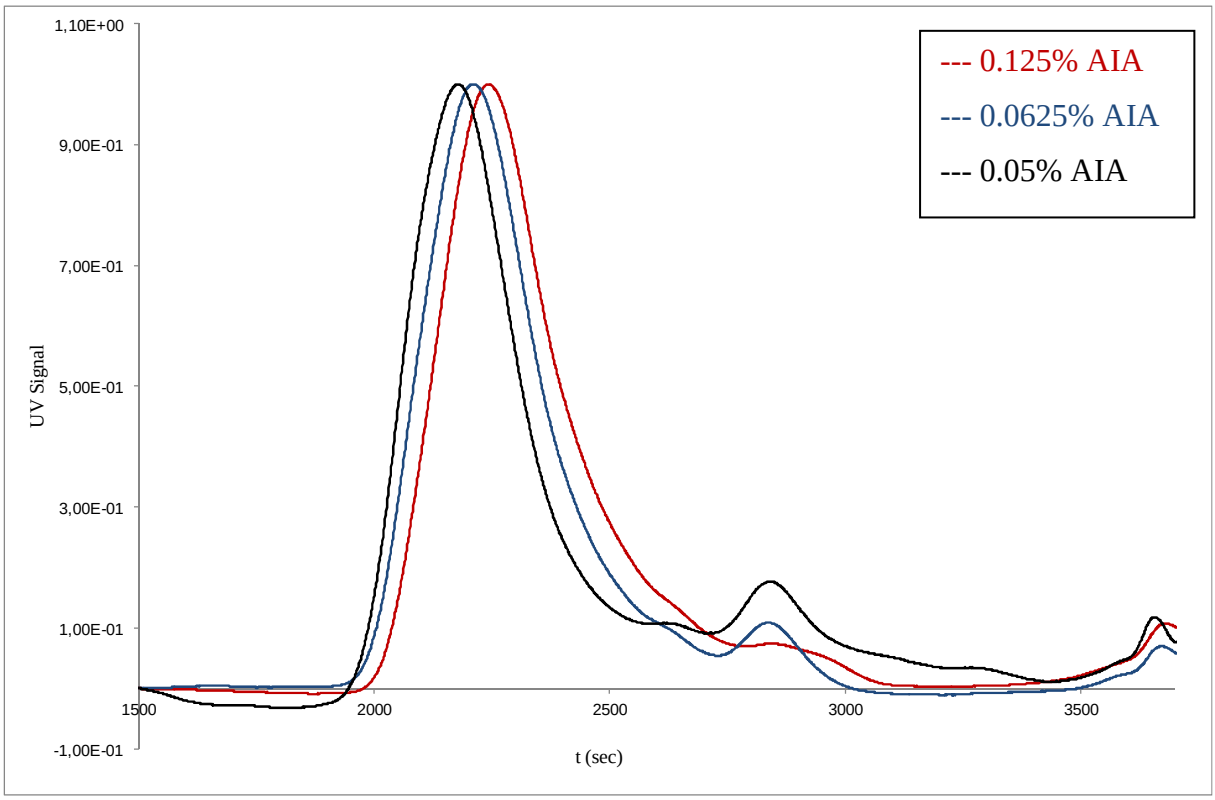

Figure 8: SEC curves of PLA with AIA after SSP

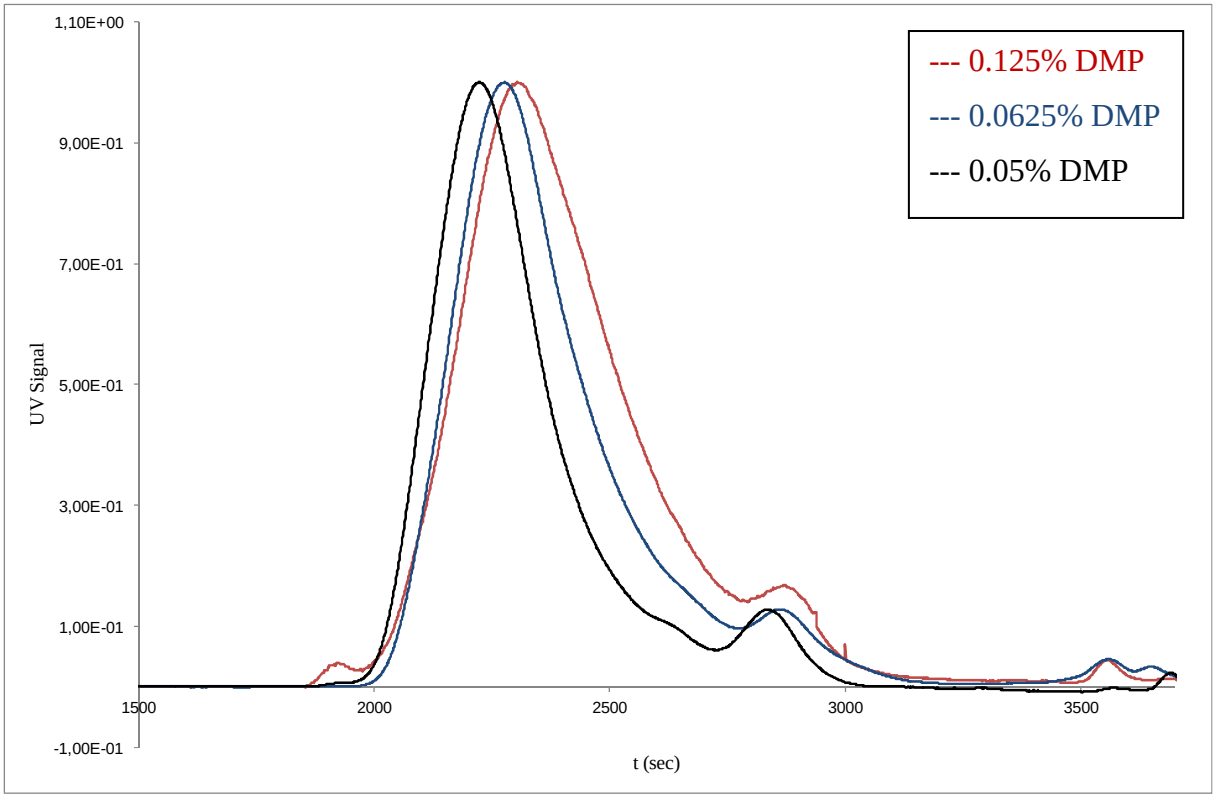

Figure 9: SEC curves of PLA with DMP after SSP

6.3 RHEOLOGY OF PLA WITH TREE ARCHITECTURE

After studying the effect of AIA and the DMP on molecular properties of PLA, rheological behavior of these polymers was evaluated by frequency sweep analysis. The analytical method is the same used for PLA with star macromolecular architecture described in chapter 5.

In particular it will be interesting to evaluate two main aspects: whether the macromolecular architecture sufficiently affects the viscosity, increasing it above that the one of the linear polymer, and the influence of low molecular weight species, formed during the SSP process, on the rheology of polymers.

Figures 10 and 11 show the rheological curves of PLA synthesized in the presence of DMP, respectively, and AIA.

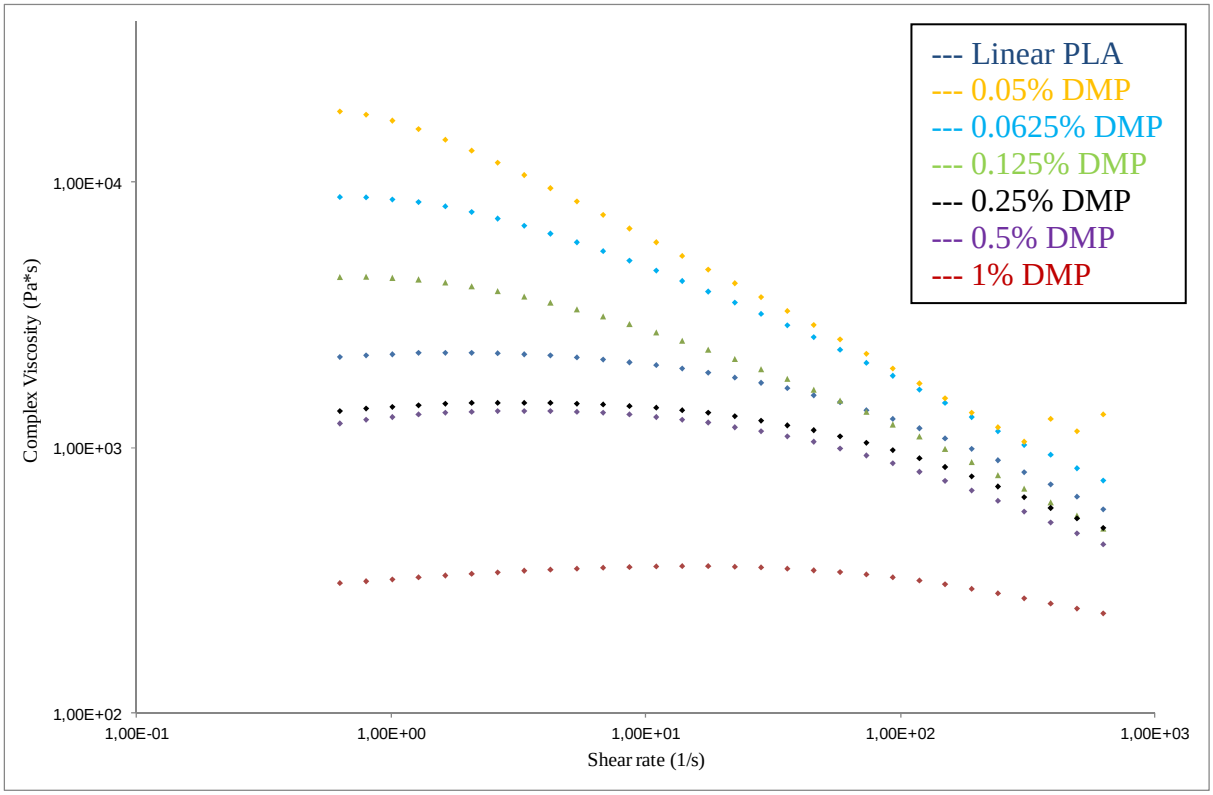

Figure 10: rheological curves of PLAs with DMP

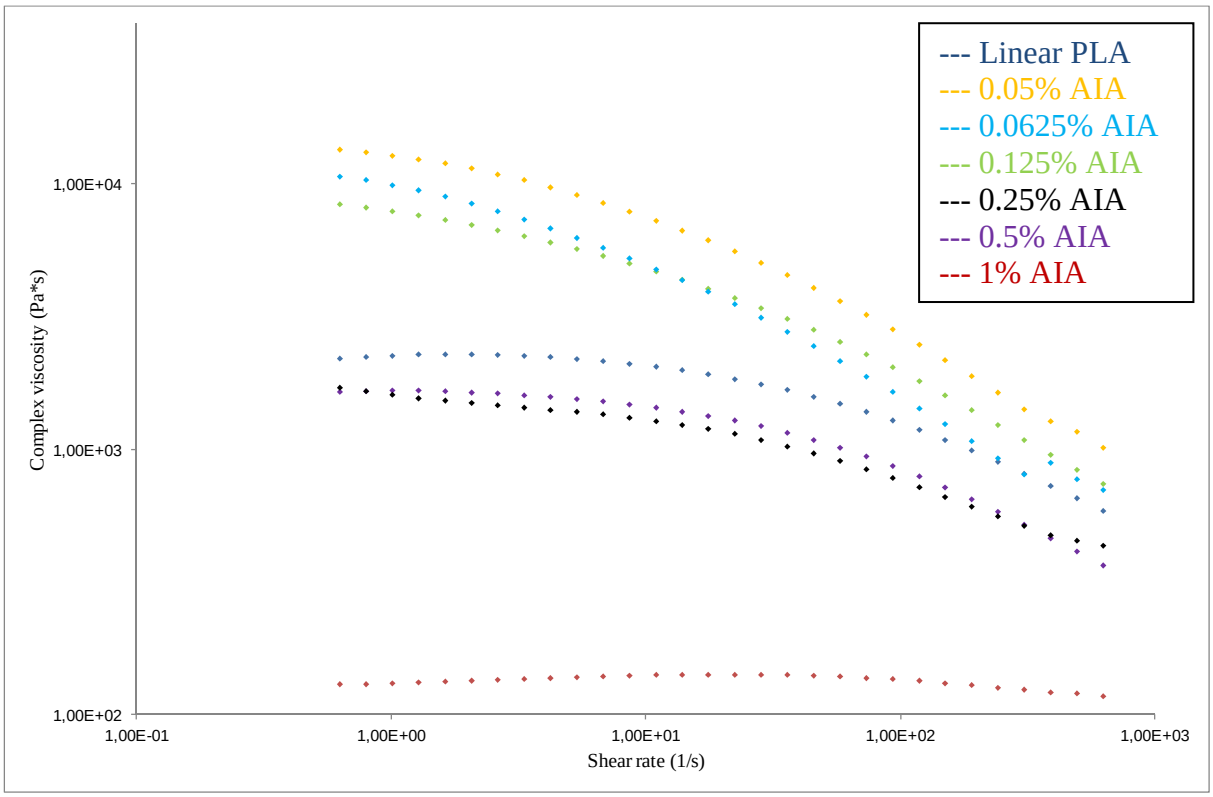

Figure 11: rheological curves of PLAs with AIA

From figures 9 and 10 we observe that complex viscosity curves of the polymers obtained in the presence of DMP and AIA in concentrations lower than 0.25% have values significantly higher compared to linear polymer. In particular, there is a very marked increase in complex viscosity in the presence of a DMP concentration of 0.05% and 0.0625% and in presence of a AIA concentration from 0.125% to 0.05%. For higher amounts of comonomers, a continuous decrease of complex viscosity is observed, and polymers with higher amounts of branching agents (up to 0.25%), are less viscous than linear polymer.

Rheological behavior confirms the first hypothesis exposed in the previous paragraph; in presence of small concentrations of branching comonomer, molecular weight is sufficiently high to guarantee the presence of extended and open chains, with linear arms having high DPn values. This factor, coupled with the fact that the average degree of branching of macromolecules is relatively low due to poor conversion of carboxyl groups, allows the formation of entanglements between different polymer chains that can interact freely and form physical "knots", called entanglements, that allow to have high melt viscosity.

On the other hand, increasing the percentage of comonomer, macromolecules will have lower hydrodynamic volume due to the increased amount of hydroxyl groups or amino groups into the feed. The decrease in molecular weight and the low percentage of ramifications, due to the equilibrium of condensation reactions, which limits the ramifications of the chains, justifies both the lower hydrodynamic volume observed by SEC analysis and the lower viscosity of the melt because the macromolecules cannot interact to form the amount of entanglements required to increase the viscosity of the material.

In chapter 5, studying the viscosity of star systems, it was observed that small amounts of multifunctional comonomer act as chain extender, increasing the molecular weight of regulated PLA in comparison to linear polymer, with a consequent increase in viscosity, which is higher than that of linear standard PLA.

Analyzing the rheological curves in figure 10 and 11, and correlating the viscosity with molecular weight data reported in table 3, despite the values of Mn are lower than those of unbranched PLA, a significant increase in viscosity especially for systems with a low-branching agent is observed. This is due to the contribution of high molecular weight species on the viscosity of the polymer.

Samples having AIA and DMP higher than 0,125% m/m have molecular weights too low, therefore the lower number of branches and the lower concentration of high molecular weight species are not sufficient to improve the rheology of the material.

REFERENCES

[1] Flory, P. J., *J. Am. Chem. Soc.*, 74, 1952, 2718.

[2] Kricheldorf, H. R., Zhang, Q. Z., Schwarz, G., *Polymer*, 23, 1982, 1821.

[3] Kim, Y. H., Webster, O. W., *Polym. Prepr.*, 29(2), 1988, 310.

[4] Muller, A. H. E., Yan, D., Wulkov, M., *Macromolecules*, 31, 1997, 7015.

Yan, D., Muller, A. H. E., Matyjaszewski, K., *Macromolecules*, 31, 1997, 7024.

[5] Malmstrom, E., Johansson, M., Hult, A., *Macromolecules*, 28, 1995, 1698.

[6] Yan, D., Zhou, Z., Jiang, H., Wang, G., *Macromol. Theory Simul.*, 7, 1995, 13.

[7] Long, T. E., Wilkes, G. L., Unal, S., Mckee, G. M., *Prog. Polym. Sci.*, 30, 2005, 507-539.

[8] Voit, B. I., Lederer, A., *Chem. Rev.*, 109, 2009, 5924–5973.

[9] Trollsas, M., Hedrick, J. L., *J. Am. Chem. Soc.*, 120, 1998, 4644-4651.

[10] Trollsas, M., Claesson, H., Atthoff, B. Hedrick, J. L., *Angew. Chem. Int. Ed.*, 37, 1998, 3132.

[11] Frey, H., Skaria, S., Smet, M., *Macromol. Rapid Commun.*, 23, 2002, 292-296.

[12] Gotschalk, C., Frey, H., *Macromolecules*, 39, 2006, 1719-1723.

[13] Cooper, T. R. Storey, R. S., *Macromolecules*, 41, 2008, 655-662.

7. Study of PLA with tree-star macromolecular architecture

7 STUDY OF PLA WITH TREE-STAR MACROMOLECULAR ARCHITECTURE

7.1 THEORY OF TREE-STAR ARCHITECTURE SYSTEMS

A system more complex than the ones described in chapters 5 and 6 can be achieved adding to the reaction mixture the main monomer, AB, a multifunctional RA_f agent and a branching agent with general formula BA_2.

In this case the star macromolecules created by the RA_f agent can react with multifunctional BA_2 comonomer and with macromolecules having a tree structures to generate more branching and complex macromolecules defined as tree-star polymers. The degree of branching and the complexity of the system depend on the percentage of the two comonomers added and on their internal ratio.

A schematic structure of a tree star macromolecule is shown in figure 1.

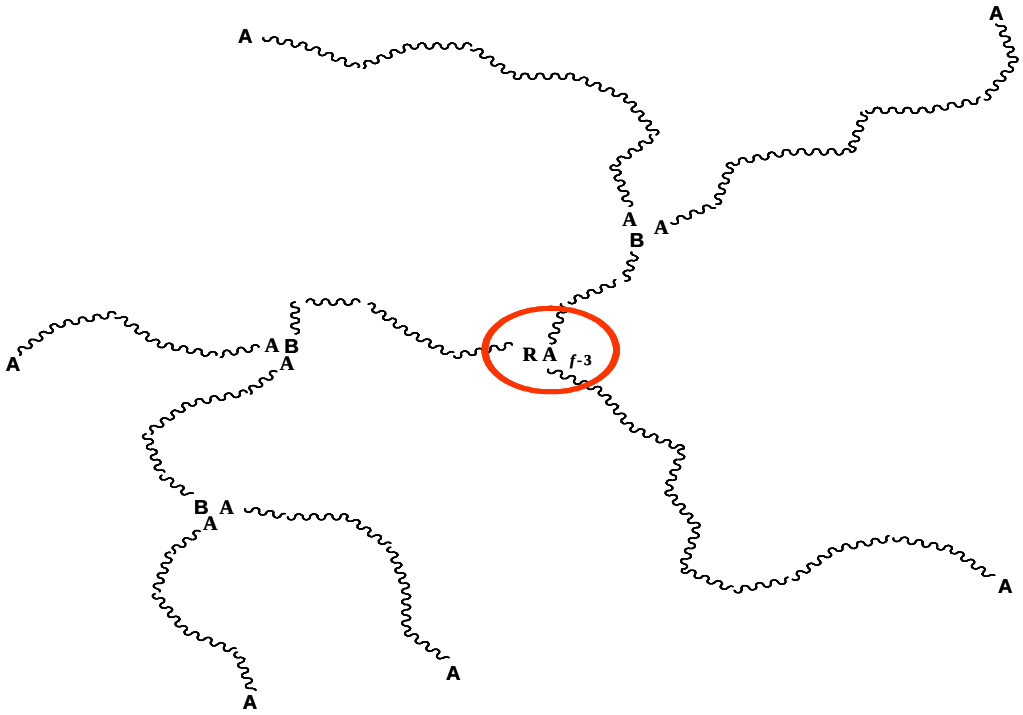

Figure 1: schematic structure of a tree-star macromolecule

In chapter 6 it was described why it is not possible to obtain branched structures directly during polymerization process using AB_2 comonomer with one or more carboxyl groups due to the non-reactivity of the COOH group with the lactide.

It is therefore necessary a SSP reaction, able to promote the reaction between the acid groups of the branching comonomer and the terminal groups of the polymer chain, to obtain polymers with tree or tree star macromolecular architecture.

For this reason an alternative combination of comonomers was chosen, different to the ones traditionally used to synthesized tree-star polymers, based on a mixture of RA_f and BA_2 comonomers, which did not include the use of a comonomer with COOH groups.

The comonomers chosen must still respect the characteristics of stability and compatibility already mentioned in chapter 5 and possibly should not require polymerization conditions different from those used for the production of linear polymer.

The system identified for this type of architecture involves the use of polyols T_x, described in chapter 5 for the synthesis of star PLAs, and pyromellitic dianhydride, benzene-1,2,4,5-tetracarboxylic dianhydride, whose structure is shown below.

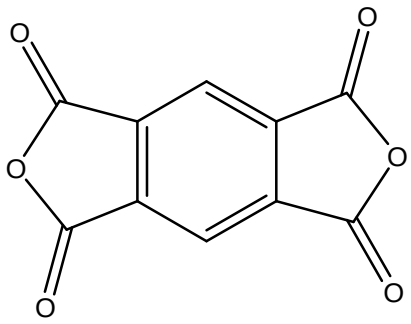

pyromellitic dianhydride

Polyols act as a central core from which the growing chains propagate; they also regulate the molecular weight, while the dianhydride acts as a link point between different star macromolecules. The dianhydride, during the polymerization, behaves as a bi-functional agent, because after the first reaction in which OH groups of polyols attack the anhydride, two free carboxylic groups which do not react in the synthesis conditions, as discussed previously, are formed. Under SSP conditions free COOH functions can further react increasing the degree of branching of the system. So the dianhydride, depending on operating conditions, can act as a bi-functional regulator or as a tetra-functional comonomer, with the possibility to modulate the properties and the behavior of the polymer, especially for what concerns the rheology.

7.2 MOLECULAR PROPERTIES OF TREE-STAR PLAs

The combined use of two different comonomers in feed allows to obtain macromolecules with very complex tree-star architecture. In these systems there is a double convergent effect: the first one is related to a decrease of molecular masses distribution promoted by the star agent, while the second one is the increase of the polydispersity index by branching comonomer.

Tree-star polymers are highly complex systems that require study and planning of feed to obtain non-crosslinked materials with good properties. The complexity of feed is however a key factor that can modify, if well controlled, the ratio between reactive groups in order to obtain polymers with different properties, especially regarding their rheological behavior.

For this study several samples of PLA have been synthesized in the presence of different polyols: T2, T3, T4 and T6 as a star agents and pyromellitic dianhydride as branching comonomer.

The method of synthesis is similar to those already optimized and used for the synthesis of linear PLAs, star PLAs and tree PLAs.

For the design of these systems we considered two parameters: the molar percentage of T_x comonomer compared to repetitive unit in the chain and the ratio between the hydroxyl groups of polyol and the carboxylic groups of pyromellitic dianhydride. By this way the effect of the unbalance of reactive groups was investigated, since it governs how polymers reach the gel point and the behavior of the different materials in rheology.

The amount of pyromellitic dianhydride in feed was calculated assuming that it acts as a tetra-functional acid comonomer: two carboxyl functionalities react after nucleophilic attack of OH groups to the carbon of anhydrides, while the other two, that arise after the ring opening of anhydride, react during the SSP process where operating conditions allow to shift the equilibrium of the reaction, as already seen in chapter 6 studying PLA with tree architecture.

Moreover, utilizing four different T_x comonomers as central core it is possible to evaluate the effect of the number and length of the arms on the molecular and rheological properties of the polymer, and also to synthesize systems with mixtures of different T_x comonomers, always with the aim to modulate the properties of the material.

Table 1 shows the samples synthesized, the feed used and the molecular properties obtained by SEC analysis and expressed as linear.

Sample	Comonomer	% Tx	% Pyromellitic dianhydride	Mn SEC	D
0	-	-	-	56909	1.982
1	T2	0.05	0.025	58433	1.893
2	T2	0.0625	0.03125	53200	1.902
3	T2	0.125	0.0625	45972	2.002
4	T3	0.05	0.0375	83042	2.477
5	T3	0.05	0.025	70701	1.878
6	T3	0.0625	0.04688	53964	2.125
7	T3	0.0625	0.03125	44812	1.960
8	T3	0.125	0.09375	29030	1.818
9	T3	0.125	0.0625	25895	1.781
10	T4	0.05	0.05	insolubile	-
11	T4	0.05	0.025	69298	2.437
12	T4	0.0625	0.0625	insolubile	-
13	T4	0.0625	0.03125	65068	2.501
14	T4	0.125	0.125	insolubile	-
15	T4	0.125	0.0625	27138	2.758
16	T6	0.05	0.075	insolubile	-
17	T6	0.05	0.025	69638	2.144
18	T6	0.0625	0.09375	insolubile	-
19	T6	0.0625	0.03125	73137	2.744
20	T6	0.125	0.1875	insolubile	-
21	T6	0.125	0.0625	29138	2.848
22	T3	0.08	0.04	63225	2.143
23	T4	0.06	0.03	66839	2.326
24	T6	0.04	0.02	70233	2.419
25	T3	0.03	0.015	118050	1.893
26	T4	0.025	0.0125	153450	1.914
27	T6	0.015	0.008	161280	2.002
28	T2-T6	25%T2-75%T6	50% T2+T6	142360	2.165
29	T2-T6	50%T2-50%T6	50% T2+T6	148500	2.184
30	T2-T6	75%T2-25%T6	50% T2+T6	147238	2.190

Table 1: feed and molecular properties of tree-star PLA

To better understand the data collected in table 1 is necessary to make some clarifications: samples 1-3 were synthesized using different percentages of T2 comonomer in combination with a molar amount of pyromellitic anhydride equal to 50% of T2 comonomer. Samples 4-21 were synthesized in the presence of three different percentages of T3, T4 and T6 comonomers in combination with two different amounts of pyromellitic anhydride: 50% m/m respect to the polyol comonomers or enough to obtain a [OH]/[COOH] ratio of 1. Samples 22-24 were synthesized using the same amount of hydroxyl groups used in sample 3, in order to have the same length of the arm that starts from the central core; samples 25-27 have the same OH groups of sample 1.

Finally samples 28-30 were synthesized using a mixture of T2-T6 comonomer in presence of 50% m/m of anhydride compared to the total moles of T2 and T6 used. The samples with 100% of T2 and 100% of T6 are respectively sample 1 and sample 27.

Looking at the data collected in table 1 polyols comonomers that, as already mentioned in chapters 5 and 6, affect the molecular weight which is regulated by the amount of OH groups included in the feed, have the biggest effect on the molecular properties.

By analyzing the values of molecular weight of the samples 4-9 the effect of the concentration of pyromellitic anhydride can be observed: an amount of anhydride balancing the hydroxyl functions leads to an increase in molecular weight and polydispersity. Increasing the number of reactive groups of the polyols (samples 10-21) leads to two different effects: the first is the inability to completely balance the number of OH and COOH groups, because in this condition the system reaches the gel point. A totally cross-linked polymer is insoluble in solvents and therefore cannot be analyzed by SEC, but the control of the feed is also important to avoid cross-linking of the material that may be particularly harmful if it should occur in a industrial plant.

For this reason, samples from 22 to 30 were synthesized in the presence of 50% molar of pyromellitic anhydride.

The second effect is the increase of the polydispersity index of the samples prepared with T4 and T6 compared to similar polymers in which T3 comonomer was used. The increase in the number of arms, in combination with the use of anhydride, leads to a considerable divergence of the system, with polydispersity values that grow with increasing the percentage of T_x comonomer in the feed. A higher number of arms contributes to having more branched structures.

Samples from 22 to 27 don't show particular behavior or differences from a molecular point of view, if not a predictable increase in the values of Mn increasing the chain length: more interesting will be the study of the melt viscosity. Also a very similar behavior has been observed for the last three samples (28-30): the combined use of a T2-T6 mixture does not change much the values of Mn and D, which increases a little increasing the % of bi-functional regulator, but modifies the rheology of polymers.

Figures 2, 3, 4 and 5 show the SEC curves of some samples described in Table 1.

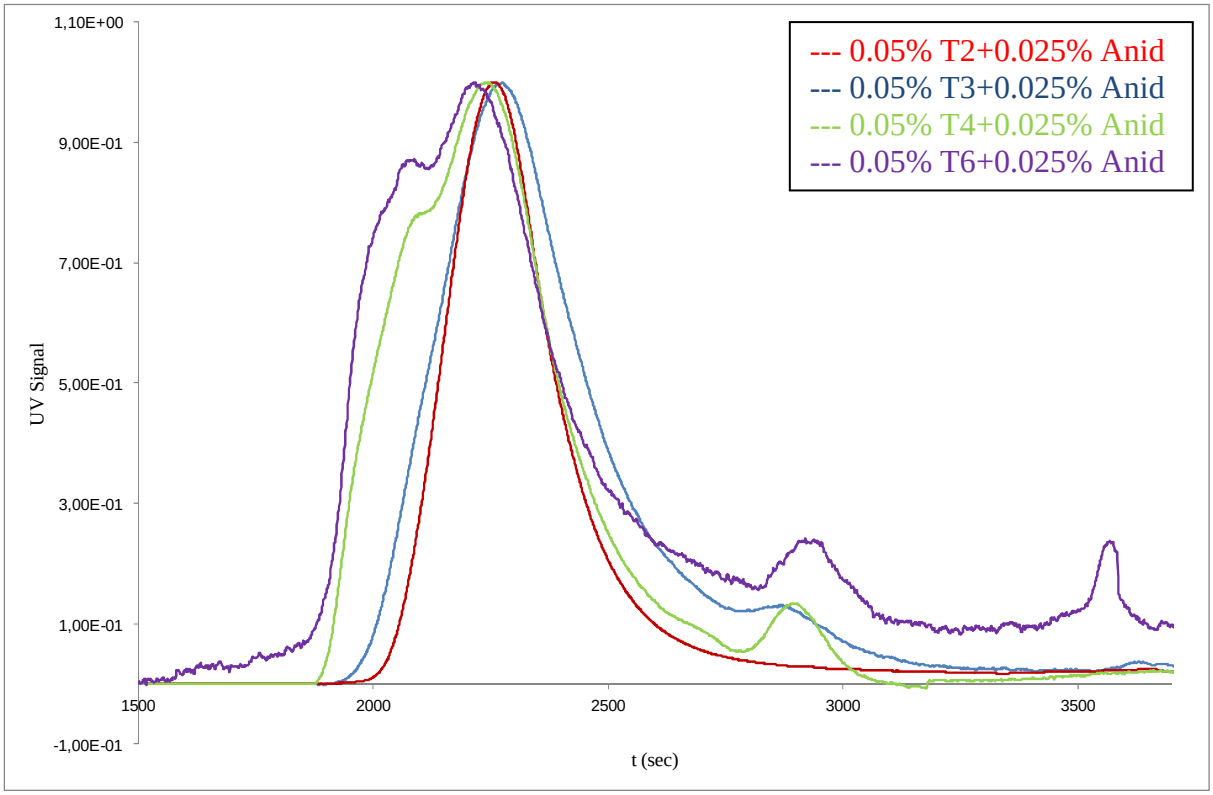

Figure 2: SEC curves of samples 1, 5, 11, 17

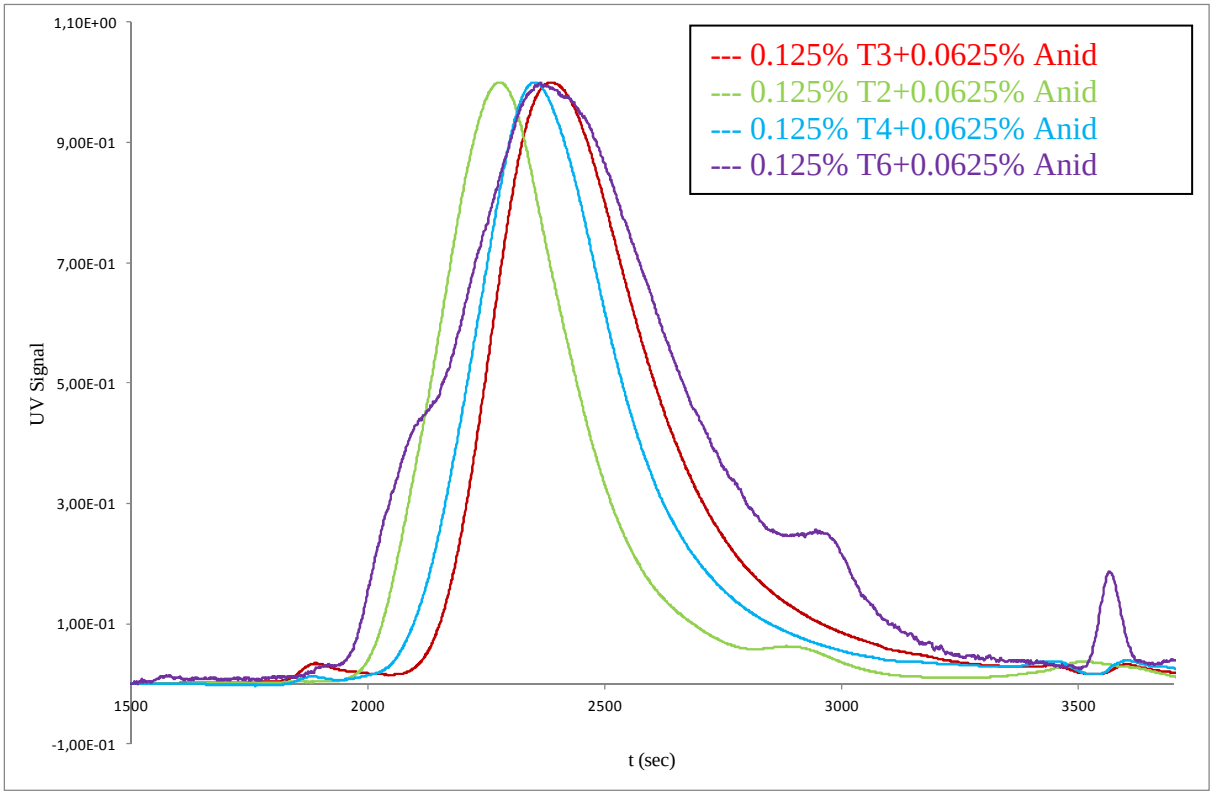

Figure 3: SEC curves of samples 3, 9, 15, 21

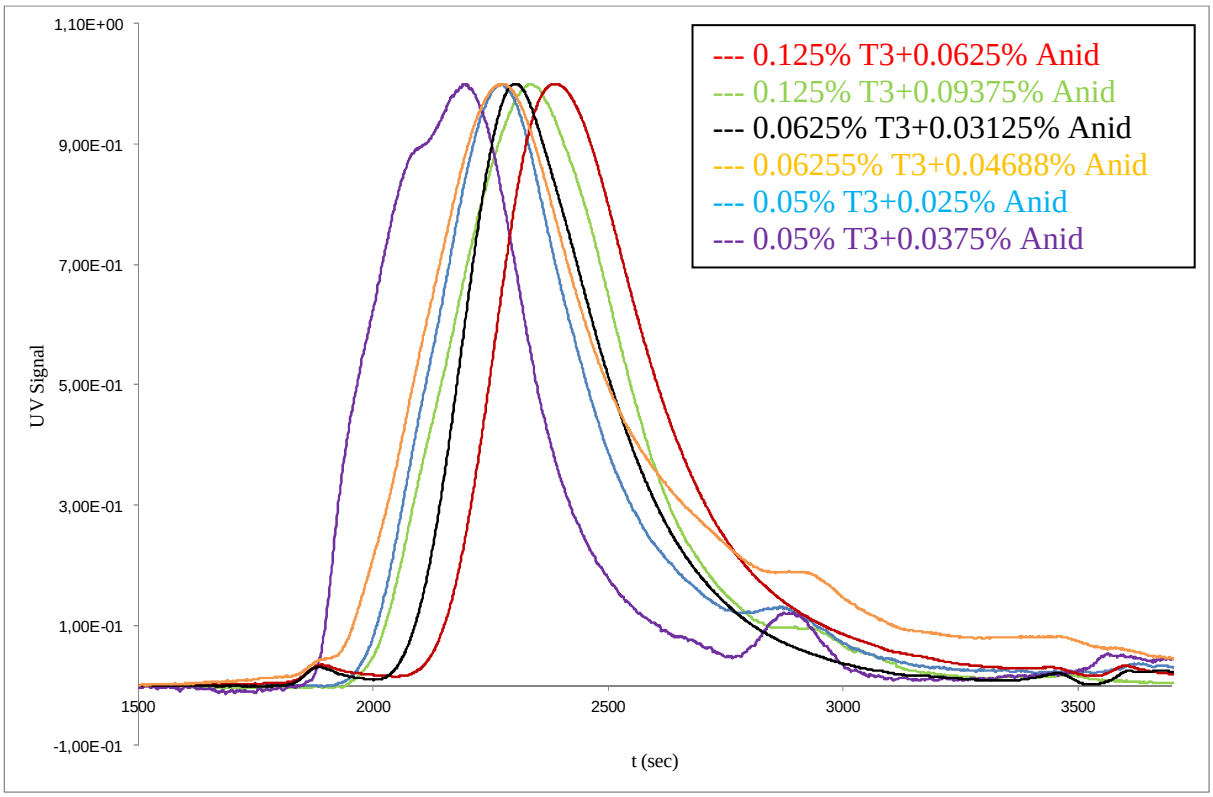

Figure 4: SEC curves of samples 4-9

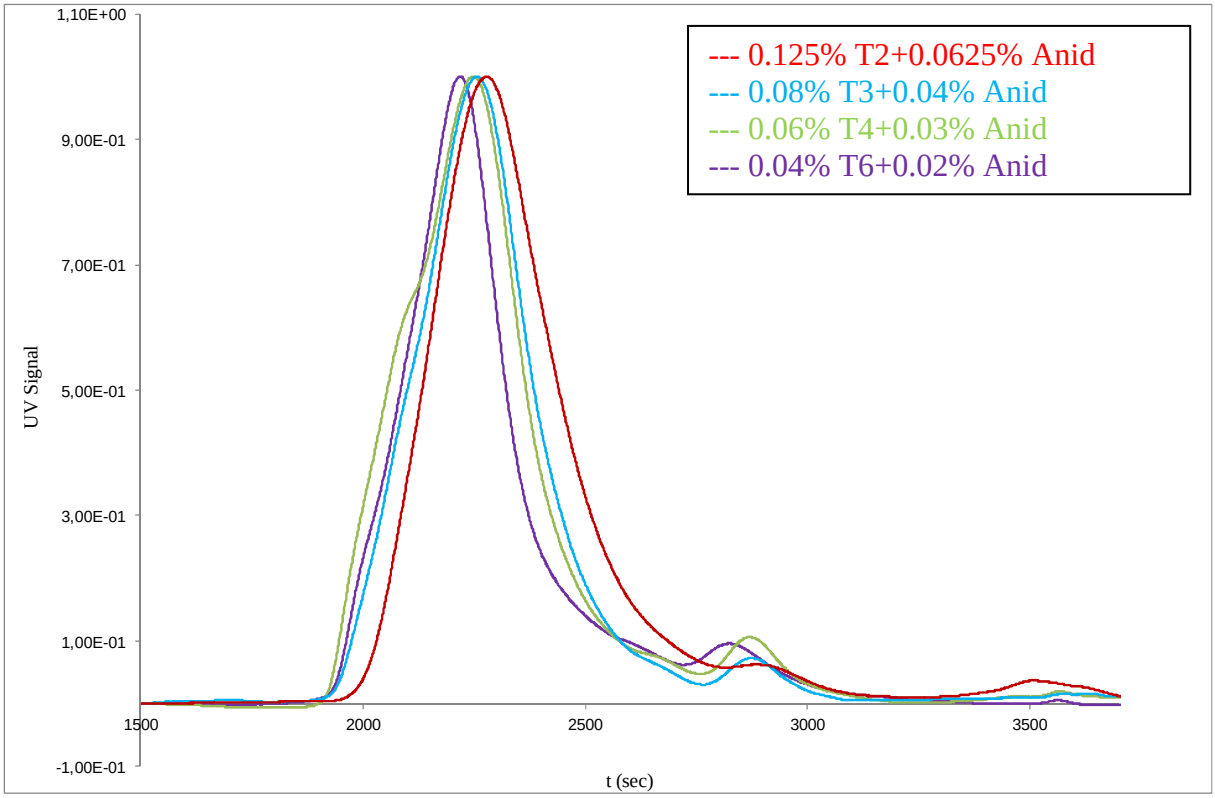

Figure 5: SEC curves of samples 3, 22-24

SEC curves of figure 2 and 3 show the effect of different polyols on Mn and polydispersity values. In the PLA synthesized in the presence of low concentration of T_x comonomer (Figure 2) there is an effect of chain extension caused by the central core, which causes an increase in molecular masses, especially in the presence of T4 and T6 regulators, as already reported in chapter 5 for star systems. It is also interesting to note that the GPC curves for polymers synthesized with T4 and T6 show a lack of homogeneity in the left side of the curve, probably due to the formation of high molecular weight species after the reaction with pyromellitic dianhydride. The higher number of arms of these two regulators leads to structures having an high degree of branching with a greater hydrodynamic volume. Using larger amounts of T_x comonomer (Figure 3) the polyol has a dominant effect compared to anhydride: going from T2 to T3 a reduction of the hydrodynamic volume due to the action of the star comonomer is observed. Increasing the number of OH groups, the possibility to have an higher level of ramifications leads to an opposite effect compared to that observed for star polymers: a slight increase of molecular mass but also a broadening of the distribution curve is observed and confirms the greater complexity of the system.

The GPC curves in figure 4 show how is possible to control the molecular weight and polydispersity of polymers changing the quantity of pyromellitic anhydride added in the feed. Looking at the SEC curves it is clear that operating with a [OH]/[COOH] ratio of 1, PLAs with molecular weight higher than the ones of polymers synthesized without balancing all the reactive functionalities are obtained: in this second case, in fact, an effect of star comonomers on molecular weight still remains.

The choice of the central polyol is also essential to obtain a non-crosslinked material with a molecular weight distribution curve as homogeneous as possible: all polymers synthesized with T3 comonomer are soluble and only in the presence of very low amounts of comonomer (0.05%) and balancing all the reactive groups SEC curves show a shoulder in the high molecular weights area.

Figure 5 shows the effect of central core: keeping constant the length of the arm an increase of Mn values, by increasing the number of hydroxyl groups of T_x comonomer, has been observed.

7.3 RHEOLOGICAL PROPERTIES OF TREE-STAR PLAs

The study of the molecular properties of polymers with high compositional complexity is not simple and easy especially in the absence of a theoretical model of growth of the polymer chain.

To evaluate the potential of materials with this kind of complex molecular architecture, it is therefore important to study their rheological behavior: the most important aspect for these polymers is, in fact, the different rheological properties compared to a linear PLA.

The rheological analysis of tree-star polymers were performed with the same procedures already used for PLA with star and tree architecture described in chapters 5 and 6. Figures 6, 7 and 8 show the rheological curves of some samples described in table 1.

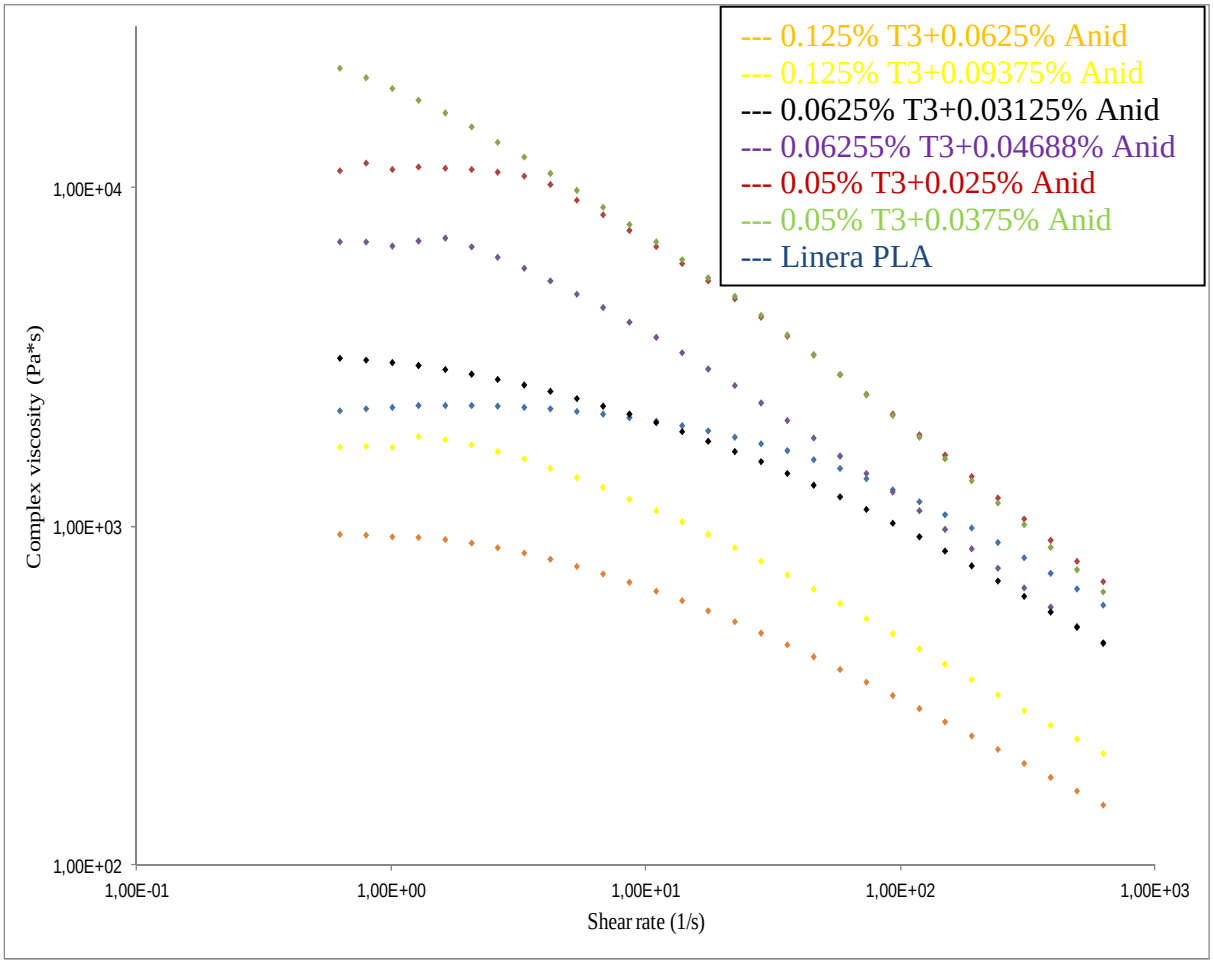

Figure 6: rheological curves of samples 4-9

The rheological curves in figure 6 show how it is possible to control the viscosity of tree-star PLA star-tree by varying the initial feed. The percentage of T3 comonomer greatly influences the viscosity of polymers: increasing the amount of T3 the rheological curves drop significantly, and T3 percentage of 0.125% the viscosity is lower than the viscosity of linear polymer. But the difference in viscosity between polymer with 0.125% of T3 and the unmodified PLA is not high, while the Mn values are quite different; there is therefore a positive effect on the viscosity of the material.

The viscosity of the materials can be modulated by changing the [OH]/[COOH] ratio: using the same percentage of T3 comonomer, the viscosity of the polymer is higher if all the reactive functionality are completely balanced. So the greater the amount of pyromellitic anhydride in the polymer the higher its viscosity.

The effect of structure on the viscosity is evident at low stress values, whereas for high shear rates the viscosity of the material is lower than that of the linear polymer, except for the materials synthesized with 0.05% of T3.

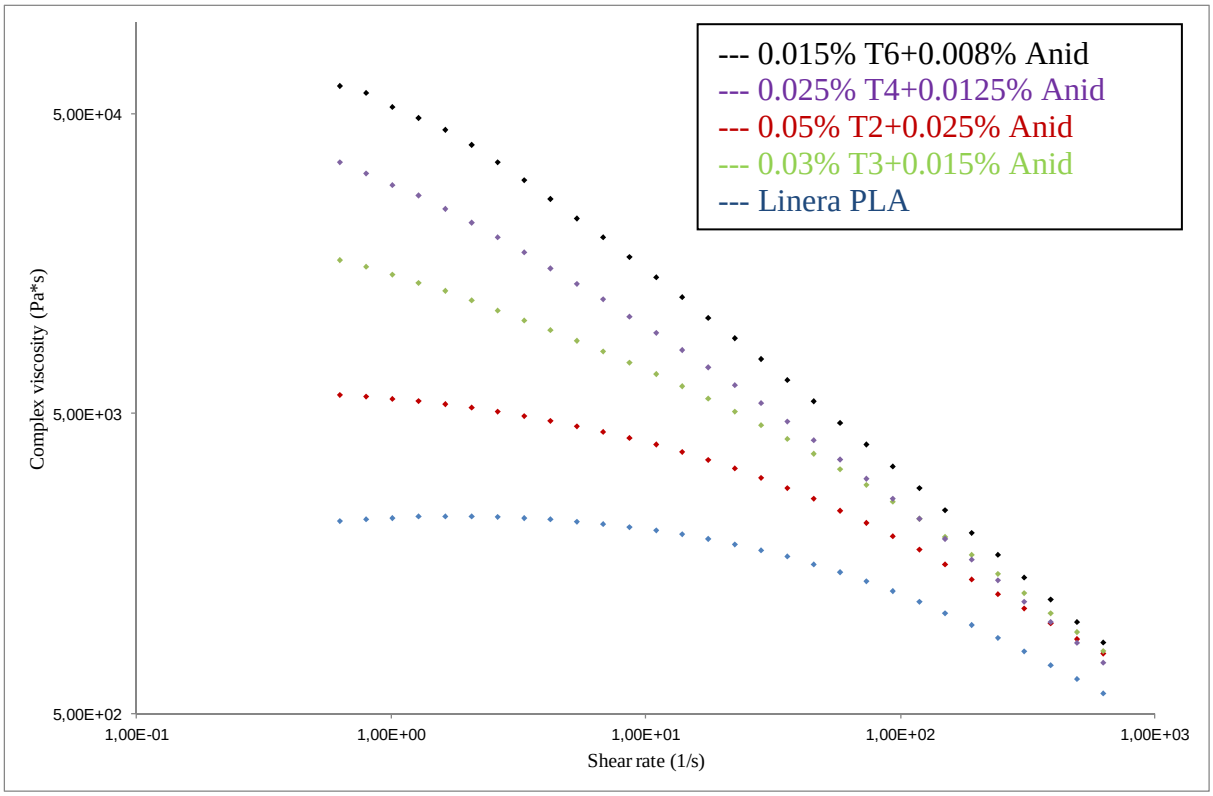

Figure 7: rheological curves of samples 1, 25-27

Figure 7 shows the effect of different types of central core on the viscosity of PLA: with a constant chain length, increasing the number of arms, the viscosity of the tree-star polymer increases a lot. It is interesting to note that the viscosity of the PLA in which the core is the T2 comonomer (red curve) at low values of shear rate reaches a plateau, while the systems with a central core with three or more arms has an upward trend. At high values of shear rate the viscosity of these materials are very similar, while the effect of the structure occurs by reducing the shear rate.

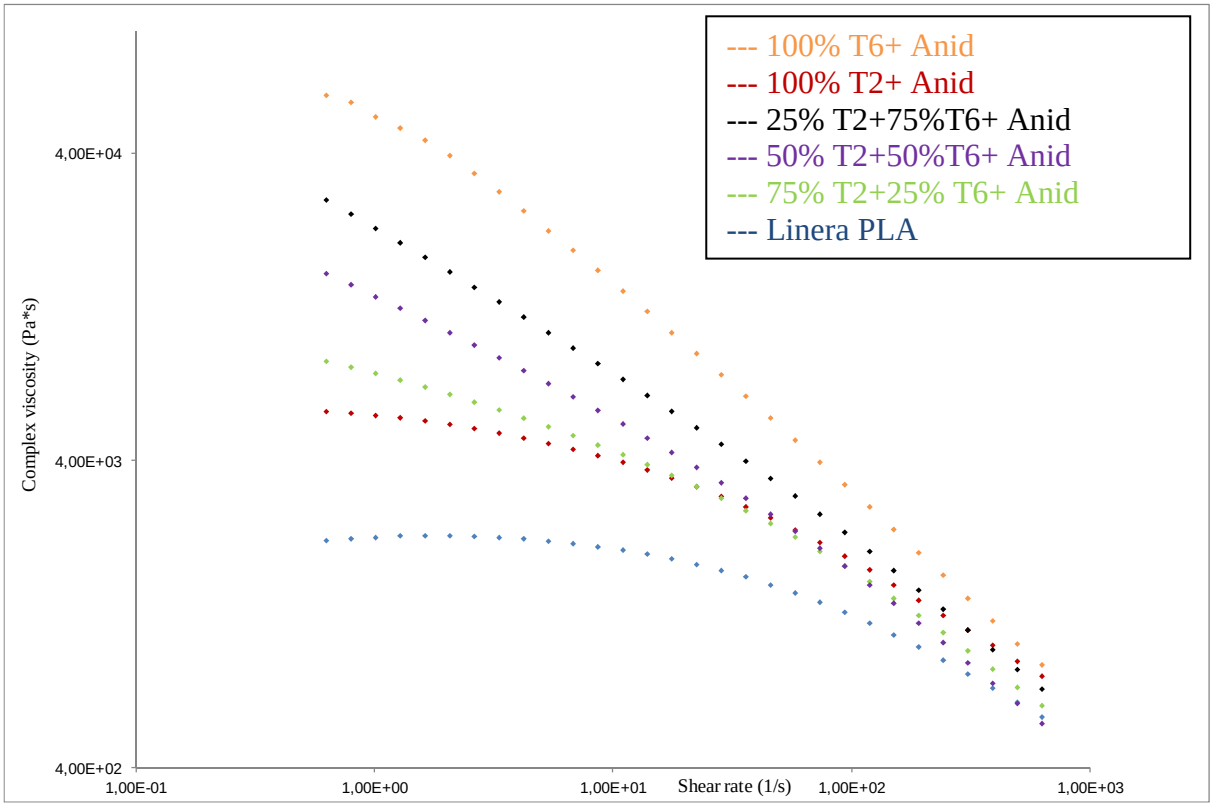

Figure 8: rheological curves of samples 1, 27-30

Figure 8 shows the effect of the core: increasing the percentage of T6 in the feed, complex viscosity increases. The rheological curves of tree-star PLA with a different feed cover a wide range of complex viscosity. So it is possible to modulate the rheological behavior of these materials by acting on the concentration of comonomers in feed.

The interesting results obtained from the SEC analysis, and especially with the rheological analysis, for tree-star PLA can be an interesting starting point for further study of these systems.

By varying the percentage of anhydride is also possible to change not only the viscosity but also to obtain materials with different molecular weights, with a homogeneous distribution curve and without reaching the gel point.

Given the possibility of using different combinations of comonomers it will be necessary to make a screening of feeds that have provided interesting preliminary results, and further study of the rheological behavior. Because of these materials appear to be quite promising, it will be interesting to study the mechanical, morphological and thermal properties to verify the possibility to use them in application fields where the PLA is currently used.

Another important aspect is that these materials can be synthesized with the same cycle of synthesis normally used for linear PLA without changing the industrial plants.

8. PLA nanocomposite materials

8 PLA NANOCOMPOSITE MATERIALS

8.1 POLYMERS AND NANOTECHNOLOGIES

Nanosciences and nanotechnologies are a new scientific and technological approach to study structure and behavior of matter at the atomic and molecular level.

The prefix "nano" means 10^{-9}, which is a billionth of a unit; from a conceptual point of view, the term nanotechnology refers to the nanoscale of atoms and molecules and to new properties that can be understood and controlled working in this field. These properties can be used and applied on a microscopic scale, for example to develop materials and devices with new functions and performance.

In the last decade, nanomaterials have been the subject of great interest because they could represent a real technological revolution for the advent of electronics and information technology.

To better understand the interest in nanotechnologies, it is sufficient consider that in 1997 funding for research and development of nanomaterials in the U.S. amounted to 116 million dollars and that within the next three years rose to 270 million dollars and they are still growing. Similar funding have been invested also in Europe and Japan.

Nanomaterials have at least one dimension lower than 100 nm and a high ratio between surface area and volume: for this reason the characteristics of surface atoms are predominant in comparison to the one of internal atoms.

The variety of nanomaterials and matrices in which they can be dispersed is very high, therefore the potential applications regard several fields: energy and environment, transports pharmaceutical, biomedical, textiles, mechanical, electromechanical, clothing, chemical and petrochemical, electronics and information technology.

Nanocomposites represent a new class of materials, in any way alternative to traditional composite materials.

Traditional composite materials are made with particles (filler) dispersed in different kind of matrices. These materials are characterized by an improvement of some properties, generally associated with an increased density and a complicated processing steps.

The use of nano-sized fillers (nanofillers) allows to achieve a high degree of dispersion of the filler in the matrix and a very high surface/volume ratio of reinforcement; thus a significant improvement of properties can be obtained, maintaining a processability similar to the one of pure material.

Moreover, in traditional composite materials, there is a clear separation at the macroscopic level between the organic phase and inorganic phase, without any significant interactions between them. Using a surface treatment on inorganic materials it is possible to obtain only a dispersion at the microscopic level. On the contrary, nanocomposites are a new class of materials characterized by a very high dispersion of phases, typically in the order of a few nanometers. Because of this dispersion, nanocomposites have unique properties not shared by conventional composites (microcomposites), and can offer new technological and economic opportunities.

As mentioned previously, the term "nanocomposite" describes a composite material in which one of the phases has at least one dimension that belongs to the scale of nanometers. A nanocomposite polymer is, therefore, defined as a nanocomposite that uses a polymer (both thermoplastic and thermosetting) as a matrix.

The improved properties of these materials are: better mechanical properties such as strength, modulus, stiffness and dimensional stability, decreased permeability to gases like oxygen, water vapor and hydrocarbons, thermal stability, flame retardance and low emission of smoke, chemical resistance, abrasion resistance and surface appearance, electrical conductivity, opacity compared to polymers with traditional fillers.

One of the most interesting characteristics of nanofillers is the possibility to dramatically reduce the amount of particles added to the polymer, reducing side effects caused by the addition of traditional inorganic fillers (higher density, lower processability and different surface aspect of the polymer). For example, only 5% or 6% w/w of nanofillers are used to obtain mechanical properties similar to the ones obtained with an amount of 15% w/w of a traditional filler, as for example calcium carbonate or short glass fibers.

The first polymer/clay nanocomposite material was produced in 1961 by Blumstein, that demonstrated the polymerization of a vinyl monomer intercalated in the structure of montmorillonite. But only in 1988 Okada and coworkers, at Toyota Central Research Laboratories in Japan, were able to obtain the first industrial application of nanocomposite polymers. In this case, the nanocomposite was obtained by the polymerization of caprolactam, that leads to the formation of a nylon 6 intercalated composite.

This material was then marketed by UBE Industries and is currently used for the construction of the belt in the engines of Toyota cars and for the production of films for packaging.

The "nanofiller" used in the polymer matrix nanocomposites can be isodimensional nanoparticles, if the three dimensions are in the order of nanometer, bi-dimensional nanoparticles if two of the three dimensions are in the order of nanometers and lamellar nanoparticles if they are characterized by a single dimension in the order of nanometers. Nanomaterials can be classified in the categories defined above basing on the kind of nanofillers used.

8.2 FILLERS FOR THE SYNTHESIS OF NANOCOMPOSITES MATERIALS

- *Oxides:* the most used are titanium dioxide, iron oxide and aluminum oxide.
- *Carbon nanotubes:* can be single wall - SWCNT - (Single-Wall Carbon Nanotubes), consisting of a single graphite sheet wrapped around itself, or multi-wall - MWCNTs - (Multi-Wall Carbon Nanotubes) formed of multiple sheets wound coaxially on each other. They have generally lengths from 100 nm to tens of μ m and diameters from 1 to 20 nm.

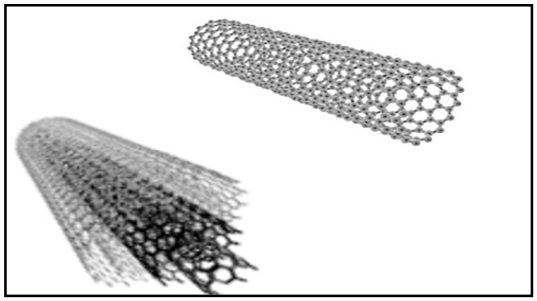

Figure 1: single wall (high) and multi wall (low) carbon nanotubes

- *Layered silicates:* include double-layer laminated hydroxides, also called anionic clays (hydrotalcite), but most of all phyllosilicates (clays) natural (montmorillonite, hectorite and saponite) and synthetic (Fluorine-mica).

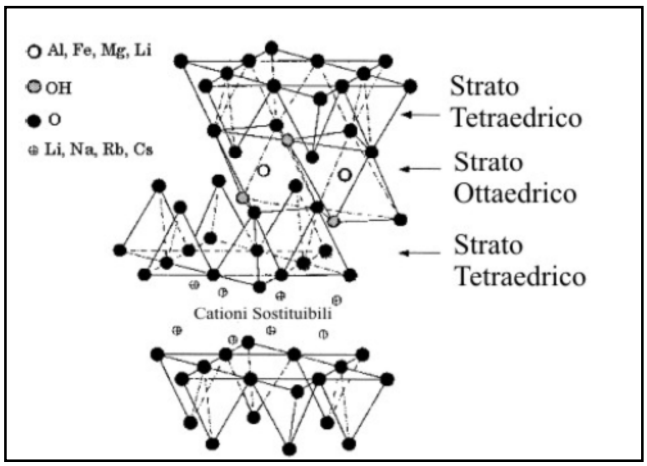

Figure 2: structure of a layered silicate

- *Colloidal fumed silica (Fumed Silica):* microporous particles with 10-50 μm dimensions, consisting of aggregates of smaller particles (5-40 nm), characterized by high specific surface area (50 - 750 m^2/g)
- *POSS*: hybrid organic-inorganic molecules in which the inorganic part consists of silicon atoms. These structures are characterized by particles with a diameter of 0.7-50 nm. The presence of reactive functional groups allows compatibility with different polymer matrices.

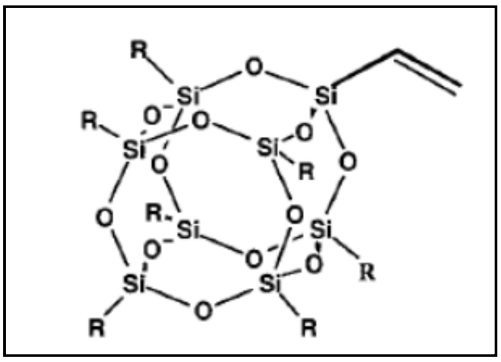

Figure 3: structure of POSS

8.3 PARAMETERS OF FILLER

Generally there are five descriptive parameters used to characterize the filler, which must be considered in the choice of a mineral, according to the desired properties for the final material.

8.3.1 Particle dimensions

This is a fundamental parameter for predicting the behavior of a material and how it can be used.
The minerals used as fillers in polymeric materials may have particles with dimensions from a few nanometers to those of the grain of sand. The techniques used to determine this parameter are:

- Light scattering
- Sedimentation techniques
- Microscopic analysis

Usually the smaller the particles the best final properties of the material, because in this way the ratio between volume and surface of the particle; therefore it is important the grinding of raw material.
Another important parameter is the distribution of particle diameters, because two minerals with the same average size of particles can be formed by a particle size distribution very different from each other.
In general, mineral A have better impact resistance than material B if the particle size distribution of A is narrower, and therefore more homogeneous, than the one of mineral B.
The fraction of bigger particles, that is more abundant in minerals with large size distribution, tends to create discontinuities in the final material, promoting breaking point and thus decreasing the impact strength.
The size distribution of particles of a mineral can also affect the viscosity of the material, modifying the rheological behavior.
Because of the importance of this parameter, the same mineral is usually available with various particle sizes and with different possible distributions of them.

8.3.2 Surface area

This property is in some way related to the size of the particles, but is mainly influenced by particle shape and porosity of the mineral. It is measured by chemical or physical adsorption measurement of gas on the surface.
In the field of polymeric materials, the rheological properties of minerals with a low surface area vary less than the one having high value of the same property, because in this latter case there is a greater interaction between filler and polymer.
To obtain an effect of improvement in viscosity it is better to use a mineral with high surface area.

8.3.3 Particles shape

Mineral particles have a very wide range of possible shapes, which have a significant impact on the properties that the filler gives to polymeric material in which it is added. The parameter used to describe the particle shape is called *aspect ratio*:

$$A_r = \frac{Length}{Thickness}$$

Obviously, rod-like particles have a high A_r value, while is not possible to apply the concept of aspect ratio to spherical particles.
Often the same particle have two values of A_r, corresponding to the ratio between the larger dimension with the two smaller one.
A mineral particles having a low value of A_r will increase the viscosity less than one with a higher value of A_r and also gives a much more higher impact resistance than a minerals with high aspect ratio.
Examples of minerals with a high aspect ratio and wollastonite and mica

8.3.4 Color

Minerals can have any color, from white to black. The nature of the color depends on various factors, and the most important are the refractive index of the mineral and the impurities present in it.

A correct choice of filler gives almost transparent compounds (for example using aluminum trihydrate), while other minerals as calcium carbonate, talc or barium sulfate, when used with pigments, can give shiny materials without any other treatment of the surface of material.

Impurities can have refraction index different than the one of mineral and may cause decomposition of the polymer during processing; this can lead to the formation of other colors in the composite.

In many cases, also the color of the pure mineral changes when it is introduced into the polymeric matrix, so it is always useful to study the changes of color with an mineral/air interaction or with a mineral/polymer interaction.

8.3.5 Specific weight

Minerals commonly used as fillers have a density range from 2.2 g/cm^3 (silica) to 4.4 g/cm^3 (barium sulfate). This factor will influence the weight of the final material, especially when the concentration of the mineral is high.

If lightweight parts are required, low volume fractions minerals with low density are necessary, while if a heavy material containing less amount of mineral is required , an high-density filler must be chosen.

8.3.6 Characteristics of layered silicates

The layered silicates commonly used in preparation of nanocomposites belong to the category of phyllosilicates. The elements commonly present in these silicates are silica and alumina or magnesium oxide. These silicates have a multi-layered structure: a layering of silica with tetrahedral structure and a layering of alumina (oxide or magnesium) with octahedral structure, as shown above in figure 2. The tetrahedral layers are formed by SiO_4 groups that form an hexagonal plane composed by Si_4O_{10}. The octahedral layers are composed of two levels of oxygen or hydroxyl groups in between are positioned aluminum atoms (or magnesium) in octahedral coordination. In total, the single silicate crystal consists of two

tetrahedral layers of silica separated by an octahedral layer; by this way oxygens at the head of the tetrahedron are shared with the octahedral layer.

The crystals (layers) described above have a thickness of about 1 nm and lateral dimensions that can vary from 30 nm to several microns depending on the type of silicate, therefore, in every type of layered silicate, the shape factor of the single crystal is very high.

If all the octahedral vacancies in the crystal are occupied by aluminum, silicate is inert, but an isomorphic substitution of trivalent aluminum with bivalent iron or bivalent magnesium with monovalent lithium is very common. The result of this substitution is that the crystal has a total negative charge. The excess of negative charge is balanced by very big cations that could not be inside the crystal and therefore are located on the edges of the same.

Silicate crystals are organized to form sandwich structures (crystallites) defined “tactoids”, held together by weak Van Der Waals forces and producing a structure with a constant gap between the layers. This gap is commonly called “interlayer space” or “tunnel”. The clay is then formed by agglomerates of these tactoids.

The intercalation of the polymer inside the interlayer space of silicate crystals is made possible by the presence of weak binding forces.

In natural layered silicates cations as Na^+ or K^+ are often present in the tunnel that balance the negative charge of the crystal. The crystals of clay are therefore hydrophilic, and the interaction with polymers having a hydrophobic nature (or with low polarity) can be quite poor.

The consequence of the lack of physical interaction can be a "immiscible system" in which the polymer is not intercalated in the layer space, and the resulting properties are close to those of traditional composites.

In order to increase the interaction between silicates and polymers a chemical treatment that makes the silicates organophilic and therefore compatible with almost all polymers is carried out. This treatment consists in replacing the cations naturally present in the tunnels with cationic surfactants such as alkyl ammonium or alkyl-phosphonium; clays that undergo this treatment are called organo-clays. The surfactants play a multiple compatibilizer action: first of all they lower the surface energy of the crystal promoting the interaction between polymer and water. Furthermore, since these cations are arranged in the tunnels and generally have a much larger dimensions than the one of cations originally present, they also increase the gap between the layers, facilitating the penetration of polymers.

In general, alkyl-ammonium or alkyl-phosphonium groups are bonded to functional groups that can interact with the polymer, or in some cases, these groups can also promote the polymerization of the monomer; the result is an increase of the interaction at the interface between the crystal clay and polymer with a consequent improvement of the characteristics of the final nanocomposite.

8.3.7 Characteristics of nanosilica

Silica is an inorganic polymeric oxide with a repeating unit of SiO_2. It has a tetragonal structure with the silicon atom in the center and four oxygen atoms at the top of the tetrahedron.
In nature it is usually present in a crystalline form in three different polymorphic structures: quartz, cristobalite and tridymite.
The thermodynamically stable form of crystalline silica on earth is the α-quartz; other forms of crystalline silica (tridymite-α and cristobalite-α), although unstable at temperature and pressure conditions on the earth, are present in nature because they return slowly to the stable phase. Silica can be found pure or in silicates: sand, clay and other minerals.
In its amorphous form it appears as a white powder and can be prepared through three main processes:

- By precipitation

$$SiO_{2\ (sabbia)} + 4Na(OH) \longrightarrow Na_4SiO_4 + 2H_2O$$
$$Na_4SiO_4 + 2H_2SO_4 \longrightarrow SiO_{2\ (P)} + 2Na_2SO_4 + 2H_2O$$

- By hydrolysis of silicon halide in vapor phase

$$SiCl_4 + 2H_2O \longrightarrow SiO_2 + 4HCl$$

- By gelation of silico alkoxydes

$$Si(RO)_4 + 4H_2O \longrightarrow Si(OH)_4 + 4ROH$$

Silica particles are usually spherical and nanometer-sized, but the high surface energy and the ability to form hydrogen bonds between different particles causes aggregation of nanoparticles to form aggregates which may reach micrometer-sized.

It is therefore important to be able in some way to break up these aggregates to obtain a better dispersion of particles in the polymer matrix and therefore use the properties related to the high surface area of silica.
Layered silicates, in particular montmorillonite, and nanosilica are the two fillers used in this research work.

8.4 NANOCOMPOSITES PREPARATION

The preparation of polymer nanocomposites is critical because of the hydrophobic nature of polymer compared to the hydrophilic one of many kinds of nanofillers. In addition, shape, size, surface morphology and distribution of the nanofillers in the polymer matrix determine the basic properties of the nanocomposite.
The main point for the synthesis of a nanocomposite material lies in the so-called "principle of maximum diversity": it consists in the fact that the particles of nanofiller must be individually dispersed in the polymer matrix so that the heterogeneous nature of the material is evidence only on the nanoscale. In theory, each nanoparticle should contribute in the same way to the overall properties of the composite.
The preparative aspect is the focus of research in this area. The first problem is the preparation of the filler, which can have one "nano" dimension (lamella), two “nano” dimensions (fiber) or three “nano” dimensions (spherical nanoparticles). All these structures have different properties. For example to get the maximum effect of reinforcing, fibers or lamellar particles should be used, since the efficiency of reinforcement depends on the length/thickness ratio. The nanofillers then must be chemically similar to the polymer ("compatibilization") to increase the hydrophobicity and promote the adhesion and dispersion in the matrix.
The nanofillers that received more attention, and for which the technology is more developed, are natural lamellar compounds (montmorillonite, hectorite, mica, vermiculite, saponite, sepiolite) which are commercially available in different forms (i.e. with different organic cations between the layers).
The second problem is the preparation of nanocomposite: it may be interesting to analyze some methods of general approach for the synthesis of polymer-layered silicates composites[1] that can also be applied to other types of fillers, including silica, and then get better in detail of PLA/fillers systems.

The main methods for the preparation of nanocomposites are:

- Exfoliation and adsorption
- Intercalation of the polymer in solution
- Intercalation of the polymer in molten state
- Template synthesis

8.4.1 Exfoliation and adsorption

In this technique a layered silicate is expanded into single layers using a solvent in which the polymer (or prepolymer in case of insoluble polymers) is soluble.
It is known that this type of silicate with layered structure, due to the weak forces that hold together the layers, can be easily dispersed in a solvent. The polymer is then adsorbed on single delaminated sheets and, when the solvent is evaporated (or the mixture re-precipitated), the reassembly of the sheet structure forms a "sandwich" in which the polymer is incorporated between the sheets to form a multilayer ordered structure. With this process also nanocomposites obtained by emulsion polymerization are synthesized where the layered silicate is dispersed in the aqueous phase.
This technique is especially used for the synthesis of intercalated nanocomposites based on polyvinyl alcohol[2,3], PEO[3-7], polyvinylpirrolidone[8], and polyacrylic acid[7].
Jeon and coworkers[9] have used this technique for the production of nanocomposites based on nitrile and polyethylene copolymers; XRD analysis on the composites showed an enlargement of the characteristic peaks showing the partial exfoliation of fillers, confirmed by TEM images in which it is possible to observe both intercalated and exfoliated lamellae.
Ogata and colleagues have applied the technique of exfoliation and adsorption for the production of PLA[10] and PCL[11] nanocomposites using montmorillonite as filler and chloroform as a solvent; in these conditions no intercalation was observed for both polyesters.
Some polymeric materials, such as polyimide, are insoluble in organic solvents; therefore the only possible way to produce nanocomposites by this mechanism and with these types of polymers is to use a polymer precursor that can be intercalated between lamella and then polymerized chemically or by using a thermal initiator.

The research group of Toyota[12] was the first to use this technique to produce nanocomposites based on polyamide.

A similar approach has allowed Oriakhi and coworkers[13] to synthesize a nanocomposite based on montmorillonite and poly(p-phenylenevinylene) using poly(p-xylenylene dimethyl sulfonium bromide) (PXDMS) as a precursor of the polymerization.

8.4.2 Intercalation of the polymer in solution

Using this technique the layered silicate is swollen in the liquid monomer (or in a monomer solution): in this way polymer can be formed between the intercalated layers. The polymerization can be initiated either by heat or by radiation, by the diffusion of an initiator or by a catalyst through the cation exchange within the intercalated lamella before the swelling of the silicate.

Many interlamellar polymerization were studied between 1960 and 1970, but only with the work initiated by the research group of Toyota[14,15] in the 90s the study of intercalated nanocomposites has gained great interest. Their studies showed how sodium montmorillonite modified with aminododecanoic acid allowed to melt caprolactam to intercalate and then to polymerize resulting nanocomposites based on nylon 6 in which the fillers were well dispersed in the polymer matrix. Depending on the chain length of acid used for the modification of montmorillonite different behaviors were observed in the polymerization process, in particular the longer the chain the higher the amount of monomer intercalated as a result of higher interlamellar space (Table 1).

$^{+}H_3N\text{-}(CH_2)_{n-1}\text{-}COOH$	Interlayer spacing of the modified clay (A°)	Interlayer spacing in presence of CL (A°)
2	12.7	14.4
3	13.1	19.7
4	13.2	19.9
5	13.2	20.4
6	13.2	23.4
8	13.4	26.4
11	17.4	35.7
12	17.2	38.7
18	28.2	71.2

Table 1: relation between interlamellar space and modifier chain length

Basing on the methodology developed by the research group of Toyota, Messersmith and Giannelis[16] modified sodium montmorillonite with aminolauric acid and then dispersed it in caprolacton which was then cured at high temperature. The composite contains 30% by weight of clay. XRD analysis show only exfoliation without intercalation.

The "in situ" intercalation of the polymer has been extensively studied for the production of nanocomposites based on polystyrene[17-19] and poliolefins[20].

Other examples of melt intercalation in 1994[21,22] were performed with epoxy resin, using an epoxy derivate of bisphenol A. Three different kinds of organophilic montmorillonite, having a cation $CH_3(CH_2)_{n-1}NH_3^+$ with n = 7,11,18, have been used.

From X-ray analysis it is deduced that the exfoliation depends on the nature of the montmorillonite, since the longest linear alkyl chains facilitate the formation of nano composite; measures of strength and modulus confirmed a significant improvement compared to pure resin for percentage of montmorillonite from 2% to 20%. These are the first examples of nanocomposites obtained by using a thermosetting polymer matrix and not a thermoplastic one.

8.4.3 Intercalation of the polymer in the molten state

This process requires that the layered silicates are mixed with the polymer in the molten state. Under these conditions, and if the surfaces of silicate are sufficiently compatible with the chosen polymer, the polymer can be arranged in interlamellar space and form an intercalated or exfoliated nanocomposites. From an application point of view this is certainly the most interesting and more used technique because it has the advantage to operate without using a solvent and with the devices commonly used for the production of composites with traditional fillers.

The thermodynamic principle behind this process is the result of a combination between enthalpic and an entropic factor: the confinement of a polymer chain in the silicate lamella space leads to a decrease in general entropy of the macromolecule, balanced by the increased conformational freedom of the cation which separates the single lamella[23].

Balazs and coworkers[24,25] have studied the contribution of two key factors considered in the formation of nanocomposites: the nature of interlamellar cation and the length of the polymer chain.

They observed that increasing the length of the alkyl chains of the cation also the distance between the lamellae could be increased by encouraging the formation of intercalated and exfoliated structures. Regarding the effect of the size of macromolecules, an increase of the length of the polymer chain results in a partial immiscibility between filler and polymer and then in a more difficult formation of intercalated structures.

The process of intercalation in the melt has been tested on numerous polymers, especially polystyrene, nylon 6 and polypropylene.

Vaia and Giannelis[26] have studied the formation of nanocomposites based on PS and different kinds of montomorillonite analyzing in detail how the type of fillers, the molecular weight of the polymer and its nature influence the process of intercalation. XRD analysis showed that the polystyrene is intercalated in the presence of interlamellar cations with chain length of at least 12 carbon atoms; moreover the kinetics of intercalation is strongly influenced by molecular weight and is much slower when the molecular weight of the polymer is higher.

Finally, the nature (polarity) of the polymer is another factor that is linked to the possibility of obtaining intercalation: the higher the polarity of the system, the higher the interaction between the polymer and silicates, the better the intercalation of polymer chains and eventually the exfoliation of the layers of filler.

Liu and coworkers[27] have prepared nanocomposites based on nylon 6 and montorillonite using a twin screw extruder. The materials had a filler content from 1% to 18%. Intercalated structures were observed by XRD analysis for composites with a quantity of clay higher than 10%. Interlamellar space was increased from 15.5 A° to 36.8 A°. DSC analysis of these materials have shown an effect of the presence of the filler on the crystallinity of nylon, in particular with the formation of gamma-phase. The montmorillonite also acts as a nucleating agent increasing the crystallization rate.

Polypropylene is certainly one of the most used polyolefins in the world, and then was one of the first polymers studied to produce nanocomposites. The main problem of PP is its apolar structure which makes it incompatible with the silicates. Kato and coworkers[28] tried to solve the problem by using a compatibilizer with polar groups, such as OH or COOH, bound to polypropylene to prepare nanocomposites with montmorillonite modified with a salt of dioctadecildimetilammonium.

The presence of these features should allow to the polymer to intercalate between the lamellae of silicate due to formation of hydrogen bonds between the oxygens of silicate surface and the OH or COOH of PP.
Since the miscibility is influenced by the number of polar groups, they must be carefully regulated in order to have the correct amount of them.
The Toyota group examined two types of PP modified with maleic anhydride, one with a acid value equal to 26 mg KOH/g and the other one with a value of 52 mg KOH/g to prepare the nanocomposite and another containing OH groups with a value of to 54 mg KOH/g.
The increase of interlamellar space from 21.7 A° to 38.2 A° and 44.0 A° for PP modified with maleic anhydride and OH groups, respectively, confirming the intercalation.
Polymers with too low content of compatibilizer show no intercalation, confirming the importance of determining the correct amount of modifying agent.

8.4.4 Template synthesis

This technique, in which the silicates are formed in situ in an aqueous solution containing the polymer and the silicate, has been widely used for the synthesis of nanocomposites based on double-layer hydroxides, but is much less developed for multi-layer silicates.
In this case polymer helps the nucleation and growth of inorganic crystals and is incorporated in the layers when they grow. This technique is particularly used for polymers that are soluble in water, such as polyvinylpyrrolidone, polyacrylonitrile, polyaniline.

8.5 PROPETIES OF NANOCOMPOSITES

8.5.1 Mechanical properties

Nanocomposites show interesting improvements compared to traditional composites both from a structural point of view (mechanical properties), and in terms of functional properties (optical and barrier properties).

The advantages of a nanocomposite, compared to a pure polymer, were demonstrated for the first time in Japan by the group of researchers from the Toyota Research Center. They realized a nanocomposite nylon 6 loaded with montmorillonite and found a remarkable improvement of all properties: increase of tensile modulus and tensile strength, lower coefficient of thermal expansion, reduced permeability, increased impact resistance.

Table 2 shows the comparison between the properties of nylon 6 and the properties of nylon 6 nanocomposite with loaded with 4% by weight of silicate.

Property	Nylon 6	Nanocomposite	Δ
Tensile Moduls [GPa]	1.1	2.1	+ 91%
Tensile Strenght [MPa]	69	107	+ 55%
HDT [°C]	65	145	+ 123%
Impact Strenght [KJ/m^2]	2.3	2.8	+ 22%
water Absorption [%]	0.87	0.51	- 41%
Thermal Expansion Coefficient	13x10^{-5}	6.2x10^{-5}	51%

Table 2: comparison between properties of nylon 6 and nylon 6 nanocomposite

In addition to a general increase of all properties it is interesting to note that the increase in tensile strength and the module is not followed by a decrease in impact resistance, as generally happens in the polymers loaded with traditional filler. These data are of considerable importance considering that the concentration of filler used is only 4%. This is very important and maybe it is the major advantage of nanocomposite systems compared to traditional composites obtained by using micrometer-sized fillers: the ability to obtain materials with higher performance loading the polymer with low percentages of nanoparticle.

The increase of heat distortion temperature from 65 °C to 145 °C has allowed Toyota to use this material to make the drive belt of the engine, where it is exposed to temperatures at which the common nylon softening. The very high reduction in water permeability makes possible to use this nanocomposite in the production of films for packaging.

The increase of the module, the same tenacity, the decrease of the coefficient of thermal expansion, the reduction of gas permeability, increased solvent resistance were observed on a lot of nanocomposites obtained with different preparation techniques. It is therefore reasonable to think that this increase in properties is a typical characteristic of nanocomposites compared to conventional composites.

The increased performance of nanocomposites compared to composite obtained with micrometric filler or compared to pure polymer is relevant considering that nanocoposites are obtained with low percentages of nanofillers; therefore nanocomposites are materials with better properties, lower density, better processability because the viscosity of polymer is higher.

It is not useful to use high concentrations of nanofillers, because if they are higher than 5% by weight a decrease of mechanical properties is observed due to the formation of aggregates of nanoparticles.

The properties of a nano-composite, however, depend on the type of system (clay-polymer-compatibilizer) and morphology. It is not always true that a nanocomposite has better properties of the pure polymer. This is true, however, for elastomers, for which there is a simultaneous increase of all the mechanical properties. This is due to the fact that the lamella of the clay are able to orient themselves parallel to the applied load and thus maximizing the mechanical properties of the material.

8.5.2 Thermal properties

From the thermal point of view nanocomposites show an increase in thermal stability and flame resistance.

The flame resistance is due to the formation, on the surface of the material, of carbonaceous element called "char". The compactness of the char reduces the interaction between oxygen and polymer. The formation of char is a common feature of all nanocomposites studied.

The char probably acts as a protective barrier, that can reduce the heat and mass transfer between the flame and the polymer.

Considering the thermal degradation of nanocomposite materials, usually studied by thermogravimetric analysis, a marked increase in degradation temperature compared to the one of pure material is observed.

8.5.3 Barrier properties

Barrier properties of nanocomposites, (low permeability), is linked to the waterproof of filler. This low permeability is due to the long path that a molecule of gas must do in order to go through a nanocomposite, since nanoparticles are not permeable and are an obstacle. Increasing the size of nanoparticle increases the permeability of the nanocomposite because increases the path of the gas molecule.

8.5.6 Optical properties

In a nanocomposite films, if there is delamination of the clay, the wavelength of light is greater than the thickness of lamella and the film is transparent. The possibility to make transparent films with low permeability opens new perspectives in the field of packaging.

8.6 APPLICATION OF NANOCOMPOSITES

Automotive

Nanocomposite materials have lower weight and better properties that allow to use them in automotive fields. In fact a nanocomposite of nylon-6 was produced for the first time on industrial by Toyota in collaboration with Ube, to cover the engine belt. The same material was used also to cover the engine. These first nylon nanocomposites, however, were very expensive and therefore were not very competitive in the automotive market; but with the innovations that followed, GM has introduced two new models of "van" presenting some parts made of a nanocomposite polypropylene.

In 2001, 8000 units of these two models were sold with these parts. The new material weighs 20% less, has a stiffness similar to the PP, has an equivalent cost, is more recyclable because it contains fewer additives and does not require different processes to be produced.

Nanocomposites of polycarbonate have been taken into account as necessary to obtain external coverings resistant to abrasion and weathering, without reducing the brightness of the surfaces. Another application concerns the system of fuel, taking advantage of the barrier properties of these new materials.

In the automotive industry there are also major potential applications of nanocomposites in different parts of the car. A study of GM shows how nanotechnology will be used, in short time, in different parts of cars especially for top class vehicles.

Pharmaceutical

In addition to increased barrier properties, the technology of nanocomposite enhances the ability to absorb UV rays and infrared radiation, characteristics that make these materials particularly suitable for blister packing. Nanocomposites, therefore can potentially extend the shelf life of the product.

A second application, very important in the pharmaceutical field, is the one in which nanostructured materials are used to obtain a controlled release of drugs in the body. From a theoretical point of view the dosage of a drug in the body should be as constant as possible over time; with conventional drugs there is a peak at the time immediately following the assumption and therefore an overdose of the drug, followed by a continuous decrease dosing during time (which also leads to a period of underdosing).

Several researchers have shown that with the use of nanomaterials is possible to obtain a gradual release of the drug in the body that provides a dosage level less variable over time increasing the effectiveness of the drug along with a decrease in systemic effects.

Medical and Biomedical Engineering

Highly engineered devices allow doctors to perform procedures for non-invasive interventions that were previously possible only through surgery. For designers of these devices the technological challenge is to reduce the size of the equipment and improve the sensitivity in handling. It is now recognized that the development of the material may provide significant improvements and increase performance. Polymers are key materials in the development of medical devices, but the choice of materials is expanding through the use of polymer composites. The medical products that can be produced with nanomaterials are composite rods, balloons, catheters and several similar devices.

Concerning the biomedical sector, the use of nanocomposites containing silver could lead to greater safety for the sterilization of equipment made of polymeric material that may be vehicles of infection or even used to eliminate them.

Electronic Devices

Nanotechnologies are widely used in electronic field. In particular the research is focused on the miniaturization of electronic components such as transistors, diodes etc.. made on semi-conducting substrates.

The technique used for the production of these components involves the creation of masks to paint on the sides of the semiconductor components. Nowadays lithography technology allows to obtain commercial transistor about 100 nm width.

Nanotechnology can reduce this size in a short time obtaining devices with the width of a few atoms. The applications in this field regard computers, portable storage drives such as memory cards for cameras, MP3 players, mobile phones, etc.

Buildings

Nanomaterials are widely used in construction sector. Currently one of the more interesting application is the use of nanometer titanium oxide mixed with paints or solvents for surface treatment of buildings to make the latter self-cleaning. To understand the importance of this application the impact of smog and pollutants on the surfaces of buildings can be considered.

The use of these coatings can dramatically reduce this problem because of the fotocatalitic effect of oxide in the presence of sunlight.
An important example of self-cleaning treatments in construction is the finish of the tiles of the sails of Sydney Opera House Theatre.
One of the main effects of the introduction of nanoparticles as a silicate, POSS, fullerenes, and many others in polymers is an improvement of flame resistance. In many types of civil construction, the regulations require the use of materials with a certain degree of flame resistance; plastics without additive do not usually have this properties. The nanocomposite can be used in the construction industry because their level of flame resistance is higher than that of pure plastics.

Materials for sports

Several companies operating in sport field produce different objects made by nanocomposite materials. For example tennis racquet (HEAD), tennis balls (WILSON) and many other devices used in sports like golf, cycling, climbing, and other as F1, etc.

Textiles

A lot of studies have been carried on in textile sector to reinforce the materials, to obtain waterproof fibers, anti-static and anti-bacterial materials. Some examples of clothing made with nanotechnologies are: clothing for ski jackets and trousers which were made using fiber produced by the American nano-tex that make clothing waterproof, breathable, stain resistant, wrinkle and with improved mechanical properties that have increased efficiency and durability.
The Japanese and Swiss Schoeller Kanedoo are developing fibers with properties similar to those produced by Nano-Tex.
Ciba Specialty Chemicals has developed nanomodified fibers able to prevent bacterial growth and bad smells.
Professor John Xin and Walid Daoud of the Textile Institute Polytechnic of Hong Kong were among the first to obtain self-cleaning fabrics using treatments that are able to deposit nanoparticles of titanium oxide on the tissues.
Nanocomposite fibers are also used for the production of clothes used in military field.

Products for cosmetics

The cosmetics industry is becoming a major user of nanotechnology. In many creams the active ingredient is "contained" in a nanoparticle; in this way a deeper penetration of the active ingredient, enhancing the functionality of the product, is obtained.

In the case of sunscreens, the use of nanoparticles such as zinc oxide, allows to increase the shielding effect of UV rays and to improve the water resistance of the product. Importantly, the nanoparticles that can be used in cosmetics are very restricted due to the possible toxicity that some types of nanofillers can have when in direct contact with the body.

Materials for coatings

Nanostructured polymers are widely used in surface coatings field. Important examples of these uses are products for aesthetic applications, products with surfaces resistant to abrasion and to corrosion, product with high hydrophobicity or hydrophilicity, products with optical properties (anti-glare, anti scratch, etc). In all these cases only the surface of materials is involved in the properties and not the total volume of material used.

The increase in surface properties is often achieved covering the material with a layer (coating) of a different material having the required properties. Research has shown that the nanostructure of these coatings and the use of nanoparticles in addition to the materials traditionally used for the production of these coatings offer the possibility of increasing the functional characteristics of the coating itself.

Nano-structured coatings are currently used in the production of organic solar cells; this application requires a very high barrier properties against oxygen and moisture in order to increase the useful life of these devices. Similar properties are required in the production of micro-batteries and micro fuel cells.

Many devices such as on-board instruments in cars, displays, etc. are covered with layers of transparent plastic to protect them from outside. In recent years, these plastics are coated with a scratch-resistant coating with antiglare properties that improve the duration and visibility of the device. The use of nanoparticles of silicon oxide and titanium oxide significantly improves the properties of the coating.

Energy Sector

The nanocomposite materials are also used in various applications related to energy. In this sector is important to distinguish between applications related to energy production, energy storage-related applications, and applications related to energy saving.

An important application of nanotechnology in the production of energy is in solar cells. In these applications are used materials like fullerenes and nanotubes. Another area of application of nanotechnology is the production of micro-batteries. Fuel cells are an energy production system that uses hydrogen as the main resource. The use of carbon nanotubes and metallic nanotubes having high porosity increase the hydrogen storage necessary for the operation of the fuel cell. It is essential to consider that the reaction product of the fuel cell is water, so this production system alternative to traditional batteries have the advantage of a low environmental impact.

Nanotechnologies are also used in the production of devices with low energy consumption and low dimension. In particular nanomaterials are used for the production of LEDs and organic LEDs (o-LED).

Aerospace Applications

The nanocomposites are currently used in various aerospace applications. One of the main problems for the structure of the aircraft is related to erosion caused by weathering. The use of nanocomposite coatings can improve the performance in terms of abrasion resistance, significantly contributing to a reduction of the thickness of paint applied (and therefore less weight) and to the long time maintenance of the aircraft. It is also increased the percentage of nanocomposite materials employed for the construction of aircraft structural parts.

8.7 POLYLACTIC ACID NANOCOMPOSITES

During the last decades the interest about polymeric materials coming from renewable sources has increased significantly so much that biopolymers begin to attract attention not only for biomedical and pharmaceutical applications but also for industrial ones. Among these materials PLA is certainly the most interesting and most studied. The limit of this polymer remains its mechanical, thermal and barrier properties that, although good if compared with those of other biodegradable polymers, is insufficient when compared with those of materials traditionally used for the production of commodities.

Considerable efforts have been made to improve the properties of PLA to make it competitive with hydrocarbon polymers; for example attempts have been made using PLA with plasticizers or mixing it with other additives.

Over the past ten years the research, both academic and industrial, has focused on the development of hybrid organic/inorganic nanocomposites that showed unexpected properties resulting from the combination of the two components. In fact, the use of inorganic fillers can improve not only the physical properties of materials, such as mechanical properties, thermal resistance, the gas barrier and chemical resistance, but also provide high-performance materials at a lower price.

In literature there are a lot of works about PLA nanocomposites; layered silicates are the most widely used fillers in the preparation of nanocomposites based on PLA, and this especially for their low cost, the availability and their high aspect ratio that allows to obtain a significant increase of the module, the heat resistance, and barrier properties. The main problem in using this type of clay is related to the need to have good dispersion of fillers in the polymer matrix, a key condition to increase property. The incompatibility between fillers and polymer, and the strong interactions that bind the layers of silicate make dispersion of clay in PLA very difficult.

Ray and Okamoto[29] have presented an interesting review on the preparation and characterization of PLA/montmorillonite nanocomposite and concluded that these materials show a significant increase in properties when compared with pure PLA; in particular Ray and Okamoto have observed an implementation of the module, both in solid state and in the melt, an increase of tensile strength and bending, a decrease in gas permeability.

Chang and cowotrkers[30] studied the effect of three different montmorillonites, Hexadecylamine-montmorillonite (MMT-C16) ammonium bromide dodecyltrimethyl montmorillonite (DTA-MMT) and Cloisite 25A, used in the preparation of PLA nanocomposites. The results obtained by them show that thermo-mechanical properties, and barrier to gases depend not only by the type of clay used, but also by the amount of filler present in the polymer matrix. In particular Chang observed that using percentages between 2% and 8% of C16-MMT and Cloisite 25A the thermal stability decreases with increasing concentration of nanoparticle used.

Dubois and colleagues[31] reported in 2003 the increase in thermal stability of PLA/montmorillonite nanocomposites compared to the properties of pure polymer.

Cabed and coworkers[32] studied the barrier behavior of PLA/kaolinite nanocomposite: the strong interaction between polymer and fillers leads to a decrease in oxygen permeability of 50%.

Table 3 shows the comparison between the properties of PLA and those of some PLA/montmorillonite nanocomposites.

Property	PLA	PLA/MMT1	PLA/MMT2	PLA/MMT3
Modulus [GPa]	4.8	5.5	5.6	5.8
Strength [MPa]	86	134	122	105
Distortion at break [%]	1.9	3.1	2.6	2
PLA_{MMT}/PLA	1	0.88	0.85	0.81

Table 3: properties of pure PLA and PLA/MMT nanocomposites

Data reported in table 3 show not only the increase of property in the presence of montmorillonite but also the relationship between the percentage of filler and the change of property.

Observing the rheological curves shown in figure 4 is clear the different rheological behavior of pure PLA compared to the viscosity of nanocomposites containing montmorillonite.

The viscosity of the material is critical because it determines the processability of the polymer. Nanocomposites have a non-Newtonian behavior, while pure PLA has a Newtonian bhavior. Therefore nanoparticles also have an effect on the viscosity of the material, increasing it significantly.

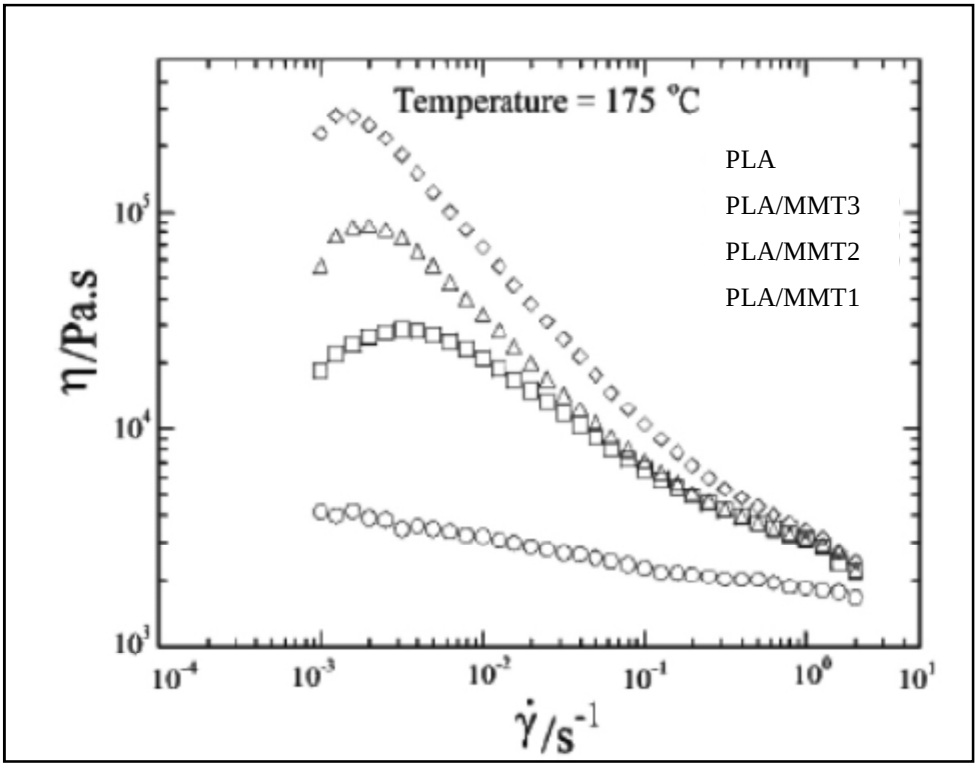

Figure 4: viscosity of pure PLA and PLA/MMT nanocomposites

In addition to multilayer silicates, several other types of fillers have been used in the preparation of polylactic acid nanocomposites; among them carbon nanotubes gained attention for their ability to significantly increase mechanical, thermal and electrical properties. Wu and Liao[33] prepared a nanocomposite using multilayer carbon nanotubes: in this study they show how this type of filler is able to strongly increase thermal and mechanical properties of PLA. Then Wu[34] used nanotubes with functionalized surface he observed that surface modification has an effect both on the dispersion of filler in the polymer and on thermal properties.

Kim and Jeong[35] have studied the properties of PLA/graphite composite, noting in particular an increase of modulus and thermal stability increasing the percentage of graphite in the composite.

Also interesting is the behavior of PLA/SiO_2 nanocomposites: Wen and coworkers[36] have studied the effect of spherical nanofillers on the thermal behavior of the PLA. Silica containing materials have degradation temperature much higher than the one of pure PLA.

An increase of the thermal, rheological and mechanical properties of nanocomposites with silica is also reported in the work of Yan[37] and Wu[38].

Figure 5 shows the TGA curves of PLA/nanosilica nanocomposites, compared with the pure polymer; the start degradation temperature increases increasing the percentage of silica in the polymer, until a content of 5%, while for higher amount of silica a decrease of temperature was observed.

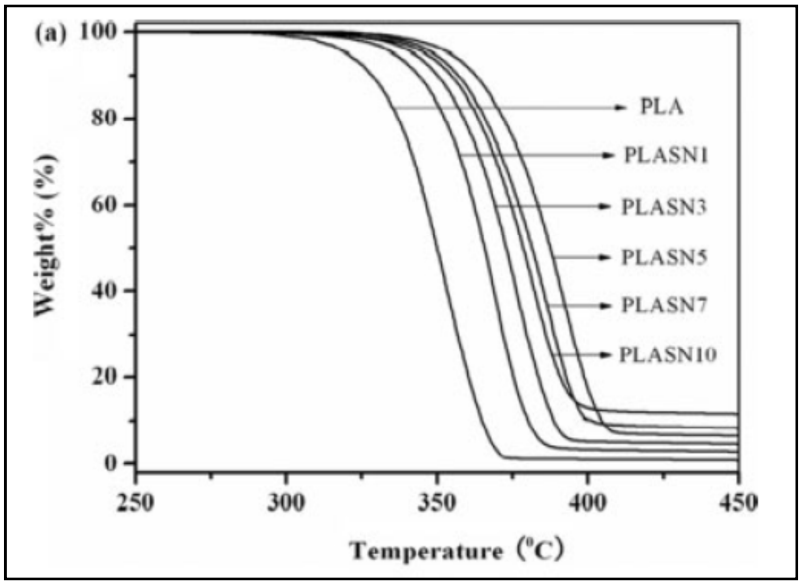

Figure 5: TGA curves of pure PLA and PLA/nanosilica composites

Figure 6 shows the effect of nanosilica on the rheological behavior of PLA: the viscosity of the composite is, in fact, significantly increased compared to the one of the pure polymer.

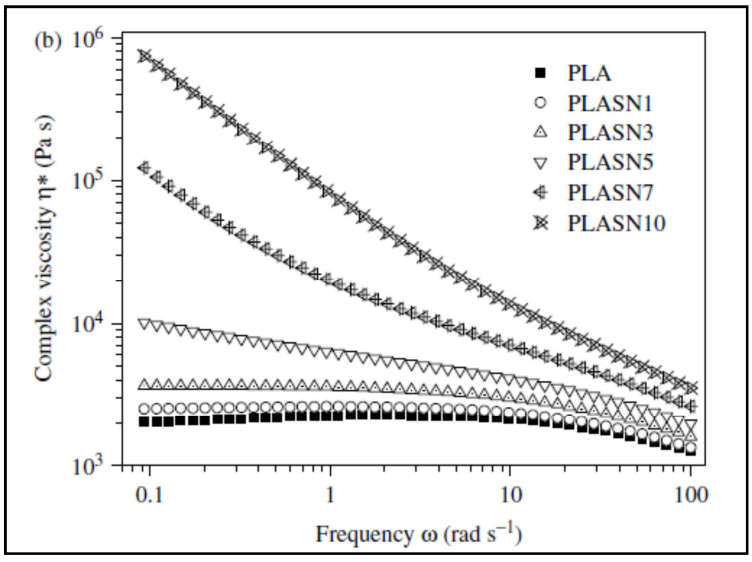

Figure 6: effect of nanosilica on PLA viscosity

Analyzing the works present in the literature, in general, there are three different methods for the preparation of nanocomposites based on PLA. Most of them are prepared adding the filler to the melt polymer[36, 39,40], using a mixer or an extruder, just as is done on an industrial scale. Figure 7 shows the profile of an extruder.

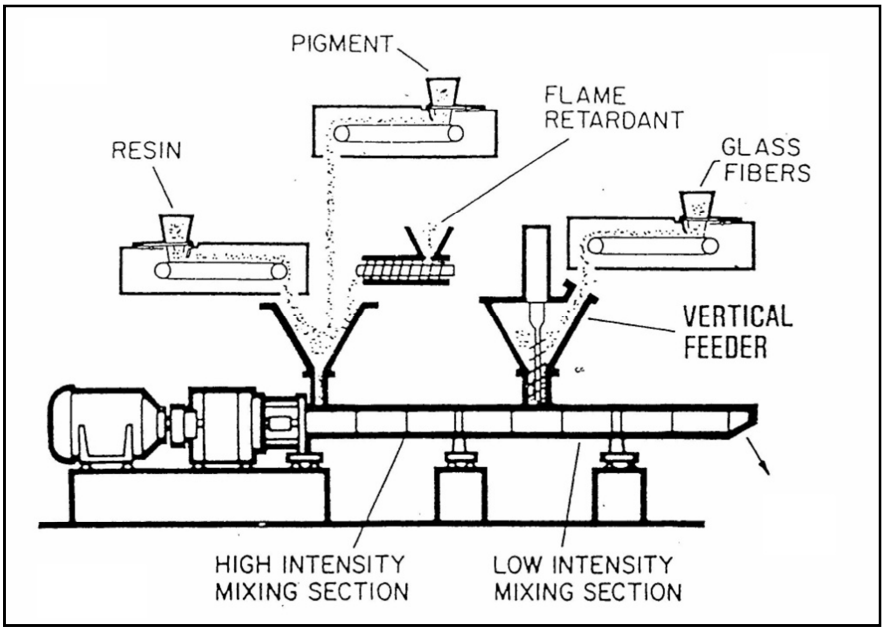

Figure 7: profile of extruder

This technique is very fast and versatile and allows to quickly prepare the polymeric material by adding different types of additives and fillers.

The polymer, as shown in figure 7, comes at the beginning of the extruder together with other additives while filler (glass fiber in the picture) comes only later: in this way, the contact time between polymer and mineral is very low.

During the compression phase the polymer and other additives, that are still in the solid state, are "pushed" to the area where the screw will melt the polymer mixing it with the fillers.

The short contact time between polymer and mineral filler, however, may lead to an unhomogeneous distribution of the filler in the material and consequently with non homogeneous properties.

With this technique also the exfoliation of the nanoparticles is far from optimal, since the contact time is low and sometimes other additives present in the extruder can interfere in the process.

A second synthetic route involves the addition of nanoparticles during the synthesis[41-44]. With this method a better dispersion of fillers in the polymer matrix can be obtained and layered silicates can be better exfoliated.

Finally, in literature[31,45,46] several works described the preparation of nanocomposites from a dilute solution of polymer and filler, which is shaken vigorously for several hours at room temperature in order to promote the dispersion of particles in polymer. The solution is then deposited and the solvent evaporated to obtain the nanocomposite material.

For this work it was decided to use the technique of in situ polymerization, adding the nanoparticles during the synthesis of the polymer. The reasons for this choice is that the interaction times between polymer and nanofillers are longer allowing to reach a very good dispersion of nanoparticles in polymeric matrix. In this way an homogeneous system, in a single processing step without the need to process the material can be obtained; by this way is also possible to study the behavior of particles during the polymerization process. The following paragraphs will describe the effect of different types of fillers used on the molecular parameters of the PLA, with particular attention to molecular weight and viscosity.

One of the problems on an industrial level, is that traditional systems are sometimes not suitable for the synthesis of “in situ” nanocomposite materials produced with this technique.

This problem occurs because the system tends to have a melt viscosity much higher when nanoparticles are present in the polymer: this can cause serious damage the plants, developed for the production of standard polymers.

Obviously a massive financial investment is necessary to change the reactor with a capacity of several tons. Such investment can be made only in the case of a high profit and present several risks. For this reason now nanocomposite materials are produced with the technique of compounding. It is interesting to study the effect of fillers on the synthesis of PLA in order to understand whether it is possible to adopt the in situ polymerization even at the industrial level.

8.8 SURFACE MODIFICATION OF NANOPARTICLES

In this work two different kinds of nanoparticles have been used: Cloisite (natural montmorillonites), purchased from Southern Clay SPA and Nanosilica. In particular three different montmorillonites have been used: sodium Cloisite (Cloisite Na^+), Cloisite 10A and Cloisite 15A, the last two modified with a quaternary ammonium salt.

Table 4 summarizes the main parameters of these minerals.

Mineral	Organic modifier	Modifier concentration	% Moisture	% Weight Loss on Ignition	Particle size d90
Cloisite Na^+	-	-	4-9%	7%	13µm
Cloisite 10A	2MBHT	125 meq/100g	<2%	39%	13µm
Cloisite 15A	2M2HT	125 meq/100g	<2%	43%	13µm
Nanosilica	-	-	2-3%	2%	10-80nm

Table 4: features of nanoparticles

2M2HT

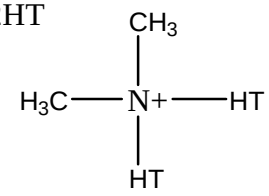

2MBHT

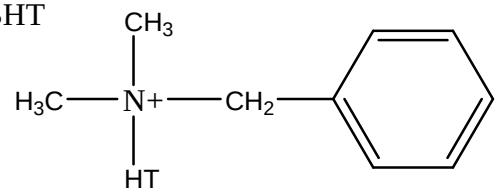

The abbreviation HT indicates a mixture of C18 (65%), C16 (30%), C14 (5%); the anion of these salts is chlorine.

Nanosilica has a surface area of 600-800 m^2/g.

For the synthesis of nanocomposites, nanoparticles and organically modified nanoparticles have been used. Contrary to what is described in the literature, where montmorillonites are modified changing the cation that divides the lamellae in order to increase the space between each layer to promote exfoliation, the idea that was developed in our laboratories in previous works has been to modify the surface of montmorillonite using a silane in order to obtain a filler having the ability to be better exfoliated during the polymerization but also to obtain a material with better properties due to the presence of coupling agent that links filler and polymer chains together.

The same strategy was adopted to modify the surface of silica; with this type of mineral that does not require exfoliation, being spherical, the use of silane can allow a better dispersion in the polymer matrix. In literature there are many papers[44] in which this technique is used.
Figure 8 shows a scheme of the surface modification reaction.

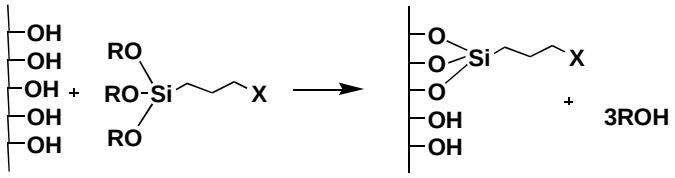

Figure 8: surface modification reaction

The procedure of surface modification is carried on placing nanoparticles under stirring in methanol with a filler/solvent ratio of 1/10; different amounts of silane are then introduced depending on the desired degree of modification. The addition is done slowly to avoid the formation of aggregates and to have a good dispersion of coupling agent. In this work three different percentages of silane - 2%, 7.5% and 15% w/w - respect to the amount of nanoparticle, have been used. Two different silane, supplied by Wacker, have been used: 3-Aminopropyltriethoxysilane (GF93) and 3-Glycidoxypropyltrimethoxysilane (GF80).
The structures of silane are shown below.

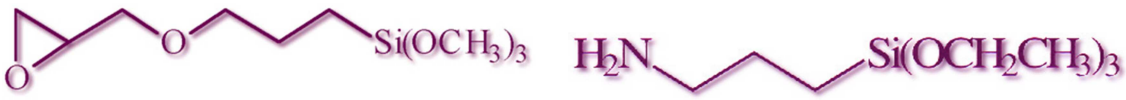

The solution was kept under vigorous stirring for 12 hours and then the solvent was removed by evaporation under nitrogen.
The unreacted silane has been removed washing nanoparticles with methanol, and then the system has been heated at 120 °C under mechanical vacuum for about 2 hours.
After these operations, nanoparticles have been finely chopped to obtain a fine powder.
To verify the efficiency of the surface modification process, nanoparticles were characterized by different techniques.

8.8.1 Determination of the amount of silane on the surface of nanoparticles

Table 5 summarizes the different nanoparticles modified in this work.

Mineral	Silane	% in weight of silane
Cloisite 15A Epox	GF80	2
Cloisite 15A Epox	GF80	7.5
Cloisite 15A Epox	GF80	15
Cloisite 15A NH_2	GF93	2
Cloisite 15A NH_2	GF93	7.5
Cloisite 15A NH_2	GF93	15
Nanosilica Epox	GF80	2
Nanosilica Epox	GF80	7.5
Nanosilica Epox	GF80	15
Nanosilica NH_2	GF93	2
Nanosilica NH_2	GF93	7.5
Nanosilica NH_2	GF93	15

Table 5: modified nanoparticles

The amount of coupling agent used was calculated considering the actual weight of the silane bounded on the surface of nanoparticle to have the same amount of silicon on nanoparticles also changing the type of silane used.

At first the surface modification was made using epoxy silane (GF80), then Cloisite 15A and nanosilica were also modified using the amino silane (GF93) to evaluate the behavior during polymerization.

Concerning montmorillonites, Cloisite 15A has been chosen as case study to test the effect of surface modification.

Nanoparticles were analyzed with different techniques: potentiometric titration, FTIR analysis, thermogravimetric analysis (TGA), solid state NMR, XRD, in order to evaluate the efficiency of surface modification process from both a quantitative and qualitative point of view.

8.8.1.1 Potentiometric titration

Nanoparticles modified with amino silane (GF93) were dispersed in hot m-cresol until a clear solution was obtained; then the solution was titrated with a 0.1M solution of hydrochloric acid in methanol.

Fillers modified with epoxy silane (GF80) were dispersed in methanol and treated with an excess of secondary amine, N, N-dibutilamine. The solution was stirred vigorously for an hour, then the methanol was removed under vacuum, to remove the excess of unreacted amine. At this point, the epoxy functionalities originally present are converted into amino groups, and they can be titrated with the same procedure used for Cloisite and nanosilica modified with GF93 silane.

Table 6 shows the data of titration of surface modified nanofillers.

Mineral	% Silane theo.	meq/Kg NH_2 theo.	meq/Kg NH_2 meas	% Silane meas.
Cloisite 15A Epox	2	236	119	1.67
Cloisite 15A Epox	7.5	840	380	5.33
Cloisite 15A Epox	15	1571	712	9.99
Cloisite 15A NH_2	2	236	148	1.22
Cloisite 15A NH_2	7.5	840	485	4.03
Cloisite 15A NH_2	15	1571	942	7.82
Nanosilica Epox	2	236	141	1.98
Nanosilica Epox	7.5	840	447	6.27
Nanosilica Epox	15	1571	798	11.19
Nanosilica NH_2	2	236	236	2.00
Nanosilica NH_2	7.5	840	671	5.57
Nanosilica NH_2	15	1571	1287	10.68

Table 6: titration data of modified nanoparticles

Data reported in table 6 were obtained analyzing the titration curves (an example is shown in figure 9).There is some agreement between the theoretical amount of silane and the values experimentally determined only for samples with 2% of coupling agent, while increasing the percentage of silane the difference between theoretical data and experimental one increases. This fact can be explained considering that silane reacts with free hydroxyl groups present on the surface of the filler that become less accessible, when modification process carries on, due to steric size generated by the silane itself. The measured values of meq/kg relative to the epoxy silane differ from the theoretical ones more than the ones of amino silane.

This may be due to the lower reactivity of this silane, which is not autocatalyzed by amino function, as occurs for GF93.

Looking at the data in the table it can be seen that the surface modification procedure seems to be less efficient for montmorillonite, and this is probably due to the multilayers structure of Cloisite that makes not available all the OH groups on the surface.

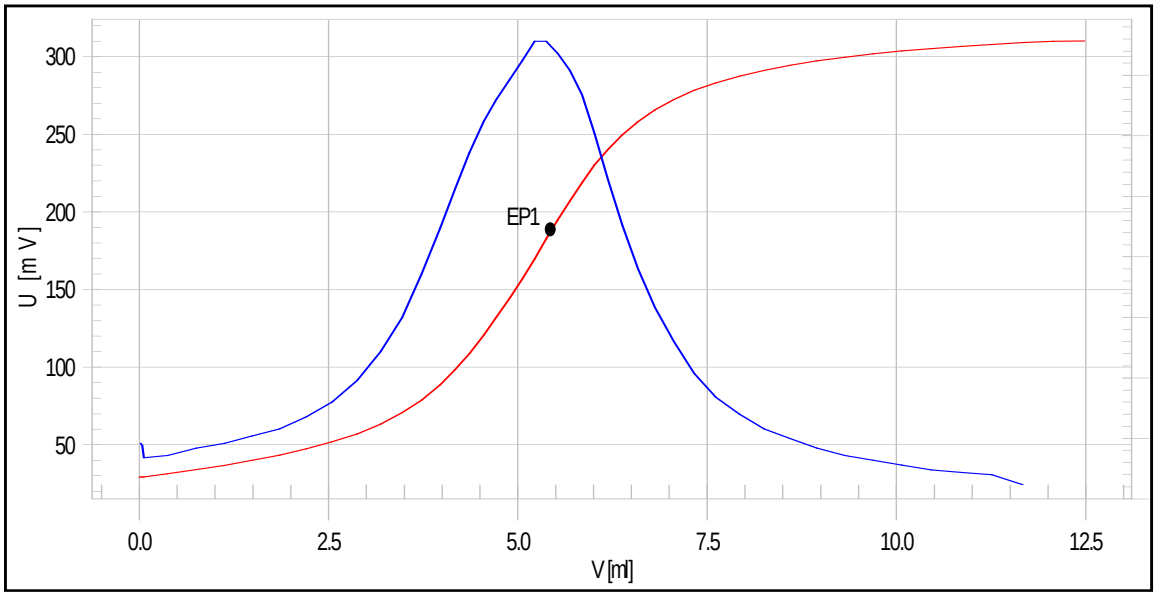

Figure 9: example of titration curve

8.8.1.2 FTIR analysis

The surface modified nanoparticles were analyzed by infrared spectroscopy in order to evaluate if modified nanoparticles present different bands compared to those of unmodified fillers. Spectra of nanosilica and montmorillonite have been taken as reference (figures 10, 11, 12 and 13).

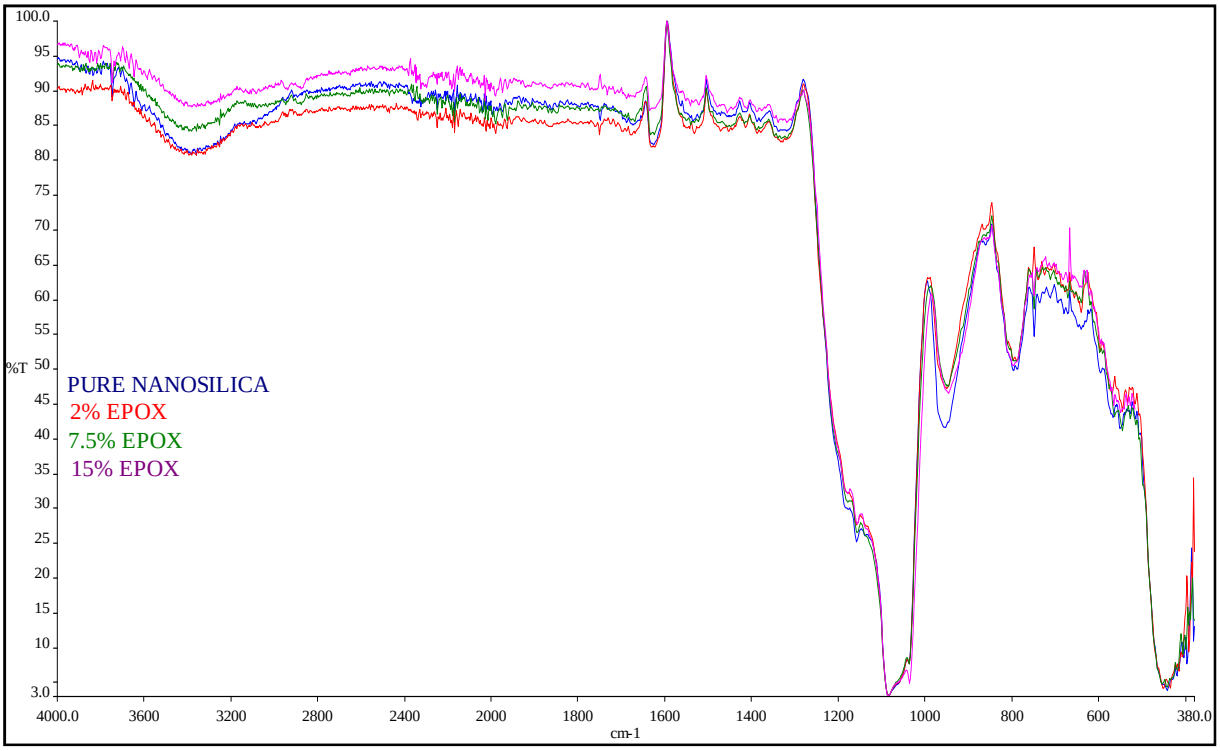

Figure 10: IR spectra of pure nanosilica and nanosilica modified with epoxy silane

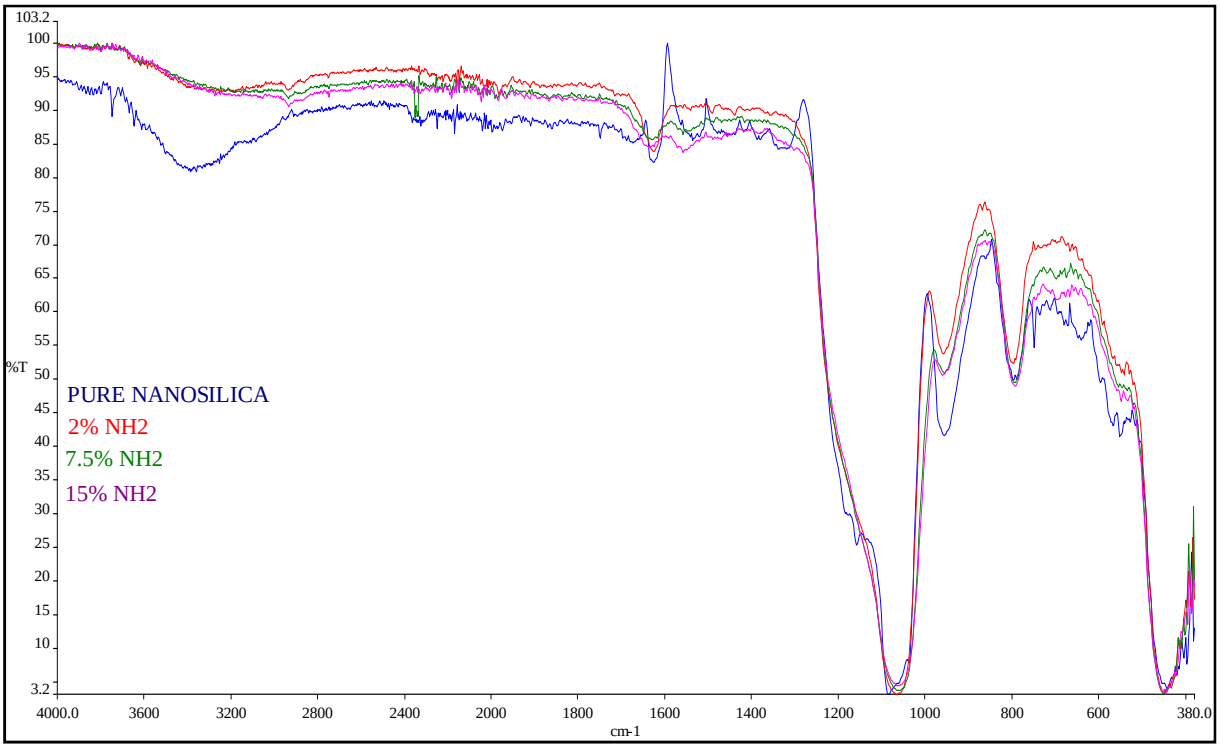

Figure 11: IR spectra of pure nanosilica and nanosilica modified with amino silane

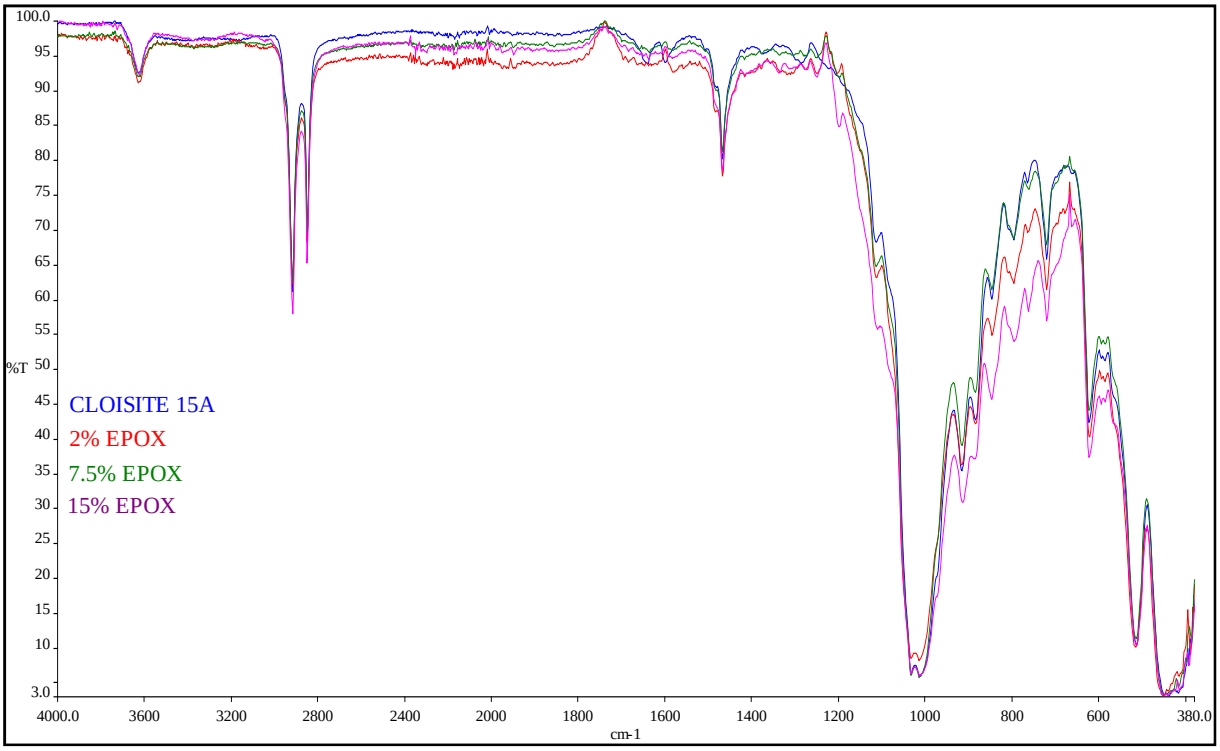

Figure 12: IR spectra of pure Cloisite 15A and Cloisite 15A modified with epoxy silane

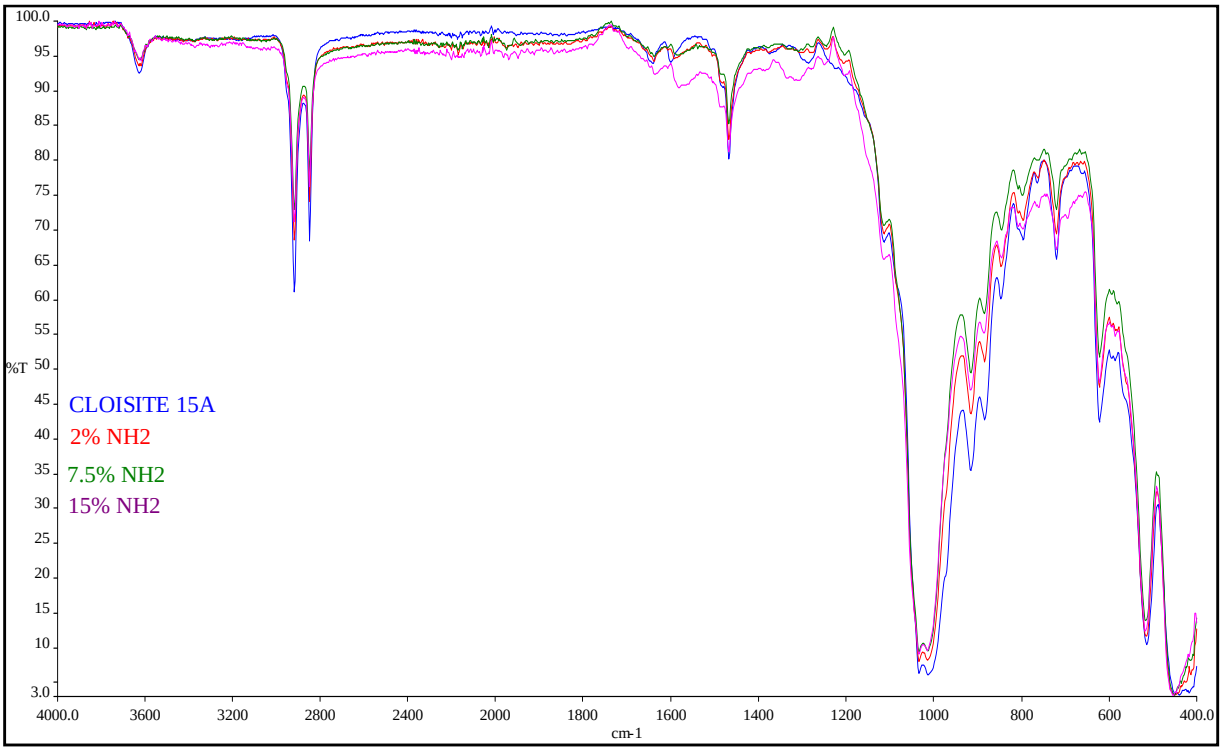

Figure 13: IR spectra of pure Cloisite 15A and Cloisite 15A modified with amino silane

Figures from 10 to 13 show that there are few differences between the IR spectra of pure and surface modified nanoparticles. The presence of silane on the surface of nanosilica (Figures 10 and 11) is difficult to detect because of the intense and weak bands of the Si-O stretching (1020-1250 cm^{-1}) and-OH (3300-3700 cm^{-1}). However, the intensity of the band between 3300 and 3700 cm^{-1} concerning the presence of silanol groups changes in presence of coupling agent, as observed by Sun[47], and in particular decreases increasing the amount of silane used for surface modification. This is particularly evident for nanosilica modified with epoxy silane. In the case of amino silane is also noticed the appearance of a band between 1500 and 1700 cm^{-1} corresponding to NH-stretching.

Regarding montmorillonites, spectra show no significant differences between modified and unmodified Cloisite.

Overall, this technology has not been very effective for our purpose, probably because of the small amount of silane used for surface modification.

8.8.1.3 TGA analysis

To determine the amount of silane effectively present on the surface of nanoparticles a study with thermogravimetric measurements was also started. Below, in figures from 14 to 17 are reported TGA curves of the nanoparticles tested.

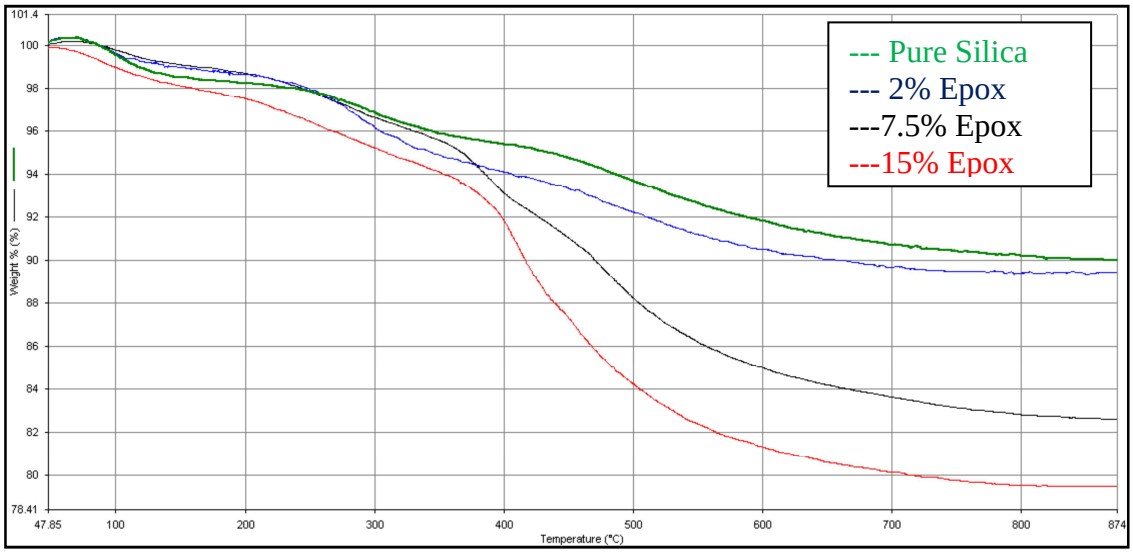

Figure 14: TGA curves of silica modified with GF80

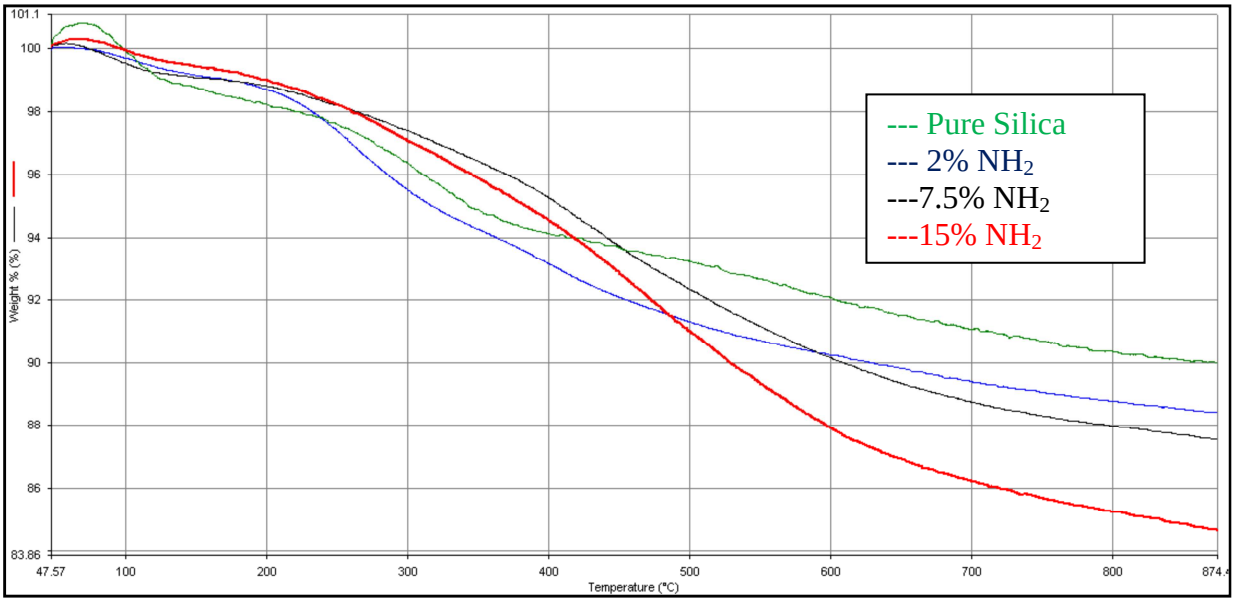

Figure 15: TGA curves of silica modified with GF93

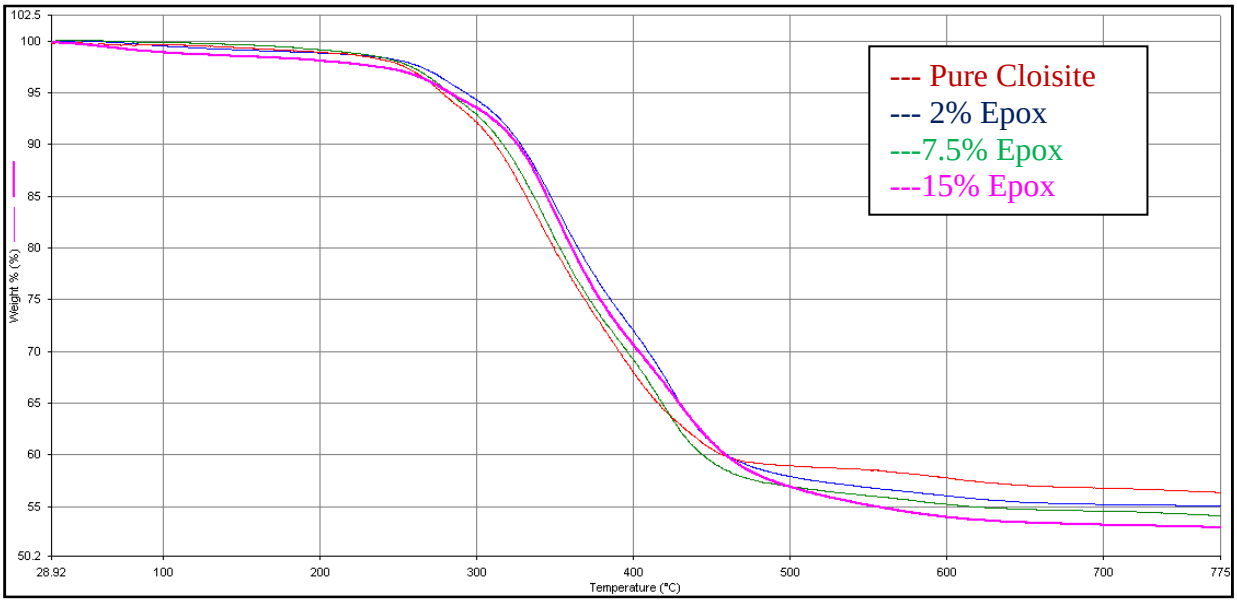

Figure 16: TGA curves of Cloisite 15A modified with GF80

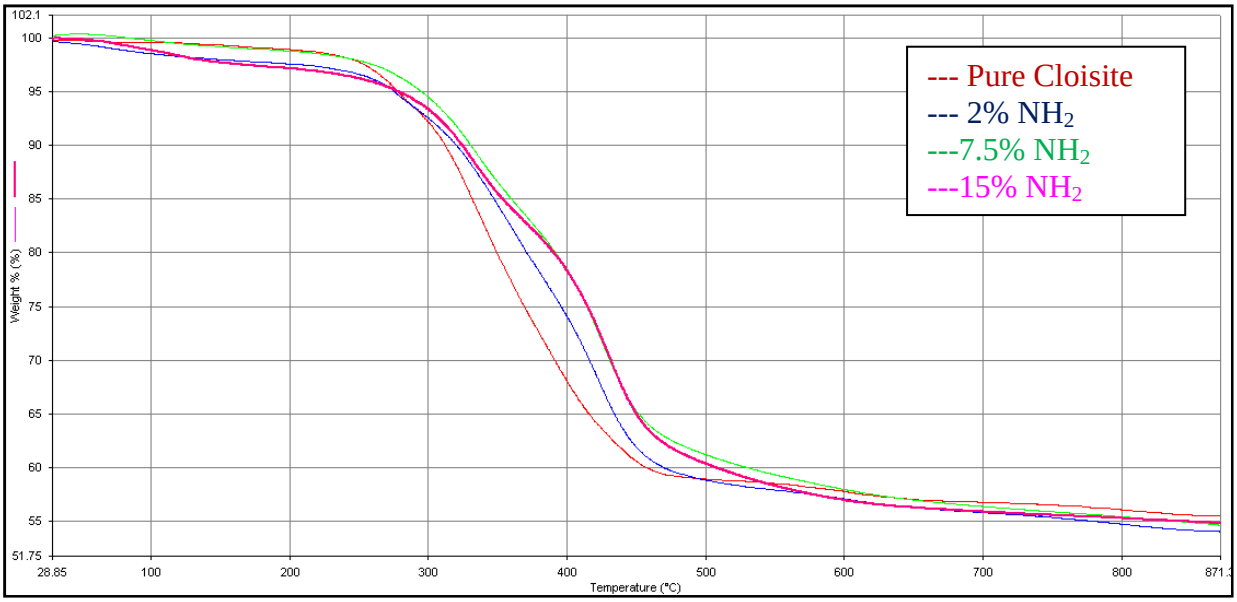

Figure 17: TGA curves of Cloisite 15A modified with GF93

Looking at the TGA curves shown in figures from 14 to 17 it is possible to observe the different behaviors depending on the type of nanoparticle and silane considered.

Considering nanosilica, an increase in loss weight, increasing the amount of coupling agent on the surface of the particles, is observed. This factor confirms that silane is actually linked to the nanoparticle and it is present in different percentages. It is interesting to note that silica modified with epoxy silane loses higher amount of weight than pure nanoparticle; on the contrary silica modified with amino silane has a loss of weight closer to that observed for the pure silica. It should also be noted, however, that curves of silica modified with epoxy silane reach a plateau, while with the amino silane degradation does not seem complete.

On the other hand, considering the behavior modified Cloisite, compared to the one of pure montmorillonite, a difference in weight loss can be observed. The loss of weight increases increasing the amount of silane, but the effect is much less pronounced than the one observed for nanosilica. This is due both to the higher amount of silane present on the nanoparticle (see table 6) and to the lower sensitivity of the measurement caused by the simultaneous degradation of ammonium ions intercalated between the lamellae of Cloisite.

Based on these considerations we can say that thermogravimetry can give a qualitative indication of the presence of silane on the surface of the nanoparticle - especially in the case of silica - while the data are not so reliable from the quantitative point of view because the loss of weight observed are not due only by degradation of silane.

8.8.1.4 Solid state ^{1}HNMR

This technique may be useful not only to determine qualitatively the presence of silane on the surface of nanoparticle, but also for a quantitative measure.

Three different samples, two nanosilica modified with 2% and 15% of epoxy silane and one Cloisite modified with 2% epoxy silane have been chosen as example to evaluate the efficiency of this technique. The spectra are shown in figures 18, 19 and 20.

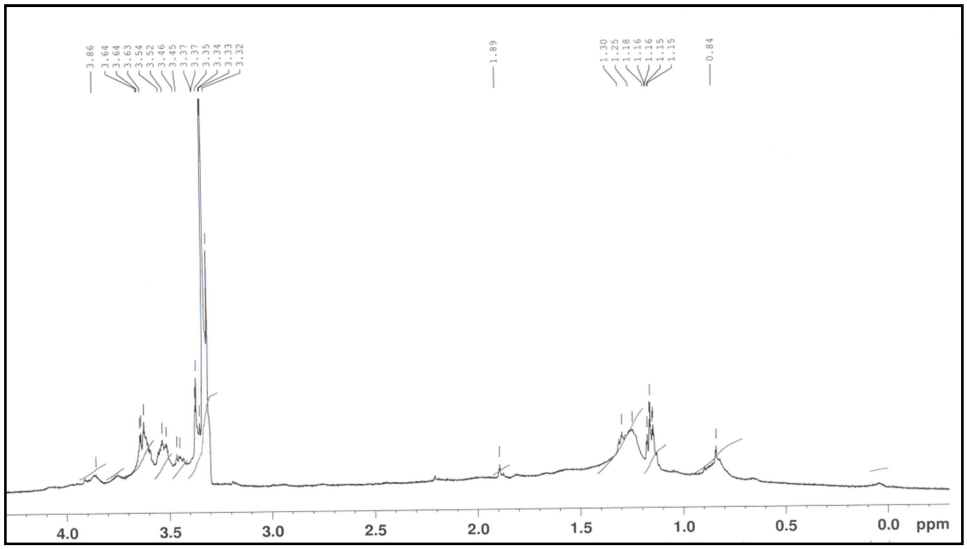

Figure 18: solid state ^{1}HNMR of nanosilica with 2% of GF80

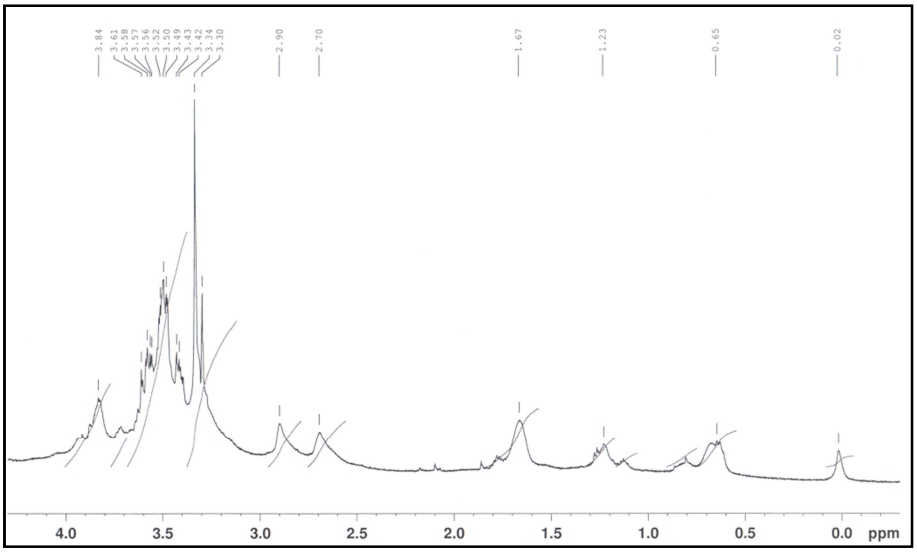

Figure 19: solid state ^{1}HNMR of nanosilica with 15% of GF80

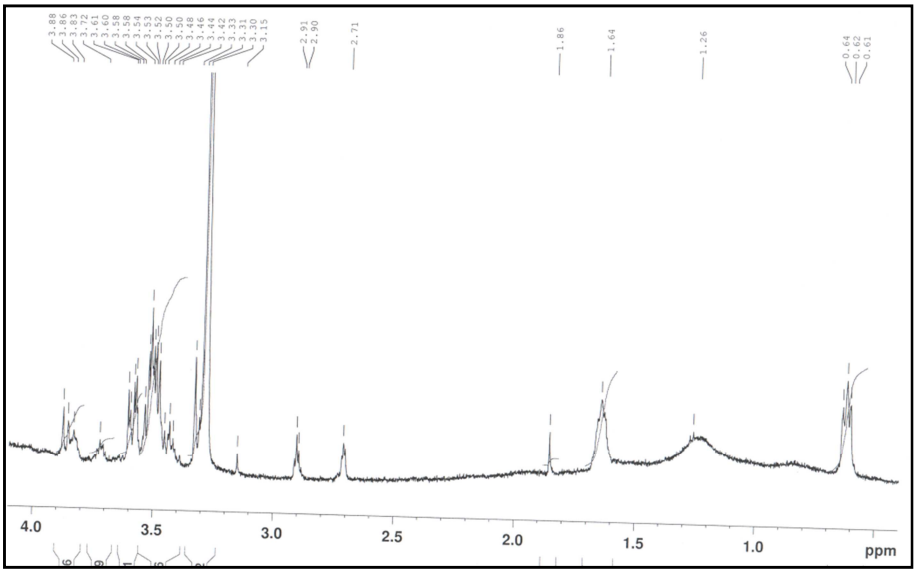

Figure 20: solid state ^{1}HNMR of Cloisite 15A with 2% of GF80

Spectra reported in figures from 18 to 20 show the presence of several peaks, particularly in the area between 4 ppm and 3 ppm. Since the only species containing hydrogen are silane used for modification of the nanoparticle, it can be easily deduced that these peaks belong to the silane. Therefore the technique is qualitatively efficient to determine the presence of coupling agent and then surface modification of nanoparticle; also the signals in the spectrum agrees with a theoretical simulation of a spectrum of silane molecule.

The quantitative determination of silane present is more difficult: in fact the peaks in the spectra are often overlapped, the baseline is not always well defined, and it can be hard to integrate the various signals: so it is not possible to determine precisely how many organic substance is actually present on the nanoparticle. It only possible observe that increasing the amount of silane from 2% (figure 18) to 15% (figure 19) there is an increase of intensity of peaks, due to the greater amount of silane used.

A more efficient quantitative determination of coupling agent could be made by improving the sample preparation technique and increasing the time of acquisition, but these are already quite long, longer than 5 hours.

Basing on what has been observed with different techniques it can be stated that the best methodology identified to measure the percentage of surface modification of nanoparticles is the potentiometric titration of amino terminal groups, directly present on the silane or obtained through reaction with an amine in the case of epoxy silane.

8.9 STUDY OF PLA NANOCOMPOSITES

8.9.1 PLA nanocomposites synthsized

The purpose of the synthesis was to produce materials containing nanofillers added directly during synthesis to evaluate the effect of nanoparticles on the polymerization process and the properties of materials obtained by this way. Table 7 summarizes the samples synthesized.

	Amount of nanoparticles (%)						
Sample	**Pure**	**2% NH_2**	**7,5% NH_2**	**15% NH_2**	**2% Epox**	**7,5% Epox**	**15% Epox**
0,5% 10A	0,5	-	-	-	-	-	-
1% 10A	1	-	-	-	-	-	-
2% 10A	2	-	-	-	-	-	-
0,5% 15A	0,5	-	-	-	-	-	-
1% 15A	1	-	-	-	-	-	-
2% 15A	2	-	-	-	-	-	-
0,5% Na^+	0,5	-	-	-	-	-	-
1% Na^+	1	-	-	-	-	-	-
2% Na^+	2	-	-	-	-	-	-
0,5% NS	0,5	-	-	-	-	-	-
1% NS	1	-	-	-	-	-	-
2% NS	2	-	-	-	-	-	-
1% 15A NH_2	-	1	1	1	-	-	-
1% 15A Epox	-	-	-	-	1	1	1
1% NS NH_2	-	1	1	1			
1% NS Epox	-	-	-	-	1	1	1

Table 7: nanocomposites synthesized

Polymers were synthesized using three different amounts of unmodified filler: 0.5%, 1% and 2% w/w respect to the monomer introduced into the reactor. Considering surface modified nanoparticles, polymers have been synthesized using a 1% of mineral because the nanocomposites with 1% of nanofillers are those that have shown a better balance between molecular properties, rheological and thermal properties.

In addition to these samples, polymers with higher content of unmodified nanoparticle (3% and 5% w/w) have been synthesized to better understand the effect on the catalyst.

8.9.2 Characterization of PLA nanocomposites

All samples synthesized in this work were characterized by SEC and rotational rheometry, in order to have information about molecular weight, distribution and about the behavior of the material in the molten state.

In fact, using these two tests together is possible to have an idea of the complexity of the considered system, obtaining information about the effect of nanoparticles on the molecular weight and viscosity. Both SEC and rheological analysis were conducted following the same procedures adopted for the samples with modified macromolecular architecture described in previous chapters. The only difference is that the solutions for SEC analysis were filtered before injection to remove the residual mineral; analysis only refers to the soluble part or to the amount of solution that passes through the filter. Any polymer bound to the mineral, especially using modified nanoparticles, remains on the filter with the filler unless the overall size of the polymer/filler nanocomposite is less than 45μm (pore size filter).

8.9.2.1 SEC analysis

Here are presented the curves for each series of nanocomposites synthesized, compared with the curve of pure PLA; the values of molecular weight and polydispersity are given in equivalent linear PLA using the calibration developed for this work and described in detail in chapter 3.

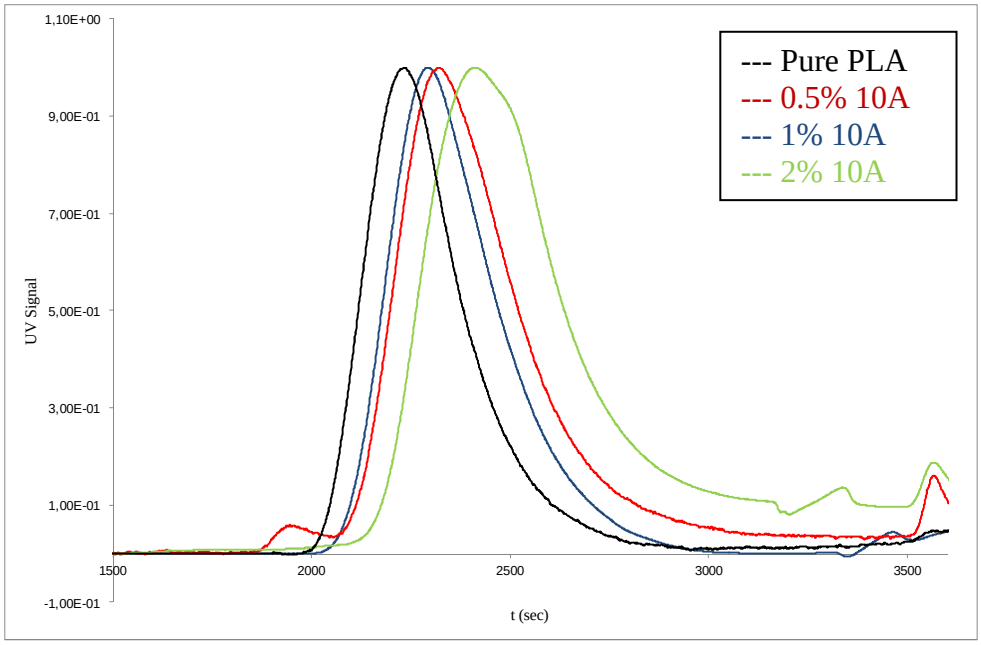

Figure 21: SEC curves of PLA nanocomposites with Cloisite 10A

Molecular weight values and polydispersity of nanocomposites shown in figure 21 are reported in table 8.

Sample	Mn	d
Pure PLA	56909	1.982
0.5% 10A	39690	1.681
1% 10A	28804	1.823
2% 10A	20248	1.931

Table 8: molecular properties of nanocomposites with cloisite 10A

A very marked effect of Cloisite 10A on the molecular weight of materials can be observed from SEC curves and data in table 8. Mn values are significantly lower than the one of pure PLA. Differences are also observed on the values of polydispersity, but the trend is not constant and is therefore difficult to interpret.

PLA NANOCOMPOSITES WITH CLOISITE 15A

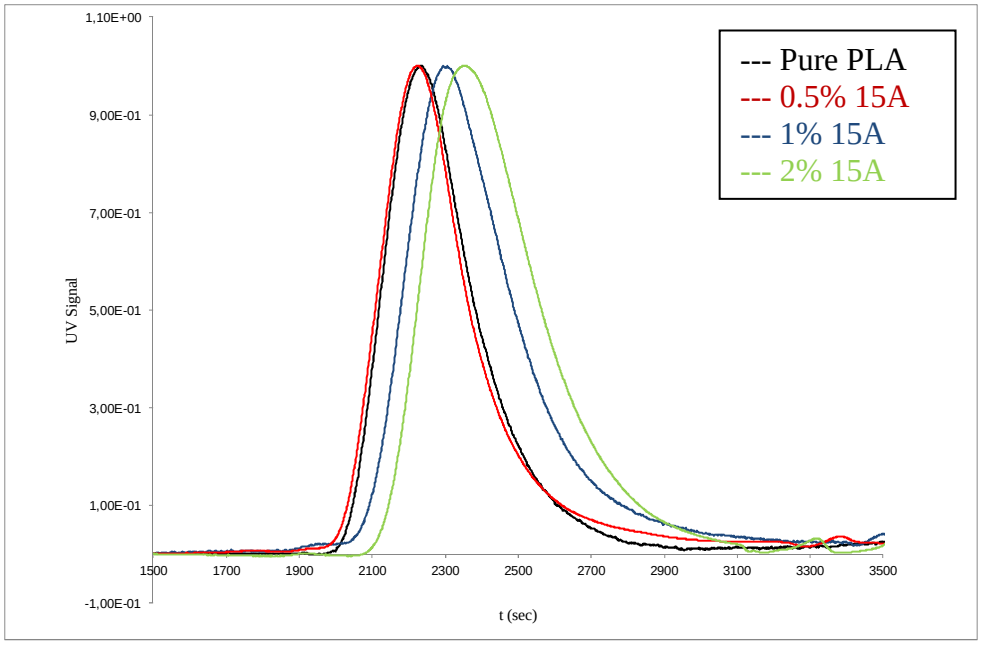

Figure 22: SEC curves of PLA nanocomposites with Cloisite 15A

Molecular weight values and polydispersity of nanocomposites shown in figure 22 are reported in table 9.

Sample	Mn	d
Pure PLA	56909	1.982
0.5% 15A	50160	1.818
1% 15A	37064	1.785
2% 15A	28594	1.734

Table 9: molecular properties of PLA with Cloisite 15A

Even in the presence of Cloisite 15A a decreasing of molecular weight increasing the percentage of fillers is observed; Mn values however are higher than the ones obtained in the presence of Cloisite 10A. The nanocomposite with 0.5% of Cloisite 15A presents a SEC curve close to that of pure PLA. Increasing the percentage of nanoparticle also polydispersity value decreases.

PLA NANOCOMPOSITES WITH CLOISITE Na^+

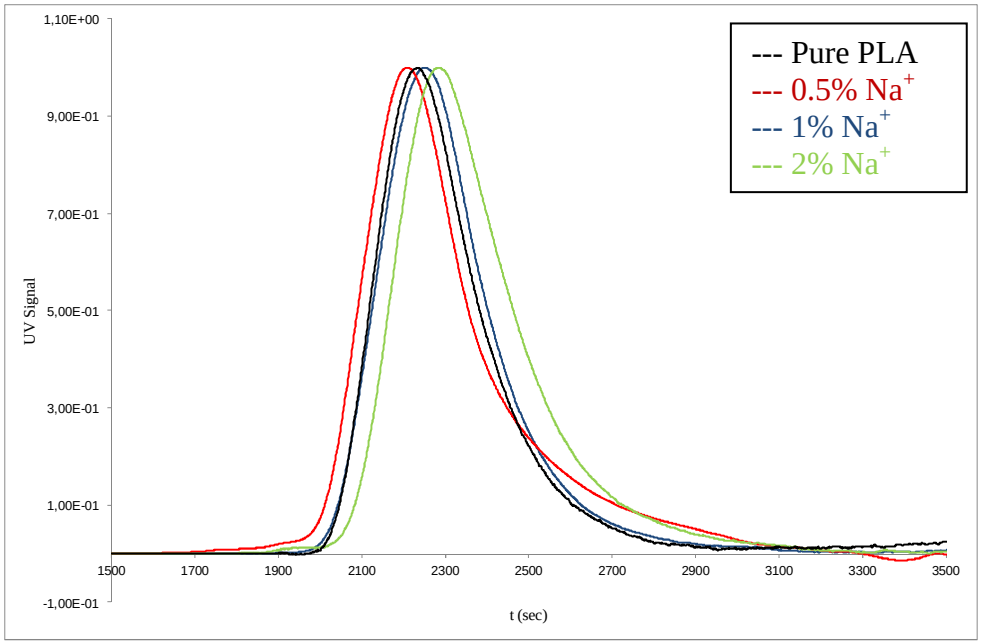

Figure 23: SEC curves of PLA nanocomposites with Cloisite Na^+

Molecular weight values and polydispersity of nanocomposites shown in figure 23 are reported in table 10.

Sample	Mn	d
Pure PLA	56909	1.982
0.5% Na^+	55136	2.418
1% Na^+	50569	1.810
2% Na^+	37744	1.949

Table 10: molecular properties of PLA with Cloisite Na^+

Molecular weight values of materials containing Cloisite Na^+ are much higher than those of other nanocomposites, even if they are still lower than those of the pure polymer, and decrease with increasing the concentration of sodium Cloisite used.

PLA NANOCOMPOSITE WITH NANOSILICA

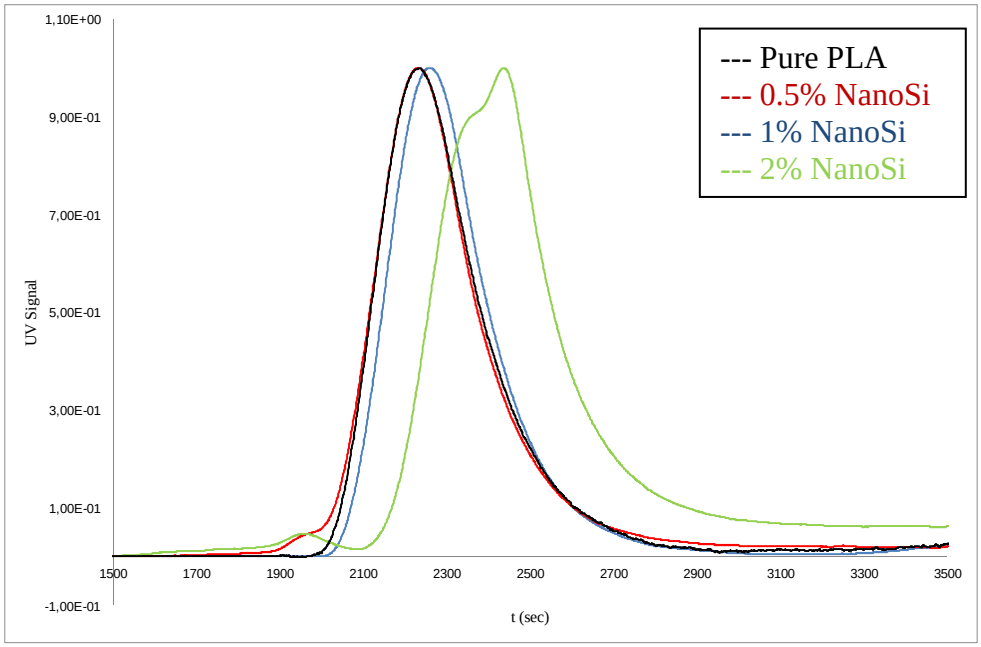

Figure 24: SEC curves of PLA nanocomposites with nanosilica

Molecular weight values and polydispersity of nanocomposites shown in figure 24 are reported in table 11.

Sample	Mn	d
Neat PLA	56909	1.982
0.5% NanoSi	52739	2.008
1% NanoSi	50008	1.710
2% NanoSi	26348	1.949

Table 11: molecular properties of PLA with nanosilica

Also in this case Mn values decrease gradually increasing the concentration of nanosilica in the composite; the difference in molecular weight is particularly evident for the material with 2% of filler.

Analyzing the Mn values of all nanocomposites it is possible to observe that there is an effect of nanoparticles on the chain growth process, especially in the case of materials synthesized with Cloisite 10A and 15A which have the lowest molecular weight values.

This may be related to the presence of ammonium cation that separates the lamellae and that, during the polymerization, may interfere with the activity of the catalyst partially turning it off. The larger size of the cation of Cloisite 10A - 2MBHT - probably makes the layer space more accessible to the growing chains, facilitating the release of the cation; this can justify why the materials with Cloisite 10A have Mn values lower than those of other nanocomposites.

The effect of the interference of the cation in the polymerization process is confirmed by the molecular weight values of polymers containing Cloisite Na^+, which are much higher than the ones of polymers with Cloisite 10A and Cloisite 15A. Also polymers with nanosilica have good molecular weight values, but lower than those of composites with Cloisite Na^+. In this case, since there is no cation in the fillers, the interference with the polymerization process may be due to the relative acidity of the nanoparticle.

In all cases, however, in presence of filler percentage higher than 1% a marked decrease of molecular weight at constant conversion have been observed.

To confirm this observation, some nanocomposites containing higher amounts of fillers have been synthesized: figure 25 shows an example of SEC curves of polymers containing 3% and 5% of nanosilica in comparison with the nanocomposite containing 2% silica.

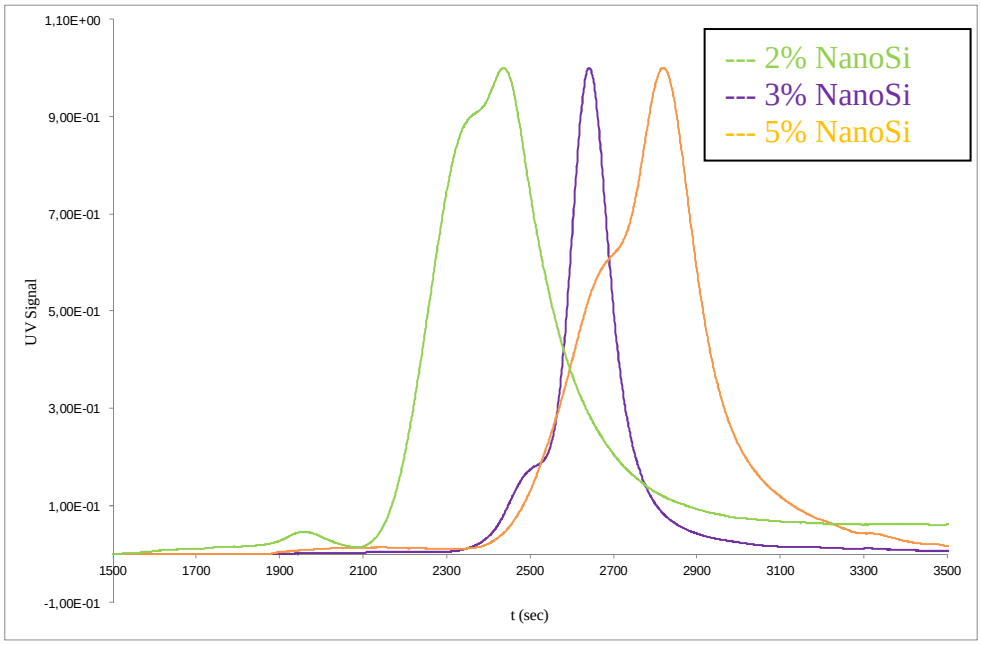

Figure 25: SEC curves of composites with 2%, 3% and 5% of nanosilica

Figure 25 shows that using higher percentages of nanoparticle molecular weight values decrease markedly, confirming the fact that nanofillers interfere with the polymerization process. Moreover the curves present a shoulder in the area of the high molecular weights, as if there were chains still growing. The decreased activity of the catalyst is confirmed by the increased amount of residue lactide remains in samples with 3 and 5% nanosilica.

Also polydispersity values decrease, except in some cases, but the trend is not easily interpretable.

Finally, a final test was performed synthesizing materials with a catalytic amount 20 times higher than the one normally used for other samples in order to determine whether the nanoparticles effectively negatively acted on the catalytic system. Figure 26 shows SEC curves of samples containing silica, synthesized with higher amount of catalyst.

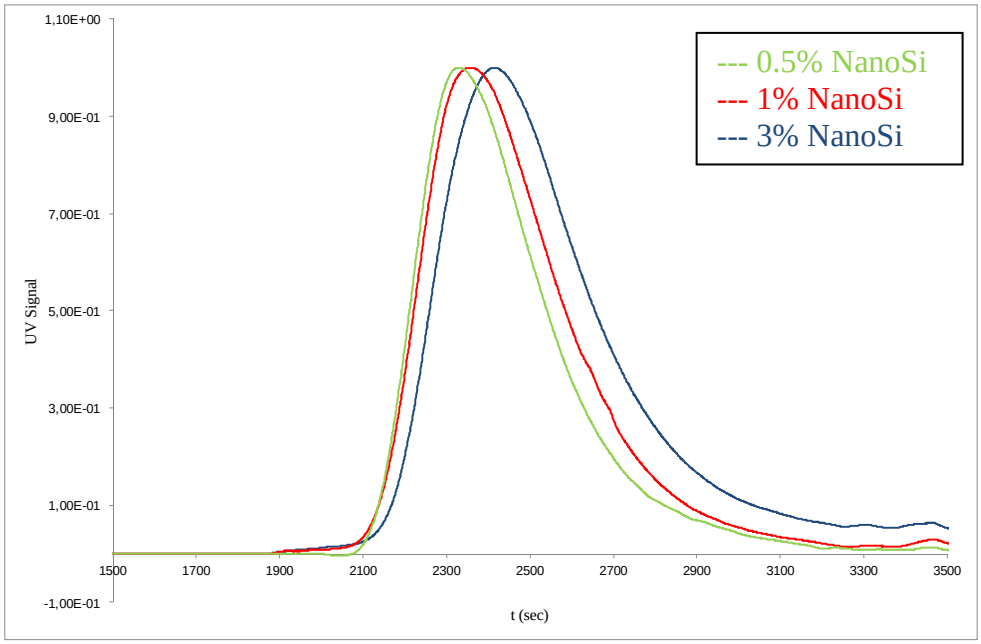

Figure 26: effect of catalyst on molecular weight value

The GPC curves of figure 26 show that increasing the percentage of catalyst in the feed is possible to obtain high molecular weight nanocomposites also with high percentages of fillers. This shows that nanofillers effectively partially disable the catalytic system limiting the growth of chains. As will be reported in the next paragraph, however, this strategy cannot be used for the synthesis of high molecular weight nanocomposites with high percentages of nanofillers because a amount of catalyst too high has negative effect on some properties of the material, such as the stability of the melt, degradation temperature, coloration.

Moreover, if PLA nanocomposites are destined for applications involving contact with food, a high amount of catalystis not accepted.

For these reasons the attention was focused on materials containing amounts of nanoparticles from 0,5 to 2% by weight, studying rheological behavior, thermal behavior (will be discussed in chapter 9) and gas barrier properties.

8.9.9.2 Rheological analysis

Here the rheological curves of nanocomposites synthesized are reported. Analyses were performed following the same procedures already described in previous chapters for the materials to complex architecture.

PLA NANOCOMPOSITES WITH CLOISITE 10A

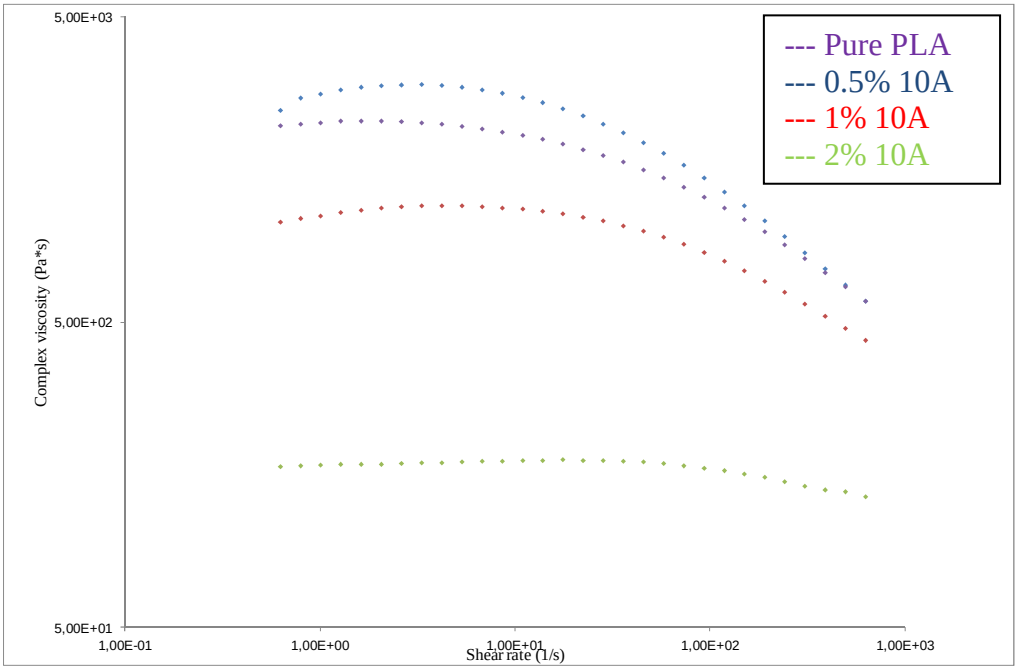

Figure 27: complex viscosity of pure PLA and nanocomposites with Cloisite 10A

The complex viscosity values measured at a shear rate of $6,28*10^{-1}$ s^{-1} are reported in table 12.

Sample	Complex viscosity (Pa*s)
Pure PLA	$2.19*10^3$
0.5% 10A	$2.46*10^3$
1% 10A	$1.06*10^3$
2% 10A	$1.68*10^2$

Table 12: complex viscosity of nanocomposites with Cloisite 10A measured at a shear rate of $6,28*10^{-1}$ s^{-1}

The values of viscosity, in agreement with the molecular weights, decreases increasing the amounts of Cloisite 10A in the feed, and this effect is particularly marked for the material with 2% of filler.

However, it is interesting to note that although the Mn values of materials are lower than those of pure PLA, the difference in viscosity between polymer nanocomposites and pure PLA is not so high, at least for concentrations of 0.5% and 1% of Cloisite 10A. Material with the 0.5% of fillers has a viscosity higher than the one of pure PLA, despite having a lower molecular weight.

Looking at the trend of the rheological curves of figure 27 it can be noted that at high values of shear rates the slope of the curves decreases increasing the percentage of filler; the curve of the sample with a 0.5% of Cloisite 10A has an inclination greater the one of the pure polymer. At low shear rates the viscosity of the composite tends to decrease slightly while that of the pure PLA is asymptotic.

PLA NANOCOMPOSITES WITH CLOISITE 15A

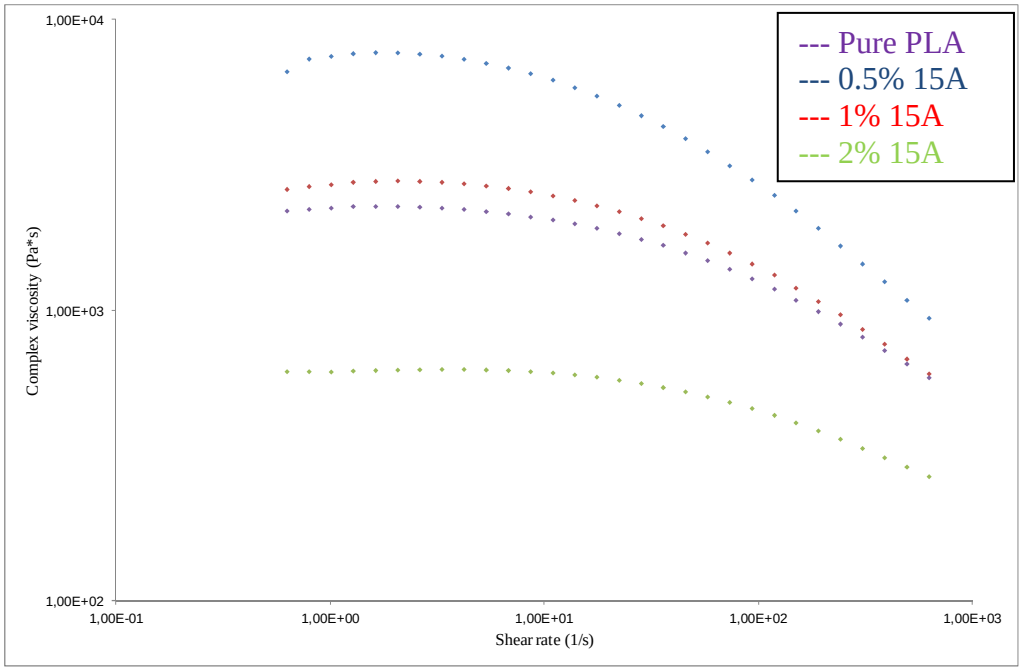

Figure 28: complex viscosity of pure PLA and nanocomposites with Cloisite 15A

The complex viscosity values measured with a shear rate of $6{,}28*10^{-1}$ s^{-1} are reported in table 13.

Sample	Complex viscosity (Pa*s)
Pure PLA	$2.19*10^3$
0.5% 15A	$6.60*10^3$
1% 15A	$2.60*10^3$
2% 15A	$6.14*10^2$

Table 13: complex viscosity of nanocomposites with Cloisite 15A measured at a shear rate of $6{,}28*10^{-1}$ s^{-1}

In the case of Cloisite 15A, the effect of nanoparticles on viscosity is more pronounced than observed for the PLA/Cloisite 10A nanocomposites.

In fact complex viscosity values are particularly high for the material with a filler concentration of 0.5%, while the polymer with 1% of fillers has a viscosity higher than the one of pure PLA despite a Mn values 20000 g/mol lower. Therefore Cloisite 15A contributes a lot to increase the viscosity of the material.

Even in this case, polymer containing 2% of nanoparticles has a low viscosity; in this case the effect of nanoparticle can not compensate the fact that Mn value of nanocomposite is about half of the one of pure PLA.

The curves of the materials with 0.5% and 1% of filler have a slope more pronounced than the one of pure PLA at high values of shear rates. At low shear rate there is a slight decrease in viscosity, as already observed for Cloisite 10A nanocomposites, especially for the material with 0.5% of filler.

PLA NANOCOMPOSITES WITH CLOISITE Na^+

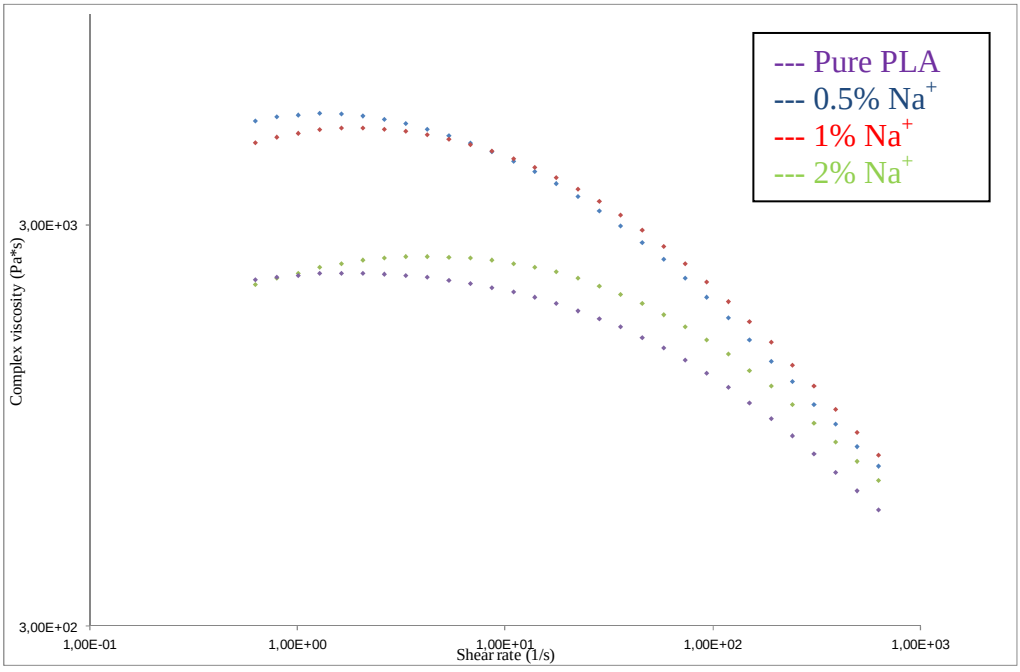

Figure 29: complex viscosity of pure PLA and nanocomposites with Cloisite Na^+

Table 14 shows the complex viscosity values measured with a shear rate of $6,28*10^{-1}\ s^{-1}$

Sample	Complex viscosity (Pa*s)
Pure PLA	$2.19*10^3$
0.5% Na^+	$5.44*10^3$
1% Na^+	$4.80*10^3$
2% Na^+	$2.13*10^3$

Table 14: complex viscosity of nanocomposites with Cloisite Na^+ measured at a shear rate of $6,28*10^{-1}\ s^{-1}$

As can be seen both from the values shown in table 14 and in figure 29, Cloisite Na^+ has more effect on viscosity of PLA. All nanocomposites synthesized with this fillers have a viscosity higher than that of the pure polymer, especially at lower values of shear rates. In particular, materials containing 0.5% and 1% of filler have a viscosity significantly higher than pure PLA, while the polymer containing 2% of Cloisite has the same viscosity of pure PLA, although the molecular weights is lower.

At high values of shear rate, composites have viscosities very similar to each other and slightly higher than that of pure PLA. The slope of the rheological curves in this zone of deformation is much more pronounced for polymers with Cloisite Na^+ than the one of unfilled polymer.

The higher increase in viscosity, observed for Cloisite Na^+, respect to Cloisite 10A and Cloisite 15A may be due to the different exfoliation of fillers during synthesis and to the higher molecular weight of the polymers with sodium Cloisite that, as already reported, less interferes with the process of synthesis.

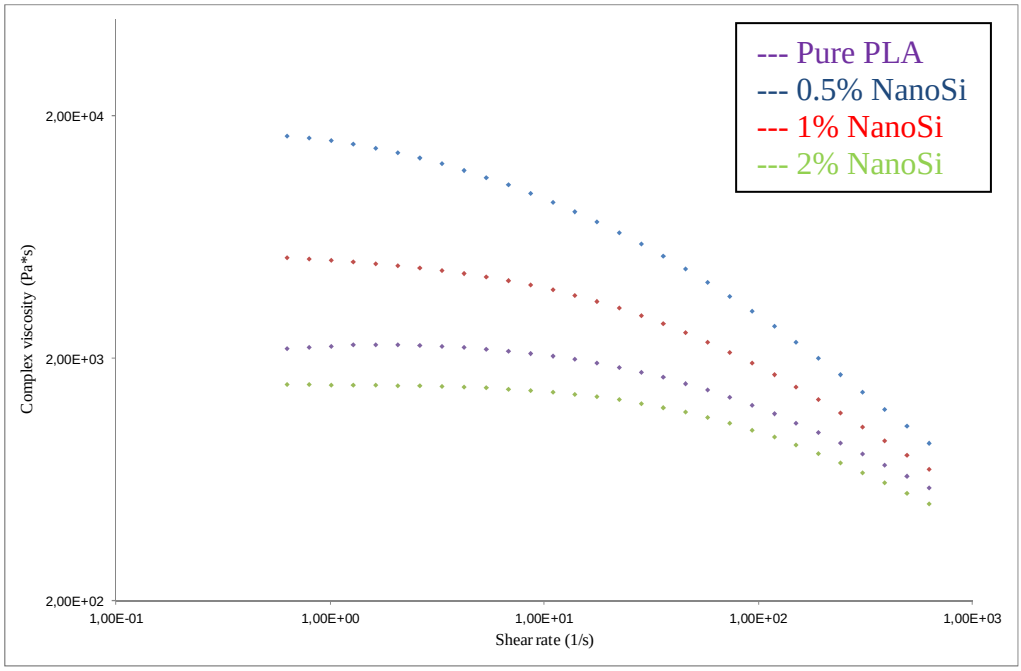

Figure 30: complex viscosity of pure PLA and nanocomposites with nanosilica

Table 15 shows the complex viscosity values measured with a shear rate of $6,28*10^{-1}$ s^{-1}.

Sample	Complex viscosity (Pa*s)
Pure PLA	$2.19*10^3$
0.5% NanoSi	$1.65*10^4$
1% NanoSi	$5.19*10^3$
2% NanoSi	$1.56*10^3$

Table 15: complex viscosity of nanocomposites with nanosilica measured at a shear rate of $6,28*10^{-1}$ s^{-1}

Nanosilica is the mineral filler that seems to have a greater effect on the viscosity of PLA; data reported in table 15 show that in presence of 0.5% and 1% of nanosilica complex viscosity increases respectively seven times and three times respect to pure polymer, although the values of Mn are lower for nanocomposites.

The behavior of material with 2% of filler is also interesting: this polymer has a molecular weight that is less than half in comparison to PLA, while its viscosity is a little lower. So there is a strong interaction between polymer and silica matrix resulting in a significant increase in viscosity.

MATERIALS WITH SURFACE MODIFIED NANOPARTICLES

One of the main requirements to obtain a nanocomposite material in which is possible to observe an increase in properties with small percentages of nanoparticles is to have a product in which the fillers are dispersed in the polymer matrix as well as possible, in order to obtain an homogeneous material.

The problem of dispersion is due to the very low compatibility between mineral and polymer: this means that filler particles have a tendency to form areas of aggregation within the polymer and that the interaction at the filler - polymer interface is very weak, creating discontinuous areas that make the material brittle, instead improving their properties.

The purpose of surface treatment is to obtain a material with a very good dispersion of nanoparticles. One of the techniques used to improve the interaction between polymer and mineral filler includes the use of coupling agents.

This term indicates a molecules that promote the adhesion between organic material (polymer) and inorganic one (mineral filler).

The silanes occupy a large share of coupling agents market: they are extremely versatile because they can be functionalized in various and this make them used with any type of polymers.

In Figures 31 and 32 is possible to observe the effect of surface modification on the dispersion of nanoparticles in the polymer matrix.

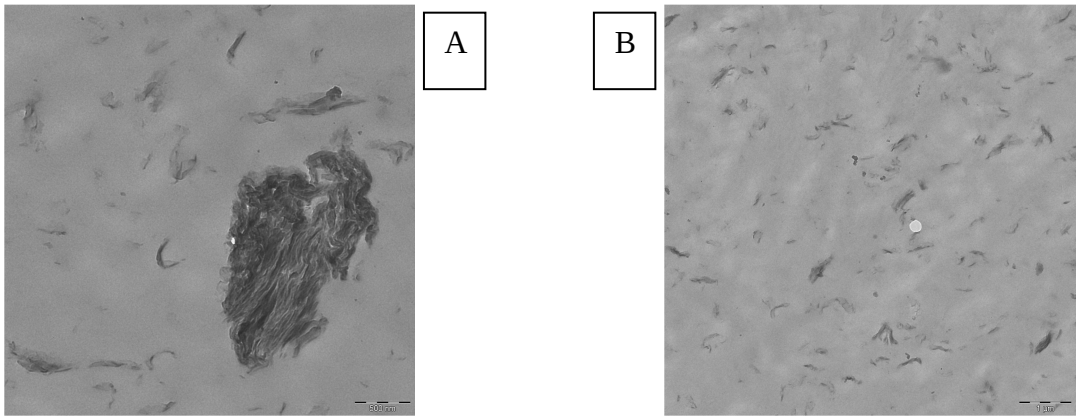

Figure 31: TEM images of PLA with Cloisite 15A (A) and surface modified Cloisite (B)

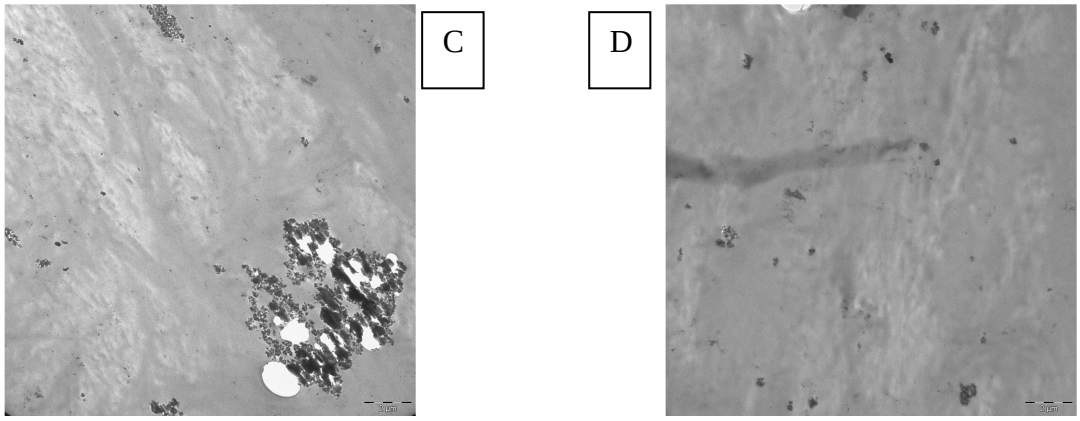

Figure 32: TEM images of PLA with nanosilica (C) and surface modified nanosilica (D)

Nanocomposites prepared with unmodified fillers (A and C) contain aggregates of micrometer size, which show how difficult it is to obtain a good dispersion of nanoparticles even if added during the synthesis. Images B and D show, on the other hand, an improvement of filler dispersion in polymer after surface modification with silane. No macroaggreagates are present.

The effects of surface modification of nanoparticles on the molecular weight and viscosity of material will be discussed.

Table 16 shows the values of molecular weight and polydispersity of materials synthesized using nanosilica and Cloisite 15A modified with amino silane (GF93) and epoxy silane (GF80).

Sample	Mn	d
1% 15A 2,0 GF80	44280	1.840
1% 15A 7,5 GF80	46500	1.895
1% 15A 15,0 GF80	46830	1.706
1% 15A 2,0 GF93	45131	1.764
1% 15A 7,5 GF93	47100	1.780
1% 15A 15,0 GF93	46128	1.815
1% NS 2,0 GF80	45800	1.780
1% NS 7,5 GF80	52014	2.025
1% NS 15,0 GF80	53194	1.996
1% NS 2,0 GF93	49380	2.000
1% NS 7,5 GF93	52000	1.955
1% NS 15,0 GF93	52115	1.763

Table 16: molecular propertis of nanocompistes with modified nanoparticles

Comparing the values in table 16 with the molecular weights of materials synthesized with unmodified nanoparticles it can be seen that the presence of coupling agent allows to obtain polymers with higher molecular weight, especially in the case of Cloisite, probably because the silane - through its functionalization- acts as a polymerization initiator and also limits the effect of catalyst deactivation caused by the nanoparticles.

Figures 33 and 34 show the rheological curves of materials synthesized using modified nanosilica (with GF80) and modified Cloisite 15A (with GF93).

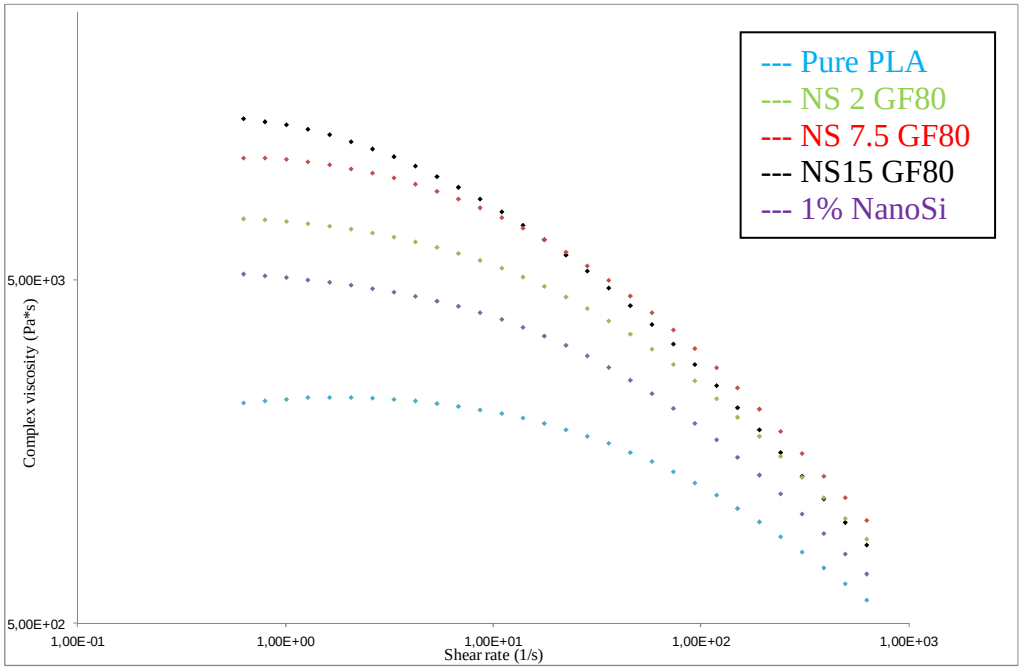

Figure 33: complex viscosity of pure PLA and nanocomposites with modified nanosilice

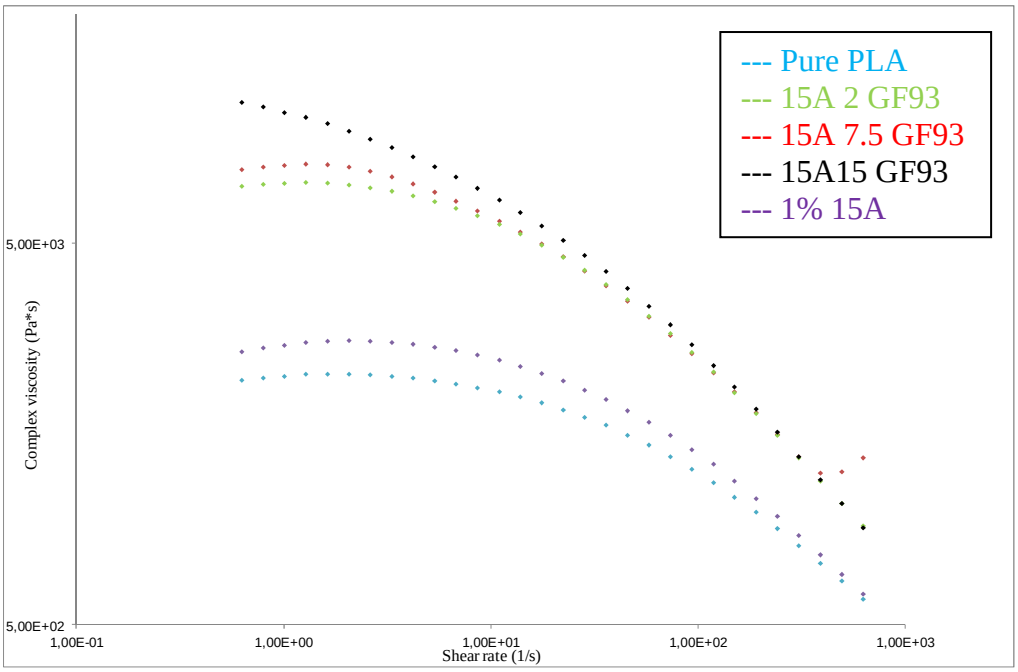

Figure 34. complex viscosity of pure PLA and nanocomposites with modified Cloisite 15A

Table 17 shows the complex viscosity values measured with a shear rate of $6,28*10^{-1}$ s^{-1}.

Sample	Complex viscosity (Pa*s)
Neat PLA	$2.19*10^3$
1% NanoSi	$5.19*10^3$
1% 15A	$2.60*10^3$
1% 15A 2,0 GF80	$7.20*10^3$
1% 15A 7,5 GF80	$7.74*10^3$
1% 15A 15,0 GF80	$1.30*10^4$
1% 15A 2,0 GF93	$7.06*10^3$
1% 15A 7,5 GF93	$7.30*10^3$
1% 15A 15,0 GF93	$1.17*10^4$
1% NS 2,0 GF80	$7.52*10^3$
1% NS 7,5 GF80	$1.10*10^4$
1% NS 15,0 GF80	$1.47*10^4$
1% NS 2,0 GF93	$5.98*10^3$
1% NS 7,5 GF93	$7.06*10^3$
1% NS 15,0 GF93	$1.58*10^4$

Table 17: complex viscosity of nanocomposites with modified nanoparticles at a shear rate of $6,28*10^{-1}$ s^{-1}

When silanes are present on the surface of nanoparticles, the effect of fillers on viscosity of materials is increased, both in the presence of GF93 and GF80. The effect is particularly marked at low values of shear rates. The different nature of the reactive groups on the surface of fillers does not influence significantly the viscosity, as reported in table 17. Materials with the same type of nanoparticle modified with different silane have very silmilar viscosity even if the reactive group available on the surface of mineral filler for the reaction with the polymer is different.

The effect of the presence of silane on the viscosity may be due to the formation of bonds between the polymer chains and the coupling agent that, at low values of shear rates enhance the effect of the formation of network that leads to an increase in viscosity. At high values of shear rates silane acts as a compatibilizer avoiding the aggregation of nanoparticles and the formation of holes.

This may explain because at high values of shear rate the viscosity is lower. On the other hand, the formation of complex inorganic-organic hybrid structures increases the relaxation times of macromolecules and this results in a relatively lower melt viscosity at shear rate values that do not allow the relaxation of macromolecules.

8.9.3 Permeability tests

As mentioned before, nanocomposite materials represent a new strategy to improve physical properties of polymers, especially the mechanical behavior, thermal stability and barrier properties.

The latter is particularly important in the food packaging[48] field where, with good mechanical properties, is required that materials have a good barrier behavior that limits the flow of oxygen, carbon dioxide, water vapor and aromas. The use of fillers with nanoscale dimensions seems to be a good way to increase the barrier behavior, but two aspects are still to improve: the compatibility between polymer and mineral filler and complete dispersion of filler in the matrix.

Based on these considerations the permeability of some of the materials synthesized in this work was measured, both nanocomposites and with complex architecture, in order to evaluate the differences with the commercial PLA and see if and how the different macromolecular architecture, or the presence of nanoparticles, affects the barrier behavior of PLA. Taking into account the model of gas permeation in a polymer in the presence of nanofillers, shown in figure 35, the overall effect of permeability variation in the complex structures of PLA synthesized in this work, should be related to both the crystalline content of PLA and to the presence of inorganic filler that interferes the permeation of gases.

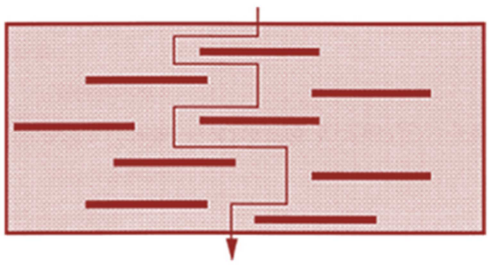

Figure 35: effect of nanoparticles on gas permeation

Permeability measurements were carried out on polymer films obtained by casting from concentrated solutions of PLA in chloroform. It was decided to use a polymer/solvent ratio of 1/5 w/w which has been shown to be the best to obtain a sufficiently viscous solution that can be stretched to form film.

The solution is deposited on a glass plate and, after the film is formed, the solvent is slowly evaporated to avoid formation of bubbles that can act as channels for gas and thus affect the measurement of permeability.

Oxygen analysis were conducted at 23 °C and 0% relative humidity as required by ASTM F2622-08, the analysis of water vapor instead are conducted at 23 °C and 90% relative humidity according to ASTM F1249-06, and CO_2 measurements were conducted at 23 °C and 0% relative humidity according to ASTM F2476-05. For all the analysis a rate of gas carrier of 73 ml/min has been used.

Table 18 shows the permeability values of some materials prepared for this work.

Sample	O_2 TR (ccmicrom/m^2 24h bar)	H_2O TR (gmicrom/m^2 24h bar)	CO_2 TR (ccmicrom/m^2 24h bar)
Standard PLA	188.27	9.48	236.66
Neat PLA	114.34	3.50	208.52
1% NanoSi	64.16	2.06	187.46
1% 15A	92.63	2.08	151.28
1% 15A 15 GF93	89.55	1.97	136.03
1% NS 15 GF93	47.93	2.19	110.09
1% NS 2 GF80	76.26	5.15	-
1% NS 7.5 GF80	57.32	5.11	-
1% NS 15 GF80	20.65	3.08	-
0.05% T2+0.025% An	90.11	4.54	-
0.025% T4+0.0125% An	47.01	4.85	-

Table 18: gas permeability of some PLA samples

Data in table 18 show the significant differences between standard PLA, or pure PLA, and materials with nanofilers or complex architecture.

A first interesting difference is observed between the permeability values of commercial PLA and of pure polymer synthesized in our laboratory. These are two unmodified PLA, so the difference in permeability can be attributed only to the different crystal content in two samples.

The difference in crystallinity, since the two films have been prepared following the same procedure, is then linked to the characteristics of material and to the microstructure. Figure 36 shows the DSC curves of commercial polymer and of PLA in the lab.

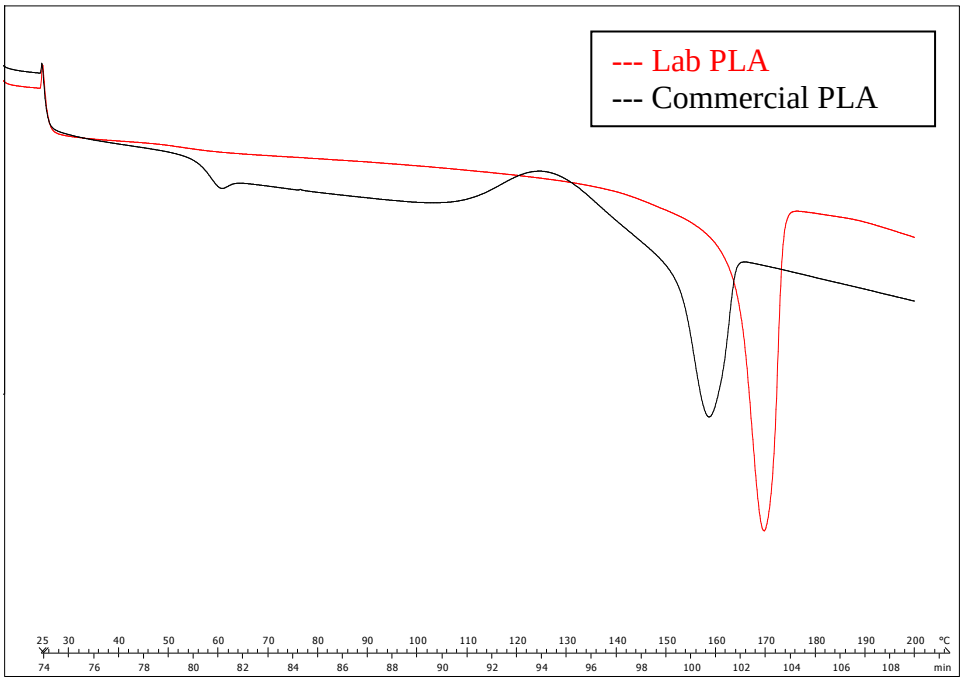

Figure 36: different crystallinity between commercial PLA and lab PLA

As expected the two materials have very different crystal content that justifies the better barrier behavior of lab PLA compared to the one of commercial PLA.

Analyzing the values of other samples a decrease in permeability in presence of 1% of Cloisite 15A and nanonilica is observed, due both to higher crystallinity of the material (will be discussed in chapter 9) and to the interference created by mineral component to the path of gas. The better dispersion of silica in the polymer matrix can justify the higher barrier effect of composite with nanoSilica compared to Cloisite.

A very marked effect related to surface modification of nanoparticles has been observed; the presence of silane improves the dispersion of fillers in the polymer matrix and increases the

content of the crystalline material. PLAs with modified nanosilica and Cloisite (GF93) have lower permeability than the corresponding polymers with unmodified nanoparticles.

Increasing the percentage of GF80 silane on the silica surface, greatly increases the barrier effect, in particular to oxygen; GF80 silane seems to be much more efficient than GF93 to the oxygen, while the water permeability is better with the GF93 and however, the values decrease using modified nanosilica.

Finally, the values for samples with complex macromolecular architecture are much lower than those of linear PLA - regarding oxygen permeability - and are worse for water vapor. All these values, however, are much more lower than one of commercial PLA.

The barrier behavior of PLA, therefore, can be controlled changing the macromolecular architecture and using nanofillers and modified nanofillers.

Table 19 shows the data reported in literature[49] about the percentage of permeability reduction in PLA composites with different kind of nanofillers added by compounding.

Sample	Clay	Clay %	R% KPO_2	R% WVTR
1	MMT Org Mod	4	12	-
2	"	5	15	-
3	"	7	19	-
4	MMT	4	14	-
5	MMT-Modificata	4	12	
6	Saponite	4	40	-
7	Mica Fluorurata sintetica	4	65	-
8	MMT	5	48	50
9	MMT modificata	5	46	-
10	Bentonite	5	6	-
11	MMT-C16-NH_2	4	42	-
12	"	6	56	-
13	"	10	58	-
14	"	10	58	-
15	Cloisite 25A	6	45	-
16	"	10	56	-
17	MMT Org. Mod	1	20	27
18	"	5	32	54

Table 19: reduction of KPO_2 and WVTR for different PLA nanocomposites

The values reported in Table 19 show clearly the effect of nanoparticles, in this case multilayer silicates, on barrier property of PLA. In particular, depending on the kind of filler used there is a proportional decrease of the permeability that also depends by the amount of fillers in feed.

Permeability data reported in table 18 show that permeability decrease more, even if in presence of significantly lower amount of filler (1% by weight), than the one used in materials described in literature[49] (minimum 4%); this confirms that the addition of fillers during synthesis allows to significantly improve some properties of materials using small amounts of nanoparticle compared to what can be obtained by compounding. This is because the polymer obtained by in situ synthesis has a better dispersion of mineral filler and a greater homogeneity which results in better properties.

As mentioned earlier the main reason why the nanocomposite in the industry are not produced by in situ polymerization is economic, essentially linked to the extensive investment required to adapt the systems currently used. However, it is clear that, even if further optimizations - mainly related to scale-up – are required, the in situ process allows to obtain materials with very interesting properties using low amounts of mineral.

REFERENCES

[1] Alexandre, M., Dubois, P., *Materials Science and Engineering*, 28, 2000, 1-63.

[2] Greenland, D. J., *J. Colloid Sci*., 18, 1963, 647-664.

[3] Ogata, N., Kawakage, S., Ogihara, T., *J. Appl. Polym. Sci.*, 66, 1997, 573-581.

[4] Parfitt, R. L., Greenland, D. J., *Clay Mineral*, 8, 1970, 305-323.

[5] Zhao, X., Urano, K., Ogasawara, S., *Colloid Polym. Sci.*, 267, 1989, 899-906.

[6] Ruiz-Hitzky, E., Aranda, P., Casal, B., Galvan, J. C., *Adv. Mater.*, 7, 1995.

[7] Billingham, J., Breen, C., Yarwood, J., *Vibr. Spectrosc.*, 14, 1997, 19-34.

[8] Levy, R., Francis, C. W., *J. Colloid Interface Sci.*, 50, 1975, 442-450.

[9] Jeon, H. G., Jung, H. T., Lee, S. W., Hudson, S. D., *Polym. Bull.*, 41, 1998, 107-113.

[10] Ogata, N., Jimenez, G., Kawai, H., Ogihara, T., *J. Polym. Sci. Part B, Polym. Phys.*, 35, 1997, 389-396.

[11] Ogata, N., Jimenez, G., Kawai, H., Ogihara, T., *J. Appl. Polym. Sci.*, 64, 1997, 2211-2220.

[12] Yano, K., Usuki, A., Okada, A., Kurauchi, T., Kamigaito, O., *J. Polym. Sci. Part A, Polym. Chem.*, 31, 1993, 2493-2498.

[13] Oriakhi, C. O., Zhang, X., Lerner, M. M., *Appl. Clay Sci.*, 15, 1999, 109-118.

[14] Fukushima, Y., Okada, A., Kawasumi, M., Kurauchi, T., Kamigaito, O., *Clay Mineral*, 23, 1988 27-34.

[15] Usuki, A., Kojima, Y., Kawasumi, M., Okada, A., Fukushima, Y., Kurauchi, T., Kamigaito, O., *J. Mater. Res.*, 8, 1993, 1179-1183.

[16] Messersmith, P. B., Giannelis, E., P., *J. Polym. Sci. Part A, Polym. Chem.* 33, 1995, 1047-1057.

[17] Akelah, A., Moet, A., *J. Mater. Sci.*, 31, 1996, 3589-3596.

[18] Doh, J. G., Cho, I., *Polym. Bull.*, 41, 1998, 511-517.

[19] Weimer, M. W., Chen, H., Giannelis, E. P., Sogah, D. Y., *J. Am. Chem. Soc.*, 121, 1999, 1615-1616.

[20] Alexandre, M., Dubois, P., Jerome, R., Garcia-Marti, M., Sun, T., Garces, J. M., Millar, D. M., Kuperman, A., *WO9947598A1*, 1999.

[21] Lan, T., Pinnavaia, T., *J. Chem. Mater.*, 6, 1994, 2216.

[22] Wang, M. S., Pinnavaia, T., *J. Chem. Mater.*, 6, 1994, 468.

[23] Vaia, R. A., Giannelis, E. P., *Macromolecules*, 30, 1997, 7990-7999.

[24] Balazs, A. C., Singh, C., Zhulina, E., *Macromolecules*, 31, 1998, 8370-8381.

[25] Balazs, A. C., Singh, C., Zhulina, E., Lyatskaya, Y., *Acc. Chem. Res.*, 8, 1999, 651-657.

[26] Vaia, R. A., Giannelis, E. P., *Macromolecules*, 30, 1997, 8000-8009.

[27] Liu, l. M., Qi, Z. N., Zhu, X. G., *J. Appl. Polym. Sci*., 71, 1999, 1133-1138.

[28] Kato, M., Usuki, A., Okada, A., *J. Appl. Polym. Sci.*, 66, 1997, 1781-1785.

[29] Ray, S. S., Okamoto, M., *Prog. Polym. Sci.*, 28, 2003, 1539–1641.

[30] Chang, J. H., An, Y. U., Sur, G. S., *J. Polym. Sci. Part B, Polym. Phy.*, 41, 2003, 94–103.

[31] Paul, M. A., Alexandre, M., Degee, P., Henrist, C., Rulmont, A., Dubois, P., *Polymer*, 44, 2003, 443–450.

[32] Cabedo, L., Feijoo, J. L., Villanueva, M. P., Lagaron, J. M., Gimenez, E., *Macromol Symp.*, 233, 2006, 191–197.

[33] Wu, C. S., Liao, H. T., *Polymer*, 48, 2007, 4449–4458.

[34] Wu, D., Wu, L., Zhang, M., Zhao, Y., *Polym. Degrad. Stab.*, 93, 2008, 1577–1584.

[35] Kim, I. H., Jeong, Y. G., *J. Polym. Sci. Part B, Polym. Phy.*, 48, 2010, 850-858.

[36] Wen, X., Zhang, K., Wang, Y., Han, L., Han, C., Zhang, H., Chenb, S., Dong, L., *Polym. Int.*, 60, 2011, 202–210.

[37] Yan, S. F., Yin, J. B., Yang, Y., Dai, Z. Z., Ma, J., Chen, X. S., *Polymer*, 48, 2007, 1688.

[38] Wu, L., Cao, D., Huang, Y., Li, B. G., *Polymer*, 49, 2008, 742.

[39] Ray, S. S., Maiti P., Okamoto M., Yamada K., Ueda K., *Macromolecules*, 35, 2002, 3104-10.

[40] Chen, G. X., Kim, H. S., Shim, J. H., Yoon, J. S., *Macromolecules*, 38, 2005, 3738-44.

[41] Paul, M. A., Alexandre, M., Degee, P., Calberg, C., Jerome, R., Dubois, P., *Macromol. Rapid Commun.*, 24, 2003, 561-566.

[42] Paul, M. A., Delcourt, C., Alexandre, M., Degee, P., Monteverde, F., Rulmont, A., *Macromol. Chem. Phys.*, 206, 2005, 484-498.

[43] Joubert, M., Delaite, C., Bourgeat-Lami, E., Dumas, P., *J. Polym. Sci. Part A, Polym. Chem.*, 42, 2004, 1976-1984.

[44] Liu, L. Z., et al., *Pigment & Resin Technology*, 39, 2010, 27-31.

[45] Hoidy, W. H., et al., *Journal of Applied Sciences*, 10, 2010, 97-106.

[46] Huang, J. W., *Journal of Applied Polymer Science*, 112, 2009, 1688−1694.

[47] Sun, Y., et al., *Journal of Colloid and Interface Science*, 292, 2005, 436–444.

[48] Arora, A., Padua G. W., *Journal of food science*, 75, 2010, 43-49.

[49] Lagaron, J., Sanchez, G. M., *Thermoplastic nanobiocomposites for rigid and flexible food packaging application*

9. Thermal properties of PLA

9 THERMAL PROPERTIES OF PLA

Standard PLA, being semi-crystalline, has glass transition temperature (Tg) and melting temperature (Tm). Above Tg amorphous PLA is rubber-like while under Tg it is in the glassy state.

Tg is around 56 °C and Tm is around 170 °C, rather low compared to one of other thermoplastic materials; this of course is reflected on the material properties and on fields of application.

Glass transition temperature and melting temperature depend both on molecular weight values and optical purity of polymer: increasing Mn value also Tg and Tm increase until they reach the values indicated but in presence of impurities Tm and Tg values decrease.

Some properties depend on crystalline content of material, like for example physical properties, mechanical properties, barrier behavior and surface appearance. Crystallinity is one of the critical points for PLA: even with high concentrations of LL Lactide isomer, therefore with a very high optical purity, crystallization is too slow to obtain a polymer with a significant crystalline fraction in standard processing conditions. Several strategies[1-5] are used to induce crystallization in PLA : the first one is the use of nucleating agents, able to lower the free surface energy barrier of nucleation process and promote crystallization at higher temperatures during cooling phase. A second possibility is to add a plasticizer to increase the mobility of polymer chains and increase crystallization rate. The third way is to vary the process conditions, for example temperature and cooling time.

In this work the first method have been chosen: different agents able to promote the nucleation and crystallization of PLA have been used; in particular the effect of nanoparticles - used in synthesis of nanocomposites described in chapter 8 - on crystallization have been evaluated. Nanofillers used are not standard nucleating agents, such as talc, but it is however interesting study the effect on this property.

Materials with complex architecture have been also analyzed in order to study possible differences in Tg and Tm, although the amount of comonomer used for modifying the architecture is very small and therefore it is more difficult that it could affect glass transition temperatures and melting temperatures.

In this chapter also the effect of nanoparticles on thermal stability of PLA will be studied, with particular attention to start degradation temperature and degradation rate.

9.1 DYNAMIC DSC ANALYSES

The study of thermal properties of PLA based nanocomposites and of PLA with complex macromolecular architecture is made to determine the possible variations in the characteristics temperatures of these polymers. DSC analyses were performed with an heating-cooling-heating cycle to determine first and second melting temperatures, crystallization temperature and glass transition temperature.
For these analyses the following program was used:

- heating from 25 °C to 200 °C at 10 °C/min
- 5 minutes isotherm at 200 °C to delete the thermal history of material
- cooling from 200 °C to 25 °C at 10°C/min
- 2 minutes isotherm at 25°C
- heating from 25 °C to 200 °C at 10 °C/min

During the first heating phase glass transition temperature T_{g1} and first melting temperature T_{m1} of PLA can be observed. These two values are characteristic of thermal and mechanical story of polymer; in fact, the same materials that have undergone different thermal processes or have different mechanical stress may have different melting temperatures and glass transition temperatures.
Polymer that has been processed, for example, gives a different result in first DSC cycle in comparison to a polymer that crystallizes slowly without any stress applied. For this reason, a comparison between the first cycle melting temperatures of different samples is not reliable. The 5 minute isotherm at high temperature, when polymer is molten, are used to erase thermal and mechanical history of the material; in this period, polymer chains relax reaching a state of minimum internal energy.
The cooling phase allows to determine crystallization temperature T_{c1}; since samples are cooled from a state of minimum energy, comparisons between different T_{c1} is significant; the reason for any differences in this case can be related to different composition and/or polymer molecular architecture.

The 2 minute isotherm at low temperature have only the purpose of allowing the sample to actually reach 25 °C, due to less effective heat transfer at low temperatures. The second cycle of heating is used to determine the glass transition temperature T_{g2}, cold crystallization temperature T_{c2} and melting temperature T_{m2}; T_{m2} can be used for a comparison between different polymers, because in this case, after the relaxation phase at high temperature, all samples underwent the same thermal history.

Figure 1 shows the DSC curves of pure PLA synthesized in the laboratory.

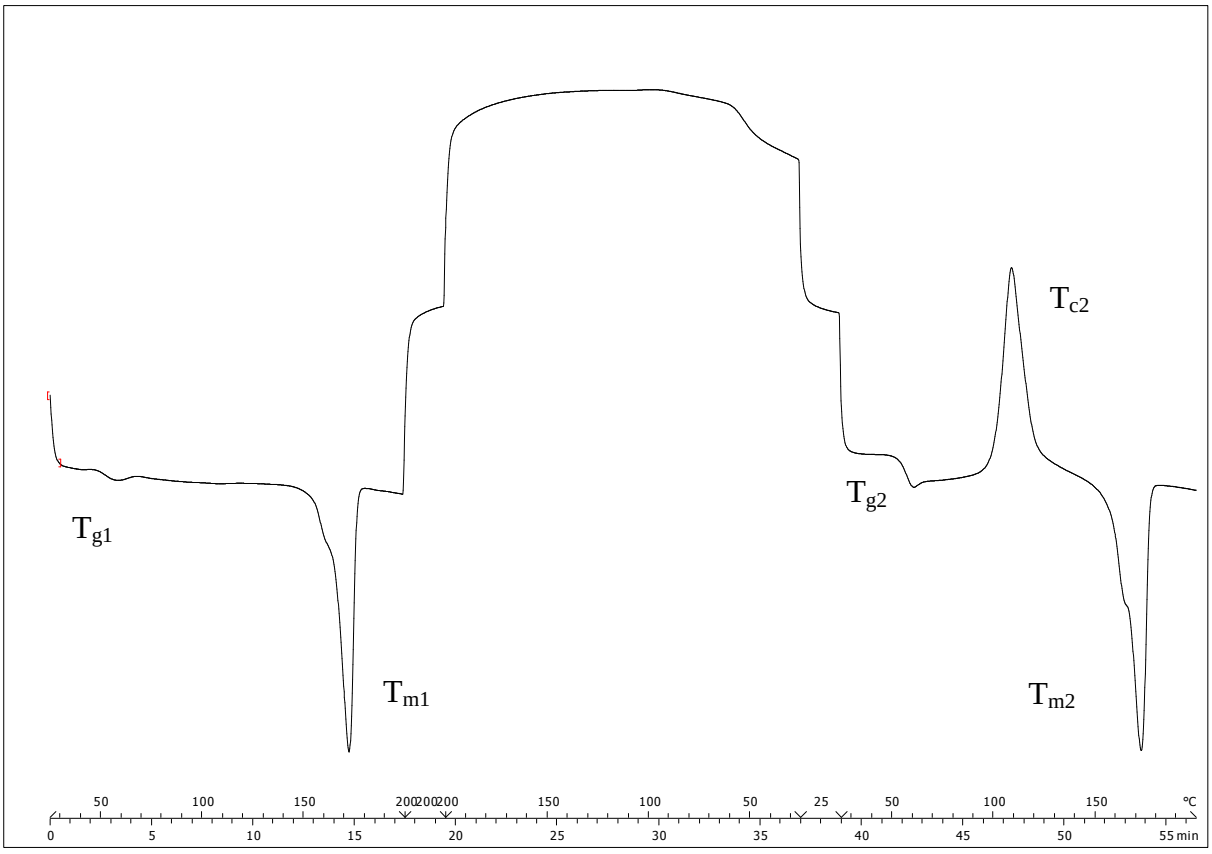

Figure 1: DSC curve of pure PLA

DSC curve in figure 1 is relative to the program of analysis described above; the first heating cycle will not be considered for the study of the material (structure, microstructure, fillers, etc.) for the reasons mentioned above. On the other hand the first heating cycle is quite important for the process technology of polymeric materials. It is interesting to observe the behavior of PLA during the cooling and heating in the second scan.

PLA is a polymer that has a low tendency to crystallize; in fact, during cooling phase, there is no crystallization even if cooling rate is relatively low. In second cycle of heating there is a very clear Tg (59.7 °C) confirming the presence of a considerable amount of amorphous phase. The mobility acquired by polymer chains allows the material to crystallize and a peak related to crystallization T_{c2} (108.6 °C) appears..

At the end of crystallization peak, melting peak appears (T_{m2}) (172.3 °C): the peak is partially overlapped with the crystallization one.

Table 1 shows thermal data of nanocomposites measured by DSC.

Sample	T_{c1} (°C)	ΔH_{c1} (J/g)	T_{g2} (°C)	T_{c2} (°C)	ΔH_{c2} (J/g)	T_{m2} (°C)	ΔH_{m2} (J/g)
Pure PLA	-	-	59.7	108.6	44.6	172.3	46.0
0.5% 10A	97.0	2.9	53.0	106.1	48.8	166.4	56.0
1% 10A	97.2	2.4	55.5	107.8	49.2	172.0	55.2
2% 10A	-	-	54.4	102.6	48.7	167.4	52.7
0.5% 15A	93.1	4.3	54.2	105.4	48.3	170.4	55.3
1% 15A	95.8	6.5	53.7	104.5	42.2	170.0	54.7
2% 15A	-	-	52.7	126.3	29.2	157.2	29.9
0.5% Na^+	96.9	5.4	54.2	103.4	43.2	172.5	54.2
1% Na^+	93.6	7.3	52.4	97.6	39.7	166.9	55.7
2% Na^+	95.2	2.5	54.6	99.3	52.9	170.3	58.1
0.5% NS	97.8	20.0	52.3	96.4	31.8	169.0	54.3
1% NS	101.7	22.4	-	-	-	174.5	41.4
2% NS	95.9	5.1	-	81.8	39.0	164.4	45.3

Table 1: thermal data of nanocomposites

Analyzing data in table 1 it can be seen that pure PLA does not crystallize during cooling. The presence of nanoparticles leads to crystallization of material during cooling, but the relationship between crystallization temperature, heat developed during the transition and amount of filler is not easily interpretable. Using Cloisite 10A, crystallization is observed in the presence of 1% of mineral and the process has very low intensity as demonstrated by the low value of crystallization heat. In presence of 0.5% and 1% of Cloisite 15A, PLA crystallizes and heats of crystallization and crystallization temperatures increase with the percentage used, but the intensity of the phenomenon is still relatively low.

Using sodium Cloisite, crystallization is always observed during cooling, but the trend in temperature and ΔH_{c1} is not linear with the percentage of filler inside the polymer.

Overall, montmorillonites promote crystallization, but the nucleating effect is not so efficient[6] like with other agents, such as talc[7] which is one of the main crystallization promoter both in academic field and in industrial one.

The addition of montmorillonites does not affect significantly cold-crystallization temperature (T_{c2}) whose values are comparable with those of pure polymer, except for nanocomposite with 2% of Cloisite 15A that from this point of view has a peculiar behavior and for materials with sodium Cloisite having lower T_{c2}. Polymers with a smaller percentage of Cloisite 15A and materials with sodium Cloisite are able to nucleate during cooling phase, and the nuclei facilitate the subsequent cold-crystallization process which occurs earlier and at lower temperatures (effect more pronounced with sodium Cloisite); probably with a 2% of Cloisite 15A, nucleation does not occurs during cooling with a consequent increase in temperature of cold-crystallization.

These considerations justify the better behavior using nanosilica, more similar to talc powder from a morphological point of view, which promotes the crystallization of PLA at higher temperatures and with an heat generation higher than the one observed with montmorillonites. In particular, the material with 1% of silica shows the most interesting results.

Materials with nanosilica, on the other hand, are those in which T_{c2} is more different from the value of pure PLA; polymer with 1% of filler does not show crystallization phenomenon during second cycle of temperature. This may be related to the higher nucleating effect of silica, compared to montmorillonite, which allows a better packing of crystal during cooling phase, with a consequent decrease in the amorphous phase of material.

Nanocomposite materials have a melting temperature lower than one of pure polymer.

Crystallinity of materials was calculated using the equation [7] 9.1).

$$\chi = \frac{\Delta H}{\Delta H^{\circ} m \times \left(1 - \frac{\% \, filler}{100}\right)} \times 100 \qquad 9.1)$$

In equation 9.1) ΔH is equal to ΔH_{c1} for cooling phase and to ΔH_{c2} and ΔH_{m2} and for heating phase; ΔH°_{m} is the enthalpy of fusion of PLA[8,9] with 100% crystallinity: its value is 93.0 J/g. Values of crystallinity were calculated basing on equation 9.1): they are reported in table 2.

Sample	χ_{c1} (%)	χ_{c2} (%)	χ_{m2} (%)	χ_{m2}- χ_{c2} (%)
Pure PLA	-	47.9	49.5	1.6
0.5% 10A	3.1	52.7	60.5	7.8
1% 10A	2.6	53.4	59.9	6.5
2% 10A	-	53.4	57.8	4.4
0.5% 15A	4.6	52.2	59.8	7.6
1% 15A	7.1	45.8	59.4	13.6
2% 15A	-	32.0	32.8	0.8
0.5% Na^+	5.8	46.7	58.6	11.9
1% Na^+	7.9	43.1	62.0	18.9
2% Na^+	2.7	58.0	63.7	5.7
0.5% NS	21.6	34.4	58.7	24.3
1% NS	24.3	-	45.0	45.0
2% NS	5.6	42.7	49.7	7.0

Table 2: crystallinity of PLA and PLA nanocomposites

As can be seen from values given in tables 1 and 2, crystals of PLA-based nanocomposites are formed in part during cooling crystallization (with the exception of the materials with 2% Cloisite 10A and 2% Cloisite 15A) and partially during the crystallization that occurs in the subsequent heating cycle (except for the nanocomposite with 1% silica). Analyzing data in table 2 we can see the different behavior of materials in relation to the kind of filler used.

In presence of Cloisite 10A, the amount of crystalline phase formed during the cooling phase (calculated by the difference (χ_{m2}-χ_{c2})) decreases with increasing percentage of filler while moving from a content of 0.5% to a concentration 1% of Cloisite 15A, crystallinity increased and then decreased again by further increasing the amount of nanoparticle, probably due to the presence of an excessive percentage of filler, which hinders the formation of crystal.

The same trend is observed for sodium Cloisite and, more markedly, for nanosilica whose nanocomposites show a greater increase of crystallinity. In all cases, however, nanocomposites are more crystalline in comparison to pure PLA because the presence of nanoparticles affects the total percentage of crystallinity of material, despite the differences related to the type of fillers used.

In chapter 8 the effect of surface modification of nanoparticles on molecular properties and rheological properties of PLA nanocomposites has been studied; materials prepared using modified fillers were analyzed by DSC and the results obtained are presented in table 3.

Sample	T_{c1} (°C)	ΔH_{c1} (J/g)	T_{g2} (°C)	T_{c2} (°C)	ΔH_{c2} (J/g)	T_{m2} (°C)	ΔH_{m2} (J/g)
1% 15A	95.8	6.5	53.7	104.5	42.2	170.0	54.7
1% 15A 2,0 GF80	98.7	12.6	54.6	105.0	26.8	172.3	42.0
1% 15A 7,5 GF80	100.6	12.8	55.3	107.8	26.0	171.1	41.6
1% 15A 15,0 GF80	97.5	1.3	52.1	104.0	46.2	166.7	48.8
1% 15A 2,0 GF93	96.1	5.1	54.4	98.9	42.8	169.1	48.5
1% 15A 7,5 GF93	-	-	54.3	102.5	45.9	167.4	49.1
1% 15A 15,0 GF93	-	-	55.9	110.0	49.2	168.0	49.8
1% NS	101.7	22.4	-	-	-	174.5	41.4
1% NS 2,0 GF80	105.6	33.5	-	-	-	174.9	41.8
1% NS 7,5 GF80	124.3	44.1	-	-	-	173.2	47.7
1% NS 15,0 GF80	130.0	57.9	-	-	-	172.9	64.5
1% NS 2,0 GF93	99.4	19.8	55.8	104.1	15.3	176.5	43.2
1% NS 7,5 GF93	119.0	41.9	-	-	173.6	173,5	44.0
1% NS 15,0 GF93	125.7	45.4	-	-	-	170.3	50.2

Table 3: thermal parameters of nanoomposites with modified nanofillers

Data in table 3 show that surface modification of nanoparticles affects the thermal behavior of materials. Nanocomposites containing Cloisite have a crystallization temperature, during cooling phase, higher than the one of polymer with unmodified filler, except for material with Cloisite modified with 7.5% and 15% of amino silane that do not crystallize during cooling.

It is interesting to note that increasing the percentage of silane on surface of Cloisite the heat associated with the process of cold-crystallization and melting increase. ΔH_{m2} values of polymer with modified Cloisite, however, is always lower than the one of nanocomposites with pure montmorillonite.

Unmodified montmorillonite partly exfoliates during polymerization, and this increases the effect of nucleation during cooling compared to pure polymer.

At low percentages of GF80, a better behavior during cooling was observed, probably due to better dispersion of Cloisite after surface modification that promotes crystallization of polymer chains linked to the fillers; the crystal that is formed is probably disturbed by the presence of clay and this may explain why ΔH_{m2} values are lower than the ones of polymer with unmodified Cloisite. Considering materials with higher amount of GF80 and those with GF93, a different behavior is observed: a lower, or absent, effect of nucleation during the cooling phase and a simultaneous increase of heat associated to the melting of crystal. This may be due to a lower exfoliation of Cloisite because of too the presence of too much silane on the surface, or to a different behavior between amino silane and epoxy silane; further analyses, especially with TEM microscopy will be needed to better understand this behavior.

The behavior of materials containing modified nanosilica is more interesting confirming the best nucleating effect of nanosilica compared to montmorillonite.

Increasing the amount of silane, crystallization process is easier and faster, with a consequent increase in the heat of crystallization.

Sample with 2% of GF93 hardly crystallizes and has a peak of cold crystallization during heating, indicating that crystallization was not complete. Sample with 2% of GF80 has a temperature and a heat of crystallization during cooling that are quite low, while materials containing higher percentages of modified silica have values of Tc, Tm, and ΔH_c ΔH_m higher than the one of nanocomposite with pure nanosilica. This because samples have greater affinity between polymer and silica. Comparing the values in table 3 it seems that epoxy silane (GF80) is more effective than amino silane (GF93); this may be attributed to the higher affinity of epoxy groups with the end groups of PLA.

This means that a greater number of polymer chains is linked to silica surface: the higher the number, the smaller the length. The material is therefore more homogeneous regarding the species present and this is reflected on crystallization phenomenon which is faster and occurs at higher temperatures, with lower temperature range from start to end, due to greater mobility of chains which nucleate and increase crystals easier. Crystal is well formed as confirmed by Tm, and ΔH_m values.

Table 4 shows values of crystallinity of materials with modified nanoparticles.

Sample	χ_{c1} (%)	χ_{c2} (%)	χ_{m2} (%)	χ_{m2}- χ_{c2} (%)
1% 15A	7.1	45.8	59.4	13.6
1% 15A 2,0 GF80	13.7	29.1	45.6	16.5
1% 15A 7,5 GF80	13.9	28.2	45.2	17.0
1% 15A 15,0 GF80	1.4	50.2	53.0	0.8
1% 15A 2,0 GF93	5.5	44.9	52.7	7.8
1% 15A 7,5 GF93	-	49.9	53.3	3.4
1% 15A 15,0 GF93	-	53.4	54.1	0.7
1% NS	24.3	-	45.0	45.0
1% NS 2,0 GF80	36.4	-	45.4	45.4
1% NS 7,5 GF80	47.9	-	51.8	51.8
1% NS 15,0 GF80	62.9	-	70.0	70.0
1% NS 2,0 GF93	21.5	16.5	46.9	30.4
1% NS 7,5 GF93	45.5	-	47.8	47.8
1% NS 15,0 GF93	49.3	-	54.5	54.5

Table 4: crystallinity of nanocomposites with modified fillers

As can be seen from table 4, the kind of silane used for surface modification of nanofillers affects the crystallinity of material. Polymers containing modified Cloisite 15A with 2% and 7.5% of epoxy silane (GF80) show an increase of crystallinity obtained during cooling (calculated by the (χ_{m2}-χ_{c2}) difference) compared to nanocomposite with unmodified Cloisite, while the behavior gets worse increasing the percentage of silane up to 15%. The ability of material to crystallize is lower, in fact only in presence of Cloisite with 2% of GF93 a crystallization is observed during cooling; the phenomenon observed in this phase is less evident than the one observed for nanocomposite with unmodified montmorillonite.

So also in presence of silane, montmorillonite remains a relatively inefficient nucleant.

On the other hand, silica is a better promoter of crystallization; data in table 3 and 4 show that materials do not have cold crystallization (with the exception of 2% GF93), confirming that during cooling the material crystallizes almost complete.

To further confirm also (χ_{m2}-χ_{c2}) values increase significantly increasing the percentage of silane on the surface of nanoparticle and, excluding the sample with 2% of GF93, these values are higher than value of nanocomposite containing unmodified silica.

Figure 2 shows a comparison between DSC curves of nanocomposites containing nanosilica modified with 15% of GF80 and GF93.

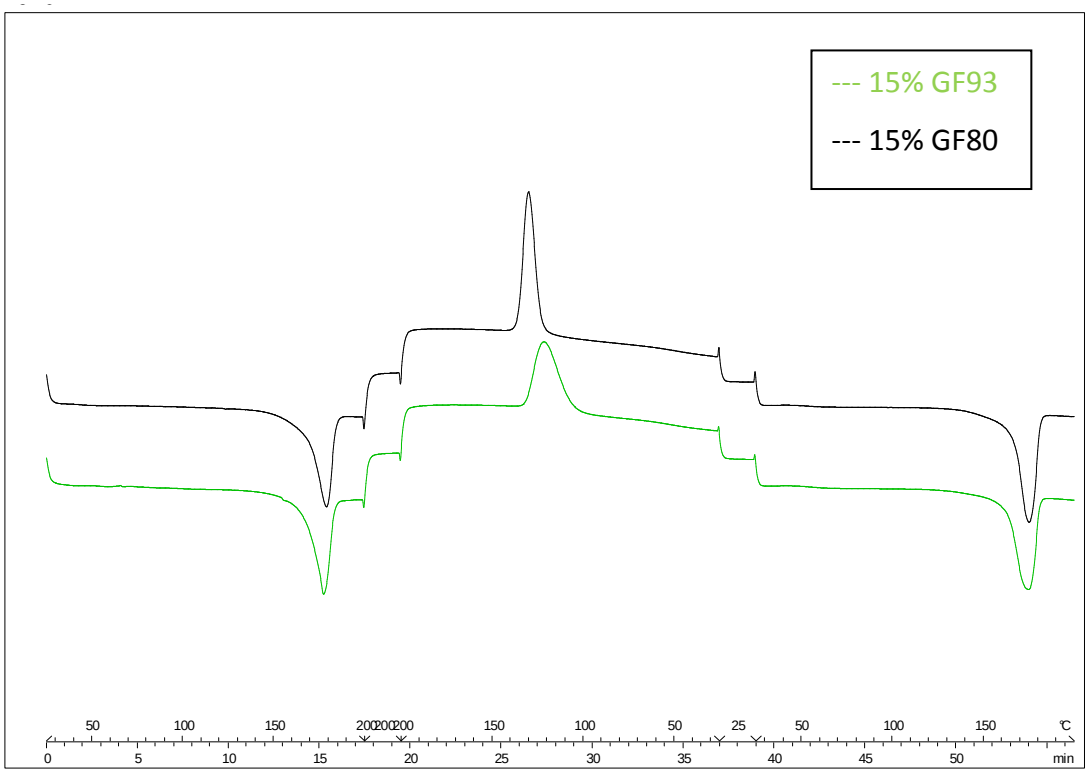

Figure 2: DSC curves of nanocomposite with modified silica

Observing DSC curves shown in Figure 2, the different behavior of the two materials during cooling can be observed; in addition to the different crystallization temperature it should be emphasized that the peak shape is different, closer to the polymer with silica modified with epoxy silane (GF80) and broader for PLA synthesized with silica modified with amino silane (GF93).

To investigate this aspect, the onset and endset values, corresponding to the beginning and end of crystallization process, were measured for pure PLA and nanocomposites containing nanosilica. The values are presented in table 5.

Sample	Onset (°C)	Endset (°C)	Δ (°C)
Pure PLA	113,5	60,7	52,8
0.5% NS	115,3	76,9	38,4
1% NS	128,7	96,6	32,1
2% NS	114,2	61,9	52,3
1% NS 2,0 GF93	122,1	75,0	47,1
1% NS 7,5 GF93	127,9	89,7	38,2
1% NS 15,0 GF93	129,4	103,0	26,4
1% NS 2,0 GF80	122,7	80,7	42,0
1% NS 7,5 GF80	133,3	120,4	12,9
1% NS 15,0 GF80	135,4	124,6	10,8

Table 5: onset and endset values of crystallization peaks

The values of onset and endset shown in Table 5, regarding the crystallization peaks, are useful for understanding the behavior of polymers; materials containing nanosilica have a non linear behavior since sample with 1% of NS is the material have lower Δ value and higher temperature of onset. Probably 0.5% of nanosilica is a not enough to improve the process and 2% is too high and probably interferes with the formation of crystal, as already discussed above. Samples with modified silica show a more linear trend.

When silanes are present at 2%, both for GF93 and GF80, the onset temperature of sample is lower than the one of 1% NS sample and Δ is higher. This phenomenon is probably caused by the presence of a few polymer chains linked on the surface of mineral along with many other chains not linked: this non-uniformity of the system, with a relatively limited interaction between macromolecules and silica results in a more difficult and slow reorganization of the polymer in its crystal phase, and explains why Δ is higher.

Increasing the amount of silane, onset value increases and Δ decreases, especially for materials containing silica modified with GF80.

This may be due, as already mentioned, to the higher reactivity of epoxy group with the polymer reason for which in these samples there is a greater amount of shorter chains (because higher regulated) on the surface of silica particles. The system is therefore more homogeneous from the point of view of the species present and thus can reorganize better and faster during cooling phase. Therefore crystallization temperatures are higher and the range in which material crystallizes is more restricted.

Nanocomposite materials have different behavior, from a thermal point of view, compared to pure polymer; it is interesting to study if materials with complex macromolecular architecture have different thermal properties, considering that the concentrations of comonomers used to obtain materials with good mechanical properties are too low to significantly affect the rigidity of chains and the crystal lattice. However, a consideration of these properties is important to have a complete knowledge of the materials studied and because even small differences, especially in temperature and kinetics of crystallization, may be important to define the best conditions for processing these materials. Thermal behavior of some PLAs with complex macromolecular architecture will be discussed below.

Table 6 shows thermal parameters of some materials with complex architecture synthesized in this work.

Sample	T_{c1} (°C)	ΔH_{c1} (J/g)	T_{g2} (°C)	T_{c2} (°C)	ΔH_{c2} (J/g)	T_{m2} (°C)	ΔH_{m2} (J/g)
Pure PLA	-	-	55.7	108.6	44.6	172.3	46.0
0.125% T1	97.1	9.9	52.8	98.8	30.4	170.1	54.6
0.125% T3	97.9	7.7	52.4	94.4	34.1	169.1	50.8
0.125% T4	-	-	54.2	115.7	42.7	167.5	42.9
0.125% T6	-	-	54.7	121.5	46.3	165.5	42.3
0.0625% T3	-	-	54.7	105.4	37.9	171.8	43.3
0.05% T3	-	-	56.6	115.8	32.7	173.6	38.9
0.125% T3+An mell	113.1	6.3	53.8	97.7	32.7	165.4	39.5
0.125% T6+An mell	104.0	7.4	51.6	96.1	30.3	167.9	45.5

Table 6: thermal parameters of PLAs with complex architecture

Thermal data in table 6 show that materials with star architecture do not have a regular behavior in terms of crystallization and melting temperatures. Material with the 0.125% of T3 crystallizes during cooling, but the phenomenon is not very intense; the value of T_{c2} is lower than the one of pure polymer or regulated with 0.125% of T1 thus showing a star effect due to the center which acts as a nucleating agent. Considering data of materials with 0.125% of T4 and 0.125% of T6 – having stars with more arms, as confirmed by SEC and rheological analyses described in chapter 5 - an opposite behavior is observed: no crystallization during cooling phase was observed and the temperature of cold-cristallization (T_{c2}) is higher than the one of linear polymer. So there is, probably, an effect correlated to the kind of comonomer used to obtain star architecture; the effect is probably related to the different solubility of comonomer in polymer.

Decreasing the percentage of T3 in the feed no crystallization during cooling was observed and T_{c2} value increases decreasing concentration of T3; this because polymer chains become longer, therefore a reorganization of crystal lattice is harder due to lower mobility of macromolecules; moreover the effect of comonomer is lower because it is present in minimum percentages.

Also the behavior of branched samples is difficult to define: both materials have a phenomenon of crystallization during cooling, but their intensity are very low. The value of T_{c1} decreases increasing branching degree as expected because the physical constraints (entanglements) between chains disturb the reorganization of macromolecules in the crystal.

Values of cold-crystallization temperature measured in second heating cycle are lower than those of linear polymer and star-shaped materials; it can be assumed that nucleation during cooling phase occurs, probably favored by the local non-homogeneities generated by comonomers (especially pyromellitic anhydride), but the kinetics of crystals growth is slower and therefore not very evident due to the higher complexity of the system. In second heating scan nuclei already formed will only increase as the system becomes more mobile as a result of heating.

In general we can say that while the presence of nanoparticles affects the thermal behavior of PLA, especially in presence of nanosilica (pure and especially modified), the effect of complex macromolecular architecture on thermal properties of materials is not so evident.

9.2 CRYSTALLIZATION KINETICS

Process of crystallization of polymers from molten state may be divided into two steps, which are usually indicated by the terms of "primary crystallization" and "secondary crystallization". Primary crystallization is divided in two stages, as shown in figure 3. In the first one - "primary nucleation" - the elements able to promote the crystallization below the thermodynamic melting temperature T_f are required. These elements may be already present in the melt in form of particles able to crystallize the polymer on them ("heterogeneous nucleation primary"), or, as in our case, they are formed by spontaneous aggregation of several chain part belonging to the same macromolecule due to the relatively high mobility of the chains ("primary homogeneous nucleation").

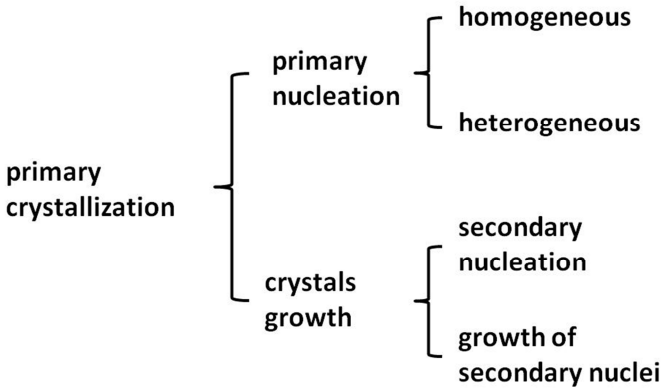

Figure 3: primary nucleation

In second step of primary crystallization, (crystals growth), the formation of secondary nuclei on crystal surfaces ("secondary nucleation") and their growth, occur.

9.2.1 Avrami equation

A lot of studies on isothermal crystallization process concerns the primary crystallization, because experiments are accessible and easy to be performed; moreover a phenomenological equation has been elaborated by Avrami[10]. These equation describes with good approximation the evolution of crystallinity degree as function of time.

Considering the initial steps of transformation, it is possible to assume that:

- primary nucleation is completely random; germs of crystallization in the sub-cooled liquid are uniformly distributed throughout the mass, regardless the degree of progress.
- At constant temperature, the number of nuclei per unit of volume of unprocessed material is dependent on the time for the primary homogeneous nucleation, and is independent for primary heterogeneous nucleation;
- The growth of each unit along any direction, r (t) = G ($t-t_o$), is independent to the development of other centers. G is the linear velocity of crystal growth and t_o is the instant at which the crystal began its growth.

The growth of primary nuclei may be on one, two or three dimensions, forming morphological structures characterized by a rod, disc or ball shapes.

Figure 4 schematically represented three spherical crystalline domains at different stages of growth, V1, V2 and V3 in the melt volume V.

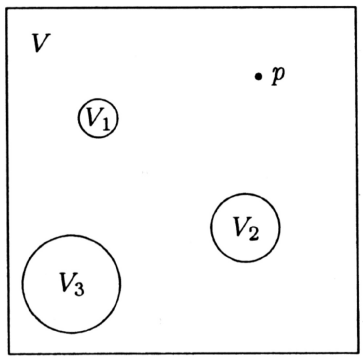

Figure 4: spherical crystalline domains model

Expression 9.2) represent the Avrami equation[10].

$$\frac{x(t)}{x_\infty} = 1 - \exp\left[-K_c t^n\right] \qquad 9.2)$$

K_c is the Avrami constant that incorporates nucleation rate (or the concentration of heterogeneous nuclei) and rate growth rate; n is the Avrami index that assumes different values depending on the dimensionality of growth and the type of primary nucleation.

The trends of equation 9.15) for different values of n are shown in Figure 5.

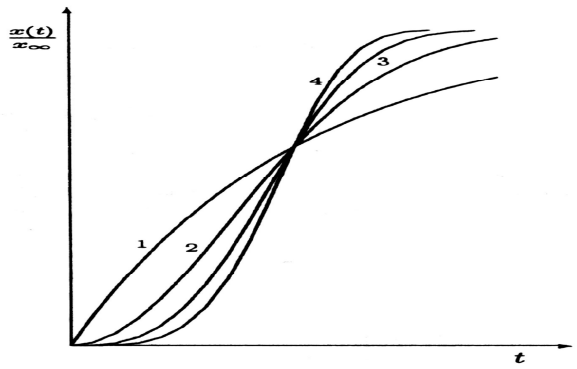

Figure 5: crystallinity degree Vs time

The index *n* is the sum of two terms, one arising from the nucleation and the other one from the growth. Nucleation gives to *n* a contribution of 0 or 1 depending if it is heterogeneous or homogeneous; the growth gives a contribution of 1, 2 or 3 depending if it is mono-, bi-or three-dimensional. The Avrami equation can be normalized as follows:

$$\log[-\ln(1-x_c)] = n\log t + \log K_c \qquad 9.3)$$

x_c is the fraction of crystallinity at time *t* respect to the full crystallization:

$$x_c = \frac{x(t)}{x_\infty} \qquad 9.4)$$

K_c and *n* values can be obtained from the intercept at the origin and from slope of the line obtained by plotting log [-ln (1-x(t)/x_∞] as a function of log (t) as shown in figure 6.

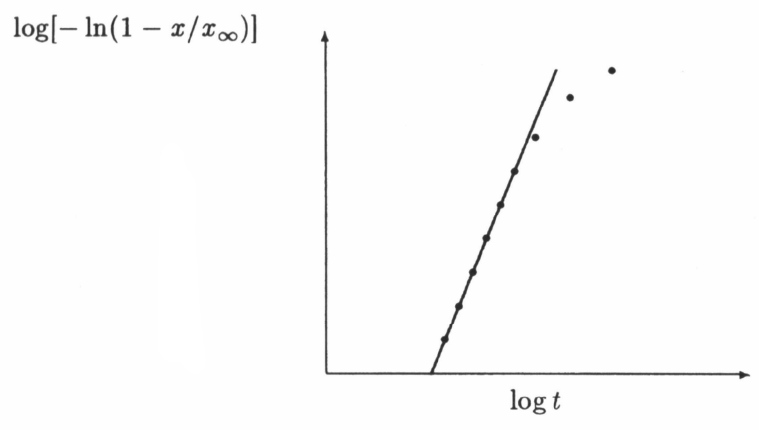

Figure 6: Avrami diagram

Crystallization kinetic can be easily followed using any technique capable of measuring physical quantities linearly dependent on the fraction of material transformed. For example, by calorimetric experiment, the increase of crystallinity in time can be measured by isothermal crystallization curve obtained with a differential scanning calorimeter: the degree of crystallinity is the ratio between the area of peak at time *t* and the total area of crystallization isotherm peak (figure 7).

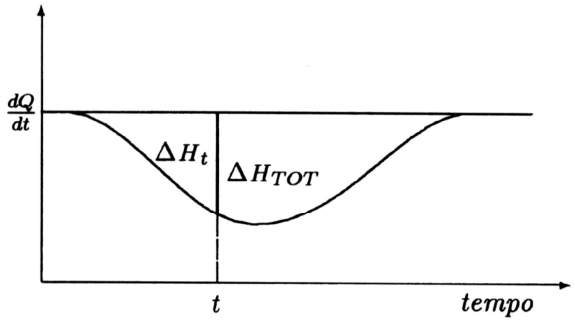

Figure 7: isothermal crystallization peak and evaluation of crystallinity at time *t*

The indications given by the experimental determination of *n* can be ambiguous. If the degree of crystallinity increases with the first power of time (n = 1), it means that the transition phase is realized through a heterogeneous nucleation with linear growth; the mechanism is unique also if n = 4 (three-dimensional growth with homogeneous nucleation).

The situation is critical for n = 2 and n = 3 because these values may correspond to two alternative mechanisms; for example if n = 2 an heterogeneous nucleation process combined with a two-dimensional growth can occur, but also an homogeneous nucleation with linear growth should be observed.

Avrami equation relates only to the process of isothermal crystallization and it is based on some approximations. This affects the reliability of the data extrapolated from it. Polymers analyzed with this method not always follow the trend of Avrami equation, especially when the isothermal crystallization temperature is relatively low. This is due to the fact that the isothermal crystallization of molten polymers usually does not end as expected by Avrami: a progressive increase in crystallinity (secondary crystallization), at very long time so that it is virtually impossible to observe the conclusion, often occurs.

For these reasons:

- Avrami equation fits the experimental data only at lower intervals of crystallization process, in which only primary crystallization occurs;
- Avrami exponent can also assume fractional values; this implies a non-uniform growth of all crystal.

This indicates that the information obtained from Avrami equation must be analyzed with great care.

The general thermal behavior of PLA nanocomposites and of PLA with complex architecture synthesized in this work has been discussed in section 9.1. In the following sections the behavior of different polymers during cooling phase will be investigated: crystallization temperatures of materials at different cooling rates and crystallization isotherm according to the Avrami equation will be evaluated .

9.2.2 Crystallization kinetics at different cooling rates

In this section the temperatures of crystallization at different cooling rates will be evaluated to better understand the behavior of material under different conditions with a particular attention to those materials which, in dynamic DSC analyses, showed the more interesting behavior. These information may be useful to better understand how different materials behave under certain process conditions, such as during molding.

The program chosen for this type of analysis provides more cycles of heating and cooling: heating is relatively rapid (20 °C/min) from 25°C to 200 °C, temperature at which the sample is kept for 5 minutes to erase the thermal history, and then the subsequent cooling is carried out with different rates in different cycles: 10 °C/min, 7.5 °C/min, 5 °C/min, 2 °C/min, 1.5 °C/min and 1 °C/min.

Crystallization temperatures of at various cooling rates for samples analyzed are reported in table 7.

Sample	T_{C10} (°C)	$T_{C7.5}$ (°C)	T_{C5} (°C)	T_{C2} (°C)	$T_{C1.5}$ (°C)	T_{C1} (°C)
Pure PLA	96,7	97,6	98,2	103,7	106,6	109,6
0,5% NS	96,7	97,3	97,7	105,3	108,3	110,6
1% NS	97,6	100,1	102,1	122,4	125,3	128,7
2% NS	96,7	97,2	98,1	105,4	109,1	111,9
NS 2,0 GF93	98,1	100,6	103,3	109,9	111,5	112,6
NS 7,5 GF93	100,2	104,1	108,1	115,6	122,3	129,9
NS 15,0 GF93	104,4	111,3	117,5	124,2	127,9	131,1
NS 2,0 GF80	101,9	109,2	117,4	128,2	131,0	132,9
NS 7,5 GF80	123,0	128,7	134,1	141,4	143,3	144,6
NS 15,0 GF80	128,3	132,7	137,8	141,7	143,8	144,7
1% 10A	97.9	98.5	101.8	105.2	112.3	116.5
1% 15A	98.4	99.0	100.2	103.7	114.1	119.6
1% Na^+	98.6	98.9	99.5	105.9	117.0	123.6
15A 2,5 GF80	99.0	99.7	100.9	119.4	120.8	123.1
15A 7,5 GF80	98.4	100.1	102.7	121.1	122.4	124.5
15A 15.0 GF80	101.8	102.4	105.9	122.0	123.1	125.3

Table 7: crystallization temperatures measured at different cooling rates

The same results are represented in figures 8, 9, 10, 11 and 12.

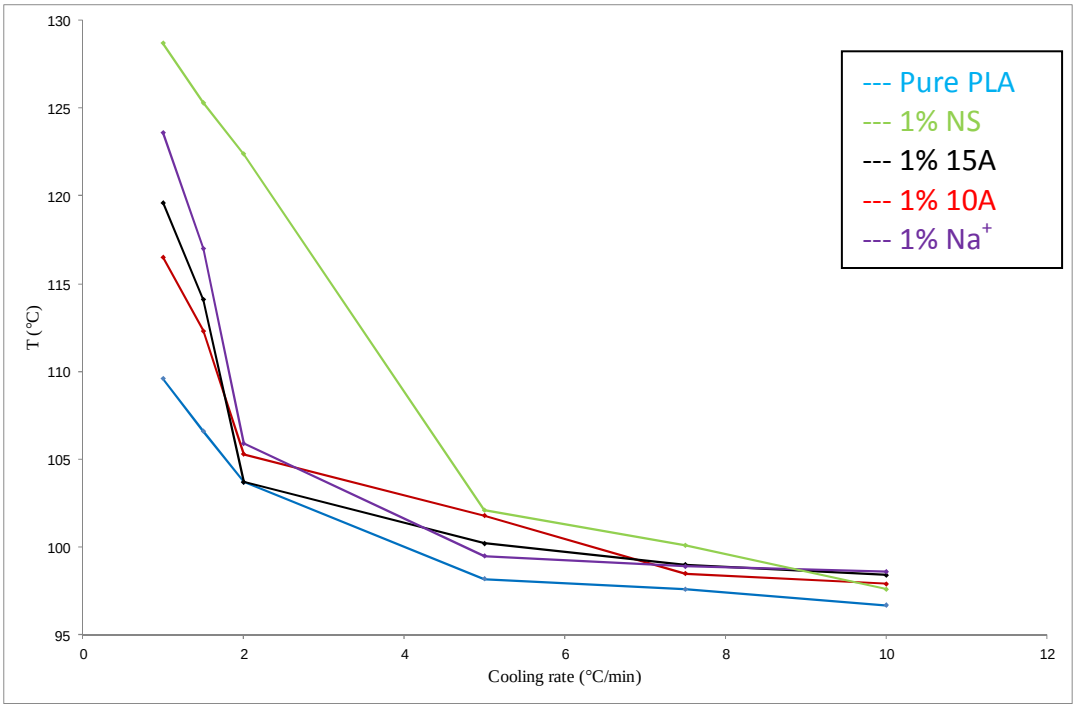

Figure 8: crystallization temperatures Vs cooling rate for nanocomposites with different fillers

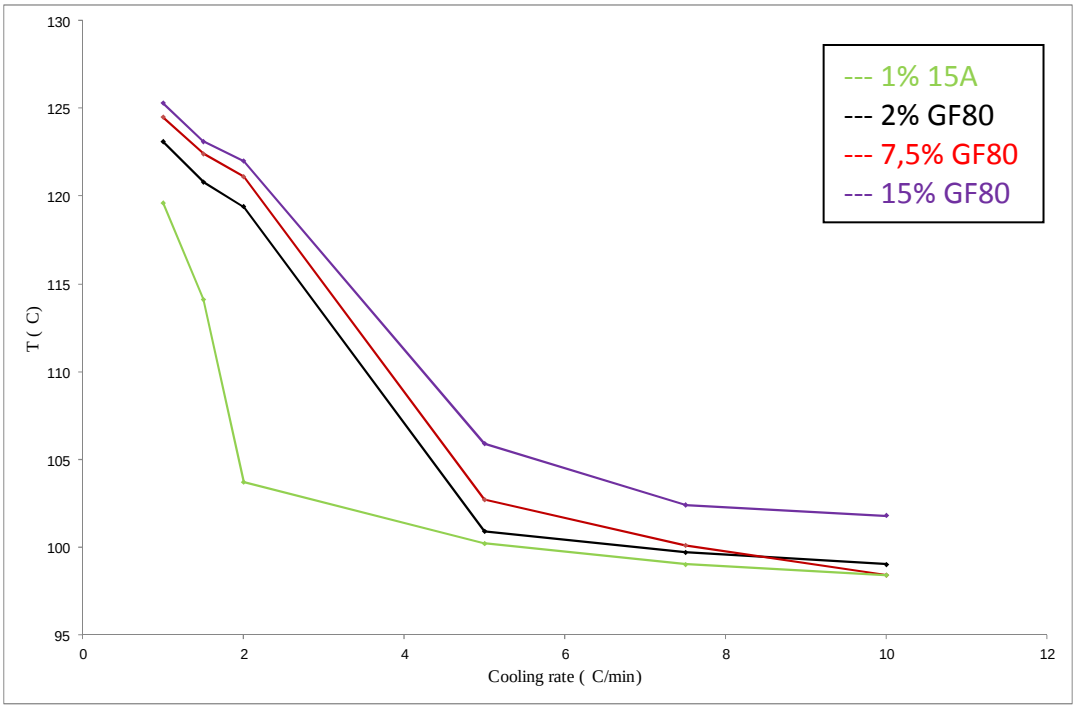

Figure 9: crystallization temperatures Vs cooling rate for PLAs with modified Cloisite 15A (GF80)

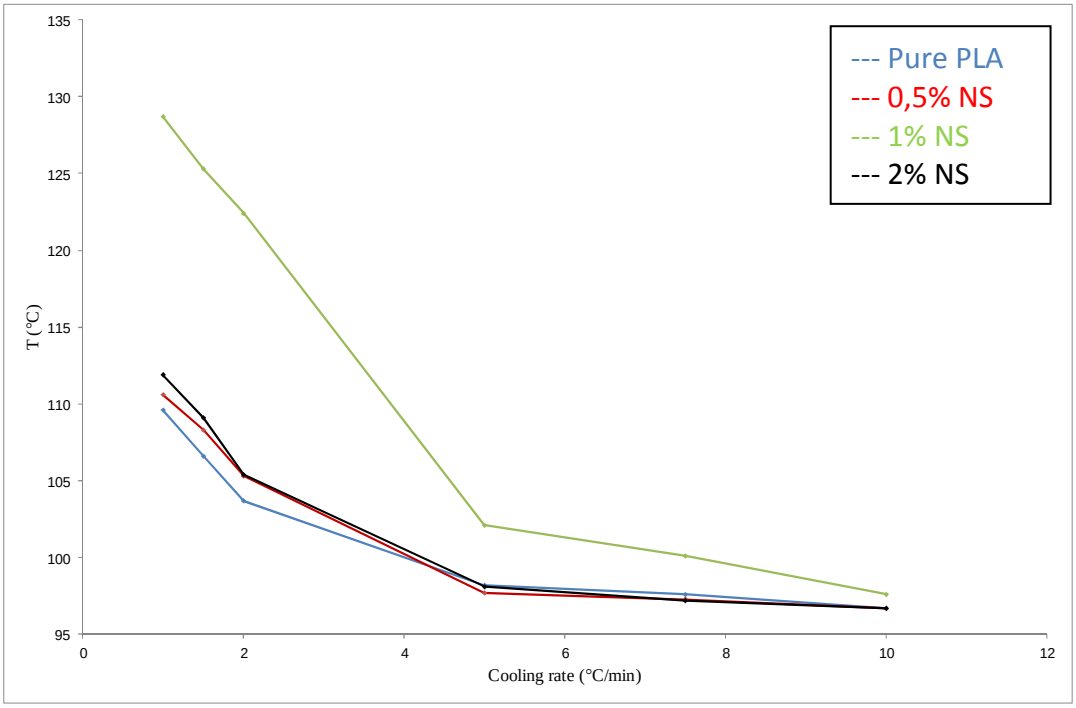

Figure 10: crystallization temperatures Vs cooling rate for PLAs with unmodified nanosilica

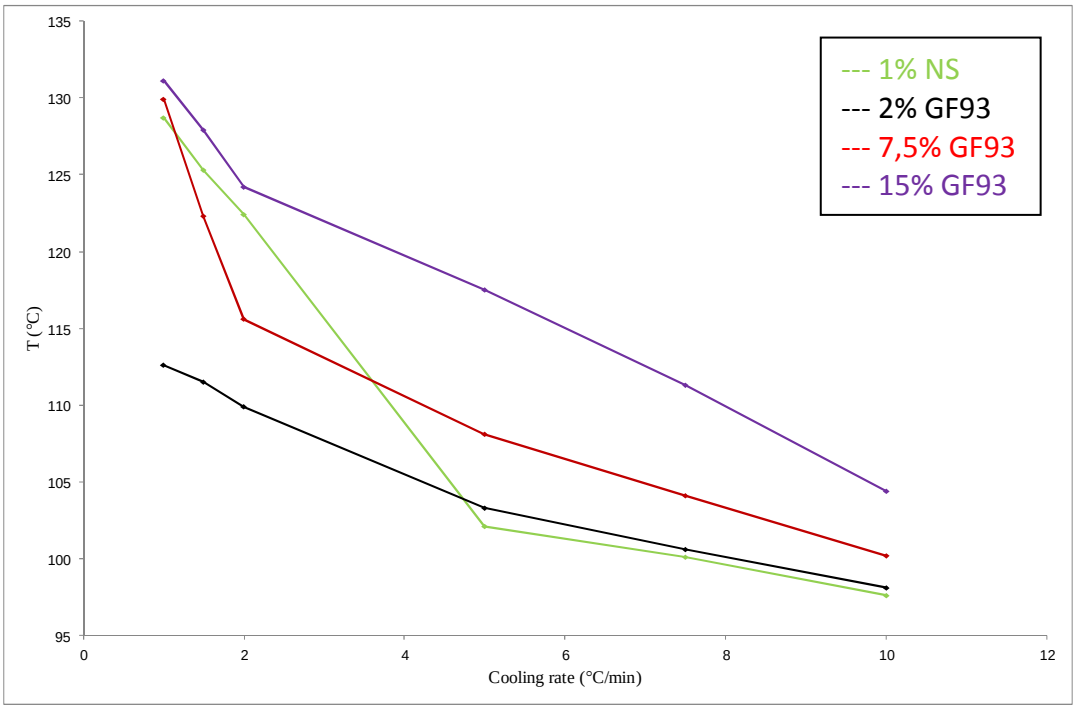

Figure 11: crystallization temperatures Vs cooling rate for PLAs with modified nanosilica (GF93)

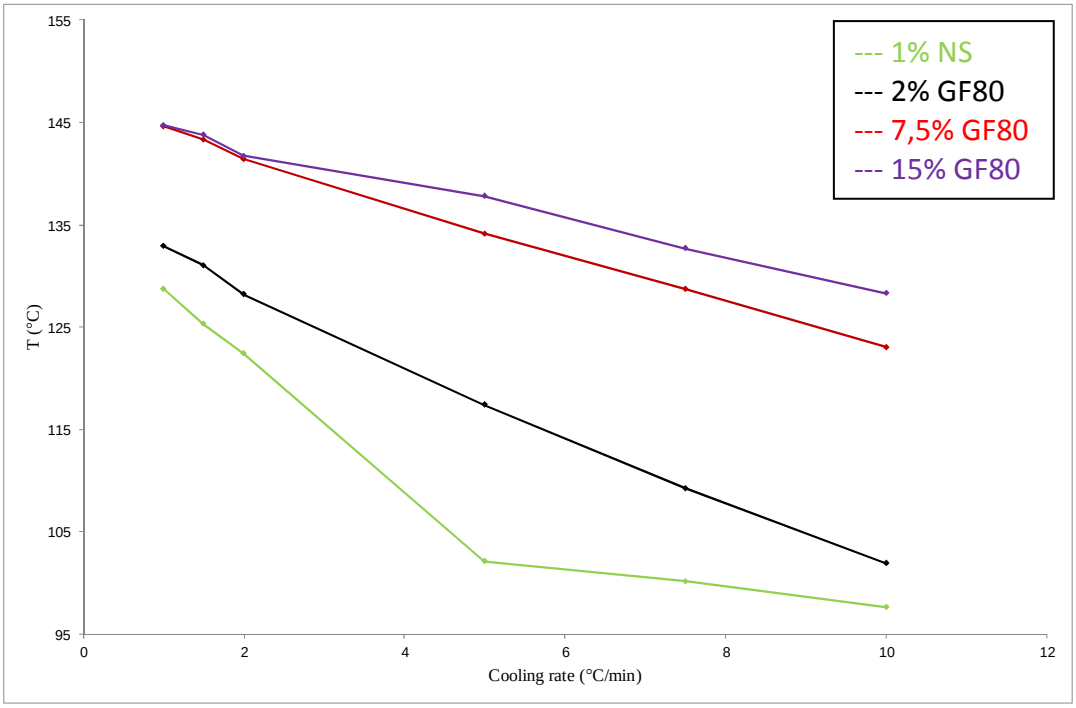

Figure 12: crystallization temperatures Vs cooling rate for PLAs with modified nanosilica (GF80)

Data in table 7 and figures from 8 to 12 show that crystallization temperature depends significantly in all series by cooling rate. At low cooling rate polymer chains will have more time to reorganize and nucleation and crystallization process will start in a lower sub-cooling situation. The presence of nanoparticles, as already reported, allows the different materials to crystallize at lower crystallization temperatures compared to pure PLA. The effect of the presence of filler is particularly evident for materials synthesized in presence of nanosilica, that crystallizes at temperatures higher than the ones of pure PLA, especially at low cooling rates.

Samples with different montmorillonites have a very similar behavior without particular differences between Cloisite 10A, 15A and Na^+, and the effect is lower than using silica (Figure 8). Sample with 1% of nanosilica crystallizes at higher temperatures while polymers with 0.5% and 2% of nanosilica fillers have lower values of T_c, which are close to those of pure PLA, especially at high cooling rate.

The surface modification of nanoparticles strongly influences the crystallization temperature, especially in presence of GF80 (Figures 9 and 12). Materials containing this silane have a T_c much higher than the one of polymer containing pure silica and pure Cloisite at all cooling rate.

This is due to the fact that in presence of silane, the system is more homogeneous both from the point of view of species and regarding the dispersion of nanoparticles in the polymer matrix; so it can better and faster reorganize during the cooling phase, together with the nucleating effect of nanosilica. The effect of GF93 (Figure 11) is evident only for large amounts of silane on the surface of silica (15%), while with lower percentages of silane the action can be seen especially at high cooling rate, while the temperatures of crystallization are lower than those of pure polymer with unmodified silica if cooling rate is slow.

Curves reported in picture 8-12 have different slopes at high and low cooling rates, with the exception of materials containing silica modified with GF80. The two different kinetics observed may be related to different crystal growth. Low cooling rates allow a better reorganization, which allows the growth of larger crystals, while when cooling rates are higher, a larger number of small crystals is formed.

Samples with GF80 probably have a more efficient nucleation chains and are able to reorganize better in the crystal at different cooling rates; this may be due to a better dispersion of nanosilica and a higher homogeneity of the system.

These information are useful from the industrial point of view and must be related to the real kinetics of cooling to which the materials are subjected during processing. Cooling rate in a normal molding process are however much higher (about 300 °C/min). Longer times during cooling after molding would be disadvantageous both in terms of productivity and economic.

Crystallization heats are difficult to evaluate because, especially at lower cooling rates, crystallization requires a relatively long time and is difficult to identify the end of the exothermic peak; however, at lower cooling rates a greater development of heat is expected, due to the better formation of crystal lattice.

9.2.3 Avrami studies of Isothermal crystallization

In the previous section, non-isothermal crystallization of PLA-based nanocomposites have been studied; the study during cooling phase is the most interesting aspect for industry because the processes on polymers designed to produce objects clearly evolve with a cooling phase and crystallization of sample to obtain the final object.

In this section, isothermal crystallization of nanocomposites with pure silica and modified silica (the most interesting from the point of view of the crystallization process) will be studied according to Avrami equation at different temperatures.

DSC analyses performed for this purpose involve an heating phase up to 200 °C, an isothermal phase at this temperature for 5 minutes to erase the thermal history of material and a rapid cooling phase (the maximum allowed by the instrument) until the temperature used evaluate the kinetics of isothermal crystallization; temperature is then maintained for 20 minutes to allow the sample to completely crystallize at low sub-cooling.

Through this study is possible to obtain Avrami index, *n*, and Avrami constant, K_c, to have information on processes of nucleation and crystal growth. Figure 13 shows an example of linearization of Avrami equation (Equation 9.3) for a sample of PLA nanocomposite; drawing the trend line the values of slope and intercept for log (t) = 0, from which K_c is derived, can be obtained.

$$\log[-\ln(1-x_c)] = n\log t + \log K_c \qquad 9.3)$$

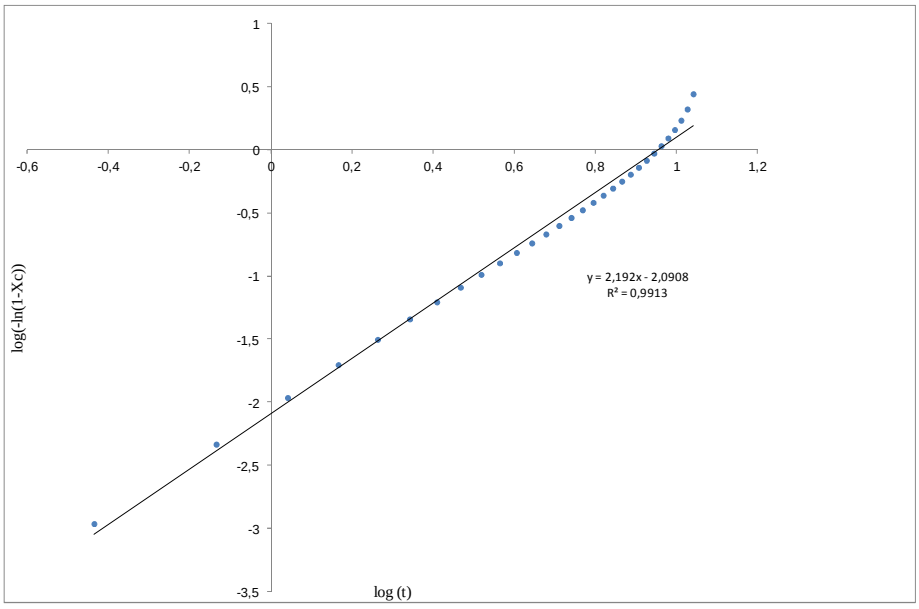

Figure 13: example of isothermal kinetics at 137°C according to Avrami equation

Figure 13 shows that considering the period in which crystallization takes place, data cannot be interpolated with a straight line, as required by Avrami method; it is possible to distinguish a region of linearity for x-axis values of about 0.8. Avrami equation is applicable only to primary crystallization and provides a linear response plotting the experimental data in a graph like that reported in figure 13; interpolating over the total range of crystallization is not significantly and it is therefore appropriate for this study consider only the area of linearity.

On the other hand, the deviations from linearity are probably due to the present of secondary crystallization process, and this is especially true when crystallization is slow.

The values of log (K_c), and n for samples studied are shown, for different isotherms of crystallization, in table 8. It does not include the values for pure polymer because in analyses conditions crystallization is not observed, confirming the difficulty of PLA to crystallize during cooling.

Sample	136°C		137°C		138°C		140°C	
	Log Kc	n	Log Kc	n	Log Kc	n	Log Kc	n
1% NS	-1,55	2,1	-1,89	2,4	-1,89	1,7	-2,21	2,4
NS 2,0 GF93	-1,99	1,6	-1,93	1,5	-1,78	1,4	-2,40	1,2
NS 7,5 GF93	-1,51	1,7	-1,63	1,7	-1,68	1,6	-1,63	1,6
NS 15,0 GF93	-1,39	2,0	-1,59	1,8	-0,88	1,8	-1,56	2,1
NS 2,0 GF80	-1,50	1,9	-1,57	2,3	-1,61	1,5	-1,76	2,1
NS 7,5 GF80	0,10	1,8	-0,02	1,5	-0,22	1,4	-0,70	1,3
NS 15,0 GF80	0,12	1,3	0,06	1,2	-0,17	1,2	-0,55	1,2

Table 8: Avrami parameters for PLA/nanosilica composites

Avrami number n varies from 1.2 to 2.4 and K_c values increases increasing the amount of silane on the surface of nanoparticle sample compared to sample with unmodified silica (1% NS). Pure PLA has very slow crystallization, then K_c and n were not measured in these analytical conditions.

Materials containing nanosilica with epoxy silane (GF80) are those with higher values of K_c; increasing the content of silane a faster kinetics of crystallization is observed; sample with 15% of GF80 has K_c 2 orders of magnitude higher than the one of material with a 1% of unmodified silica unmodified.

This confirms the higher tendency to crystallization in the presence of a high content of silane; surface modification makes it possible to increase the kinetics of crystallization which will be faster and occur in a narrower temperature range, in addition to increasing the temperature of crystallization. The effect on Avrami number (*n*) is less pronounced but the sample with 15% of GF80 shows the lowest values among all samples and in general the values of *n* are lower for samples containing modified nanoparticles. As already reported in literature[11], the trend of *n* is not very significant: for example PLA with 15% of GF80, seems to have a heterogeneous crystallization with a linear growth of crystal (n = 1). On the other hand, sample with 15% of GF93 has *n* close to 2: this could indicate a mechanism with a two-dimensional crystal growth, or a mechanism with a linear growth of crystals. Sample with 1% unmodified silica has a value of *n* close to 2, because of its nature (silane is not present on the surface of the nanoparticle), this value probably indicates a heterogeneous crystallization with a two-dimensional growth of crystals.

It is interesting to compare the curves of isothermal crystallization of each material: in figure 14 an example is reported.

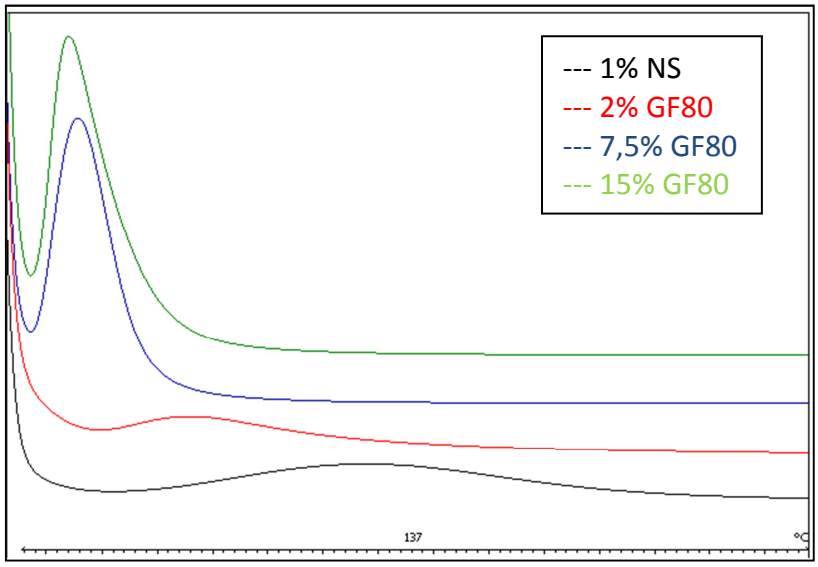

Figure 14: isothermal crystallization of samples with modified silica at 137°C

Figure 15 shows what is reported in table 8. Increasing the percentage of silane on the surface of nanoparticle, material crystallizes faster. The effect is particularly evident for high concentrations of coupling agent.

9.3 TGA ANALYSES

Thermal stability of materials based on polylactic acid is one of the aspects that received more attention, in order to identify possible strategies to increase start degradation temperature to improve the possible applications of PLA and to facilitate the processing of this polymer.

Degradation reactions of PLA, which proceed through random breaking of the polymer chains, involve the ester bonds present in large amounts in polymer chain. These reactions include depolymerization and oligomerization to form cyclic species.

In particular low molecular weight PLAs, having a high concentration of free hydroxyl end groups are more vulnerable to a faster degradation at high temperatures, because the OH groups promote depolymerization reactions mentioned above.

An important aspect that must be taken into consideration in the process of degradation of PLA is the amount of catalyst used in the polymerization reaction: an higher amount of catalytic species in the final product is able to catalyze the degradation reactions accelerating the demolition of polymer [12].

Degradation of PLA forms mainly lactide or other comonomers present in feed and oligomers; also catalytic species, if not removed, are subject to degradation. The removal of volatile and low molecular weight species, in particular lactide, combined with the blocking of hydroxyl end groups are two strategies to increase the thermal stability of PLA, but may not be sufficient to guarantee the necessary stability avoiding the degradation during processing. For this reason, stabilizers are used. Also mineral fillers are an effective way to increase the temperature at which degradation of PLA begins: there are numerous examples in the literature but, as already mentioned in chapter 8, they describe materials prepared in compounding in which is often present a stabilizer. For this reason, in this work it was decided to evaluate the thermal stability of nanocomposite materials based on PLA obtained through in situ polymerization and without using any type of stabilizer, in order to evaluate the real effect of mineral filler on the degradation of polymer.

Tables 9 and 10 show the data of thermal degradation of materials containing montmorillonite and nanosilica, pure and modified, compared with the pure polymer.

Sample	$T_{1\%}$ (°C)	$T_{5\%}$ (°C)	$T_{50\%}$ (°C)	$T_{95\%}$ (°C)	$\Delta T_{1\%-95\%}$ (°C)
Pure PLA	248	275	320	352	104
0,5% NS	270	305	354	382	113
1% NS	313	335	372	389	76
2% NS	297	346	381	392	95
NS 2,0 GF93	273	314	357	375	102
NS 7,5 GF93	254	284	334	372	118
NS 15,0 GF93	253	278	325	376	123
NS 2,0 GF80	286	315	364	390	104
NS 7,5 GF80	275	301	350	383	108
NS 15,0 GF80	264	280	326	381	117

Table 9: thermal data about degradation of nanocomposites with silica

The increase of thermal stability of PLA due to the presence of nanoparticles has already been observed and documented in literature[13,14], and the effect on thermal stability of silica and silanes in our samples can be seen looking data in table 9. Thermal stability increases significantly, especially increasing the content of silica; at low amount of filler (0.5% by weight) the start and end degradation temperature ($T_{1\%}$ and $T_{95\%}$) increased up to 30 °C compared to those of pure PLA, and the effect is much more pronounced further increasing the content of nanosilica. Sample containing 2% of pure silica, even if with a start degradation temperature slightly lower than material with 1% of silica, has a value of $T_{5\%}$ which is 70 °C higher than the one of the pure PLA reaching 346 °C. No stabilizers were added therefore the higher thermal stability is entirely due to the presence of nanosilica.

On the other hand, when the degradation process starts, decomposition seems to proceed faster than that observed for pure polymer, since $\Delta T_{1\% -95\%}$ increased from 104 °C for PLA to 76 °C for the sample with 1% of nanosilica. Material with 0.5% of filler has a kinetics of degradation slower than the one of pure PLA.

There is, therefore, an effect correlated to the presence of mineral, which delays the start of degradation process, but on the other hand the presence of OH groups on silica surface can accelerate the degradation mechanism.

Table 9 also shows the data of thermal decomposition of nanocomposites prepared using modified nanosilica. It is interesting to observe the behavior of these materials compared to PLA and to polymers containing 1% of unmodified silica. Start and end degradation temperatures ($T_{1\%}$ and $T_{95\%}$) decrease increasing silane content, but are still higher than those of pure polymer. This type of behavior observed increasing the amount of surface modification can be explained considering that silanes have a tendency to degrade at relatively low temperatures, often below those of polymer therefore the degradation process of nanocomposite materials starts at lower temperatures. Nanocomposites with GF80 have degradation temperatures slightly higher than those of GF93 series, but data are very similar. Temperature values collected in table 9 also show that samples with modified nanosilica, both GF93 and GF80 have values of $\Delta_{T1\%-95\%}$ that increase when the percentage of silane on the surface of nanoparticle is higher, until to become greater than the one of pure PLA. As explained above, silanes have lower degradation temperatures and can thus promote the process of degradation, but once the silane is completely degraded, the system behaves very similar to the sample containing 1% of unmodified nanosilica. This hypothesis is confirmed by $T_{95\%}$ values , which are very similar for all systems containing 1% of silica, regardless of the amount of silane present.

Data reported in table 9 are shown in figures 15, 16 and 17.

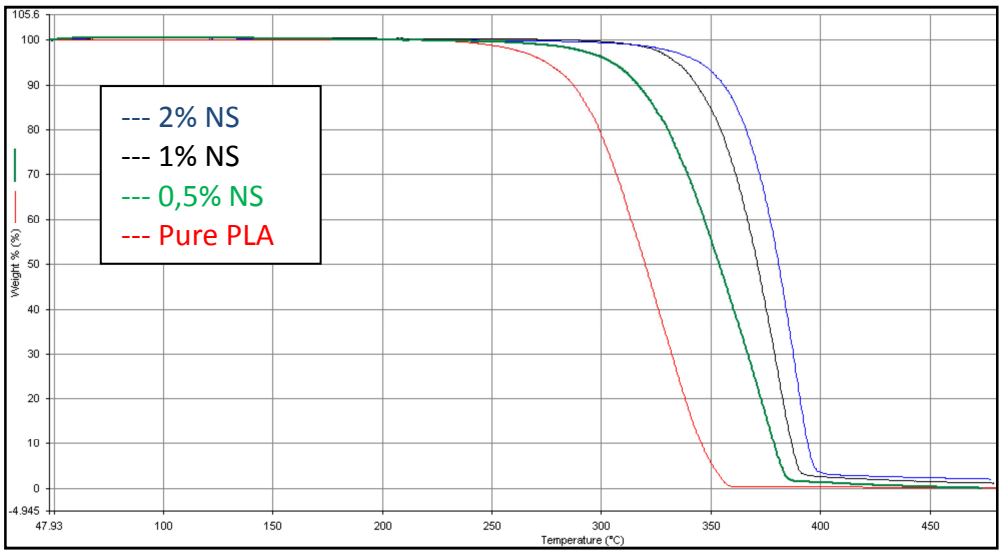

Figure 15: TGA curves of nanocomposites with pure silica

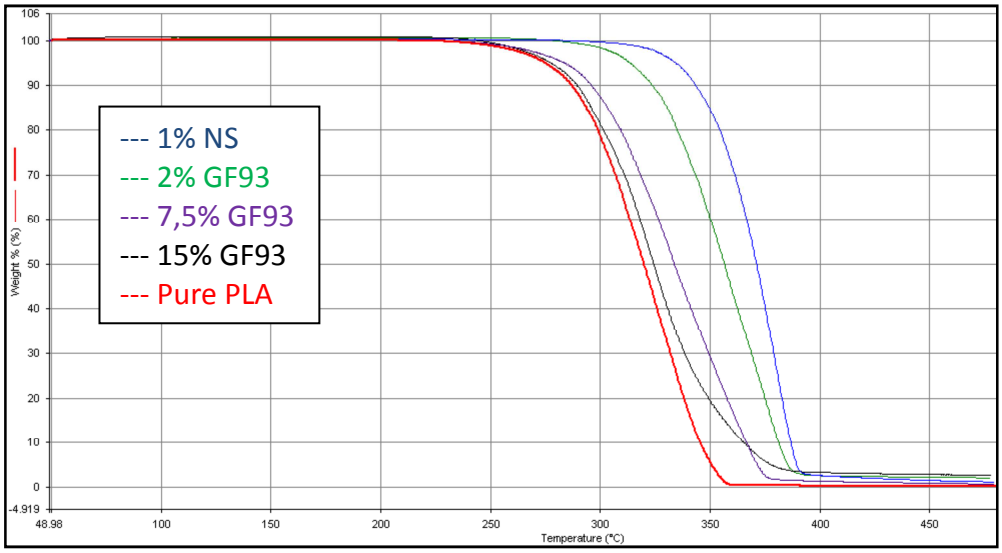

Figure 16: TGA curves of nanocomposites with modified silica (GF93)

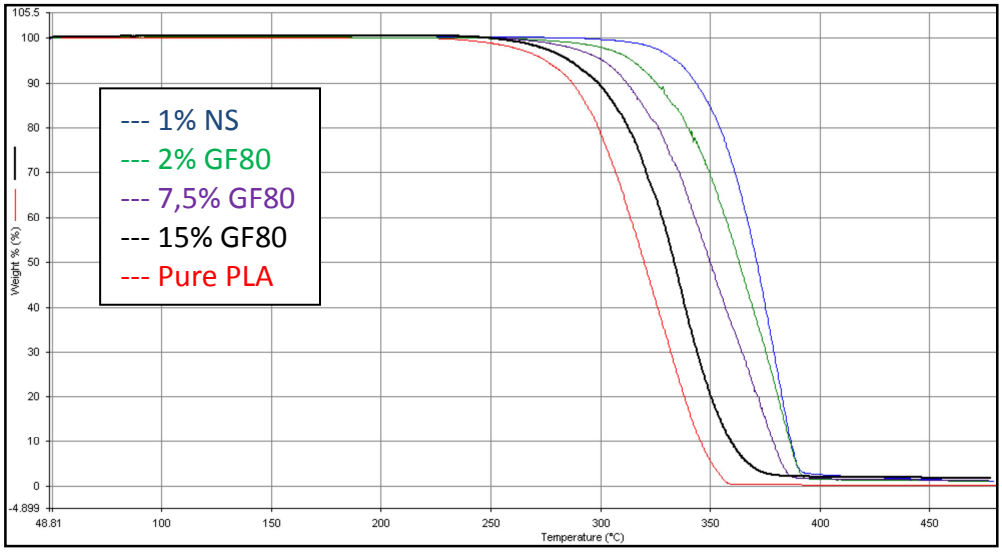

Figure 17: TGA curves of nanocomposites with modified silica (GF80)

In table 10 the degradation temperatures of materials with montmorillonite are reported.

Sample	$T_{1\%}$ (°C)	$T_{5\%}$ (°C)	$T_{50\%}$ (°C)	$T_{95\%}$ (°C)	$\Delta T_{1\%-95\%}$ (°C)
Pure PLA	217.4	262.3	312.1	331.3	113.9
0.5% 10A	249.1	277.8	311.6	327.5	78.4
1% 10A	257.1	286.2	320.7	337.8	80.7
2% 10A	267.0	294.2	327.6	344.3	77.3
0.5% 15A	254.9	275.7	312.0	328.6	73.7
1% 15A	257.1	287.3	319.5	336.0	78.9
2% 15A	283.7	299.5	330.7	353.2	69.5
0.5% Na^+	252.9	278.5	315.6	336.5	83.6
1% Na^+	254.5	279.3	320.6	341.4	86.9
2% Na^+	264.5	294.7	331.3	353.4	88.9

Table 10: thermal data about degradation of nanocomposites with montmorillonite

First of all is necessary to explain why values of pure PLA present in table 10 are different to those reported in table 9: as stated before, the amount of catalyst used in the polymerization process greatly affects the degradation of material, especially for what concerns the start decomposition temperature. As mentioned in chapter 8, the presence of nanoparticles interferes with the growth of chain due to the decrease of catalyst activity, and this is particularly evident in presence of montmorillonites making it necessary to use a higher amount of catalyst to obtain materials with good molecular weight. For this reason it was not possible to compare, from a point of view thermal stability, composites with montmorillonite with the same pure polymer used as standard for materials with silica. Therefore PLA with the same amount of catalyst used for the polymerization of materials containing Cloisite have been synthesized and use as reference to evaluate the role of montmorillonite on the degradation process. The degradation temperatures of this polymer are lower than the ones of standard reported in table 9.

Data collected in table 10 show that montmorillonites have an effect on thermal stability of PLA; degradation temperatures are higher than ones of pure polymer and they increase increasing the amount of filler, just as observed for unmodified silica-containing materials.

Also with Cloisite a decrease in the range of degradation compared to that of pure PLA is observed, and this may be caused by the combined action of OH groups on the surface of nanoparticles and degradation of the cation present between lamella. Materials with sodium Cloisite have a wider range of degradation, probably because sodium cation affects less the process of degradation compared to the ammonium cations present in Cloisite 10A and 15A.
In Figures 18, 19 and 20 are plotted the values collected in table 10.

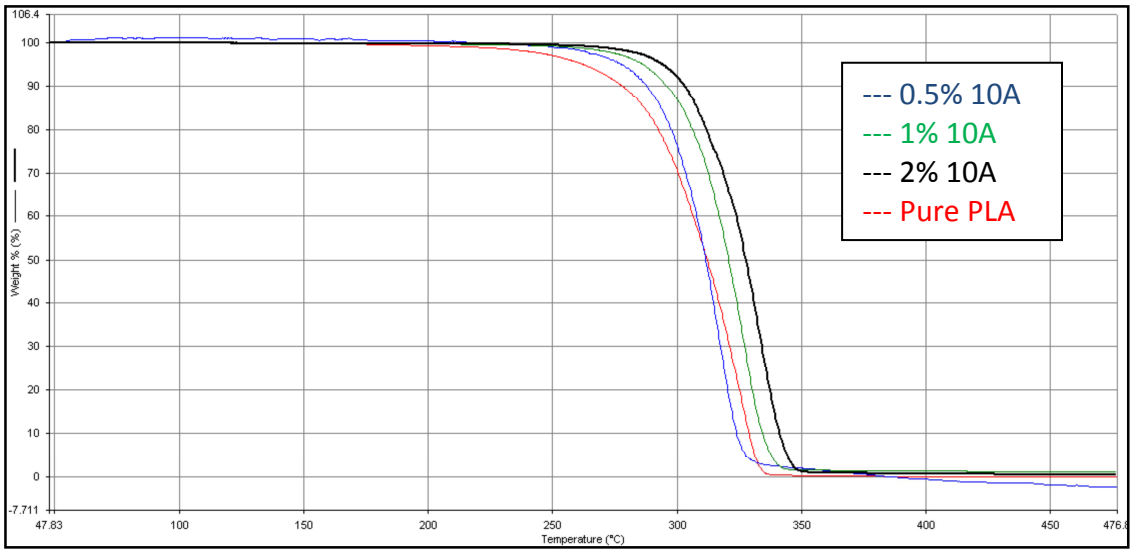

Figure 18: TGA curves of nanocomposites with pure Cloisite 10A

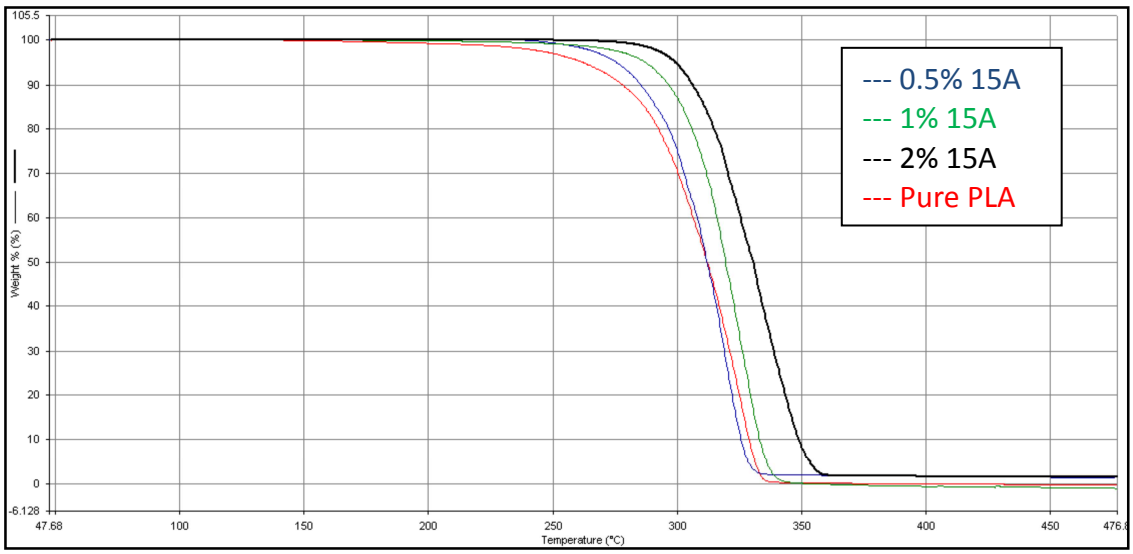

Figure 19: TGA curves of nanocomposites with pure Cloisite 15A

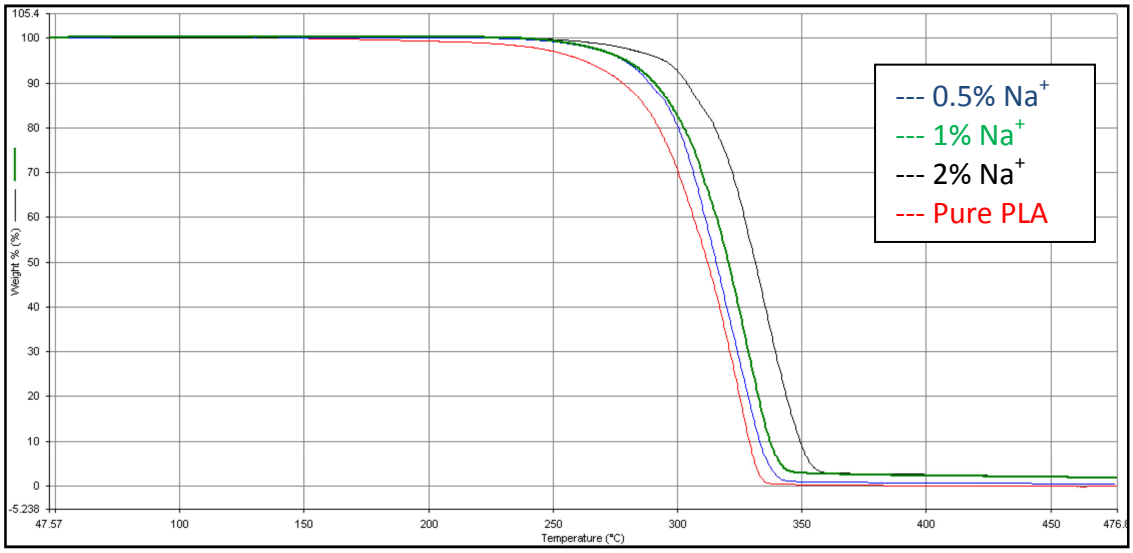

Figure 20: TGA curves of nanocomposites with pure Cloisite Na^+

Figures 15-17 and 18-20 show the effect of mineral filler on degradation of different materials. The weight of the residue after the decomposition is in agreement with the amount of nanoparticle used. The increase in thermal stability is related to the nature of the filler used; in the case of silica it can be attributed to the stability of Si-O-Si bonds compared to C-C bond which increases the energy required for decomposition of the material. This may also explain why in the presence of silanes, increasing the percentage of C-C bonds present, the start degradation temperature is lower than the one of composite prepared with unmodified silica. Montmorillonites act with a double effect, forming a cover over the surface of the material, and a barrier to reduce the diffusion of volatile species forming during the degradation of the material.

REFERENCES

[1] Vasanthakumari, R., Pennings, A. J., *Polymer*, 24, 1983, 175.

[2] Kolstad, J. J., *J. Appl. Polym. Sci.*, 62, 1996, 1079.

[3] Schmidt, S. C., Hillmyer, M. A., *J. Polym. Sci. Part B, Polym. Phys.*, 39, 2001, 300.

[4] Ray, S. S., Maiti, P., Okamoto, M., Yamada, K., Ueda, K., *Macromolecules*, 35, 2002, 3104.

[5] Shieh, Y. T., Liu, G. L., *J. Polym. Sci. Part B, Polym. Phys.*, 45, 2007, 2870.

[6] Nam, J. Y., Ray, S. S., Okamoto, M., *Macromolecules*, 36, 2003, 7126.

[7] Battegazzore, D., Bocchini, S., Frache, A., *Polymer Letters*, 5(10), 2011, 849–858.

[8] Fukada E.: 32, (1995), 593–609

[9] Turner J. F., Riga A., O'Connor A., Zhang J., Collis J., *Journal of Thermal Analysis and Calorimetry*, 75, 2004, 257–268.

[10] Avrami, M., *Journal of Chemical Physics*, 7**,** 1939, 1103.

[11] Yougang G, Yudong Z, Xiangmin X, Puyu Z., *Zhongguo Suliao*, 24(12), 2010, 30-35.

[12] Jamshidi, K., Hyon, S. H., Ikada, Y., *Polymer*, 29, 1988, 2229–34.

[13] Fukushima, K., Tabuani, D., Abbate, C., Arena, M., Rizzarelli, P., *European Polymer Journal*, 47, 2011, 139–152.

[14] Xin, W., Kunyu, Z., Ya, W., Lijing, H., Changyu, H., Huiliang, Z., Shan, C., Lisong, D., *Polym. Int.*, 60, 2011, 202–210.

10. Experimental methods

10 EXPERIMENTAL METHODS

This chapter contains all the experimental procedures used in this research work for the synthesis and characterization both for polymers synthesized and for nanoparticles.

10.1 SURFACE MODIFICATION OF NANOPARTICLES

10 grams of nanoparticles were suspended in 100 mL of methanol, in a 500 mL flask; the suspension was vigorously stirred with a magnetic stirrer.
Silane was diluted with methanol in order to have a silane/methanol ratio of 1/5 w/w. The amount of silane depends on the percentage of surface modification. The silane is then added to the dispersion of nanoparticles: the addition is done slowly to avoid the formation of aggregates and to have a very good dispersion of coupling agent. After the addition, the solution was kept under vigorous stirring for 12 hours and then the solvent was removed by evaporation under nitrogen. The nanoparticles were washed with methanol to remove unreacted silane and then heated to 120 °C (only in the case of amino silane) with mechanic vacuum for about 2 hours. After these operations nanoparticles have been chopped to obtain a fine powder.

10.2 SYNTHESIS OF PLA

10.2.1 Linear PLA and PLA with complex macromolecular architecture

All PLAs, both linear and with different macromolecular architecture, were synthesized using LL-lactide, comonomers and tin 2-ethylhexanoate as a catalyst. The reactions were conducted at 190 °C for 2 h under nitrogen flow in order to ensure an inert atmosphere inside the reaction system. The nitrogen flow was very slow (about one bubble per second observed in the bubble counter) since there are no by-products to push away.

10.2.2 PLA nanocomposites

PLA nanocomposites were prepared adding different percentages (w/w respect to lactide) of mormorillonite and nanoSilica. As in syntheses described in 10.2.1, tin 2-ethylhexanoate and comonomers were also added. The reagents were dried directly in the reaction flask at 80 °C under mechanic vacuum for 12 hours before polymerization. The reaction conditions are the same used for the synthesis of liner PLA and PLA with complex architecture.

10.3 SEC ANALYSES

SEC analyses were performed using methylene chloride as solvent. The system used for the analyses is composed by:

- Pump: Waters 1515 isocratic HPLC pump
- UV detector: Waters 2487 dual λ absorbance detector
- Columns: six columns styragel HR4-HR4-HR3-HR3-HR5-HR2.

SEC measurements were made at a wavelength of 230 nm. 1.2-dichlorobenzene was used as internal reference. The columns are calibrated in terms of linear equivalent PLA.
Solutions of the nanocomposite samples were filtered with 45 microns filter, before injection into the column, in order to prevent that nanoparticles or aggregates of them could damage the SEC system. The analysis thus refer only filtered part of polymer.

10.4 RHEOLOGICAL ANALYSES

Rheological analyses were performed with Physica MCR 300 rotational rheometer with a parallel plate geometry (Φ = 25 mm). Analyses were conducted in frequency sweep experiments on samples after SSP process at 150 °C in mechanic vacuum. Deformation was set equal to 5% and curves of complex viscosity as function of frequency were recorded, ranging from 100 Hz to 0.01 Hz.

10.5 NMR ANALYSES

^{1}HNMR analyses were performed with a Bruker instrument operating at 400 MHz. Samples were dissolved in deuterated chloroform and a delay time (and signal acquisition) of 20 seconds was used to obtain a quantitative results.
^{13}CNMR analyses were performed following the same protocol used for ^{1}HNMR analyses.

10.6 DSC ANALYSES

10.6.1 Determination of melting temperature and crystallization temperature

Melting temperature and crystallization temperature were measured by DSC analyses using this program:

- heating from 25 °C to 200 °C at 10 °C/min
- 5 minutes isotherm at 200 °C to delete the thermal history of material
- cooling from 200 °C to 25 °C at 10°C/min
- 2 minutes isotherm at 25°C
- heating from 25 °C to 200 °C at 10 °C/min

10.6.2 Determination of crystallization temperatures at different cooling rates

Crystallization temperatures at different cooling rates were measured by DSC analyses using these programs:

Cycle 1:

- heating from 25 °C to 200 °C at 10 °C/min
- 5 minutes isotherm at 200 °C
- cooling from 200 °C to 25 °C at 10°C/min
- 2 minutes isotherm at 25°C

Cycle 2:

- heating from 25 °C to 200 °C at 10 °C/min
- 5 minutes isotherm at 200 °C
- cooling from 200 °C to 25 °C at 7.5 °C/min
- 2 minutes isotherm at 25°C

Cycle 3:

- heating from 25 °C to 200 °C at 10 °C/min
- 5 minutes isotherm at 200 °C
- cooling from 200 °C to 25 °C at 5 °C/min
- 2 minutes isotherm at 25°C

Cycle 4:

- heating from 25 °C to 200 °C at 10 °C/min
- 5 minutes isotherm at 200 °C
- cooling from 200 °C to 25 °C at 2 °C/min
- 2 minutes isotherm at 25°C

Cycle 5:

- heating from 25 °C to 200 °C at 10 °C/min
- 5 minutes isotherm at 200 °C
- cooling from 200 °C to 25 °C at 1.5 °C/min
- 2 minutes isotherm at 25°C

Cycle 6:

- heating from 25 °C to 200 °C at 10 °C/min
- 5 minutes isotherm at 200 °C
- cooling from 200 °C to 25 °C at 1 °C/min

10.6.3 Isothermal crystallization

Isothermal crystallization temperatures were measured by DSC analyses using these program:

- heating from 25 °C to 200 °C at 30 °C/min
- 5 minutes isotherm at 200 °C
- cooling from 200 °C to temperature selected to study the crystallization at 100 °C/min
- 30 minutes isotherm at selected temperature

Isothermal temperatures to study Avrami crystallization were: 136 °C, 137 °C, 138 °C, 140 °C.

10.7 TGA ANALYSES

Thermogravimetric analyses were performed using a TGA4000 Perkin Elmer instrument; tests on polymeric materials have been conducted in nitrogen atmosphere with a program that provides a single heating cycle from 30 °C to 550 °C at 20 °C/min.
The analyses of nanoparticles were conducted using a temperature program involving heating from 30 °C to 900 °C at 20 °C/min in nitrogen atmosphere.

10.8 PERMEABILITY TESTS

Permeability tests at oxygen, water vapor and carbon dioxide were performed using a MultiPerm Permeability instrument purchased by ExtraSolution SrL.
The standards for the different tests are: ASTM F2622-08 for oxygen, ASTM F1249-06 for the water vapor and ASTM F2476-05 for CO_2.
Samples for analyses were prepared dissolving 10 grams of polymer in 50 grams of chloroform.
Solution was deposited on a glass plate and stretched to form a film thickness of about 100 microns. Solvent was slowly evaporated to avoid formation of bubbles that can act as channels for the permeation of gas.
Films were conditioned as required by ASTM rules before analyses.

Conclusions

CONCLUSIONS

In the last decade, the industrial interest towards polymeric materials deriving from renewable sources has increased significantly mainly to find substitutes for conventional polymers of petrochemical origin. This phenomenon is mainly due to two reasons: the need to lower the environmental impact of plastics and the need to separate the polymer market from that of oil. In this scenario, aliphatic polyesters are certainly the most widely used class of polymers on which the interest (both academic and industrial) has been focused. These polymers are easy to synthesize, stable in many environments, but may also be highly biodegradable; this class of materials includes a series of polymers derived from the condensation of diols (ethylene glycol, butane diol, etc..) and acids (adipic acid, succinic acid, etc..).

This work was born in a project funded by Cariplo foundation and aimed at the development of polymeric materials based on PLA for applications in packaging field.

Research project was focused on two main aspects: the synthesis of materials with complex macromolecular architecture and the use of nanoparticles, directly added in the process of synthesis; especially the first issue had not been widely investigated yet for PLA polymers.

The importance of changing the molecular architecture of a polymer through the synthesis of complex structures is remarkable; complex macromolecular architectures give properties (for example low melt viscosity, shear sensitivity) that allow to increase the fields of applications of traditional polymers without changing the transformation processes and without increasing the cost of the final product.

The addition of micrometer-sized mineral fillers in compounding in a polymeric matrix is rather well known and widely used, both in academic and in industry. In recent years interest in the use of nano-sized fillers that offer the possibility of a greater increase of properties using a smaller amount of mineral filler has grown considerably.

The first aspect of the work was the study of systems with complex macromolecular architecture obtained through the use of different multi-functional comonomers. The comonomers used are RA_f type in order to obtain star structures, A_2B for tree architecture and a combination of RA_f and pyromellitic dianhydride for tree - star polymers.

Since star structures are the simplest ones, they were used to verify the reactivity of comonomers in polymerization reaction of lactide and the ability to obtain structures with controlled macromolecular architecture.

First reactions were carried out in solution, to have higher control of the synthesis conditions, and then polymerization reaction were carried on in bulk, working in conditions as similar as possible to those used industrially. This methodological approach allowed to test the reactivity of comonomers used to obtain star structures in both synthesis conditions, also observing the influence of the type of polymerization on the distribution of molecular masses.
Operating in solution the polydispersity of the materials is very narrow, close to 1 regardless of the functionality of the monomer used, while bulk polymerization conditions promote intramolecular and intermolecular transesterification reactions that lead to an increase in polydispersity, without epimerisation, as confirmed by NMR analysis.
SEC analysis of star PLA synthesized in bulk showed a decrease of molecular masses distribution due to presence of multifunctional agent.
Once verified the ability to control the macromolecular architecture materials with a more complex architecture, tree and tree – star polymers have been synthesized. From a molecular point of view these polymers are characterized by a broadening of the distribution of molecular masses.
rheological properties of these materials have great importance on an industrial level because they are directly related to manufacturing processes and help to define, for different materials, the possible fields of application connected to mechanical properties, temperature and also processability of materials. Star shaped PLAs show a higher fluidity of the melt, with the same molecular weight, compared to linear polymer and this is due to the lower hydrodynamic volume of star macromolecules and especially to the lower average length of the arms that start from the comonomer compared to the chains of linear polymer. Consequently, star macromolecules have fewer physical constraints to flow and a consequent lower melt viscosity. The nature of PLA, especially the type of bonds present in the chain and the repetitive unit length, requires an high value of DPn to obtain a material with good mechanical properties; for this reason very low amounts of comonomer are required to achieve a sufficiently high molecular weight. In this way the main feature of these materials, the higher fluidity of the melt, is partially lost. For this reason star shaped PLA are not particularly useful and interesting from an industrial point of view. On the contrary branched PLA have shown, for low concentrations of branching comonomer, a high melt viscosity compared to equivalent linear polymers; this property is due to the chains with tree architecture that, for a relatively low degree of branching, are very extensive, accessible and can form many entanglements that are responsible for high viscosity of the melt.

Relatively higher concentrations of branching comonomer make the macromolecules more branched, more compact, less accessible and with less opportunity to interact with other macromolecules to give entanglements: consequently there is a decrease of hydrodynamic volume measured by SEC analysis and a decrease in melt viscosity. Among the branched polymers, those with tree – star architecture are the most interesting ones because they show a higher shear sensitivity and also the possibility to modulate the rheological behavior by varying the ratio of the two comonomers in feed.

The thermal properties of materials with modified macromolecular architecture are not substantially different than those of analogous linear polymers, and this depends on the difficulty of PLA to crystallize during cooling, which cannot be overcome by changing the macromolecular architecture.

Second aspect of the research was the study of nanocomposite materials based on PLA. The work has focused on the use of two classes of nanoparticles: the montmorillonite (Cloisite 10A, 15A and Na^+) and nanosilica. At first fillers were used as such and added directly during polymerization. The presence of mineral filler interferes with the polymerization process limiting the growth of the chain and the molecular weight; for this reason a maximum amount of fillerof 2% w/w, respect to monomer, has been used.

The presence of nanoparticles positively influences the viscosity of nanocomposite materials, which is higher than the one of pure polymer. Thermal behavior is also affected by the presence of nanoparticles: mineral fillers increase the thermal stability of PLA and act as nucleating agent, promoting the crystallization of material during cooling phase. In particular, the analyses show that materials containing nanosilica have an overall behavior better than polymers with montmorillonite.

Then surface of nanoparticles was modified by using two organosilanes as coupling agents.

It has been optimized a method to modify the surface of nanosilica and Cloisite 15A and different techniques to have a qualitative and/or quantitative determination of couplig agent present on the surface of nanoparticles have been tested. The most satisfactory results were obtained by titration of functional groups of silane. Other kinds of analyses give only qualitative results.

Surface modified nanoparticles were used to synthesize new nanocomposite materials. It was found that the presence of silane has a significant influence on material properties, which are different from those of pure PLA, but also from those of materials synthesized with unmodified fillers.

The results obtained from rheological and DSC analyses are particularly interesting. Viscosity is significantly affected by the presence of silanes, especially at low values of shear rates; also temperature and kinetics of crystallization during cooling change in presence of modified nanoparticles.
The results obtained are very encouraging since the materials have shown interesting properties even if the amount of filler in the feed is very low compared to that usually added with the technique of compounding: a significant improving effect of properties has been observed after surface modification of filler.
Gas permeability of nanocomposite materials compared to that of pure PLA was also tested, both on linear samples and on the ones with complex architecture: the presence of nanoparticles significantly increase the barrier behavior respect to pure polymers and also compared to commercial PLA.

Materials studied in this work, both with complex macromolecular architecture and nanocomposites, have different properties but they both are very interesting, allowing the use of these materials in different fields of application. Changing the architecture and controlling macromolecular structure can be advantageous for different manufacturing processes (injection molding, blow molding or spinning) that require different viscosities pf the materials.
Nanocomposites produced with the technique of in situ polymerization can be applied in the field of packaging, given the lower permeability to gases, for injection molding, having the ability to crystallize more quickly, or in applications at higher temperatures.

Another important aspect that can justify the interest and the industrial development of these materials is the possibility to produce them with the normal processes of synthesis already used and optimized for the standard linear PLA. This is clearly a great advantage from the industrial point of view because it allows to produce materials with different properties, without developing new industrial production processes.
The study of a new class of materials that combine the two central aspects of this research, the complex molecular architecture and the use of modified nanoparticles, has provided interesting preliminary results. Within a certain range of the ratio between comonomers in the feed, non-crosslinked materials have been obtained, and rheological curves of some of the samples synthesized have a range of complex viscosity interesting from an industrial

viewpoint. This behavior gives an opportunity to continue research and development of new materials, both to deepen what already studied and to explore new and interesting issues.